Sebastiano Foti

Multistation Methods for Geotechnical Characterization using Surface Waves

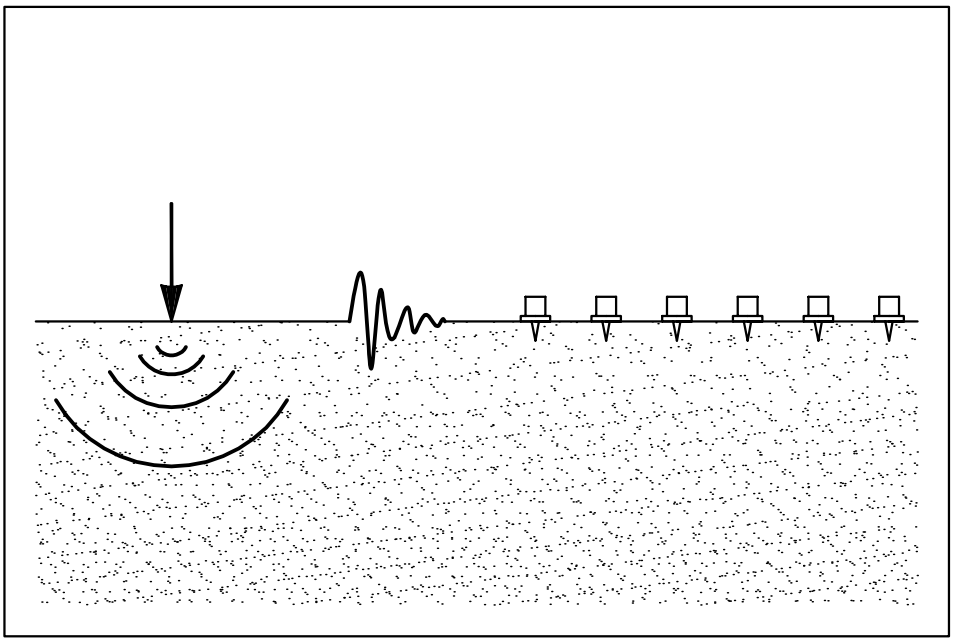

Dottorato di Ricerca in Ingegneria Geotecnica

Politecnico di Torino
Politecnico di Milano
Università degli Studi di Genova
Università degli Studi di Padova

Politecnico di Torino
Politecnico di Milano
Università degli studi di Genova
Università degli studi di Padova

Dottorato di Ricerca in Ingegneria Geotecnica (XII ciclo)
(PhD Degree in Geotechnical Engineering)

Multistation Methods for Geotechnical Characterization using Surface Waves

A thesis presented by

Sebastiano Foti

Approved:

Prof. Renato Lancellotta
Adviser

Prof. Renato Lancellotta
Head of the PhD Programme in Geotechnical Engineering

February 2000

Ai miei genitori
A Lucia

Acknowledgements

I'm extremely pleased for the high number of people who collaborated with me and especially those with whom I shared my time during my PhD. For sure I will not be able to mention them all, but everyone has my sincere gratitude.
My advisor Prof. Renato Lancellotta, no words can express enough my gratitude to him. I have a great debt to him and I'm sure it will not be possible for me as a pupil to surpass my Master. Even those who have never met him personally know of his scientific value, but only those who are lucky enough to work with him can tell about his high human qualities.
I would like to express my gratitude to Prof. Jamiolkowski. Since the start of my PhD program his suggestions have always been of great value to me and finally his peer review has been very important during the writing of this dissertation.
The turning point of my research on surface wave propagation and soil characterization has been the period I spent as a research scholar at GeorgiaTech with Prof. Glenn Rix. My gratitude to him is not only due to the knowledge he transmitted to me but also to his warm hospitality. During that period I learned so much and I want to thank also the whole Georgia Tech faculty and my colleagues who gave me great help.
A word of gratitude to Dr. Carlo Lai as well, who is a good friend first of all. He contributed to my knowledge in the field tremendously. His highly valuable suggestions have always been very precious to me and his rigorous approach has been a constant example to follow.
The experimental work of the final year of my PhD would not have been possible without the help and the contributions of Prof. Luigi Sambuelli, Dr Valentina Socco and Mr Andrea Rafanelli. Moreover their geophysicists' point of view is for me continuously stimulating.
ENEA-Saluggia staff conceded the access to their testing field and kindly gave us all the support we needed.
Dr. Giampiero Deidda of Cagliari University helped the Author for the τp processing.
My sincere gratitude goes to all my colleagues at Politecnico di Torino and especially to Daniele, Guido, Herbert, Marco and Roberto. Thanks to them I have the privilege of spending my days in a stimulating, friendly and serene working environment.
I think that nobody would ever be able to thank his own parents sufficiently. Continuous support and encouragement are but only one of the wonderful gifts I received from mine. And these have been very precious to me since the start of university.
Last but not least my girlfriend Lucia. Without her continuous presence and love I could not have afforded any of the sacrifices that have led to this work. In addition several illustrations of this dissertation are due to her patience.

Abstract

This dissertation deals with soil characterization methods based on surface wave propagation applied to geotechnical engineering purposes. This topic has gained much interest in the last decade because of the appealing possibilities given by non-invasive methods, which are at once very flexible and cost effective.

An overview of the properties of Rayleigh waves in layered linear elastic and linear viscoelastic media is presented, together with their applications for site characterization, of whose the SASW (Spectral Analysis of Surface Waves) method is by far the most well-known in geotechnical engineering.

The research has been mainly focused on the application of multistation methods, compared with the classical two-station approach typical of the SASW method.

Results from both numerical simulations and experimental testing are reported to compare two-station and multistation methods and to clarify the advantages that can be obtained using the latter ones.

In particular the research has been developed following two different directions: on the one hand the application of classical geophysical analysis tools (such as *fk* domain analysis and slant stack transform) to tests performed with impulsive sources. On the other one the possibility of obtaining from surface wave testing not only a stiffness profile, but also a damping ratio profile for the site. In this respect a new method for simultaneous measurements of Rayleigh dispersion and attenuation curves is proposed.

Regarding the first topic, the necessity of a multistation approach to determine the experimental dispersion test is essentially related to the spatial variation of phase velocity. Analyses in the frequency-wavenumber domain and in the frequency-slowness domain are very powerful approaches, still there was a need of studying the effects of the change of scale from geophysical applications to geotechnical ones. Indeed because of the peculiar properties of Rayleigh waves, surface testing is strongly affected by the distance travelled by the analysed wave. The numerical simulations performed in the research show that the phase velocity obtained using multistation methods with a limited number of receivers close to the

source is not a modal value as it is for geophysical applications, but an apparent phase velocity arising from modal superposition.

The experimental tests showed the good performances of multistation methods when compared to the SASW method. In particular some drawbacks of the latter method, due essentially to its two-station nature, are avoided and the field-testing appears to be very promising for future applications. In particular the application of the frequency-wavenumber domain analysis can lead to much faster and more stable estimates of the experimental dispersion curve and the process is easily automated, with a great saving of time and less requirement for subjective decisions. Another important advantage is given by the stability with respect to a near field effects that lead to a better reconstruction of the dispersion curve for the low frequencies and hence to a deeper characterization.

The necessity of a new method for the simultaneous determination of surface wave dispersion and attenuation curves is linked to the strong coupling existing between the two. Such coupling is extremely important for the subsequent inversion process, in a consistent method leading from the field measurements to the stiffness and damping profiles.

The proposed method uses a new testing configuration, designed to measure the experimental transfer function. Successively a regression process of the complex quantity with the corresponding expression obtained modelling soil as a linear viscoelastic layered system leads to the experimental dispersion and attenuation curves.

Some preliminary results are reported showing very encouraging results, also if a more extensively testing programme is required for the complete validation of the method.

Sommario

La tesi tratta la caratterizzazione geotecnica dei terreni attraverso misure di propagazione di onde superficiali. Nell'ultimo decennio questo argomento è stato oggetto di un intenso interesse da parte della comunità scientifica in virtù delle attraenti possibilità date dalla flessibilità di tali metodi e dalla loro efficacia anche dal punto di vista del contenimento dei costi di esecuzione.

Una panoramica generale delle proprietà delle onde di Rayleigh in mezzi linearmente elastici o viscoelastici, con particolare riguardo al caso dei mezzi stratificati, introduce il tema, riportando le peculiarità che fanno di queste onde un potente strumento per la caratterizzazione. Segue un'analisi dei metodi utilizzati per l'identificazione dei terreni, dei quali il metodo SASW (Analisi Spettrale delle Onde Superficiali) è certamente il più noto in ambito geotecnico.

L'obiettivo principale della ricerca è centrato sull'uso di metodi a più stazioni per il rilevamento e l'analisi delle onde superficiali, in luogo del classico schema a due ricevitori, correntemente utilizzato per l'esecuzione delle prove SASW. Per chiarire i vantaggi connessi e le differenze che possono riscontrarsi sono state svolte alcune analisi comparative, utilizzando sia simulazioni numeriche della propagazione delle onde sia dati sperimentali, ottenuti in apposite campagne di prova.

La ricerca si è sviluppata essenzialmente su due diversi temi: da una parte si è indagata l'applicabilità di strumenti classici della Geofisica (come le analisi nel dominio frequenza-numero d'onda e nel dominio frequenza-lentezza, ottenuto mediante l'applicazione della trasformata di Radon) nel caso di prove eseguite con sorgente impulsiva. L'altro aspetto è legato alla possibilità di utilizzare le informazioni presenti nel treno d'onda per ottenere non solo un profilo di rigidezza ma anche un profilo di smorzamento relativo al sito in esame: a tale riguardo viene proposto un nuovo metodo basato sull'applicazione del concetto di funzione di trasferimento.

Per quanto riguarda il primo aspetto, un punto essenziale riguarda gli effetti di scala, ossia le differenze che possono attendersi laddove le tecniche di analisi utilizzate in Geofisica vengano applicate a problemi di caratterizzazione su scala

Geotecnica e dunque su dimensioni ridotte. Infatti, la dispersione, che è una caratteristica peculiare delle onde di Rayleigh in mezzi stratificati, produce effetti notevoli sul treno d'onda, effetti fortemente legati alla distanza che intercorre tra la sorgente ed il punto in cui l'onda viene rilevata. Le simulazioni numeriche condotte nell'ambito della presente ricerca mostrano come la velocità di fase ottenuta utilizzando metodi a più ricevitori sia fortemente condizionata dalla sovrapposizione dei diversi modi di Rayleigh, perlomeno nei casi di profilo inversamente dispersivo. Questo costituisce una forte differenza rispetto al caso geofisico nel quale vengono rilevate le velocità modali. Conseguentemente, il processo d'inversione deve essere basato su algoritmi che tengano conto della sovrapposizione modale come nel caso della prova SASW.

I risultati sperimentali, riguardanti su un sito normalmente dispersivo, sono molto incoraggianti. In particolare le tecniche a più stazioni permettono di superare alcuni svantaggi della classica tecnica SASW, legati essenzialmente all'adozione di due soli punti di misura. L'applicazione dell'analisi nel dominio frequenza-numero d'onda porta a stime più stabili della curva di dispersione ed è oltretutto possibile automatizzare la procedura, con notevole riduzione dei tempi di elaborazione ed eliminazione di alcune scelte soggettive che condizionano la tecnica attualmente in uso. Infine è importante evidenziare la possibilità di ottenere maggiori informazioni relative agli strati più profondi del terreno.

Per quanto riguarda il nuovo metodo delle Funzioni di Trasferimento, questo si basa sull'uso di una sorgente armonica per misurare in situ le grandezze sperimentali, che sono poi utilizzate per un processo di regressione nel campo dei numeri complessi. Tale algoritmo è basato sull'espressione teorica degli spostamenti in superficie per un mezzo viscoelastico lineare, coerentemente con una struttura matematica che può essere convenientemente utilizzata per il successivo processo d'inversione delle curve di dispersione ed attenuazione sperimentali, volto ad ottenere i profili di velocità e smorzamento delle onde di taglio.

I risultati preliminari derivanti dall'applicazione del nuovo metodo appaiono molto incoraggianti, sebbene un programma di prove più esteso sia necessario per la sua completa validazione.

Contents

Table of Figures

List of Tables

Chapter 1

Introduction

1.1 Motivation

Soil behaviour under cyclic loading or dynamic conditions is of interest for a wide range of problems, from foundation vibrations to site response during earthquake.

In particular the important role that stiffness and dissipative characteristic of geomaterials at shallow depth play in site amplification of the motion caused by earthquakes, push towards the need for adequate characterisation (Gazetas 1982).

In this regard both laboratory and in situ tests have a great importance. The advantages and disadvantages of the two classes are well known. The possibility of testing geomaterials in their more or less undisturbed state (particularly important for hard-to-sample soils) and the wider scale of application are two of the main advantages of in situ testing.

The stiffness and damping of soils are strongly related to the magnitude of strains involved. In this respect the attention will be in the following restricted to seismic methods based on wave propagation, from which soil parameters at very low strains are obtained.

Seismic methods are often divided into two broad categories: invasive tests and non-invasive tests. While the methods of the first category require a bore-hole (Cross-hole, Down hole, P-S suspension logging) or the insertion of a probe in the soil (Seismic cone), the methods of the second one are conducted from the free surface (Reflection, Refraction and SASW tests).

In general the latter ones are usually affected by a larger degree of

uncertainties, but they present some advantages such as the possibility of testing larger portions of soil and moreover they are usually more cost-effective.

Since its introduction in the mid-Eighties, the SASW (Spectral Analysis of Surface Waves) method has gained a large role into in situ testing for stiffness at very low strains.

1.1.1 In situ testing through surface waves detection

Surface waves travel in a medium along a free boundary and hence they are easily detected using transducers placed on the free surface of a body. Moreover they have some inherent properties that make them very useful for identification problems. Their use in geotechnical characterisation has recently spread out because modern equipment allows for a satisfactory analysis and an adequate inversion process, necessary to infer from the detected particle motion the properties of the medium in which the wave propagates.

The main advantages of the SASW test are essentially related to its non-invasive nature that allows the characterisation of hard-to-sample soils without the need for boreholes, a need that strongly affects invasive methods from an economic point of view. Moreover with respect to other non-invasive methods, such as seismic reflection and seismic refraction, the SASW test gives a good resolution at shallow depth, as required for geotechnical characterization, and it is more flexible.

A distinctive features of SASW, compared with cross-hole and down-hole methods that are the most widely adopted in situ seismic methods in geotechnical practice, is related to the volume of soil tested. Indeed the results of the SASW test must be considered an estimate of the average properties of the site, which can be an advantage for example in the case of seismic amplification studies.

The process of detecting and analysing surface waves has been successfully applied to many characterisation problems, showing a great flexibility of the basic idea. In the following some of the applications that can be found in the geotechnical literature are reported:

- Pavement system identification: it is a natural application of the method since such systems are typically horizontally layered media. A difficulty is given by the inherent inversely dispersive nature (caused by the presence of stiff top layers), that strongly complicates the inversion procedure (Heisey et al. 1982, Al-Hunaidi 1992, Haegeman and Van Impe 1997).
- Waste disposals: the use of non invasive methods to get the mechanical parameters is in this case a great advantage due to the difficulties and the danger associated to the collection of samples and to the realisation of

boreholes. Moreover the advantage of getting average properties is in this case emphasised, because of the scale of intrusions (Rix et al. 1998, Haegeman and Van Impe 1998).

- Offshore characterization: theoretical and experimental studies have been carried out by the researchers of the University of Texas at Austin to assess the possibility of applying the test on the seafloor (Manesh 1991, Luke 1994).
- Soil improvement: the repetition of the test before and after the application of soil improvement processes can give an important insight into their effectiveness. In this regard, also the simply comparison of the dispersion curves can give useful information, without the need for an accurate and time-consuming inversion process (Andrus et al. 1998).
- Frozen soils: similarly to the case of soil improvement, the repetition of the test in different periods of the year can give important hints about the seasonal variations of soil stiffness in cold regions, caused by freezing cycles (Alkire 1992).
- Obstacle detection: a very appealing possibility is given by the use of surface wave to detect underground obstacles, studying the effects that they produce on the propagating wave (Gucunski et al. 1996, Ganji et al. 1997, Gucunski et al. 1998).
- Borehole SASW: although it is somewhat different from the other applications being an invasive method, also this new seismic method is based on surface wave propagation. The measurements are in this case performed on the edge of a borehole (Kalinski et al.1998; Kalinski et al. 1999).

1.2 Research Objectives

The use of surface waves for geotechnical site characterization has been originally proposed during the Fifties and then it has been practically set apart up to the mid-Eighties when the SASW test was proposed. The main reason of the poor success of the Steady State Rayleigh method was the lengthy procedure of data acquisition on site. The SASW method, using the concepts of signal analysis and impulsive sources acting on the ground surface, drastically reduces the acquisition time in situ.

The basic idea of soil characterization through surface wave propagation can be summarised as follow. In a vertically heterogeneous medium the phase velocity of Rayleigh wave is a function of frequency and this dependency is strictly related

to the mechanical parameters of the medium. Hence if the dispersion curve (i.e. the relationship phase velocity vs. frequency) is measured experimentally, it is in principle possible to get from it the mechanical parameters of the medium.

The implementation of the above concept requires essentially three separate steps: in field testing an arbitrary characteristic of particle motion associated to wave propagation is experimentally measured; subsequently a signal analysis procedure is applied to extract from the records the experimental dispersion curve; finally using an inversion algorithm based on an appropriate model, the mechanical properties of the soil are obtained.

The present research has been focused mainly on the first two steps, working on field test configuration and experimental dispersion curve evaluation.

In current SASW practice, the dispersion curve is obtained using a two-receiver test configuration and spectral analysis tools to get the frequency dependent time delay from the difference in phase of the two signals. Such procedure, although simple and easily implemented, has certain drawbacks.

The use of only a pair of receivers leads to the necessity of performing the test using several testing configuration and the so-called common receiver midpoint geometry. This results in a quite time-consuming procedure on site for the collection of all the necessary data.

Once the raw data are obtained on site, the evaluation of the experimental dispersion curve has to be done back in the office and requires the expertise of the operator, since many non-trivial choices need to be made based on data quality and testing configuration. In this respect the main obstacle to automation of the process is the requirement for phase unwrapping, that is often a ticklish task. So the dispersion curve evaluation from field data is very time-consuming and moreover it introduces a high degree of uncertainty.

Starting from the usual practice of SASW, the present research is an attempt to give answer to two different important questions:

- ✓ Can multistation testing configurations be profitably used for geotechnical characterization and which advantages can they give compared to the classical SASW test?
- ✓ Is it possible to get more than the stiffness profile from surface waves analysis?

The first aspect has been analysed using, as a starting point, the multistation methods (well known in geophysics) and the knowledge about 2D transforms. Such methods have to be translated to the scale of interest of geotechnical engineering. Since the change of scale has very important consequences on Rayleigh wave propagation, the use of such methods needs to be accurately investigated using both numerical simulations and experimental tests on site.

As far as the second point is concerned, the possibility of obtaining from

surface wave testing not only the stiffness profile but also the damping ratio profile has been explored during the last years at the Georgia Institute of Technology (Spang 1996, Lai 1998, Rix et al. 1999b). Such researches emphasise the necessity of simultaneously collect and analyse data and hence the need for a consistent experimental procedure.

1.3 Dissertation Outline

The dissertation has been organised in two different blocks. The first part is methodological: it tries to give an insight into the characteristic of surface waves in soil deposits and their use for site characterization. The remaining part presents some applications of the methods and the relative conclusions.

More in detail, in Chapter 2 the models used to reproduce soil behaviour at very small strain and a brief summary of wave propagation theory are presented. Chapter 3 is entirely devoted to Rayleigh waves, which are the type of surface waves more widely used for characterisation problems. In particular the essential features of Rayleigh waves propagation in homogeneous and layered either linear elastic or linear viscoelastic media are presented from a theoretical point of view and then some application are reported regarding both numerical simulations and experimental data.

In Chapter 4 an overview of the methods currently used in practice and newly proposed for soil characterization using surface waves is presented. Particular emphasis has been posed on the following methods: the SASW method that can be considered the current state of practice in geotechnical engineering; the new transfer function approach that is proposed for the simultaneous measurement of soil stiffness and damping profiles; the multistation methods based on frequency-wavenumber and frequency-slowness analysis, which are considered a good alternative to the conventional SASW test.

Chapter 5 reports some simulations of actual tests that have been conducted using synthetic seismograms to check the effectiveness of multistation methods in comparison with the SASW method. In particular the purpose of the simulation was to assess the results that can be expected from the application on a geotechnical scale of the multistation methods that are successfully applied on a geophysical scale. To generalise the results, the comparison has been made considering three different hypothetical profiles to cover both normally dispersive and inversely dispersive cases.

Chapter 6 presents the testing sites and the field equipment that have been used for the experimental testing, which results are reported in Chapter 7. In

particular the testing program was divided in two parts: the tests conducted using impact sources with multichannel acquisition of data and the tests conducted with a controlled harmonic source to get both stiffness and damping profiles.

Finally in Chapter 8 some comments and conclusions are summarised, together with the indication of some specific topics, about which some further research efforts are needed in the future.

Appendix A reports some basic aspects of the signal processing tools that have been used in this research.

Chapter 2

Dynamic properties of soils and wave propagation

The dynamic behaviour of soils is very important for different problems belonging to the classes of foundation vibrations and earthquake engineering. The need of specific characterization tools has brought to many different procedures for experimental soil mechanics both in laboratory and in situ.

As in every problem related to the mechanics of materials, the first important step for the global modelling of a general phenomenon is the assessment of the specific experimental behaviour and the search for an appropriate model that has to be at the same time accurate and manageable.

The case of soils is particularly complex if compared to other construction materials because of the inherent characteristic of being a natural material, in comparison to man-made materials.

As for many other materials the mechanical behaviour of soil is strongly dependent on the magnitude of strains that are developed for each type of problem. A linear model can be appropriate at very small strains but as deformation increases the behaviour becomes strongly non-linear.

Usually many dynamic problems, such as vibrations, imply small strains and this can be really of great help for modelling, since simple models can work quite well.

Quite often, to simplify the modelling process in presence of large strains, equivalent linear models are considered. In this case the mechanical properties can be derived by the small strain ones using appropriate decaying laws.

For dynamic problems, the response of soils to an external perturbation is not

only related to its stiffness, but also to its damping properties, so that a viscous component is usually introduced to account for dissipation mechanisms.

In this chapter a concise review of experimental soil behaviour and of related models is presented. It is important to point out that the attention is focused on the phenomenological aspect of the behaviour, i.e. to the macroscopic relation between causes and effects, with no attempt of going into the microscopic scale where the mechanisms that effectively determinate the behaviour take place.

Once such framework, which is necessary to describe the soil behaviour, has been established, the relationships between waves and mechanical parameters will be considered.

2.1 Experimental behaviour of soils

Many factors have a strong influence on soil behaviour. Most of them have been extensively studied using several kinds of laboratory and in situ tests. They can be roughly divided in external factors and specific soil properties. One of the most important external factors is the strain magnitude. The behaviour of soils at different strain levels has been the object of many experimental investigations, especially in laboratory where the testing condition can be fully controlled. Based on these results, some conventional threshold values have been set: they separate strain ranges for which a different phenomenological behaviour can be assigned to the soil. The main interest in this respect is obviously related to the choice of an appropriate model to predict soil behaviour at different strain levels.

For static loads, the soil behaviour can be modelled for increasing strain magnitude respectively as linear elastic, non-linear elastic, non-linear elasto-plastic or perfectly plastic medium. Some efforts have been recently made to implement new mechanical models able to catch all the essential features of soil behaviour (e.g. hypo-plastic models).

For the description of soil dynamic behaviour, the dissipative phenomena that take place also at very low cyclic shear strains in soils must be taken in consideration. By its definition, an elastic model is not able to describe energy dissipation and hence different models, as for example a visco-elastic one must be used.

Some important features of soil behaviour are reported in the following for the different intervals of cyclic shear strains (Vucetic 1994).

For very small shear strains the soil behaves essentially as a linear medium. Usually the associated threshold shear strain is defined with respect to the decay of the shear stiffness modulus G. Indeed, if a secant modulus is defined for each shear

strain considering an equivalent linear elastic model, a decaying curve can be obtained for the ratio between the secant modulus and the initial (tangent) one. The linear threshold strain γ_{tl} is then defined as the shear strain such that the ratio G_s/G_0 is equal to 0.99. Clearly for this first zone there is no decaying of the stiffness and a linear elastic model would appropriately model the soil response. Nevertheless it must be noted that energy dissipation take place as it is confirmed by Figure 2.1 that shows an hysteretic loop at very small strains for which the area is not null and hence there is dissipation. Thus a linear-viscoelastic model is more appropriate for cases where energy dissipation is of interest (basically dynamic excitations).

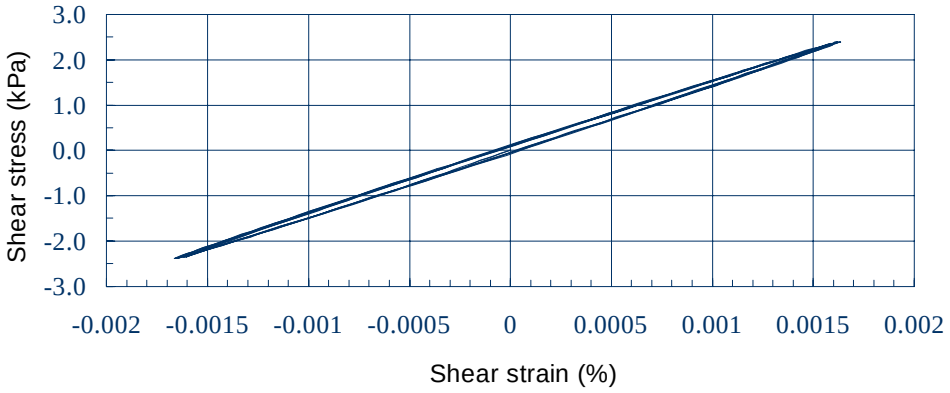

Figure 2.1 Hysteretic loop from testing in a resonant column device (Noto clay, frequency 1Hz) (after Lai et al. 1999)

The small strain range is comprised between γ_{tl} and the volumetric threshold shear strain γ_{tv}. In this range the stiffness degradation is not very large and the soil behaviour is non-linear, but permanent changes in the microstructure are absent or negligible. Also in this case an elastic or viscoelastic model, depending on the applications, can give a good approximation of the material response to cyclic loads.

The name volumetric threshold shear strain indicates that above this strain level the permanent change in the soil microstructure under cyclic loads cause a permanent variation of volume in drained conditions or an increase of excess pore water pressure in undrained conditions (Figure 2.2). Clearly such conditions are far from the ones of elastic models and hence a plastic component need to be

introduced, switching to elasto-plastic or visco-elasto-plastic models.

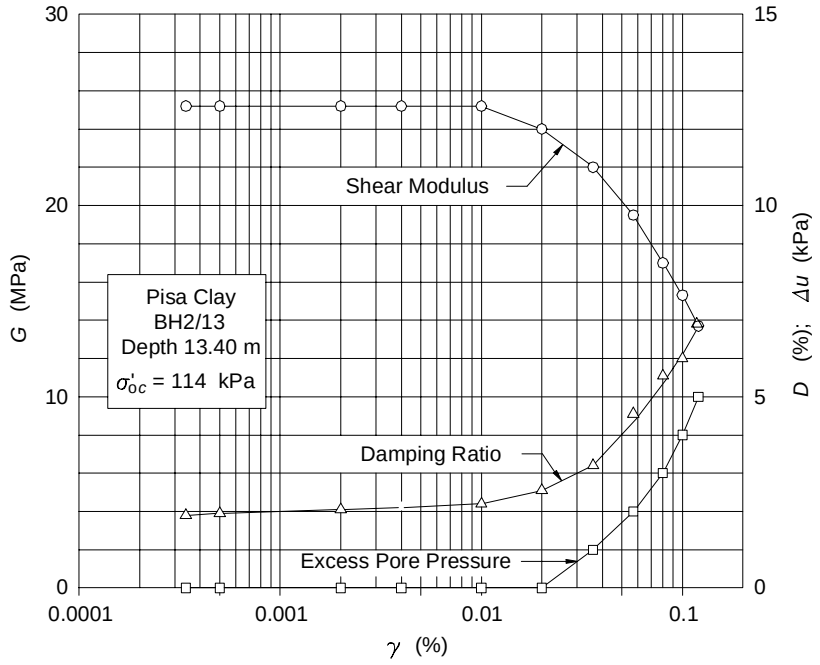

Figure 2.2 Effects of shear strain on the soil parameters (after Lancellotta 1993)

Then the degradation of material properties continues up to reach the failure condition, at which level residual values of stiffness are present and the material behaves as perfectly plastic.

The increase of strains produces not only stiffness degradation, but also an increase of the internal disorder in the material and hence an increase of the dissipative properties, as it is shown in Figure 2.2 in terms of material damping. This last quantity is defined in relation to the area included in a hysteretic loop (see Paragraph 2.3.3).

A complete relationship between stiffness and strain, as those shown in Figure 2.3, can be obtained only through laboratory testing. An interesting possibility for modelling soil non-linearity is constituted by the association of a direct measurement of the initial shear stiffness, for example through in situ seismic techniques, and the use of decaying curves to get the equivalent linear parameters

for the whole range of strains.

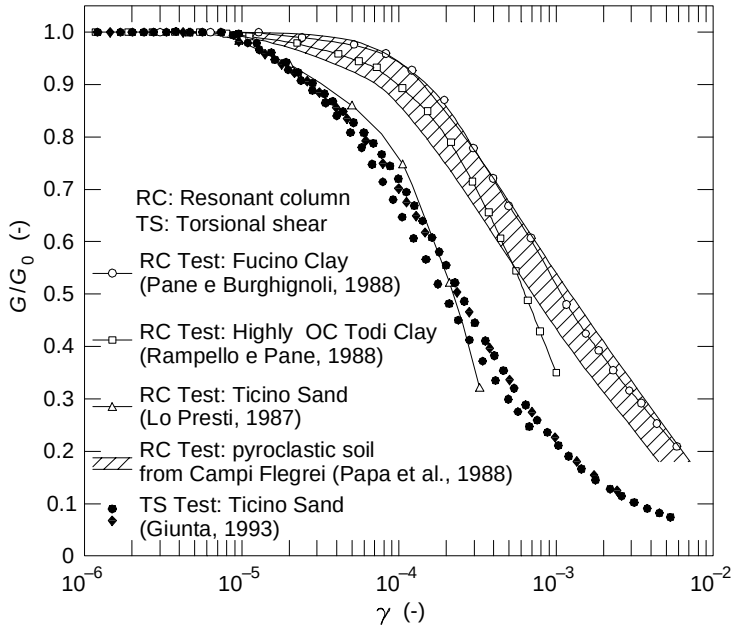

Figure 2.3 Degradation of Stiffness from laboratory tests (from Lancellotta and Calavera 1999)

2.2 Modelling soil behaviour at very small strain

As shown above soil behaviour is strongly influenced by the magnitude of strains involved in the process. Seismic methods for soil characterization involve very small strains and hence the description of appropriate models for soil will be in the following restricted to the ones used in such range of strains.

Mainly two different models are used to represent soil behaviour at very low strain: linear elasticity and linear visco-elasticity. Also if the first one violates the experimental evidence of energy dissipation, it is still used in many cases for its simplicity.

2.2.1 Linear Elasticity

Elastic media do not show any energy dissipation and are characterised by a bi-univocal correspondence between stress σ and strain ε. Considering the inherent tensor nature of these two quantities, such relationship can be written in index notation as:

$$\sigma_{ij} = a_{ijkl} \cdot \varepsilon_{kl} \tag{2.1}$$

where $\boldsymbol{a}$ is a 4th order tensor. Considering the symmetry of stress and strain tensors and the existence of an elastic potential, the number of the independent constants, that define the tensor $\boldsymbol{a}$, reduces from 81 to 21.

The above relationship is valid for a generally anisotropic medium. Some assumptions on the isotropy of the medium can further reduce the number of constants. For example for a transversely isotropic medium, that can be a good approximation of soil behaviour in many cases, the number of independent elastic constants reduces to 5.

If the hypothesis of complete isotropy is assumed, the number of independent constants further reduces to 2, and the above Equation 2.1 can be rewritten as:

$$\sigma_{ij} = \lambda \cdot \varepsilon_{kk} \cdot \delta_{ij} + 2\mu \cdot \varepsilon_{ij} \tag{2.2}$$

where δ_{ij} is the Kronecker delta function and the two elastic constants are λ and μ (known as Lamé's parameters).

Under some special loading condition, it can be useful to express the stress-strain relationship using other definition of the elastic constants, such as for example the Young's modulus E, the Poisson's ratio ν or the bulk modulus K (see Table 2.1). Table 2.2 reports a summary of the most widely used pairs of parameters with the relative cross relationships.

Anisotropy is also an important issue but it will not be addressed in this thesis. Nevertheless it is important to remark that, as seen above, it strongly increases the number of parameter that need to be taken in account for the characterization of a medium. Usually soils are strongly anisotropic media, but the problem of assessing this feature is still widely open, especially for what concerns in situ testing.

Table 2.1 Definition of elastic constants

Name	Symbol	Definition	Notes
Young's modulus	E	$\frac{\text{longitudinal stress}}{\text{longitudinal strain}}$	Free transversal deformation
Shear modulus	G	$\frac{\text{shear stress}}{\text{shear strain}}$	
Poisson's ratio	ν	$\frac{\text{longitudinal strain}}{\text{transversal strain}}$	Free transversal deformation
Bulk modulus	K	$\frac{\text{idrostatic pressure}}{\text{volumetric strain}}$	

Table 2.2 Relationship between elastic constants

	λ, μ	***G, ν***	***E, ν***	***K, G***
λ	λ	$\frac{2G\nu}{1-2\nu}$	$\frac{\nu E}{(1+\nu)(1-2\nu)}$	$K-\frac{2}{3}G$
μ≡G	μ	G	$\frac{E}{2(1+\nu)}$	G
K	$\frac{(3\lambda+2\mu)}{3}$	$\frac{2G(1+\nu)}{3(1-2\nu)}$	$\frac{E}{3(1-2\nu)}$	K
E	$\frac{\mu(3\lambda+2\mu)}{\lambda+\mu}$	$2(1+\nu)G$	E	$\frac{9KG}{3K+G}$
ν	$\frac{\lambda}{2(\lambda+\mu)}$	ν	ν	$\frac{3K-2G}{2(3K+G)}$

2.2.2 Linear Visco-Elasticity

Visco-elastic models are those in which the elastic behaviour is coupled with some viscous component that produces energy dissipation. This feature can lead to the possibility of modelling more appropriately soil behaviour at very small strain

allowing for energy dissipation.

Since in a viscous medium the energy dissipation is related to the time derivative of strain, the relationship between stress and strain is not anymore algebraic as in the elastic case but it is integro-differential.

The simplest viscoelastic model is composed by an elastic spring coupled with a viscous dashpot. The coupling can be either in series (Maxwell model) or in parallel (Kelvin-Voigt model). Anyway such a simple model is not able to catch all the essential features of soil behaviour.

The generalisation of such models leads to the analogous of Equation 2.1, that in this case is a linear integral functional (Christensen 1971):

$$\sigma_{ij} = \int_{-\infty}^{t} G_{ijkl}(t-\tau)\frac{d\varepsilon_{kl}(\tau)}{d\tau}d\tau \tag{2.3}$$

where **G** is a 4th order tensor-valued function called the relaxation function. In analogy to the elastic case, for a isotropic linear visco-elastic material, the number of independent component reduces to 2, say the shear and bulk relaxation functions ($G_S(t)$ and $G_B(t)$). From a physical point of view the relaxation function represents the stress response in time when a unit Heaviside step function strain is applied (respectively in terms of shear or bulk stress and strain) (see Figure 2.4).

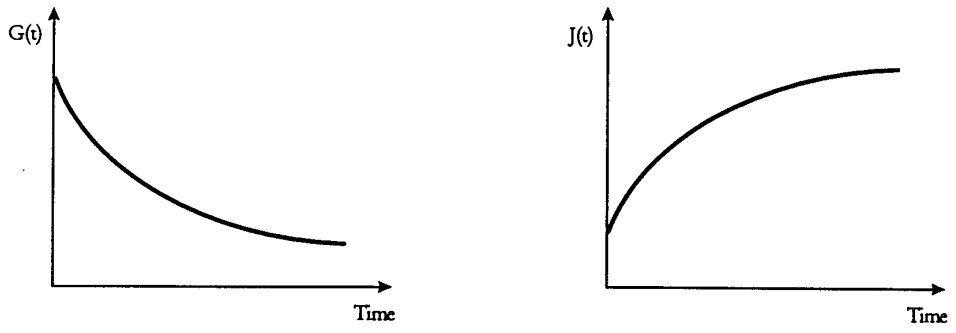

Figure 2.4 Typical shape of relaxation [G(t)] and creep [J(t)] functions for a viscoelastic solid (from Lai 1998)

By inverting Equation 2.3, it is possible to write the relationship that links the strains to the stresses in an integro-differential form. In this case the 4th order tensor-valued function will be the creep function and the particularisation to linear isotropic media leads to a couple of functions, say the shear and bulk creep

functions ($J_S(t)$ and $J_B(t)$). Also in this case an analogous physical interpretation can be given in terms of strain response to an applied unit step function stress (see Figure 2.4).

The application of linear visco-elasticity appears to be very complex considering the integral relationships that are involved. Nevertheless using the Fourier transform it is possible to show that the solutions to boundary value problems for viscoelastic media can be borrowed from linear elasticity using the correspondence principle. According to this principle, for time-invariant harmonic boundary conditions the solution can be obtained from the solution of the elastic problem substituting the viscoelastic complex-valued moduli to the elastic real-valued moduli. Since any arbitrary boundary condition can be seen as the superposition of harmonic boundary condition through the Fourier analysis, the solution relative to the harmonic boundary conditions can be used with the Fourier synthesis to get the solution of the general problem.

The general expression for the complex-valued viscoelastic tensor modulus can be found considering a harmonic in time strain or stress history (Lai 1998). If the former is considered, the prescribed strain can be written as:

$$\varepsilon_{kl}(t) = \varepsilon_{0_{kl}} \cdot e^{i\omega t} \tag{2.4}$$

Under this assumption, Equation 2.3 becomes an algebraic equation that links stress and strain through a complex-valued frequency dependent tensor modulus $G^*_{ijkl}(\omega)$:

$$\sigma_{ij}(t) = G^*_{ijkl}(\omega) \cdot \varepsilon_{0_{kl}} \cdot e^{i\omega t} \tag{2.5}$$

with

$$\begin{aligned} \mathrm{Re}(G^*_{ijkl}(\omega)) &= G_{(e)\,ijkl} + \omega \cdot \int_0^\infty G_{ijkl}(\tau) \cdot \sin\omega\tau \cdot d\tau \\ \mathrm{Im}(G^*_{ijkl}(\omega)) &= \omega \cdot \int_0^\infty G_{ijkl}(\tau) \cdot \cos\omega\tau \cdot d\tau \end{aligned} \tag{2.6}$$

Note that the complex tensor modulus is a function of frequency and that the real and imaginary components are linked each other.

Analogous relationships can be found for the creep function when a harmonic in time stress history is imposed.

Again, the particularisation of the general case to the homogeneous isotropic linear-viscoelastic medium leads to the introduction of a pair of independent

complex-valued moduli, say the complex shear and bulk moduli.

2.3 Waves

The effect of a sharply applied, localised disturbance in a physical medium rapidly spreads over in space, this is commonly addressed as wave propagation (Graff 1975). Analogously a wave is defined as a disturbance that travels in the medium and carries energy (Doyle 1995). Many techniques for soil characterization at very small strain levels are based on measurements of particle motions associated to wave propagation. This is made possible by the strong link existing between wave propagation characteristics and the mechanical parameters of the body, which is interested by the phenomenon.

2.3.1 Waves in linear elastic media

Since at very small strain the soil doesn't show any degradation of stiffness both with strain level and with cycles of loading and unloading, the linear elastic model is considered a good approximation of its behaviour when the dissipative cyclic behaviour is not of interest. Moreover the simplicity of the elastic model can be profitably used to clarify the relation between wave propagation and stiffness of the medium.

The indefinite equilibrium equation can be written in index notation as:

$$\sigma_{ij,j} + \rho \cdot f_i = \rho \cdot \ddot{u}_i \tag{2.7}$$

where σ_{ij} is the stress tensor, u_i is the displacement vector of a material point, ρ is the mass density per unit volume and f_i is the body force per unit mass.

Considering a homogeneous isotropic linear elastic medium and using the Lamé's parameters λ and $\mu \left(\equiv G\right)$ to describe its behaviour, the relationship between stress and strain is expressed by Equation 2.2. Recalling that the small strain tensor is given by:

$$\varepsilon_{ij} = \frac{1}{2}\left(u_{i,j} + u_{j,i}\right) \tag{2.8}$$

and substituting into 2.7, after some manipulations it is possible to obtain the Navier's equations for the indefinite medium:

$$(\lambda + \mu) \cdot u_{j,ji} + \mu \cdot u_{i,jj} + \rho \cdot f_i = \rho \cdot \ddot{u}_i \tag{2.9}$$

or in vector notation:

$$(\lambda + \mu)\nabla\nabla \cdot \mathbf{u} + \mu\nabla^2\mathbf{u} + \rho\mathbf{f} = \rho\ddot{\mathbf{u}} \tag{2.10}$$

The Navier's equations are quite complex and they appear to be very hermetic from a physical point of view. A simpler set of equations can be obtained applying Helmholtz's theorem, which allows the decomposition of a vector field into the gradient of a scalar and the curl of a zero divergence vector (Graf 1975). Hence the displacements can be expressed introducing the scalar and vector potentials Φ and $\mathbf{H}$ such that:

$$\mathbf{u} = \nabla\Phi + \nabla \times \mathbf{H}, \qquad \nabla \cdot \mathbf{H} = 0 \tag{2.11}$$

Note that the condition $\nabla \cdot \mathbf{H} = 0$ gives the necessary constraint to allow for the determination of the three components of $\mathbf{u}$ from the four components of the couple $\Phi, \mathbf{H}$.

Also the body force vector can be decomposed analogously:

$$\mathbf{f} = \nabla f + \nabla \times \mathbf{B}, \qquad \nabla \cdot \mathbf{B} = 0 \tag{2.12}$$

Substituting 2.11 and 2.12 into 2.10 and rearranging it is possible to get:

$$\nabla\left[(\lambda + 2\mu)\nabla^2\Phi + \rho \cdot f - \rho \cdot \ddot{\Phi}\right] + \nabla \times \left(\mu\nabla^2\mathbf{H} + \rho \cdot \mathbf{B} - \rho \cdot \ddot{\mathbf{H}}\right) = 0 \tag{2.13}$$

and this equation can be satisfied only if both bracketed terms vanish.

In absence of body forces four wave equations are obtained from 2.13:

$$\begin{aligned} (\lambda + 2\mu)\nabla^2\Phi &= \rho \cdot \ddot{\Phi} \\ \mu\nabla^2\mathbf{H} &= \rho \cdot \ddot{\mathbf{H}} \end{aligned} \tag{2.14}$$

The four equations above can be solved separately, imposing the relevant boundary conditions, and then the solution can be obtained by summing the displacements.

It can be shown that the first equation of 2.14 (the scalar one) correspond to the propagation of longitudinal waves (also known as compression or dilatational or irrotational or Primary, since they constitute the first arrival in seismic records). The other three scalar equations of 2.14 (corresponding to the vector equation) are relative to the propagation of shear waves (also named distorsional or rotational or equivoluminal or Secondary, since they constitute the second arrival in seismic records).

It is important to remark that a fundamental hypothesis for the application of

Helmholtz's decomposition is the isotropy of the medium. In anisotropic media the decomposition of the displacement field in a dilatational component and a distorsional component, each one independent of from the other, is not anymore possible.

The velocities of Primary and Secondary waves can be obtained from the wave equations 2.14:

$$V_P = \sqrt{\frac{l + 2m}{r}} \tag{2.15}$$

$$V_S = \sqrt{\frac{m}{r}} \tag{2.16}$$

The ratio between the two body wave velocities can be expressed as a function of the Poisson Ratio alone:

$$g = \frac{V_S}{V_P} = \sqrt{\frac{m}{l + 2m}} = \sqrt{\frac{1 - 2u}{2(1 - u)}} \tag{2.17}$$

hence, since for real media $0 \le n \le 0.5$, the longitudinal wave travels always faster than the shear one ($V_P > V_S$), thereby justifying the names Primary and Secondary waves.

The above waves are often called body waves, because they travel in the interior of a medium. In contrast there are the so-called surface waves, that travel in a very shallow zone close to the free surface of an halfspace. They are essentially of two different kinds: Rayleigh waves (which will be extensively treated in Chapter 3) and Love waves. The latter ones can exist only in presence of a waveguide, i.e. of a softer superficial layer above stiffer materials, and can be seen as generated by multiple reflections of energy trapped in this layer. Their existence was shown by Love in 1911 and the particle motion associated to them is transversal with respect to the direction of propagation.

A representation of the particle motion associated to the propagation of body and surface waves is reported in Figure 2.5.

Another class of waves is the one of the interface waves, among which the most important are Stoneley waves, also known as generalised Rayleigh waves. These waves travel across a mechanical impedance (i.e. rV) discontinuity and they rapidly attenuate going away from the interface. It can be shown that such waves can exist only for given values of the ratio between stiffness properties of the two adjacent layers (Graf 1975).

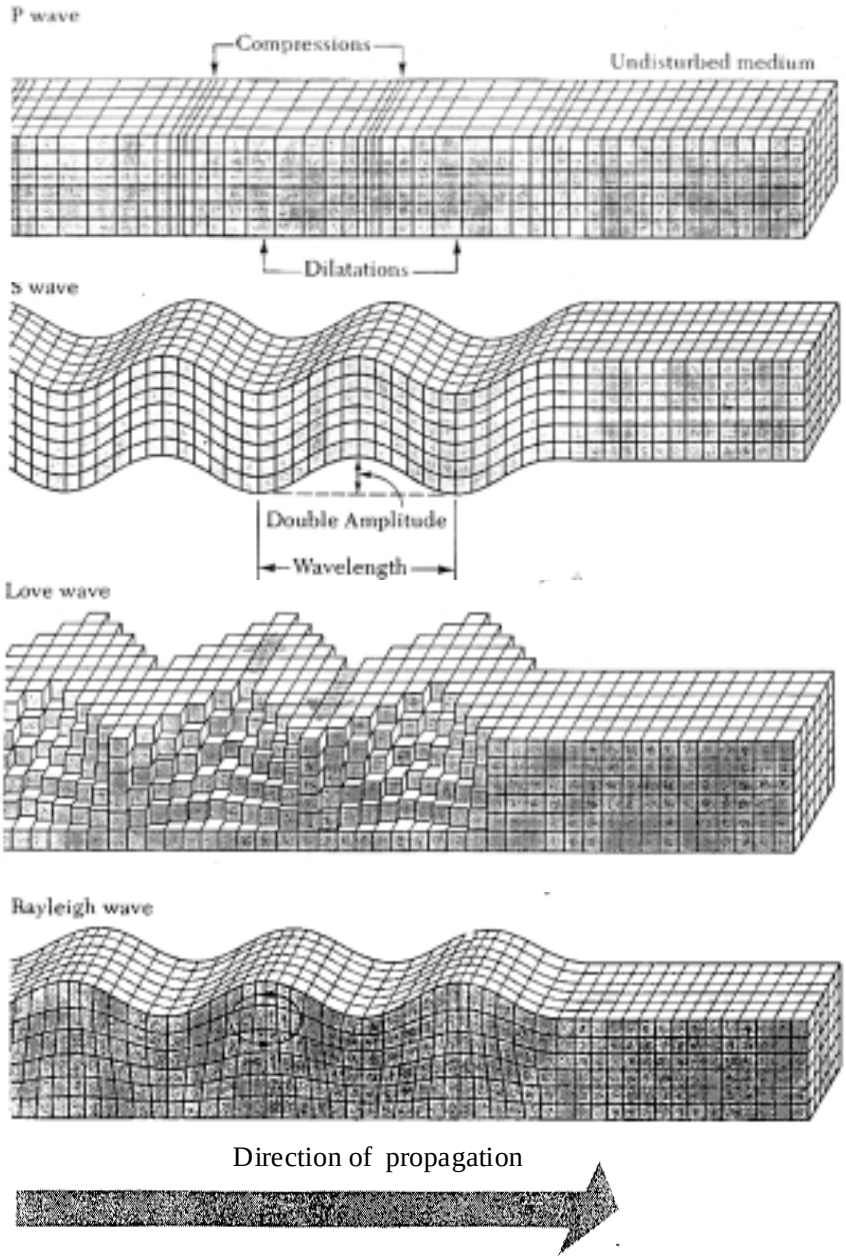

Figure 2.5 Particle motion associated to body and surface waves propagation (from Bolt 1976)

Consider now the specialisation of the wave equation for the case of the mono-dimensional propagation along direction x (the case of a shear wave will be taken as example):

$$\frac{\partial^2 u}{\partial x^2} = \frac{1}{V_S^2}\frac{\partial^2 u}{\partial t^2} \tag{2.18}$$

If a harmonic in time solution is assumed in the form:

$$u = f(x)e^{-i\omega t} \tag{2.19}$$

and plugged in 2.18, a ordinary differential equation is obtained:

$$\frac{d^2 f(x)}{dx^2} + \frac{\omega^2}{V_S^2} f(x) = 0 \tag{2.20}$$

which solution $f(x)$ is also harmonic and combined with 2.19, after some manipulation, gives the general solution for a harmonic wave propagating in the positive x direction:

$$u(x,t) = A \cdot e^{i(kx-\omega t)} \tag{2.21}$$

where A represents the amplitude of the wave and the argument of the complex exponential its phase ϕ. The wavenumber k is given by ω / V_S.

Rewriting the phase in the following form:

$$\phi = (kx - \omega t) = k(x - V_S \cdot t) \tag{2.22}$$

it is clear that V_S represents the phase velocity of the wave. Note that the harmonic wave has infinite length and hence it has no wavefront, so only considering its phase a velocity can be assigned to the wave (Graf 1975).

The distance between to successive points in space having equal phase is referred as the wavelength and it is related to the wavenumber by the relationship: $\lambda = 2\pi / k$.

The other relevant quantities that are used to describe the wave motion are the period T and its inverse the frequency f, which is related to the circular frequency ω by the relation: $\omega = 2\pi f$.

Since the above definitions are recurrent in the dissertation, a summary is reported in Table 2.3, together with the relative dimensions.

Table 2.3 Definition of wave characteristics

A	Amplitude	
ω	Circular frequency	[radians/time]
f	Frequency	[cycles/time]
λ	Wavelength	[length]
k	Wavenumber	[1/length]
V	Phase velocity	[length/time]
T	Period	[time]

2.3.2 Waves in linear viscoelastic media

If the dissipative behaviour shown by soils also at very low strain levels (see Paragraph 2.1) is of interest, the linear elastic constitutive model is no more sufficient. In this case a linear visco-elastic model (Paragraph 2.2.2) can be a good approximation of the soil behaviour. The use of viscoelasticity in conjunction with the causality principle leads to the so-called material dispersion, i.e. the phase velocity can no longer be considered independent on frequency (Aki and Richards 1980).

Starting from the indefinite equilibrium (Equation 2.7), the use of a viscoelastic model would lead to a complicate general equation, since in this case a set of integro-differential equations links stress and strain tensors (Equation 2.3).

According to the correspondence principle of linear viscoelasticity, the wave equations for linear viscoelastic media can be obtained from the elastic ones substituting the complex-valued viscoelastic moduli to the real-valued elastic ones. Recalling Paragraph 2.2.2 it must be remarked that the above sentence is applicable to the harmonic case and the extension to general cases can be done through the Fourier synthesis. Following an alternative procedure, the correspondence principle is also applicable directly to the general case using the Laplace Transform.

The insertion of complex moduli in the relationships that define the body waves velocity (Equations 2.15 and 2.16) leads to complex-valued velocities of propagation to be inserted in the harmonic expression of Helmoltz's Equations (2.14).

The general solution for longitudinal or shear wave propagation is formally the same, with the only change due to the substitution of the complex valued phase velocity. Taking for example the solution relative to one-dimensional shear wave propagation (Equation 2.21), the corresponding solution in the linear viscoelastic case can be written as:

$$u(x,t) = u_0 \cdot e^{i\left(\frac{\omega}{V_S^*}x - \omega t\right)} \tag{2.23}$$

where u_0 is a constant to be evaluated using the boundary conditions.

In analogy to the elastic case the factor ω / V_S^* is the complex wavenumber associated to the wave propagation. Considering the real and imaginary part of the complex velocity of propagation, it can be useful to rewrite the displacement field associated to wave propagation (Equation 2.23) as follows:

$$u(x,t) = A \cdot e^{\omega \cdot \mathrm{Im}\left(\frac{1}{V_S^*}\right)x} e^{i\left(\omega \cdot \mathrm{Re}\left(\frac{1}{V_S^*}\right)x - \omega t\right)} \tag{2.24}$$

from which it is clear that while the real part of the complex wavenumber is related to the velocity of propagation of the wave but not to its amplitude, the imaginary part is related to the attenuation in space of the amplitude of the perturbation, because of the dissipative phenomena due to the viscous component. Hence, using an approximation, the complex wavenumber can be rewritten as the sum of a real wavenumber, associated to the real phase velocity that characterise the propagation, and a real attenuation coefficient α_S, that measures the spatial amplitude decay as the wave propagates in the viscoelastic medium:

$$k_S^* = \frac{\omega}{V_S^*} = \frac{\omega}{V_S} + i\alpha_S \tag{2.25}$$

The phase velocity and the attenuation coefficient can be explicitly written as a function of mass density ρ and complex shear modulus G_S^*, and since the latter one is in general frequency dependent also the phase velocity and the attenuation factor will be in general frequency dependent (Lai 1998):

$$\begin{aligned} V_S(\omega) &= \left[\mathrm{Re}\left(\sqrt{\frac{\rho}{G_S^*}}\right)\right]^{-1} \\ \alpha_S(\omega) &= \omega \cdot \mathrm{Im}\left(\sqrt{\frac{\rho}{G_S^*}}\right) \end{aligned} \tag{2.26}$$

The frequency dependency of phase velocity caused by the inherent nature of the viscoelastic model is generally addressed as material dispersion, in contrast to geometrical dispersion that arise as a consequence of the medium heterogeneity (see Chapter 3). In presence of a dispersive behaviour the shape of a general

waveform change as the wave propagates, because the different component of the Fuorier transform of the pulse travel with different velocities (Aki and Richards 1980).

It is also important to remark the close link existing between phase velocity and attenuation coefficient. Indeed this is a consequence of the interdependence between real and imaginary component of the complex modulus G_S^* (see Equation 2.6) (Lai 1998).

The case of the longitudinal wave is formally analogous and will not be explicitly reported.

2.3.3 Waves and characterization

The use of wave propagation for the determination of stiffness properties of a medium is well established in the practice of material characterization in general. The classical basis in this regards are constituted by the elastic case, in which once the velocity of propagation of a given kind of body waves is determined, the stiffness can be directly determined using relationships such as 2.15 or 2.16.

In the field of geotechnical engineering the methods based on the measurements of wave propagation are generally addressed as seismic methods. A variety of methods for in situ and laboratory tests have been established in the past to determine stiffness at very small strain levels using body wave propagation (Kramer 1996).

Cross-Hole and Down-Hole methods (see Chapter 6) are fully part of the standard of practice for in situ testing, while the use of piezoelectric bender elements in laboratory apparatuses has widely spread out in the last years.

Other in situ methods are seismic cone (that is an extension of the down-hole or cross-hole methods with the use of respectively one or two special CPT probes) and P-S well logging (in which an instrumented probe is lowered in a single borehole and it acts both as generator and receiver of body waves). More widely used for geophysical purposes, but still useful in some cases for geotechnical applications are seismic reflection and refraction methods (see Chapter 6).

The use of wave propagation for the determination of dissipation characteristic of a medium is less widely adopted, but still very promising (see Paragraph 4.4 for some indications on proposed methods). In this case the interest is focused on the decay in space of the propagating wave.

In geotechnical engineering, the dissipative characteristic of a medium are typically expressed in terms of damping ratio, that can be defined with reference to a stress-strain loop at a given frequency, as:

$$D(\omega) = \frac{1}{4\pi}\frac{\Delta W(\omega)}{W(\omega)} \tag{2.27}$$

(see Figure 2.6 for the definition of the above quantities).

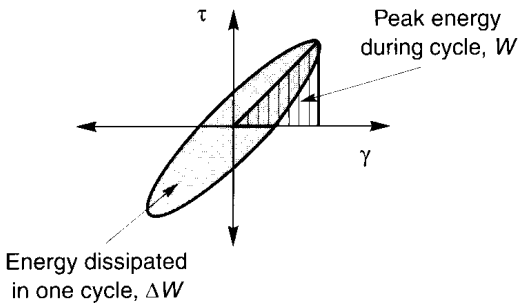

Figure 2.6 Definition of damping ratio from a hysteretic loop

Also seismologists use a dimensionless definition of energy dissipation, the quality factor Q (Aki and Richards 1980), that is related to the damping ratio by the relationship:

$$Q(\omega) \approx \frac{1}{2D(\omega)} \tag{2.28}$$

Both D and Q must be defined for shear and longitudinal waves independently. It is commonly observed that the shear damping ratio is higher than the longitudinal damping ratio (Herrmann 1986).

It must be noted that the determination of the damping ratio directly from the definition can be pursued only in special experiments. More often it is measured indirectly by the temporal decay of amplitude or by the spatial decay of amplitude of a propagating wave (Aki and Richards 1980).

Both methods are founded on the observation that for a medium with linear stress-strain relationship, the wave amplitude is proportional to the square root of energy and hence the damping ratio can be expressed also as:

$$D(\omega) = \frac{1}{2\pi}\frac{\Delta A}{A} \tag{2.29}$$

Under the assumption that the direction of propagation x coincides with the

direction of maximum attenuation, the spatial variation of amplitude is given by:

$$A(x) = A_0 \cdot e^{-\frac{\omega x}{2VQ}} = A_0 \cdot e^{-\alpha x} \tag{2.30}$$

where A_0 is the amplitude at $x = 0$, ω is the circular frequency, V the phase velocity and α is defined as the attenuation coefficient. From Equation 2.30 the relationship between the attenuation coefficient, that can be under certain condition measured experimentally, and the damping ratio, that is the objective of the measurement, can be extracted:

$$D = \frac{\alpha V}{\omega} \tag{2.31}$$

It is important to distinguish geometrical attenuation, due to the spreading of energy over wider and wider extension of the wavefront as the wave moves away from the source (see Paragraph 3.2.1 and in particular Equation 3.8), from material attenuation, due to dissipative characteristic of the medium. Other kinds of energy dissipation, such as for example scattering of energy between interfaces, often interfere with the two above and they can make the use of wave propagation for material damping determination less accurate.

The determination of stiffness and damping characteristics of the medium with the above methods is totally uncoupled. Nevertheless it has been seen that linear viscoelasticity can be considered from many point of view appropriate for modelling the dynamic behaviour of soil at very small strains. Moreover as shown in Paragraph 2.3.2, in a linear viscoelastic medium, phase velocity and attenuation coefficient of body waves are linked each other. It derives the necessity of developing new testing procedures to simultaneously determine stiffness and damping as required for coherence to the framework of linear viscoelasticity. A procedure for laboratory coupled measurements has been recently proposed by Lai et al. (1999).

Chapter 3

Rayleigh Waves

3.1 Overview

Waves that propagate in a medium can be roughly divided into two main categories: body waves and surface waves. Surface waves are generated only in presence of a free boundary and they can be essentially of two types: Love waves and Rayleigh waves. Love waves can exist only in presence of a soft superficial layer over a stiffer halfspace and they are produced by energy trapping in the softer layer for multiple reflections. Rayleigh waves are always generated when a free surface exists in a continuous body.

John Strutt Lord of Rayleigh firstly introduced them as solution of the free vibration problem for an elastic halfspace in 1885 ("On waves propagated along the plane surface of an elastic solid"). In the last sentences of the above paper, he anticipated the importance that such kind of wave could have in earthquake tremor transmission. Indeed the introduction of surface waves was preceded by some seismic observations that couldn't be explained using only body wave theory, which was well known at that time. First of all the nature of the major tremor was not clear, because the first arrivals were a couple of minor tremors corresponding to P and S waves respectively. The greater amount of energy associated to this late tremor if compared to that of body wave was a strong evidence of less attenuation passing through the same medium and this could be explained only assuming that this further kind of wave was essentially confined to the surface (Graff 1975).

Another main contribution regarding the forced vibrations was successively

given by Horace Lamb ("On the propagation of tremors over the surface of an elastic solid", 1904), who solved the problem of a point harmonic force acting on the ground surface. He also proposed the solution for the case of a general pulse, by using the Fourier synthesis concept.

Usefulness of surface waves for characterization problems has been soon clear due to some important features and especially to the possibility of detecting them from the surface of a solid, with strong implications on non-invasive techniques development (Viktorov 1967).

In this chapter an overview will be given about specific properties of Rayleigh waves, with special aim at soil characterization purposes, leaving more comprehensive treatment to specific references.

Also some numerical simulations and some experimental data will be presented in the view of clarifying some important aspects related to Rayleigh waves propagation and to its modelling.

3.2 Homogeneous halfspace

3.2.1 Linear elastic medium

If the free boundary condition is imposed on the general equations for wave propagation in a linear elastic homogeneous medium, the solution for surface Rayleigh wave can be deduced from the P-SV components of the wave. It is important to note that a SH wave propagating on a free boundary can exist only under restrictive layering condition (and in that case it is usually called Love wave) and hence it cannot exist for the homogeneous halfspace.

The Navier's equations for dynamical equilibrium in vector formulation can be expressed as:

$$(\lambda + \mu)\nabla\nabla \cdot \mathbf{u} + \mu\nabla^2\mathbf{u} + \rho\mathbf{f} = \rho\ddot{\mathbf{u}} \tag{3.1}$$

where $\mathbf{u}$ is the particle displacement vector, ρ the medium density, λ and μ the Lamè's constants and $\mathbf{f}$ the body forces. Neglecting the latter contribution, the free vibration problem is addressed.

The solution can be searched using Helmholtz decomposition and assuming an exponential form (Richart et Al. 1970). The motivation for assuming the exponential form is that by definition a surface wave must decay quickly with depth.

Imposing the boundary conditions of null stress at the free surface:

$$\mathbf{\acute{o} = 0} \tag{3.2}$$

the surface wave solution can be found. In particular for the case of plane strain, discarding the solutions that give infinite amplitude at infinite depth, a solution (Rayleigh wave) can be found only if the following characteristic equation is satisfied by the velocity of propagation of the surface wave:

$$K^6 - 8K^4 + (24 - 16\gamma^2) \cdot K^2 + 16 \cdot (\gamma^2 - 1) = 0 \tag{3.3}$$

where K and α are the following ratios between velocities of longitudinal (P), distortional (S) and Rayleigh (R) waves:

$$K = \frac{V_R}{V_S} \tag{3.4}$$

$$\gamma = \frac{V_S}{V_P} \tag{3.5}$$

This equation is a cubic on K^2 and its roots are a function of Poisson Ratio ν since, as shown in Paragraph 2.3.1, $\gamma^2 = \frac{1-2\nu}{2(1-\nu)}$. It can be shown (Viktorov 1967) that for real media ($0 < \upsilon < 0.5$) only one real and acceptable (i.e. in the range 0 to 1) solution exists. The relationship between velocities of propagation of the different waves as a function of Poisson Ratio is reported in Figure 3.1.

An approximate solution of the characteristic equation (3.3) has been suggest by Viktorov (1967):

$$K = \frac{0.87 + 1.12\upsilon}{1 + \upsilon} \tag{3.6}$$

From Figure 3.1, it is evident that the difference between shear wave velocity and Rayleigh wave velocity is very limited, being the latter slightly smaller than the former. In particular the exact range of variation is given by:

$$0.87 < \frac{V_R}{V_S} < 0.96 \tag{3.7}$$

Note that there is no dependence of Rayleigh wave velocity on frequency, i.e. a homogenous linear elastic medium is characterised by a unique value of Rayleigh wave velocity.

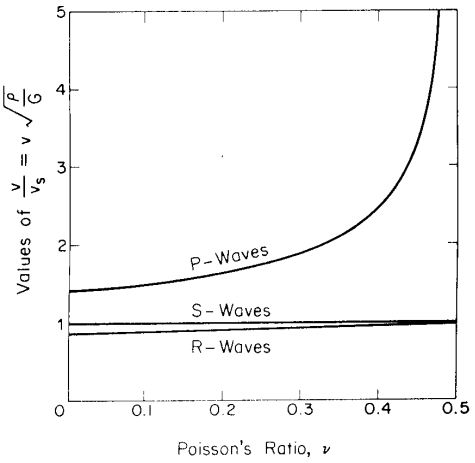

Figure 3.1 Relation between Poisson's ratio and velocity of propagation of compression (P), shear (S) and Rayleigh (R) waves in a linear elastic homogeneous halfspace (from Richart 1962)

It is important to remark that since the solution has been obtained using Helmholtz decomposition, the surface wave can be seen as the superposition of two separate components: one longitudinal and the other transverse. They propagate along the surface with the same velocity but they have different exponential laws of attenuation with depth. Obviously the wave fields are such that the superposition of the two gives a null total stress on the boundary of the halfspace.

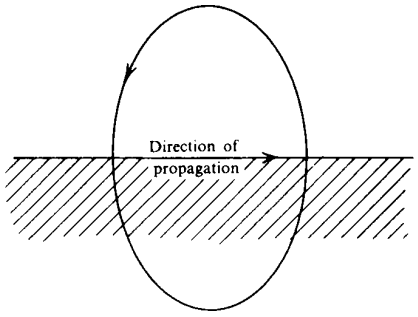

Figure 3.2 Particle motion on the surface during the passage of a Rayleigh waves in an elastic homogeneous halfspace

As far as the displacement fields are concerned, they can be computed introducing the solution of the characteristic equation into the respective formulations. The resulting horizontal and vertical components of motion are out of phase of exactly 90° one with the other, with the vertical component bigger in amplitude than the horizontal one, hence the resulting particle motion is an ellipse. On the ground surface the ellipse is retrograde (e.g. counter-clockwise if the motion is propagating from left to right as shown in Figure 3.2), but going into depth the ellipse is reversed at a depth equal to about $1/2\pi$ of the wavelength.

Another important remark is that being the decrease with depth exponential, the particle motion amplitude becomes rapidly negligible with depth. For this reason it can be assessed that the wave propagation affects a confined superficial zone (see Figure 3.3), hence it is not influenced by mechanical characteristics of layers deeper than about a wavelength.

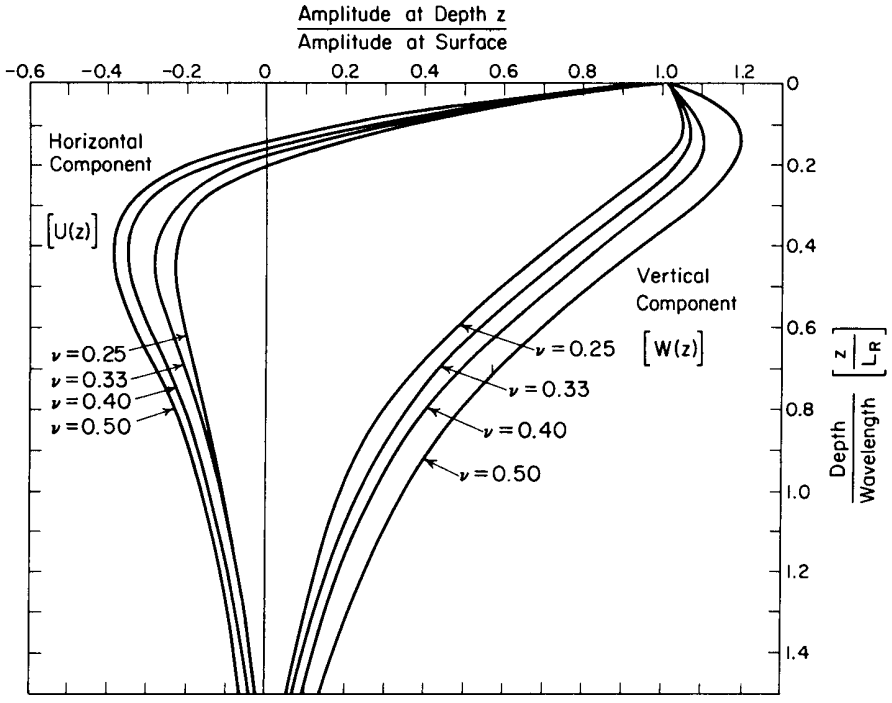

Figure 3.3 Amplitude ratio vs. dimensionless depth for Rayleigh wave in a homogenous halfspace (from Richart et Al. 1970)

The solution for a line or point source acting on the ground surface can be found in the Lamb's paper that has been cited above. In this regard it is important to remark that, due to the axial-symmetry of the problem, the disturbance spreads away in the form of an annular wave field. The reduced geometrical attenuation of surface waves can be directly associated to this property.

Also Lord Rayleigh, although he didn't solve the case of a point source, had a similar intuition about surface waves: *"Diverging in two dimensions only, they must acquire at a great distance from the source a continually increasing preponderance"* (concluding remarks of the above cited paper).

The geometric spreading factor, i.e. the factor according to which the waves attenuate as they go away from the source, can be estimate with the following physical considerations about the wave fronts.

Considering a buried point source in an infinite medium, the released energy spreads over a spherical surface and hence its attenuation is proportional to the square of distance from the source. Since the energy is proportional to the square of displacements, the latter ones attenuate proportionally to distance. Analogously since Rayleigh waves, that are generated by a point source acting on the ground surface, propagate with a cylindrical wave-front, their energy attenuation must be proportional to distance and displacement attenuation to the square root of distance. Concerning the geometrical attenuation of longitudinal and shear waves along the free surface, it is not possible an analogy to previous cases, but it can be shown that because of leaking of energy into the free space the displacement attenuation goes with the square of distance (Richart et al. 1970). In summary for a linear elastic halfspace a simple power law of the following type can express the radiation damping consequences on waves amplitude:

$$\frac{1}{r^n} \quad \text{with} \quad n = \begin{cases} 2 & \text{for longitudinal and shear waves on the surface} \\ 1 & \text{for body waves into the solid} \\ \frac{1}{2} & \text{for Rayleigh waves} \end{cases} \tag{3.8}$$

where r is the distance from the point source.

Back to Lamb's work, the displacements at great distance r from a vertical harmonic point force $F_z \cdot e^{i\omega t}$ can be expressed as:

$$u_z = F_z \cdot \frac{b_z}{\sqrt{r}} \cdot e^{i\left(\omega t - kr - \frac{\pi}{4}\right)} \tag{3.9}$$

$$u_r = F_z \cdot \frac{b_r}{\sqrt{r}} \cdot e^{i\left(\omega t - kr + \frac{\pi}{4}\right)} \tag{3.10}$$

where u_z and u_r are the vertical and radial displacements, b_z and b_r are functions of the mechanical parameters of the medium and k is the wavenumber that is defined by the following relation:

$$k = \frac{\omega}{V_R} \tag{3.11}$$

The two displacements are out of phase of 90° and hence the particles describe an elliptical path, as it was predicted by the solution of the homogeneous problem related to free vibration.

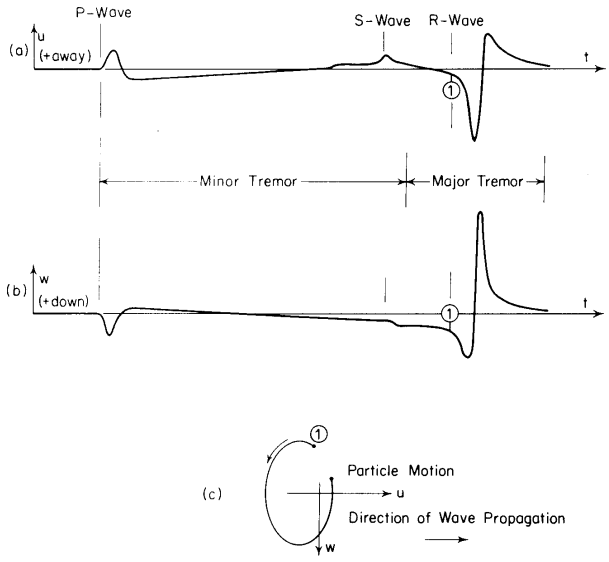

Figure 3.4 Complete wavefield predicted by Lamb (1904) for a surface point source on an elastic halfspace (a) horizontal radial motion; (b) vertical motion; (c) particle path of Rayleigh waves.

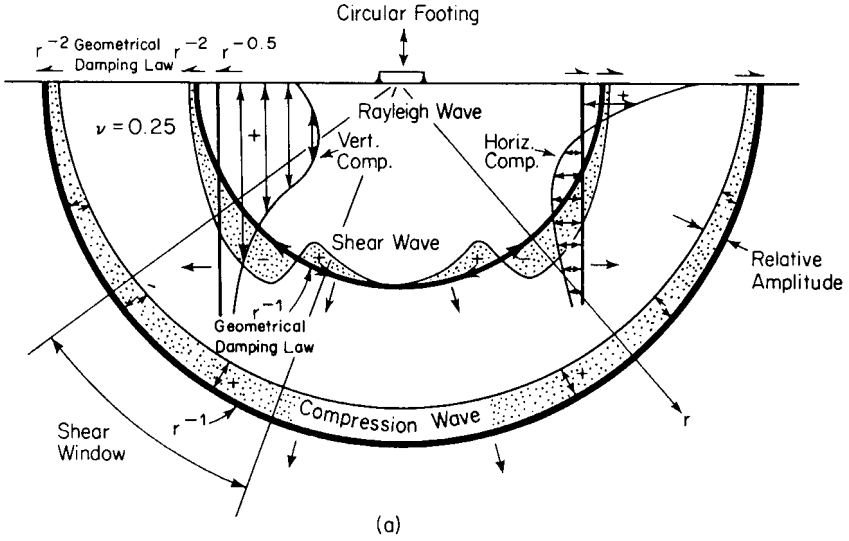

Wave Type	Per Cent of Total Energy
Rayleigh	67
Shear	26
Compression	7

(b)

Figure 3.5 Harmonic vertical point source acting on the surface of a homogenous, isotropic, linear elastic halfspace: (a) Complete displacements wave field; (b) Partition of energy between different types of waves (from Woods 1968).

The position of a given characteristic point of the wave (such for example a peak or a trough) is described by constant values of the phase:

$$(\omega t - kr) = const \tag{3.12}$$

thus with some manipulation and recalling Equation (3.11) it is clear the reason why V_R is often denoted as Rayleigh wave phase velocity.

Considering a circular footing vibrating harmonically at low frequency over a homogeneous isotropic linear elastic halfspace, Miller and Pursey (1955) showed that 2/3 of the total input energy goes into Rayleigh waves and the left fraction is

divided between body waves (see Figure 3.5b). Adding this information to the above considerations about geometrical attenuation, the conclusion is that at a certain distance from the source the wavefield is essentially dominated by the Rayleigh waves. This is essentially the same conclusion reached by Lamb (1904), who divided the wave contributions in two minor tremors (P and S) and a major tremor (R) (Figure 3.4).

All the important features of the complete wave-field generated by a low frequency harmonic point source are summarised in Figure 3.5.

3.2.2 Linear viscoelastic medium

As seen in Chapter 2, also at very low strain levels soil behaviour can't be considered elastic, indeed cycles of loading and unloading show energy dissipation. Recalling the actual nature of soil, it is intuitive that dissipation is essentially due to the friction between particles and the motion of the pore fluid, and hence it occurs also for very small strains, when the soil is far from the plasticity conditions.

To account for dissipation, an equivalent linear viscoelastic model can be assumed at small strains. In this regard the correspondence principle can be used to extend the result obtained in the case of a linear elastic medium. According to it, the velocity of propagation of seismic waves can be substituted by a complex valued velocity that accounts for the attenuation of such waves. Adopting this principle Viktorov (1967) showed that the attenuation of surface waves in a homogeneous linear viscoelastic medium is governed primarily by the shear wave attenuation factor. In particular he found that the Rayleigh wave attenuation α_R could be expressed as a linear combination of the longitudinal wave attenuation α_P and the shear wave attenuation α_S, according to the expression:

$$\alpha_R = A \cdot \alpha_P + (1 - A) \cdot \alpha_S \tag{3.13}$$

where is A a quantity depending only on the Poisson Ratio. Since A is always smaller than 0.5, the shear wave attenuation is prevalent in determining the Rayleigh wave attenuation. Moreover for Poisson Ratio values higher than 0.2, A is less than 0.2 (see Figure 3.6).

The wave field generated by a vertical harmonic point source acting on the ground surface can be obtained applying the correspondence principle to the Lamb's solution. For example substituting a complex wavenumber in (3.9) it is possible to evaluate the vertical displacements as:

$$u_z = F_z \cdot \frac{b_z^*}{\sqrt{r}} \cdot e^{i\left(\omega t - k^* r - \frac{\pi}{4}\right)} \tag{3.14}$$

where obviously also the quantity b_z^* is changed since it is dependent on the mechanical parameters, that now are those of the viscoelastic medium.

The complex wavenumber is defined as:

$$k^* = k - i\alpha = \frac{\omega}{V_R(\omega)} - i\alpha(\omega) \tag{3.15}$$

where $\alpha(\omega)$ is the material attenuation of surface waves and V_R is now frequency dependent because of material dispersion. With some manipulations of Equation (3.14) the phase and the amplitude of the displacements can be separated as follows:

$$u_z = F_z \cdot \frac{b_z^*}{\sqrt{r}} \cdot e^{-\alpha r} \cdot e^{i\left(\omega t - kr - \frac{\pi}{4}\right)} \tag{3.16}$$

and in this formulation the exponential effects due to the material attenuation is evident. Note also that the quantity $\frac{e^{-\alpha r}}{\sqrt{r}}$ represents the combined effect of material and geometrical attenuation as the wave spreads out from the source.

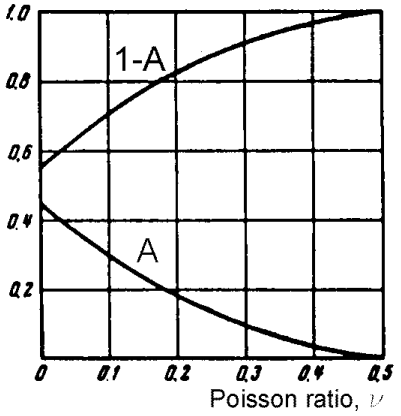

Figure 3.6 Body waves attenuation participation factors vs. Poisson ratio (Viktorov 1967)

3.3 Vertically heterogeneous media

3.3.1 Linear elastic medium

For heterogeneous and anisotropic media the mathematical formulation of Rayleigh waves becomes very complex and there can be cases of anisotropic media where they do not exist at all. However in the case of transverse isotropic medium with the free surface parallel to the isotropy plane (common situation for soil systems) Rayleigh waves exist and the analogous of the Lamb solution can be found (Butchwald 1961).

As far as heterogeneity is concerned, when the mechanical properties of the medium are assumed to be dependent only on depth z, the formal expression of the Navier's equations, neglecting body force, is:

$$(\lambda+\mu)\nabla\nabla\cdot\mathbf{u}+\mu\nabla^2\mathbf{u}+\mathbf{e}_z\frac{d\lambda}{dz}\nabla\cdot\mathbf{u}+\frac{d\mu}{dz}\left(\mathbf{e}_z\times\nabla\times\mathbf{u}+2\cdot\frac{\partial\mathbf{u}}{\partial z}\right)=\rho\ddot{\mathbf{u}} \quad (3.17)$$

where $\mathbf{e}_z$ is the base vector for the direction perpendicular to the free surface.

Lai (1998) has showed that introducing in (3.17) the condition of plane strain (that causes no loss of generality) and assuming the classical exponential form for the solution, the final solution is given by a linear differential eigenvalue problem. Assuming the usual boundary condition of null stress at the surface, the eigenvalues $k(\omega)$ can be found as the values that makes equal to zero the equivalent of the Rayleigh characteristic equation, that in this case can only be written in implicit form (Lai 1998):

$$\mathsf{F}_{\mathrm{R}}\left[\lambda(z),\mu(z),\rho(z),k_j,\omega\right]=0 \quad (3.18)$$

It is noteworthy to remark some important features of this equation. First of all the dependence on the frequency means that also the relative solution will be frequency dependant and hence the resulting wave field is dispersive, meaning that its phase velocity will be a function of frequency. This dispersion is related to the geometrical variations of Lamé's parameters and density with depth and hence it is often called geometric dispersion. The equation (3.18) itself is often named dispersion equation.

For a given frequency the solutions of the dispersion equation are several while in the case of the homogeneous halfspace there was only one admissible solution of the characteristic equation. This means that many modes of propagation of the Rayleigh wave exist and the solution of the forced vibration case must account for them with a process of mode superposition.

Substituting each one of the eigenvalues (wavenumbers) in the eigenproblem formulation, four eigenfunctions can be retrieved. They correspond to the two displacements and the two stresses associated to that particular wave propagation mode.

The existence of several mode of propagation can be explained physically through the concept of constructive interference (Lai 1998).

3.3.1.1 Mathematical formulations for layered media

In the formulation of the dispersion equation (3.18) there was no explicit reference to any law of variation of the mechanical properties with depth. The problem can be solved once a law of variation is specified. In general it is not possible to solve the problem analytically and a numerical solution is needed.

In this respect one classical assumption is that of a stratified medium with homogeneous linear elastic layers. This modelling procedure, that has been established for seismological purposes, assume a stack of layers, each one characterised by its thickness, elastic parameters and density (Figure 3.7). Obviously a price is paid in terms of generality but the eigenvalue problem can be established using a matrix formulation for a single layer and then building the global matrix, which governs the problem.

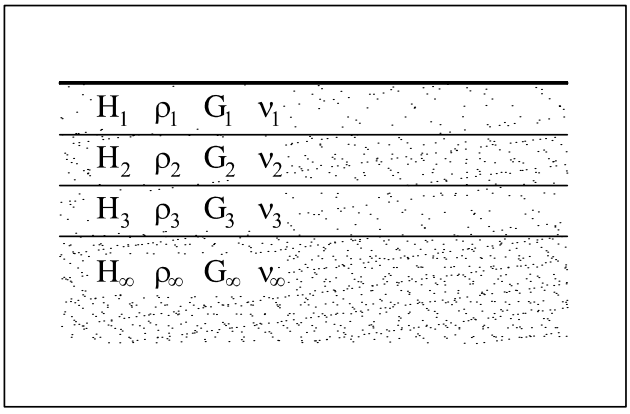

Figure 3.7 Stack of homogeneous isotropic elastic layers

Many version of this general procedure, also known as propagator-matrix methods (Kennett 1983), have been formulated, differing in the principles on which the single layer matrix formulation is based and consequently in the assembling process.

The oldest and probably the most famous method is the Transfer-Matrix method, originally proposed by Thomson (1950) and successively modified by Haskell (1953).

The Stiffness-Matrix method proposed by Kausel and Roesset (1981) is essentially a reformulation of the Transfer-Matrix method, having the advantage of a simplified procedure for the assembly of the global matrix, according to the classical scheme of structural analysis.

The third possibility is given by the construction of reflection and transmission matrices, which account for the partition of energy as the wave is propagating. The wave field is then given by the constructive interference of waves travelling from a layer to another (Kennett 1974, 1979; Kerry 1981).

Once the dispersion equation has been constructed using one of the above methods, the successive and very computationally intensive step is the use of a root searching technique to obtain the eigenvalues of the problem. Great attention must be paid in this process because of the behaviour of the dispersion function. Indeed some solution searching techniques can easily fail due to the strong oscillations of the dispersion function especially at high frequencies (Hisada 1994, 1995). In this respect since these methods are borrowed from seismology, the frequencies involved in the soil characterization methods have to be considered high.

Recalling the starting point of the above considerations (Equation (3.17)) the eigenvalues, and hence the correspondent eigenfunctions, that have been computed are the solution of the homogeneous problem, i.e. in absence of an external source. The obtained modes constitute the solution of the free Rayleigh oscillations of the considered medium.

If a source exists, the correspondent inhomogeneous problem must be solved. In this case a term that represents the external force is included in Equation (3.17). The solution comes from a mode superposition process. Sometimes this problem is addressed as the three dimensional solution because waves spread out from the source following a 3D axial-symmetric path, whereas the free modes represent plane waves and hence are addressed as the solution of the 2D problem.

For our purposes it is relevant the case of a point source acting on the ground surface. Lai (1998) has given an interesting solution for the case of a harmonic point load $F_z \cdot e^{i\omega t}$. According to its formulation, if body wave components are neglected (i.e. in far field conditions) the displacements induced by the load are given by:

$$u_\beta(r,z,\omega) = F_z \cdot \mathsf{G}_\beta(r,z,\omega) \cdot e^{i\cdot\left[\omega t - \psi_\beta(r,z,\omega)\right]} \tag{3.19}$$

where β stands for the generic component either vertical or radial, $\mathsf{G}_\beta(r,z,\omega)$ is

the *Rayleigh geometrical spreading function*, that models the geometric attenuation in layered medium, and $\psi_\beta(r,z,\omega)$ is a composite phase function.

An interesting comparison can be made between Equation (3.19) and its equivalent for a homogeneous halfspace (Eq. (3.9) and (3.10)), in which case the mode of propagation was only one. First of all the geometric attenuation for the homogeneous halfspace is much simpler. On the other side phase velocity is coincident with that of the only one mode of propagation, while in the case of the layered medium also the phase velocity comes from mode superposition and for this reason is often indicated as *effective* or *apparent* phase velocity.

In analogy to Equation (3.12), the position of a given characteristic point of the harmonic wave (such for example a peak or a trough) is described by constant values of the phase:

$$\left(\omega t - \psi_\beta(r,z,\omega)\right) = const \tag{3.20}$$

hence differentiating with respect to time, under the hypothesis that the function $\psi_\beta(r,z,\omega)$ be smooth enough, it is possible to obtain the effective phase velocity $\hat{V}_R$ (Lai 1998):

$$\hat{V}_R(r,z,\omega) = \frac{\omega}{\dfrac{\partial \psi_\beta(r,z,\omega)}{\partial r}} \tag{3.21}$$

It is very important to note that since the effective Rayleigh velocity is a function not only of frequency but also of the distance from the source, it is a local quantity (see Lai 1998 for a comprehensive discussion on this topic).

3.3.1.2 Physical remarks

Some physical aspects are implicitly included in the mathematical formulations of vertically heterogeneous media described above. It can be useful trying to describe them in a more phenomenological way.

First of all the geometrical dispersion, i.e. the dependence of Rayleigh phase velocity on frequency can be easily explained recalling the characteristics of shallowness of this waves. As exposed in Paragraph 3.2.1 for a homogeneous linear elastic halfspace the exponential decay of particle motion with depth is such that the portion of the medium that is affected by the wave propagation is equal to about one wavelength. Since the wavelength λ_R is related to the frequency f by the following relation:

$$\lambda_R = \frac{V_R}{f} \tag{3.22}$$

it is clear that low frequency waves will penetrate more into the ground surface. Hence in the case of a vertically heterogeneous medium, surface waves at different frequency will involve in their propagation different layers and consequently the phase velocity will be related to a combination of their mechanical properties. Consequently the surface waves velocity will be a function of frequency. The above concept is summarised in Figure 3.8, where the vertical displacements wave field in depth at two different frequencies is presented for a layered medium.

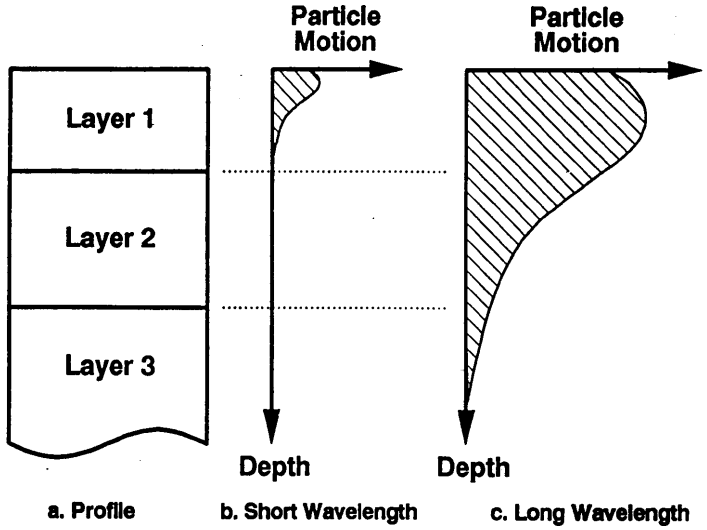

Figure 3.8 Geometrical dispersion in layered media (from Rix 1988)

It is important to remark that the shape of the dispersion curve (Rayleigh phase velocity vs. frequency or wavelength) is strongly related to the variation of stiffness with depth. Usually a distinction is made between a layered system for which the stiffness is monotonically increasing with depth and another one in which there is the presence of stiffer layers over softer ones. The first case is indicated as normally dispersive profile, the latter one as inversely dispersive profile. An example is presented in Figure 3.9, where the shape of the dispersion curve is presented in the phase velocity-wavelength plane. This representation is often used since for the aforementioned reasons it gives a clear picture of the variation of stiffness with depth.

Obviously in real media the alternation of stiff and soft layers can be much

more complex if compared to the above cases, still Figure 3.8 gives an idea of the relation existing between the stiffness profile and the dispersion curve.

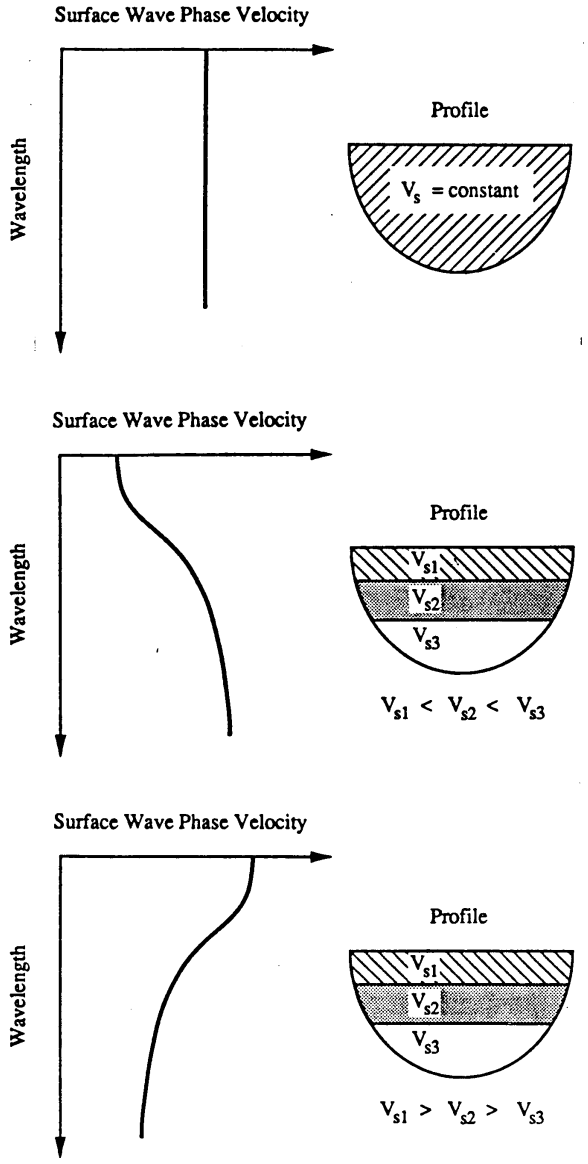

Figure 3.9 Examples of non dispersive (homogeneous halfspace), normally dispersive and inversely dispersive profiles (from Rix 1988)

Another important feature of surface waves propagation in layered media is the existence of several modes of propagation. This can be explained physically by the presence of constructive interference between curved ray-paths for continuously varying heterogeneous media and between transmitted and reflected waves for layered media (Achenbach 1984). The presence of several modes of propagation makes the forced case very complex since the active energy that the source introduces into the medium is propagating away with a superposition of the different modes. It is not possible to say a priori which mode dominates and in general there is the transition from the predominance of a mode to that of another one for different frequencies (Gukunski e Woods 1992). For these reasons the case of an impulsive source is particularly complex. Nevertheless usually, for normally dispersive profiles and in absence of strong stiffness jumps, the fundamental mode of propagation dominates the wavefield. In such cases the effective phase velocity practically coincides with the phase velocity of the fundamental mode. Hence resolving only the eigenvalue problem, with no need to account for mode superposition is sufficient for the construction of a good approximation of the effective dispersion curve.

Moreover also geometrical attenuation becomes very complex in the case of layered media and a geometric spreading function need to be introduced (see Equation (3.19)). Regarding this aspect (that is very important when also displacements amplitudes are of interest), if the above conditions for the predominance of the first mode of propagation are satisfied, further complications can be avoided by taking the usual factor of homogeneous halfspace $1/\sqrt{r}$ for geometrical attenuation.

Another important note can be made about the path described by particle motion on the ground surface. For the homogeneous halfspace vertical and horizontal components are 90° out of phase in such a way that as the wave is propagating the particle motion describes a retrograde ellipse. In the case of a layered medium the path is always elliptical but not necessarily retrograde. Moreover in presence of dissipative phenomena (that are likely to occur in soils) the phase difference between vertical and horizontal displacements can be different from 90° and the axes of the ellipse are not necessarily vertical and horizontal respectively (Haskell 1953).

An important consequence of surface wave dispersive behaviour in layered media is the existence of a group velocity. Up to now, when talking about velocity of propagation of surface waves, we used the term phase velocity, that is the velocity of a wave front (locus of constant phase points), such as a peak or a trough. For a dispersive medium, this is not the same as the velocity of a pulse of energy, indeed the latter can be seen (Fourier analysis) as composed of several

single frequency signals, each one travelling with its own velocity because of dispersion. Figure 3.10 clarifies this concept. The velocity of the wave train, i.e. the velocity of the envelope is indicated as group velocity, in contrast with that of the carrier that is the phase velocity. Obviously for a non-dispersive medium group velocity and phase velocity coincide.

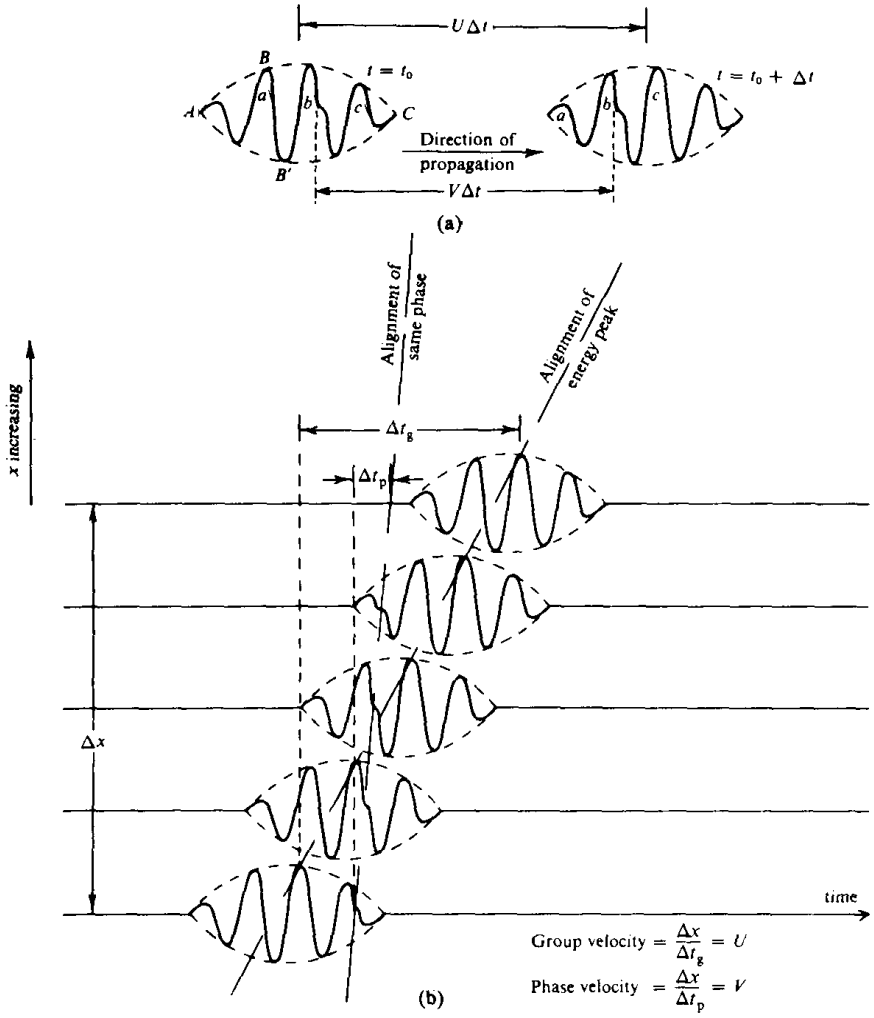

Figure 3.10 (a) Group U and phase V velocities. (b) Arrival of a dispersive wave at different geophones (from Sheriff and Geldart 1995)

The group velocity U can be computed using the following expressions, which involve the derivative of phase velocity with respect to frequency f or to wavelength λ (Sheriff and Geldart 1995):

$$U = \frac{d\omega}{dk(\omega)} \approx V + f\frac{dV}{df} = V - \lambda\frac{dV}{d\lambda} \tag{3.23}$$

where all the values are the average ones over the dominant frequency range.

From the above expression it is clear that if modal phase velocity decrease with increasing frequency (normally dispersive profiles), V is greater than U and hence the carrier travels faster than the envelope. Thus in such cases if a phase disturbance appears at the beginning of the pulse, then it overtakes and finally it disappears in the front (as shown in Figure 3.10). Obviously everything reverses for the case of an inversely dispersive profile.

3.3.2 Linear viscoelastic medium

It is important to distinguish two different cases: one is that of the weakly dissipative medium, the other one is the more general case were no assumption is made on the magnitude of the dissipation (Lai 1998).

For weakly dissipative media the solution can be obtained directly from the solution of the linear elastic eigenvalue problem substituting in the relevant expressions the real elastic phase velocities of body waves with the correspondent complex values:

$$\begin{aligned} V_P^*(\omega) &= V_P(\omega)\cdot\left[1 - iD_P\right] \\ V_S^*(\omega) &= V_S(\omega)\cdot\left[1 - iD_S\right] \end{aligned} \tag{3.24}$$

where D_P and D_S are the damping ratios.

Instead in the general case the correspondence principle has to be applied to the formulation of the eigenvalue problem, so that it becomes a complex eigenvalue problem and its solution is not trivial. A solution based on the generalisation of the transmission and reflection matrix techniques and appropriate root searching for complex dispersion equation can be found in Lai (1998). An expression, which is formally analogous to Equation (3.19), can be established for the displacement field generated by a harmonic point source:

$$u_\beta(r,z,\omega) = F_z \cdot \mathsf{G}_{\beta\nu}(r,z,\omega)\cdot e^{i\cdot\left[\omega t - \psi^*_{\beta\nu}(r,z,\omega)\right]} \tag{3.25}$$

where $G_{\beta v}(r,z,\omega) \neq G_{\beta}(r,z,\omega)$ is the geometric spreading function for the layered viscoelastic medium and the function $\psi^{*}_{\beta v}(r,z,\omega)$ in the exponent is now complex-valued.

In relation to what exposed in Paragraph 3.3.1.2, it is important to recall that in the case of a viscoelastic layered medium, material dispersion is added to geometrical dispersion, hence the phenomenon is more complex, with respect to the way in which it was explained for layered elastic media.

3.4 Numerical examples

Some numerical simulations regarding the case of linear elastic stratified medium are presented hereafter. The results have been obtained using a freeware computer program developed by Hisada and modified formerly by Lai (1998) and successively by the Author. The construction of the eigenvalue problem is based on the formulation of transmission and reflection matrices, initially proposed by Kennet (1975) and successively modified with the contribution of several researches (Luco and Apsel 1983, Apsel and Luco 1983, Chen 1993). The relative theory can be found in Hisada (1994, 1995).

The basic purpose of these numerical simulations is to illustrate some basic features of Rayleigh waves in vertically heterogeneous media, that have been delineated in the theory above.

Two stiffness profiles are considered to show the differences between normally dispersive and inversely dispersive media. This difference has a huge influence on characterization problems, because the presence of stiff layers over softer ones produces the shift of the dominating mode from the fundamental one towards the higher ones.

3.4.1 Normally dispersive profile

Firstly the very simple case of a layer over a homogeneous halfspace is considered. The model parameters are reported in Table 3.1. They are such that the medium is normally dispersive, the stiffness being monotonically increasing with depth.

Table 3.1 Normally dispersive profile

Thickness (m)	V_S *(m/s)*	V_P *(m/s)*	*Density* (kg/m^3)
10	300	600	1800
∞	400	800	1800

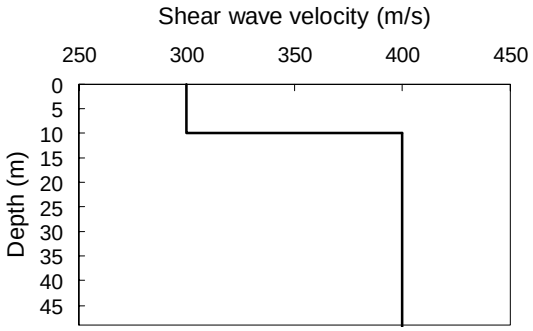

Figure 3.11 Normally dispersive profile

Once the Rayleigh dispersion equation (3.18) has been built using matrix multiplication on the matrices of the top layer and of the homogenous halfspace, the Rayleigh homogeneous eigenproblem can be solved. The corresponding eigenvalues are the wavenumbers corresponding to the modes of propagation for each analysed frequency. From the wavenumbers, the phase velocities can be easily derived inverting Equation (3.11). Figure 3.12 shows the Rayleigh mode phase velocities for the above model in the frequency range that is of practical interest in soil characterization problems. It is important to note that for low frequencies only one free Rayleigh mode exists while as the frequency increases other modes arise.

For each frequency, substituting one of the eigenvalues in the matrix formulation it is possible to find out the four eigenfunctions that represent, for the corresponding free Rayleigh mode, the depth dependence of stresses and displacements. The displacements eigenfunctions relative to a frequency equal to 50 Hz are plotted in Figure 3.13, while Figure 3.14 represents the vertical component stress eigenfunctions at the same frequency. Since the eigenvalues at frequency 50 Hz are three, there exist three eigenfunctions for each displacement or stress characteristic. In the view of characterization purposes, it is very

important to observe the typical shapes of these eigenfunctions.

The fundamental mode eigenfunctions show a depth dependence very similar to the case of a homogeneous halfspace, for which a single mode of propagation exists (see Figure 3.3). In particular they attenuate very rapidly with depth, showing that when the fundamental mode is predominant the deeper strata are not interested by the wave propagation phenomenon. This is the basis of simplified procedures for the estimation of stiffness profile from the dispersion data (see Figure 4.3). Note that for higher modes the shape of the eigenfunctions changes substantially and the deeper zones of the soil are strongly involved. As it will be shown in the successive Paragraph, higher modes are very important for inversely dispersive profile, thus for such soils the estimate given by the method of Figure 4.3 gives poor results and more accurate procedures need to be used.

Figure 3.15 depicts the variation of group velocity as a function of frequency for the different Rayleigh modes. Because of the geometric dispersion phenomenon it is substantially different from the phase velocity. It is important to remark that the asymptotic behaviour for increasing frequencies is the same for all the different modes and for both group and phase velocities. This is evident for the first mode, being its group velocity rapidly converging to the same value of the phase velocity. It can be explained by the fact that for very high frequencies (very short wavelengths) the Rayleigh wave 'sees' only the first layer and hence travels in a homogeneous medium with no geometric dispersion, so there is no distinction between phase and group velocity. As a consequence, the asymptotic value of Rayleigh velocity can be evaluated using Equation 3.6 and in this case ($V_S = 300\,m/s$ and $\nu = 0.33$) it results:

$$V_R = \frac{0.87 + 1.12\upsilon}{1+\upsilon} \cdot V_S = 0.93 \cdot V_S = 280\ m/s$$

Also it is important to note that, for a given frequency, the phase velocity is always greater or at least equal to the group velocity. As seen in Paragraph 3.3.1.2, this is a typical feature of normally dispersive profiles, for which phase velocity monotonically decreases with frequency increase (see Figure 3.12).

Once the homogeneous boundary value problem that corresponds to the free Rayleigh vibration has been solved, obtaining the eigenvalues and the associated eigenfunctions, a mode superposition technique can be used to derive the solution of the inhomogeneous problem, that correspond to the forced vibrations. As seen in Paragraph 3.3.1.1, the resulting effective phase velocity, is not only function of frequency, but also of spatial position, hence a correct representation of this quantity would require a three dimensional plot.

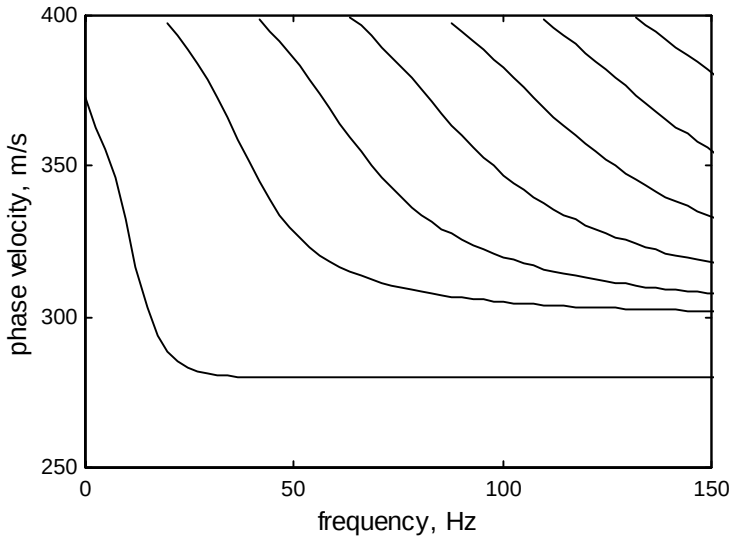

Figure 3.12 Rayleigh modes phase velocity

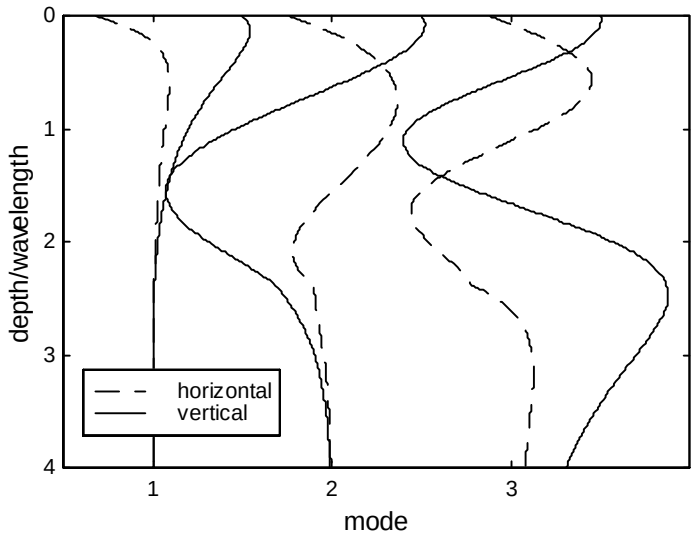

Figure 3.13 Normalised displacements eigenfunctions for a frequency of 50 Hz

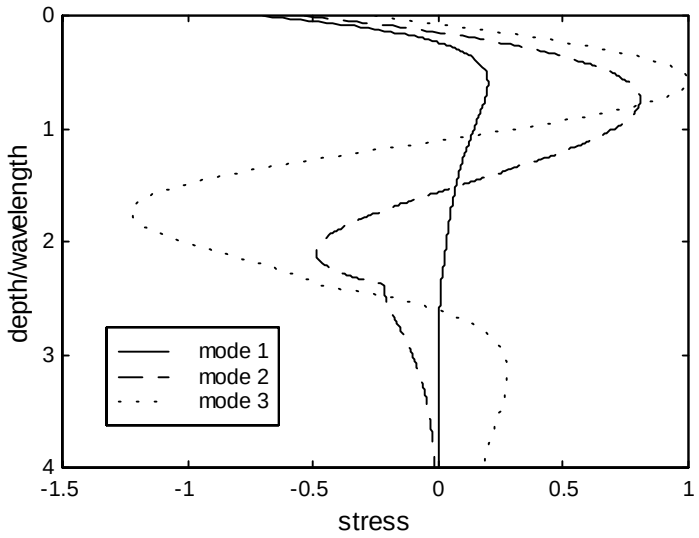

Figure 3.14 Normalised stress eigenfunctions for a frequency of 50 Hz (vertical component)

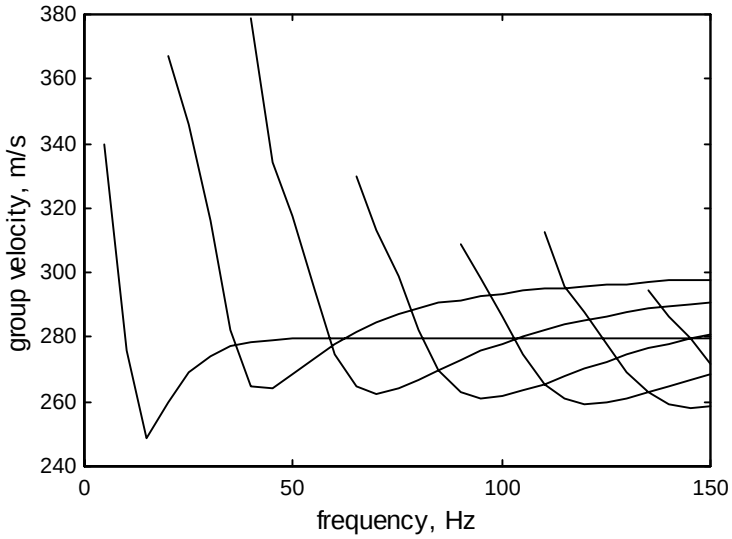

Figure 3.15 Rayleigh modes group velocity

To make a simple comparison between effective and modal phase velocity a conventional definition as been adopted, evaluating the effective velocity considering a two-receiver model with the first receiver at a distance equal to two wavelengths from the source and the second one at four wavelengths (see Figure 5.1). The choice of having the two receivers at a great distance from the source is due to the fact that going away from the source there is a sort of stabilisation in the velocity values.

The comparison between modal and effective phase velocity is reported in Figure 3.16 from which it is clear that for normally dispersive media higher modes have practically no influence and hence the effective phase velocity coincides with the phase velocity of the fundamental Rayleigh mode.

Another important consequence of mode superposition is the difference between the geometric attenuation in an homogeneous halfspace and the *Rayleigh geometrical spreading function* that models the geometric attenuation in a layered medium, introduced in Equation (3.19). Figure 3.17 reports the comparison between the two for different frequencies, showing that the difference is negligible at low frequencies and becomes sensible as frequency increases, because of the increasing number of modes.

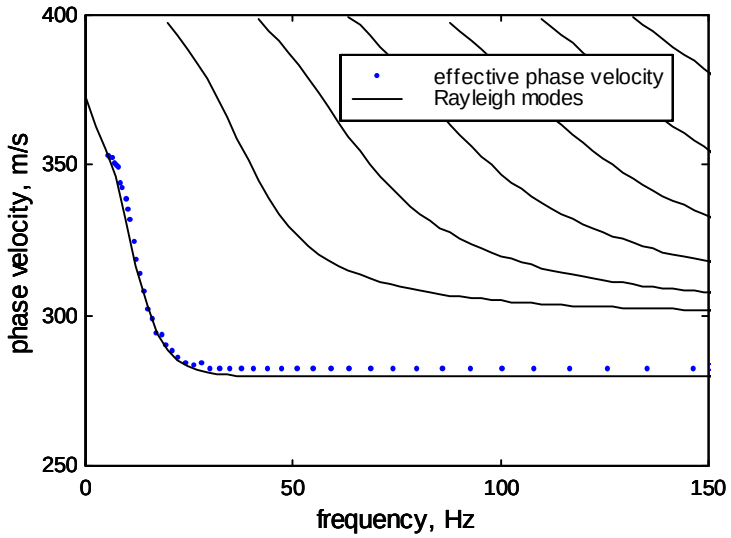

Figure 3.16 Comparison between effective and modal phase velocities

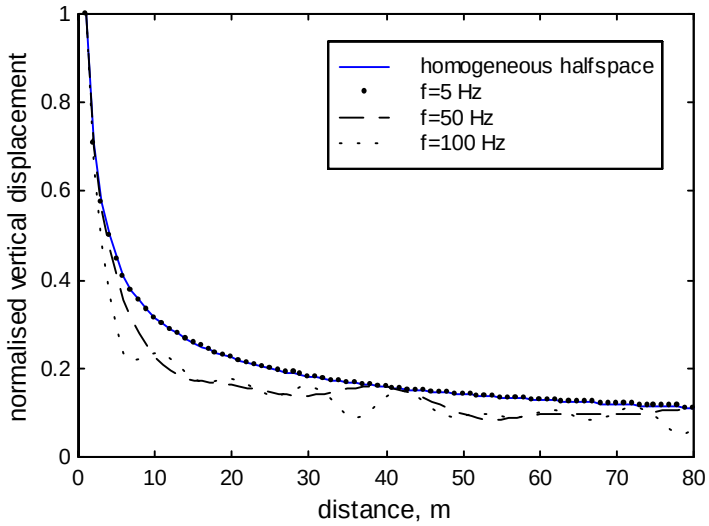

Figure 3.17 Geometrical attenuation in layered media

3.4.2 Inversely dispersive profile

To illustrate the case of an inversely dispersive profile a two layers over halfspace model has been selected, with the intermediate layer softer than the cover and the halfspace. The model parameters are reported in Table 3.2 Inversely dispersive profile.

Table 3.2 Inversely dispersive profile

Thickness (m)	V_S *(m/s)*	V_P *(m/s)*	*Density* (kg/m^3)
10	400	800	1800
10	300	600	1800
∞	400	800	1800

With regards to the solution of the eigenproblem that is associated to the free Rayleigh vibration, the only essential difference with respect to the previous analysed case of a normally dispersive profile, is given by the shape of the modal dispersion curves (Figure 3.18). Note that in this case, the phase velocity is not

monotonically decreasing with frequency.

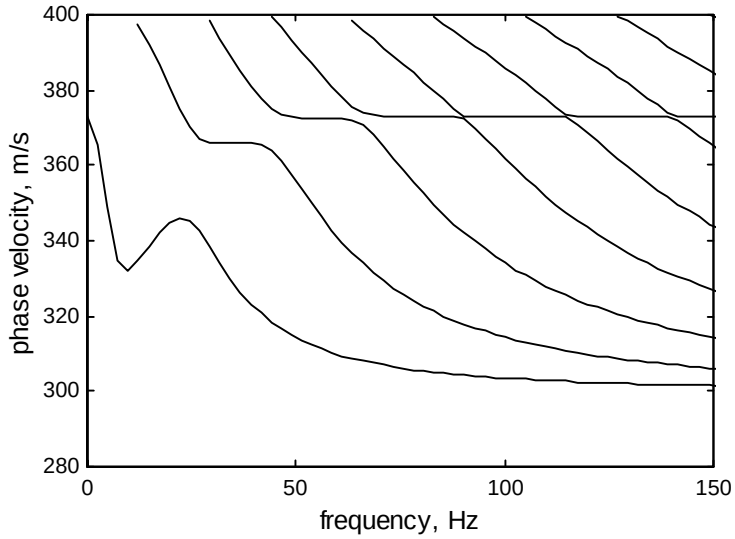

Figure 3.18 Rayleigh modes phase velocity

The very important difference with the case of a normally dispersive profile is relative to the forced vibration problem. Indeed in this case the fundamental mode is dominant only at low frequencies, while as frequency increases and more modes participate to the definition of the wavefield the dominant mode changes. This fact has huge consequences on the propagation phenomenon. First of all the effective phase velocity that can be measured on the ground surface is now a combination of the individual mode phase velocities. This is clear in Figure 3.19 where the effective phase velocity is compared to the modal quantities. It is important to note that also in this case the asymptotic value at which the effective phase velocity tends as frequency increases is the Rayleigh wave velocity characteristic of the surface layer, also if in this case the dominant mode continuously changes to satisfy this requirement. Indeed the Rayleigh wave phase velocity for high frequencies can be evaluated, as for the previous case, considering that the surface layer is characterised by $V_S = 400\,m/s$:

$$V_R = \frac{0.87 + 1.12\upsilon}{1+\upsilon} \cdot V_S = 0.93 \cdot V_S = 373\ m/s$$

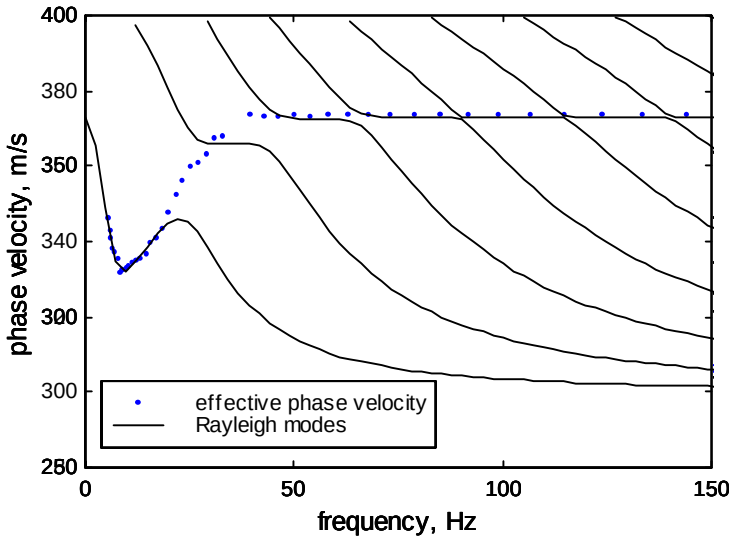

Figure 3.19 Comparison between effective and modal phase velocities

The influence of higher modes has very serious consequences also on the extent of soil that is involved in the surface wave propagation phenomenon. Recalling the shape of the eigenfunctions of Figure 3.13 and Figure 3.14, which are very similar to those of the inversely dispersive profile, the influence of higher modes clearly results in an increased possibility of identifying deep layers in a characterization problem.

3.5 Experimental evidence

Some experiments have been conducted to detect the surface wave particle motion that is induced by impulsive sources acting on the ground surface. The main purpose was to investigate their shape in the view of clarifying the relation between Rayleigh waves (that induce an elliptic particle motion) and body waves (that in this respect should act as a disturbance).

The description of the field equipment and of the testing site can be found in Paragraph 6.2. The test was conducted with impulsive sources (either a sledgehammer or a seismic weight drop source) and a series of composite receivers, in which a vertical geophone was coupled to a horizontal one. Since the

adopted receivers were velocity transducers, the signals have been integrated to get particle displacements.

A nice example of experimental elliptic path is represented by the arrival of the main disturbance at a receiver placed at 36m from the weight drop source (Figure 3.20). Note firstly that the particle path is not retrograde has one could expected in a homogeneous elastic medium. Moreover the ellipse axis are not vertical and horizontal has it would have been in a layered elastic medium.

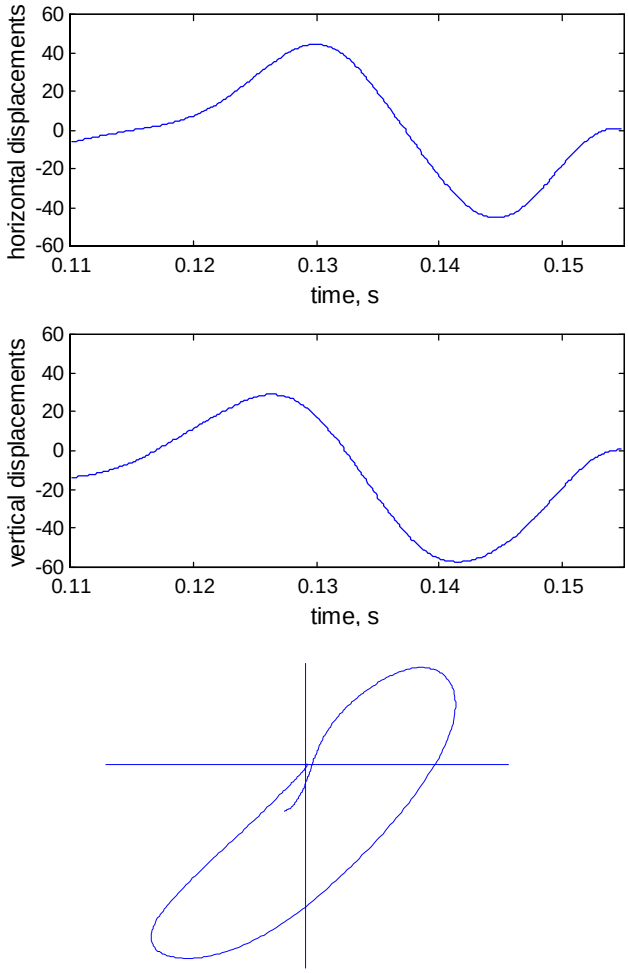

Figure 3.20 Arrival of main disturbance at a composite receiver placed at 36m from the source and resultant particle motion path

The elliptic path associated to surface waves has been detected in most of the recorded signals, nevertheless it was often perturbed by incoherent or coherent noise. Other two examples are reported in Figure 3.21 with the complete path relative to two different receivers, which were placed close to the impact source. Both particle paths show the presence of segments of elliptic path with the addition of some noise. In particular the first one shows initially a retrograde ellipse that is successively perturbed by some disturbance. Note also that as the point of detection is moved farther from the source the number of elliptical or quasi-elliptical paths increases. This aspect is associated to mode separation and to the widening of the pulse as the wave travels along the surface. As it will be clarified in the following.

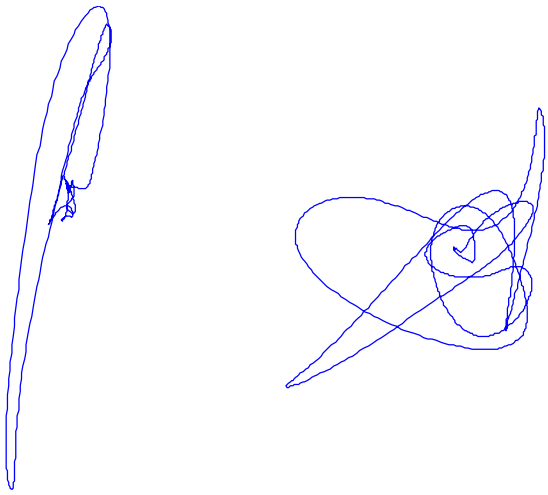

Figure 3.21 Particle paths observed at 6m and 12m from the source

A typical feature that can be experimentally observed in surface waves traces is the spreading of the signal. The difference between phase and group velocity breaks the initial impulse given by an impact source acting on the ground surface in a composite wave-train (see Figure 3.22). This aspect is very important because it is linked to mode separation at great distance, an effect that is very important in the view of characterization problems. At short distances from the source, the signal is composed essentially by a narrow impulse, in which the different modes are combined, while as the wave travels along the surface the modes separate because of their different velocity.

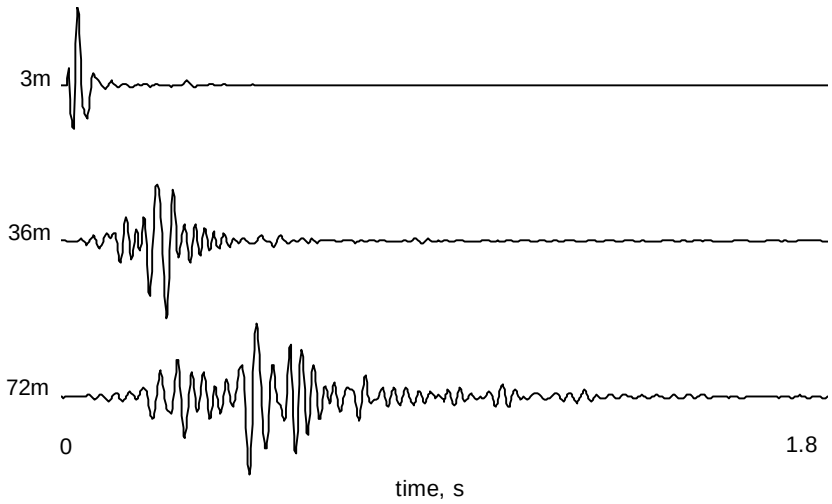

Figure 3.22 Signals recorded at different distances from the source (receivers: vertical velocity transducers, source: weight drop, site: ENEA)

3.6 Summary

Rayleigh waves are generated by the presence of a free surface in solids and they travel in a confined zone along the free surface. Their properties have been extensively treated in this Chapter and are summarised in the following.

Concerning Rayleigh waves in a homogenous halfspace:

- ✓ Their velocity of propagation is quite similar to that of shear waves. The ratio between the two is a function of the Poisson ratio, but it is comprised in a very narrow range (0.87 to 0.96).
- ✓ The associated particle motion is elliptical retrograde on the surface, with the major axis vertical.
- ✓ The propagation involves only a limited superficial portion of the solid, having thickness nearly equal to one wavelength.
- ✓ Geometrical attenuation as the wave departs from a point source is related to the square root of distance and hence it is less sensible than for body waves.
- ✓ Considering a circular footing vibrating at low frequency, about 2/3 of the

input energy goes in surface waves and only the remaining portion in body waves.

- ✓ Their material attenuation is much more influenced by shear wave attenuation than by longitudinal waves one.

For a layered system, the following points regarding surface wave propagation are worthily highlighted:

- ➢ The phase velocity is frequency dependent also for an elastic medium (geometric dispersion).
- ➢ In general for a given frequency several free vibration modes exist, each one characterised by a given wavenumber and hence a given phase velocity. The different modes involve different stress and displacement distributions with depth.
- ➢ It is necessary to distinguish group velocity from phase velocity.
- ➢ Particle motion on the ground surface is not necessarily retrograde.
- ➢ In presence of an external source acting on the ground surface it is necessary to account for mode superposition that has some major consequences:
  - The geometrical attenuation is a complicate function of the mechanical properties of the whole system.
  - The effective phase velocity is a combination of modal values and it is spatially dependent.
  - Because of the difference between phase velocity and group velocity, mode separation takes place going away from the source and hence the pulse changes shape.

Finally it is noteworthy to mention the main lessons learned from the numerical simulations:

- ❖ For a normally dispersive profile the fundamental mode is strongly predominant on the higher modes at every frequency. This has some very important consequences:
  - The effective phase velocity is practically coincident with the fundamental mode one.
  - The wave propagation interests a portion of the medium nearly equal to a wavelength
- ❖ For an inversely dispersive profile it is very important to account for mode superposition.

Chapter 4

Surface Waves and Soil Characterization

4.1 Overview

The motivations for using Surface waves for soil characterization derive by the inherent nature of this kind of waves and by some specific properties of them. Indeed such waves travel along a free surface, so that it's relatively easy to measure the motion associated to them, and they carry important information about the mechanical properties of the medium.

For this reason many applications have been developed in the fields of Science of Materials. This interest led to many publications and books explaining the features of surface waves from a physical and from a mathematical point of view (see, e.g. Viktorov 1967).

The specific features of surface wave propagation in stratified medium make them very interesting also in the field of Earth's constitutive materials characterization. Applications started to be developed for earthquake seismology with the attempts to infer the characteristics of the rocks through which earthquake generated waves travel (Dorman and Ewing 1962).

Before the introduction of surface waves theory, many features of actual seismograms were unexplained. In particular surface waves have a great influence on the motion associated to Earthquakes and recorded on seismological stations far from the epicentre.

Soon researchers started to use information carried by seismograms to get a deeper knowledge regarding the substructure of the Earth and the related layering

system. The wave-theoretical approach based on modelling the (mainly Love and Rayleigh) wave propagation to fit the observed phase velocities or amplitudes spread out starting from the early sixties with the advent of digital computers. This research founded the basis of all the tools needed for soil characterization: mathematical models of layered systems, techniques to obtain wave propagation parameters from point measurements of motion, inversion algorithms (Aki and Richards 1980, Ewing et al. 1957, Doyle 1995).

Applications to site characterization at a geotechnical scale started at the end of the Fifties with the Steady State Rayleigh Method. Successively, after a period during which there was small interest in this field, they had a strong impulse during the Eighties with the introduction of the SASW method. Meanwhile also geophysicists started to consider surface waves, which before were seen only as an undesired side effect, as a potential tool for underground explorations.

This Chapter is devoted to trace an overview of the methods that have been proposed to characterize stratified soil systems. Some of these methods have been extensively used in practical applications and can be considered as a State of Practice in soil characterization, while some other have not, still they are very important for possible future improvement of the testing technique. Also the Steady State Rayleigh Method will be briefly described: although it is not anymore in use, it can be considered the starting point of geotechnical applications. Obviously more details will be reported about the techniques that have a strict relation with the present dissertation, while the other methods will be presented only for completeness, referring the appropriate references for further details.

4.2 Characterization of layered media using Rayleigh Waves: basic concepts

As seen in Chapter 3, Rayleigh waves in a homogeneous isotropic linear elastic halfspace are not dispersive, i.e. their velocity of propagation is a function of the mechanical properties of the medium, but it is not a function of frequency. In stratified media the phenomenon of geometrical dispersion arises, for which the phase velocity of Rayleigh wave is a function of frequency. This can be easily explained considering a medium composed by a stack of homogeneous isotropic linear elastic layers and recalling the extent of soil deformation caused by a perturbation of a given wavelength travelling on the surface (Figure 3.8). Such a system is then characterised by a dispersion curve, i.e. a given relation between frequency and phase velocity of surface waves.

This property can be used for identification purposes, indeed measuring the

dispersion curve that is associated to a given site, it is possible through an inversion process to infer from it the stiffness profile of the underlying medium.

There are two critical aspects in this scheme: one is the necessity of assuming a consistent soil model, the other concerns the non-uniqueness, which is a major problem for every inversion problem.

Regarding the soil model, nearly all methods for soil characterization assume that the underlying system is constituted by a succession of parallel layers, each one constituted by a homogeneous and isotropic elastic material. Clearly this is only an approximation of the reality and the more the real conditions are distant from this hypothesis the less the method is reliable. In particular not always sharp interfaces are present between layers, in this condition a continuos variation of soil deformation characteristic with depth, e.g. due to the increase in geostatic stresses, is interpreted as the presence of fictitious layers. This is not a major problem if we keep in mind that the results of surface wave testing is an estimate of the soil stiffness as a function of depth and it doesn't want to be a exact picture of the underground situation.

The serious problem can be instead represented by lateral inhomogeneities and bedding inclinations in the strata. This kind of factors can strongly distort the real stiffness profile. For this reason it can be useful to perform measurements not only along a straight line, but also along a different direction and try to evaluate the differences to assess the effectiveness of the hypothesis of plane and parallel layers.

As far as the non-uniqueness is concerned, this remains a problem of difficult solution. The inversion process need a starting hypothesis of stiffness profile and this need to be chosen carefully because it can strongly influence the final result. Any information about the site is very important to set some constraints on the solution. Information about interface position not only mitigates the non-uniqueness, but also speeds up the convergence of the inversion process (see Par. 4.3.2.3).

4.3 Traditional geotechnical testing using surface waves

The use of techniques similar to those used in seismology has always been appealing for geotechnical engineers. The scale factor plays in this case a very important role. Indeed it is not only a matter of frequency (and hence wavelength) of interest, but the distance between the source and the receivers combined with the dispersion features of surface waves has enormous effects on the recorded waveform. On a seismological scale, the difference between group velocity and

phase velocity causes the separation of the different modes, while the usual distances of a geotechnical survey are not large enough. Thus the information extracted from signals are related to the superposition of several modes. This has heavy consequences on the inversion process that undoubtedly is not only lighter but also better conditioned when information regarding separate modes is available.

The general procedure of most common methods for soil characterization can be summarised in the following three essential steps:

1. Generation of a perturbation on the surface of the deposit using a dynamic point source (generally acting in the vertical direction).
2. Detection of the subsequent wave through some sensors placed on the ground surface and determination of the dispersion curve (Rayleigh phase velocity vs. frequency).
3. Determination of the stiffness profile with an inversion process.

The success of the above procedure is strictly related to the condition that Rayleigh waves predominate in the generated wavefield. This is usually verified at a certain distance from the source, because most of energy that is transmitted to the medium by a vertical point source goes into Rayleigh waves and they attenuate with distance less than body waves (see Par. 3.2.1).

The first test for soil characterization using surface waves was proposed and developed at the end of the Fifties (see Par. 4.3.1). The time consuming testing procedure and the lack of precision due to the simplified inversion process caused the poor diffusion of the method.

The spreading of geotechnical surface waves characterization in standard practice started during the Eighties when the Researchers of the University of Texas at Austin (Texas, USA) introduced the *Spectral Analysis of Surface Waves* method (see Par. 4.3.2). Since then, the interest in the scientific and professional community has rapidly grown up, because of the advantages of such non-invasive methods.

Nowadays the SASW is considered a distinctive tool for in situ testing and it is commonly used not only on natural soils but, thanks to its flexibility and to its non-invasive nature, also on pavements systems and on waste disposals.

This interest led also to the development of many variants of the method, based on application of different sources or signal analysis tools. An appealing possibility is given by methods based on ambient noise also named passive methods because they do not generate any perturbation (see Par. 4.6).

Another important improvement in the execution of tests based on surface waves propagation gives the possibility of obtaining not only the stiffness of geomaterials but also their dissipative properties (see Par. 4.4).

4.3.1 Steady State Rayleigh Method

The first method developed for soil characterization at a small scale was the Steady State Rayleigh Method, proposed by Jones (1958; 1962) and then adopted at the Waterways Experimental Station, USA (Ballard 1964).

This method was undoubtedly less refined than successive ones and than seismological methods, nevertheless it must be recognised the big merits of getting into the physics of the problem and understanding the strong potentiality of surface waves for characterization purposes.

The initial application was made using ultrasonic frequencies on concrete slabs to assess their thickness and deformation characteristics. The success of this technique led to the extension to soil deposits, with the use of lower frequencies.

The idea that velocity of propagation could be related to subsoil condition came from a series of experiments with mechanical vibrators that showed as this velocity was a function of frequency on sites where soil properties were found to be variable with depth.

In his field experiments Jones tried to use both Rayleigh and Love waves to characterize the underground soil. In particular the field equipment was composed of a mechanical vibrator and a single receiver. To investigate Rayleigh wave propagation the vibrator was placed vertically, so that the transmitted action was perpendicular to the free surface, while for Love waves the vibrator and the receiver were orientated to produce and detect vibrations in a horizontal direction transverse to the testing line.

In both cases the dispersion curve was obtained moving the receiver along a straight line starting from the source, working at a given frequency, and looking for positions such that vibrator and receiver were in phase. The average distance between two different positions is the wavelength associated to that particular frequency. Repeating the process for different frequencies the whole dispersion curve could be obtained.

Once dispersion curves for Rayleigh and Love waves were obtained, approximate procedures based on the results of theoretical analysis on wave propagation were used to infer shear moduli of the subsoil system.

It is important also to remark that Jones saw in surface waves a useful tool for assessing the results of ground improvement processes such as compaction or rolling. Actually this is one of the straightforward applications, since for this purpose also the dispersion curve itself gives some indications about the success of compaction, with no need for a refined inversion process.

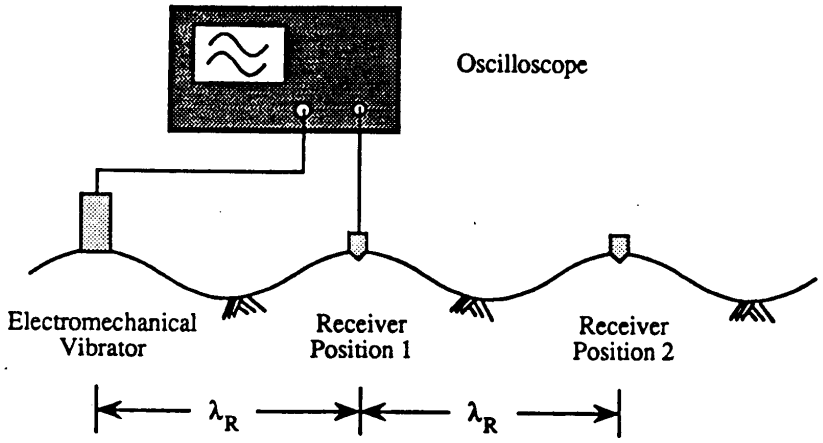

Figure 4.1 Steady State Rayleigh method: field procedure (from Rix 1988)

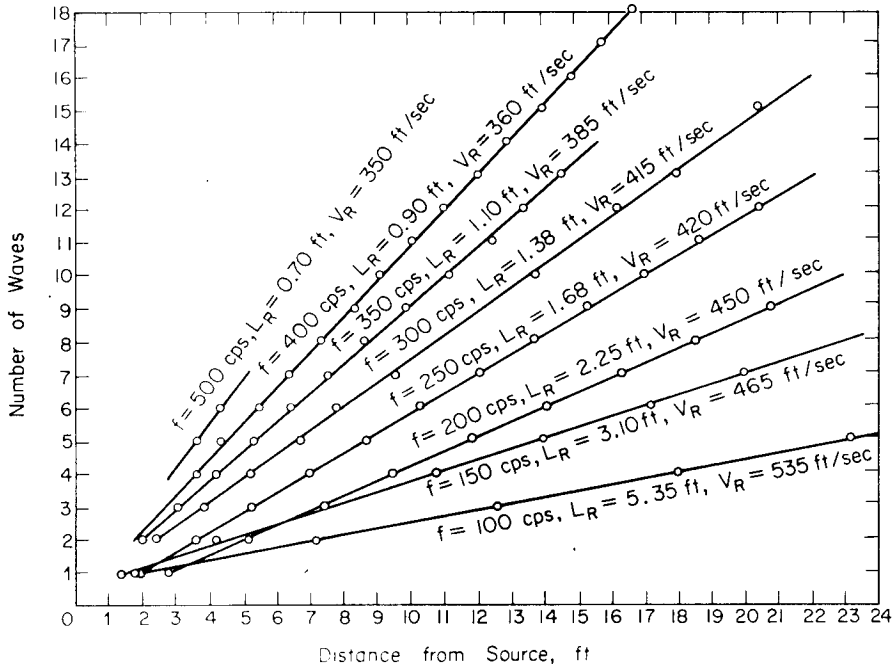

Figure 4.2 Determination of the average wavelength of Rayleygh waves by SSR Method (from Richart et Al. 1970)

The procedure of Steady State Rayleigh Waves method is illustrated in Figure 4.1. A vertical-acting sinusoidal vibrator, working at frequency f, is placed on ground surface and one vertical receiver also laying on ground surface is used to detect the particle motion. The receiver is moved away from the vibrator until they are in phase. The distance between any two adjacent receiver positions is assumed to be the wavelength at that particular frequency. To improve the precision, the following procedure can be applied: points corresponding to some different location at which the receiver is in phase with the source are represented in a diagram source-receiver distance vs number of cycles (Figure 4.2). The slope of the straight line connecting the points represents the inverse of wavelength for the current frequency.

From wavelength λ_R, phase velocity of surface waves V_R is determined by using the relationship:

$$V_R = f \cdot \lambda_R \tag{4.1}$$

By changing the frequency f and repeating all the above steps, it is possible to obtain the characteristic dispersion curve (V_R vs. λ_R) of the site.

The soil stiffness is inherently linked to Rayleigh wave phase velocity, but this relation can't be expressed in an explicit form. A simple procedure that can be used to estimate the stiffness profile directly from the dispersion curve is based on the following remarks.

In chapter 3 it was shown that the motion induced by surface waves is confined in the upper part of the soil (Figure 3.3). Thus it can be assumed that the energy that is associated to the perturbation travels in shallow zone, which depth is about one wavelength. On the other side shear waves velocity is closely related to V_R and can be estimated as (see Equation 3.7):

$$V_S \approx 1.1 \cdot V_R \tag{4.2}$$

Considering a sort of weighted stiffness of the underlying layers, this shear wave velocity is considered to be the characteristic value at depth equal to one half or one third of wavelength. This process can be considered as a sort of direct mapping from the (V_R ; λ_R) space to the (V_S ;z) space (see Figure 4.3). Repeating this procedure for the available data the stiffness profile is obtained.

This simple inversion procedure was ideated to comply with the limited possibilities of numerical elaboration at the time when the SSRM method was proposed. It works quite well for sites where the stiffness of soil increases gradually with depth, but it can lead to serious mistakes if the upper layers are stiffer than the deeper ones. Still it can be very useful to obtain a first estimate of

the stiffness profile to be used as basis for more complex inversion algorithms (see Par. 4.3.2.3).

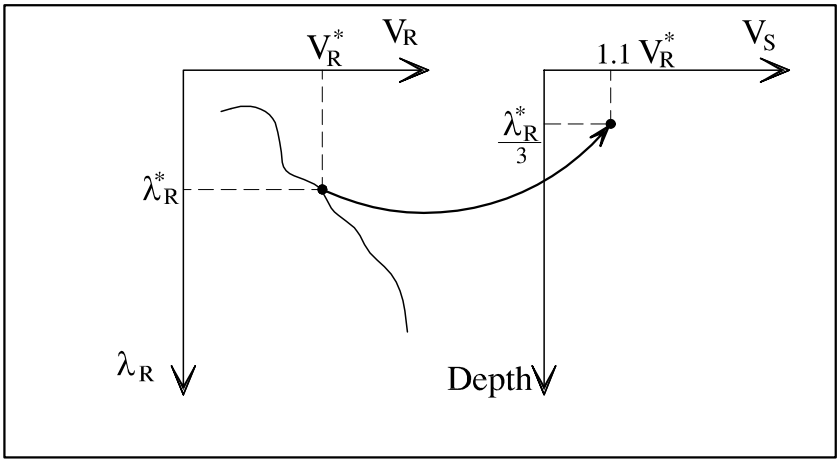

Figure 4.3 Simplified inversion process proposed for the SSRM

4.3.2 Spectral Analysis of Surface Wave (SASW) Method

Information over a broad frequency range can be obtained at one time by using an impulse source and processing the associated transient signals, which can be detected on the ground surface. SASW test is based on this observation and on the same basic idea of SSRM method.

Although it can be considered a relative young method, having been proposed and developed during the Eighties (Heisey et al. 1982, Nazarian and Stokoe 1984, Stokoe et al.1988), it is nowadays a widely used method for in situ testing.

This attempt to use the original idea of Jones in a more productive and efficient way was made possible by the technological improvements of equipment for scientific research: the availability of portable digital instruments and the increased accessibility of powerful tools for computing. The result was a much faster, for what concerns field-testing, and more accurate, for what concerns the inversion process, method for soil characterization.

The whole test can be synthesised in three different steps that lead to the final result of a stiffness profile for the site: data collecting on field, dispersion curve evaluation and inversion process.

4.3.2.1 Field Testing

The test is performed using a vertical impulse applied to the ground surface and recording the transient signal, composed mainly of Rayleigh waves over a certain frequency range, by means of two receivers placed along a straight line starting from the impulse point (Figure 4.4). The distance between the source and the first receiver is usually taken equal to that between the two receivers. This choice is not a strict requirement, but represents the result of the balance between the influence of different factors, tested through several parametric analysis based on numerical simulations (Sanchez-Salinero 1987). In the following the discussion is referred to this configuration.

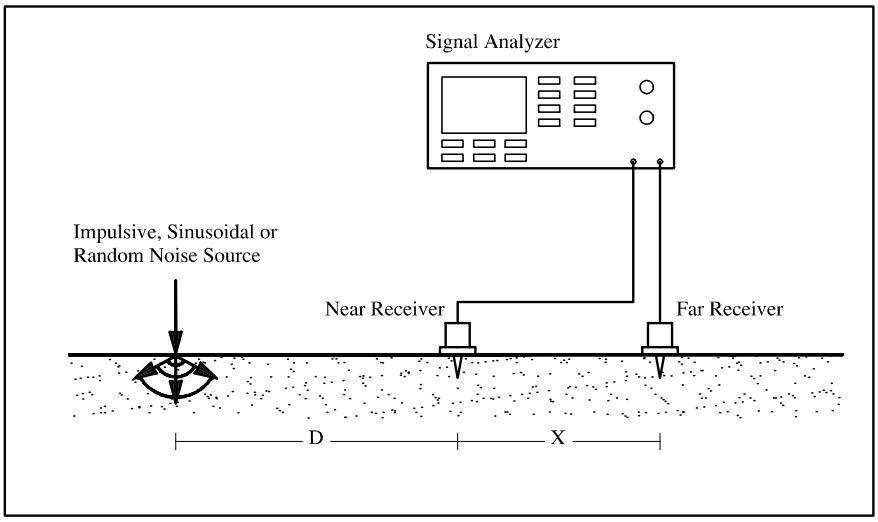

Figure 4.4 SASW method field configuration

Several repetition of the test are made for each geometrical configuration and the recorded signals are averaged, to improve the signal to noise ratio.

Only information regarding a limited range of frequency can be obtained by a given source-receivers configuration, due to many factors such as attenuation, spatial aliasing, near field effects (see Par. 4.3.2.2).

By changing receiver positions and using different sources the dispersion curve can be constructed over a wide frequency range, sufficient for the purposes of characterization. Short spacing (0.5-5 m) and weak impulse sources (such as a small hammer) are used for high frequencies (short wavelengths), while long

distance (up to 60 m) and heavy impulse sources (e.g. a massive concrete cube drop or the movements of a bulldozer) are suitable for the low frequency range (long penetration: information on deeper layers). This choice is also related to the attenuation of signals for both geometric and material attenuation: signals that have to be detected at great distance must be generated by a heavy source, which is able to generate an energetically rich perturbation.

The choice of inter-geophones distances are dictated by consideration about the frequency range of points in the dispersion curve that are obtained from each configuration: usually the choice is such that there is a certain overlap between information from one measurement and information from the successive one. Receivers are moved according to one of the following geometrical schemes:

- Common receivers midpoint array (Figure 4.5)
- Common source array (Figure 4.6)

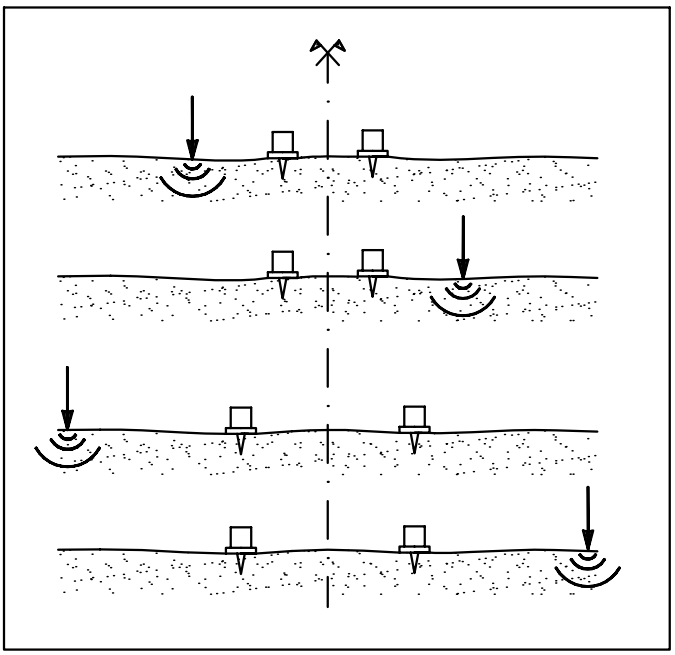

Figure 4.5 Common Receiver midpoint array with source position reversing

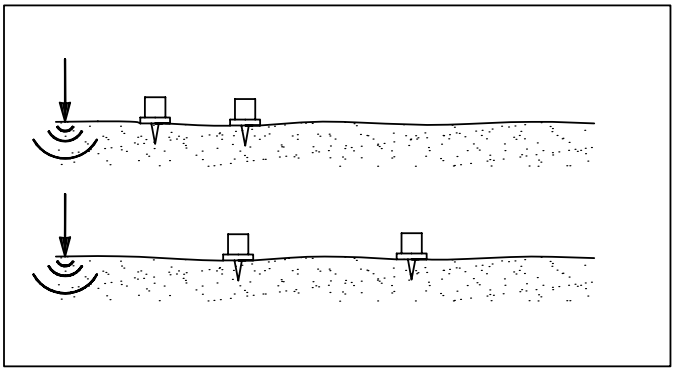

Figure 4.6 Common Source array

The choice of one or the other scheme is essentially related to site condition and source portability. Common receiver midpoint point array is often preferred because it allows the reversing of the source, i.e. for each testing arrangement the measure is performed before with the source on one side and then on the other one with respect to geophones midpoint. This expedient has mainly two objectives: one is to compensate for any internal phase distortion in the geophones that could false the results. On the other side, this is an attempt to mitigate the effects of local discontinuities, lateral inhomogeneities and bedding inclination. With respect to this last aspect it is important to remark that the SASW method and in particular the inversion process is strongly based on the hypothesis of plane and parallel layers, so any perturbation to this condition has to be treated carefully. Small differences from the ideal case should not be a great problem, but big ones are likely to invalidate the whole test results.

The usual choice for receivers is to have two vertical transducers of velocity. For pavement systems, acceleration transducers are sometimes adopted because they are more suitable for the high frequencies that are needed to characterize the very thin shallow layers.

Some researches have proposed the use of both vertical and horizontal transducers to get more information from the particles motion, being this motion in Rayleigh waves elliptical either retrograde or prograde (see Par. 3.3.1.2). This further information is proved to be useful in understanding which mode of Rayleigh waves is predominant (Tokimatsu et al. 1992a).

4.3.2.2 Signal processing and dispersion curve construction

The particle motion velocity (or acceleration) recorded at the two receivers is used to evaluate the Rayleigh wave phase velocity as a function of frequency. This step involves the computation of the time delay associated to the wave arrival at the two successive positions. Being this time delay frequency dependent, an appropriate algorithm has to be used.

The two signals in time domain ($y_1(t)$ and $y_2(t)$) (Figure 4.7) are firstly translated in frequency domain using a Fast Fourier Transform, obtaining the related linear spectra ($Y_1(\omega)$ and $Y_2(\omega)$). Using spectral analysis techniques, it is then possible to get information about the quality of the records and eventually the phase velocity as a function of frequency.

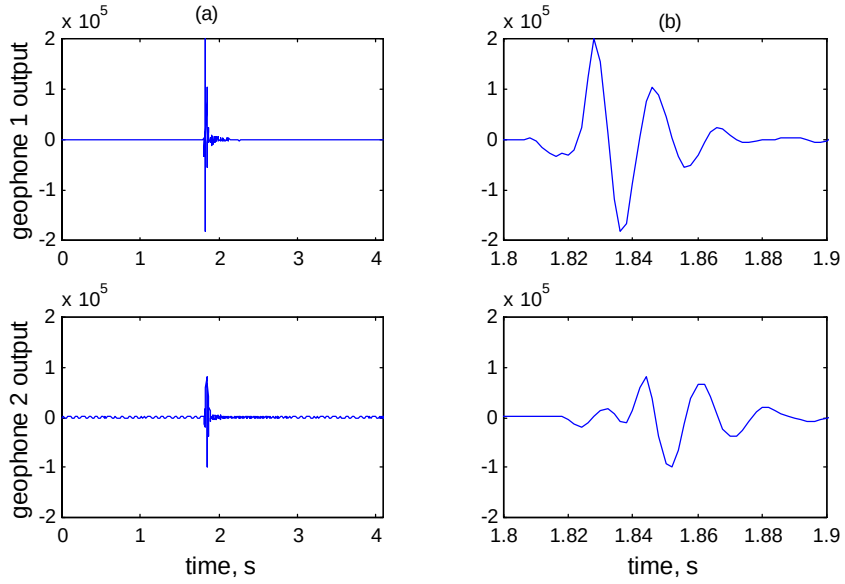

Figure 4.7 Example of SASW signals: (a) whole signals; (b) wave-train arrivals. (site: ENEA; source: 6kg hammer; d=2m)

The assessment of signal quality is made using the "coherence function", namely a spectral quantity obtained comparing different registrations, that is a measure of the degree by which input and output signals are linearly correlated. A value close to unity is an index of good correlation and hence the recorded signals

can be considered genuine and unaffected by ambient noise.

Phase velocity as a function of frequency can be obtained from the phase of the average Cross-Power Spectrum. The quantities involved in the evaluation of the dispersion curve, in the succession according to which they are evaluated, are the following:

- Auto-power spectra (Figure 4.8c,d):

$$G_{11}(\omega) = Y_1(\omega) \cdot \overline{Y_1(\omega)} \tag{4.3}$$

$$G_{22}(\omega) = Y_2(\omega) \cdot \overline{Y_2(\omega)} \tag{4.4}$$

- Cross Power Spectrum:

$$G_{12}(\omega) = Y_1(\omega) \cdot \overline{Y_2(\omega)} \tag{4.5}$$

where $\overline{\ }$ denotes the complex conjugate

- Phase of Cross Power Spectrum (Figure 4.8a):

$$\Theta_{12}(\omega) = \tan^{-1}\left(\frac{\mathrm{Im}(G_{12}(\omega))}{\mathrm{Re}(G_{12}(\omega))}\right) \tag{4.6}$$

- Coherence function (Figure 4.8b):

$$\gamma_{12}^2(\omega) = \frac{G_{12}(\omega) \cdot \overline{G_{12}(\omega)}}{G_{11}(\omega) \cdot G_{22}(\omega)} \tag{4.7}$$

- Time delay between the receivers:

$$t(\omega) = \frac{\Theta_{12}(\omega)}{\omega} \tag{4.8}$$

- Phase velocity of Surface waves:

$$V_R(\omega) = \frac{D}{t(\omega)} \tag{4.9}$$

where D is the distance between the two receivers.

- Wavelength:

$$\lambda_R(\omega) = \frac{V_R(\omega)}{f} \tag{4.10}$$

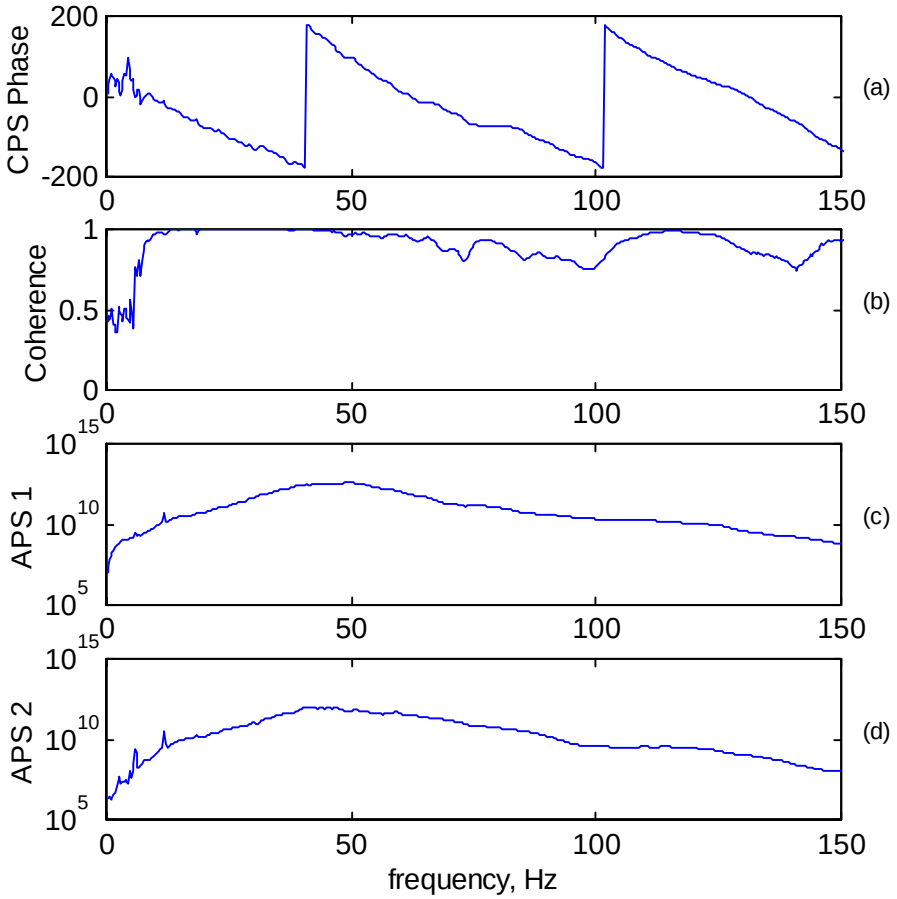

Figure 4.8 Spectral quantities evaluated from the signals of Figure 4.7: (a) Phase of the cross-power spectrum; (b) Coherence function; (c) Auto-power spectrum (first receiver); (c) Auto-power spectrum (second receiver).

The use of the cross-power spectrum phase for the evaluation of the frequency dependent time delay is based on the hypothesis that the wave group under consideration is composed of a single mode of propagation and hence the phase velocity is function only of frequency (Aki and Richards 1980). Under such assumption the signal that is associated to a wave propagating along the x direction can be expressed as a superposition of harmonic waves of the same mathematical

form of that propagating in a homogenous halfspace (Equation 3.9):

$$y(x,t) = \frac{1}{2\pi} \int_{-\infty}^{+\infty} |y(x,\omega)| \cdot e^{i\cdot[\omega t - k(\omega)x + \phi(f)]} \cdot d\omega \tag{4.11}$$

where $y(x,\omega)$ is the amplitude spectral density, $k(\omega)$ is the wavenumber and $\phi(\omega)$ is a constant phase term due to effects other than propagation. The Fourier transform of such signal is:

$$Y(x,\omega) = \int_{-\infty}^{+\infty} y(x,t) e^{i\omega t} dt = |y(x,\omega)| \cdot e^{i\cdot[\phi(\omega) - k(\omega)x]} \tag{4.12}$$

hence considering the cross-power spectrum relative to two different detection of the same wave along the x-axis at location x_1 and x_2:

$$\begin{aligned} G_{12}(\omega) &= Y_1(\omega) \cdot \overline{Y_2(\omega)} = \\ &= |y(x_1,\omega)| \cdot e^{i\cdot[\phi(\omega) - k(\omega)x_1]} \cdot |y(x_2,\omega)| \cdot e^{-i\cdot[\phi(\omega) - k(\omega)x_2]} = \\ &= |y(x_1,\omega)| \cdot |y(x_2,\omega)| \cdot e^{i\cdot k(\omega)\cdot(x_2 - x_1)} \end{aligned} \tag{4.13}$$

and recalling that

$$k(\omega) = \frac{\omega}{V_R(\omega)} \tag{4.14}$$

Equation (4.8) can be obtained with few manipulations.

It is important to note that according to the concept of mode superposition, which has been exposed in Paragraph 3.3.1.1, the quantity $k(\omega) \cdot x$ that appears in the phase of Equation (4.11) and successive ones is not correct for a layered medium. Recalling the mathematical description of surface waves in layered elastic media that has been reported in Chapter 3, it is clear that the process described above results in an approximate estimate of the effective phase velocity, that is described by Equation 3.21, substituting the differentiation with finite increment differentials. The strong implication is that the measured quantity, besides being approximate, is also function of the spatial locations where the wave is measured. In particular for the cases in which there is no predominant mode of propagation the consequences can be very serious (see Chapter 5). This must be kept in mind when interpreting the dispersion curves obtained in the SASW test.

Using the procedure that is outlined by Equations (4.3) to (4.9) for each source-receivers arrangement, it is possible to obtain a certain number of points of

the dispersion curve. The frequency range over which the above estimate of phase velocity can be considered reliable depends on signal to noise ratio and on some consideration regarding receivers location and wavelength, as stated in the preceding paragraph and explained in details hereafter.

As far as noise is concerned the most of the selection is based on the coherence function (Fig. 4.7b). Looking at its mathematical definition it is clear that if it is evaluated for a single pair of signals it loose significance since it will be equal to one over the whole frequency range. Properly coherence is calculated from mean spectra of an ensemble of measurements. The more the signals that are detected by the second receiver are (linearly) related to those of the first one, the more the coherence will be high (eventually equal to one for those frequency at which the signal strongly prevails over noise and the relationship between the signals is linear). Note that the use of an higher number of impulses, i.e. repetitions of the test, for the same configuration will result in general to a prevalence of the actual signal over uncorrelated noise and hence in higher values of the coherence function.

The auto-power spectra (Fig. 4.7c,d) give an estimate of the frequency distribution of energy for each signal. Frequency ranges where their values are high are likely to be those in which the generated signal is stronger and hence it prevails over uncorrelated noise. This is the reason why lighter sources are used for smaller receivers spacing, since these sources generate much more energy at higher frequency (see Paragraph 8.3).

Since most of the time field data are collected using a signal analyser, the in-situ visual inspection of the above spectral quantities can constitute an important preliminary judgement about the quality of data and the necessity of more repetitions.

The other aspect in the selection of reliable results is the so-called filtering criterion (Ganji et al. 1998). This is based on some basic restrictions on the information that can be obtained from each given source-receivers configuration in the view of mitigating body wave (near field) effects and signal deterioration caused by attenuation.

The estimation of the near field of the point source, i.e. the location where it cannot be assumed that the whole motion is related only to Rayleigh waves propagation, is one of the major problem in the SASW test. Initially it was proposed to discard all data for which the distance between the source and the first receiver was less than one third of the obtained wavelength (Heisey et al. 1982). Successively some numerical analysis showed that this criterion underestimates the extension of the near field (Sanchez-Salinero 1987).

Usually a near field extension of half wavelength is assumed for a normally dispersive soil (i.e. where stiffness is increasing with depth) whereas about two

wavelength is a more prudential estimate for a strongly inverse dispersive soil (i.e. where a soft layer is present below or trapped between stiffer ones). These indication are based on numerical simulation of the complete wavefield generated by a point source (Tokimatsu 1995) for different layer configurations. Nevertheless there is still an open discussion about the influence of direct and reflected/refracted body waves on the recorded signals.

It is important to remark that being the Rayleigh waves dispersive in layered media, the distance at which the condition of far field can be assumed is not a constant, but depends on the frequency analysed. For example considering a wrapped cross power spectrum phase (Fig. 4.7a), discarding data affected from an half wavelength long near field is equivalent to cut information given by an initial section of 180 degrees (i.e. the portion between 0 and the first jump).

On the other side, because of attenuation, data relative to inter-receiver distance higher than about three wavelengths are usually strongly affected by noise (Stokoe et al 1988) and therefore it is preferable to discard them.

In summary, assuming that no strong contrasts of stiffness are present, for each receivers configuration the following restriction are applied to select data:

$$\frac{D}{3} < \lambda < 2D \tag{4.15}$$

in which λ is the estimated wavelength and D the inter-geophone distance, that is taken equal to the distance source-first geophone.

A clear interpretation of filtering criteria is given by Figure 4.9, showing the whole set of data that can be obtained by a given experimental setup and the subset that is considered acceptable.

It is important to remark that although other more prudential (especially for what concerns the near field extent estimation) criteria have been proposed, they are often of small practical interest for soil characterization. Indeed, since they make prohibitive to obtain information for long wavelengths, the inversion process cannot be used to infer stiffness at adequate depth. In summary an engineering judgement is required in choosing the filtering criterion: it is necessary to balance the loss of accuracy that can arise from near field effects and the importance of additional information for the inversion process (Rix 1988).

One crucial step in the above signal processing procedure is the unwrapping of the cross power spectrum phase. Any standard Fourier transform algorithm produce a modulo-2π representation of the phase spectrum that is very difficult to interpret and unsuitable for further processing (Poggiagliolmi et al. 1982). The passage to an unwrapped (full-phase) curve (Figure 4.9) is necessary for the computation of time delay as a function of frequency using Equation (4.8).

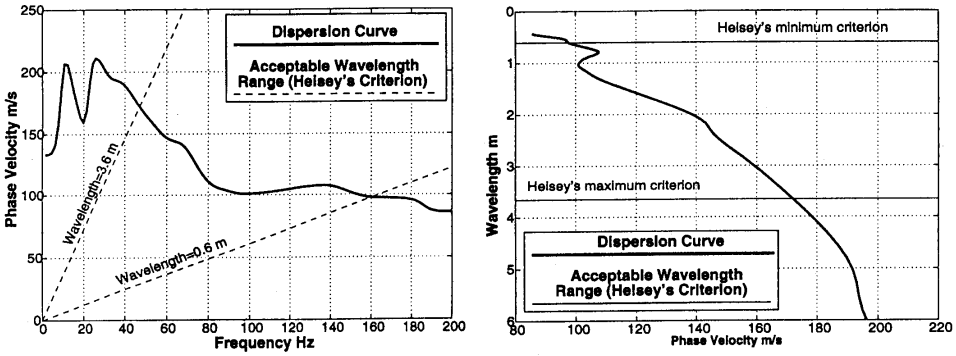

Figure 4.9 Example of application of filtering criteria to the dispersion curve correspondent to one source-receivers configuration (from Gukunski et Al. 1998)

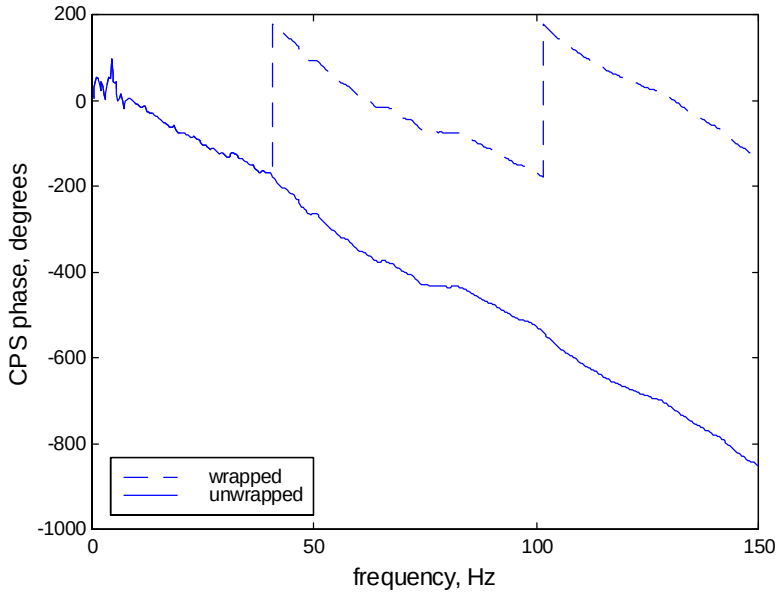

Figure 4.10 Unwrapping process of the cross power spectrum phase of Figure 4.8(a)

Usually this step is conducted using some automated algorithms (Poggiagliolmi et al. 1982), but many problems can arise due to the influence of noise that can produce fictitious jumps in the wrapped phase. Not always the

operator judgement can solve this problem and still it remains a subjective procedure (Al-Hunaidi 1992).

The whole ensemble of data collected using a series of geophones configurations have to be assembled to create only one final dispersion curve covering a wide enough range of frequency. Moreover since the inversion process can't manage very large amount of points, a quantitative reduction of the available information is required. Usually for any sub-set in frequency (or wavelength) the average value of phase velocity is assigned to the central frequency (or wavelength) of the sub-set. Still there are a couple of problems: one is that the choice of reducing points in the frequency or wavelength domain must be made consistently with the domain successively adopted for the inversion process. The other one is about the significance of adopting the mean value of a population that hardly can be seen as a statistical distribution (this because the number of overlapping information in a given frequency range is arbitrary, depending on testing configurations, quality of data, etc.).

As seen above, the construction of the experimental dispersion curve is strongly affected by the operator's experience, since a selection of significant and corrected data is actually required. Moreover since it is time consuming and it involves many manipulations of the data, it is usually conducted in the office after data collection in the field. This can be considered a limitation of the testing procedure, since a critical visual inspection of the experimental dispersion curve on the field could lead to a real time judgement, with subsequent decisions about the necessity of collecting some extra data.

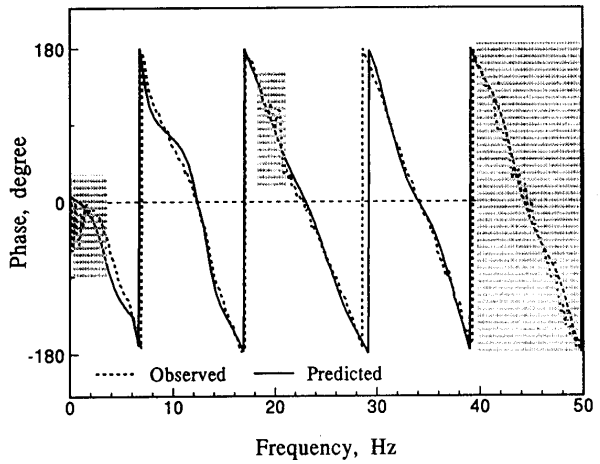

Figure 4.11 Example of least-square approximation of Cross Power spectrum phase for automated dispersion curve evaluation (from Nazarian and Desai 1993)

To comply with this problem an automated method has been proposed for the dispersion curve generation from raw field data (Nazarian and Desai 1993). It is based on a procedure for estimating the phase of the cross power spectrum at each frequency using a weighted least-square best-fit solution that approximates the original data (Figure 4.11). The weighting function is based on the values of the coherence function and the final result is a smoother dispersion curve, if compared to that computed with the manual procedure.

4.3.2.3 Inversion process

Finally the soil mechanical parameters have to be estimated from the dispersion curve. Usually this task is accomplished assuming a model of horizontally stratified elastic medium (Figure 4.12). This process is named inversion. The unknown are four for each layer, i.e. thickness, density, shear modulus and Poisson ratio. Many parametric studies have been devoted to assess the influence of each one of these parameters (Nazarian 1984, Sanchez-Salinero 1987). The general conclusion is that the influence of density and Poisson number is negligible, so that they can be estimated on the basis of experience without sensible effects on the final result.

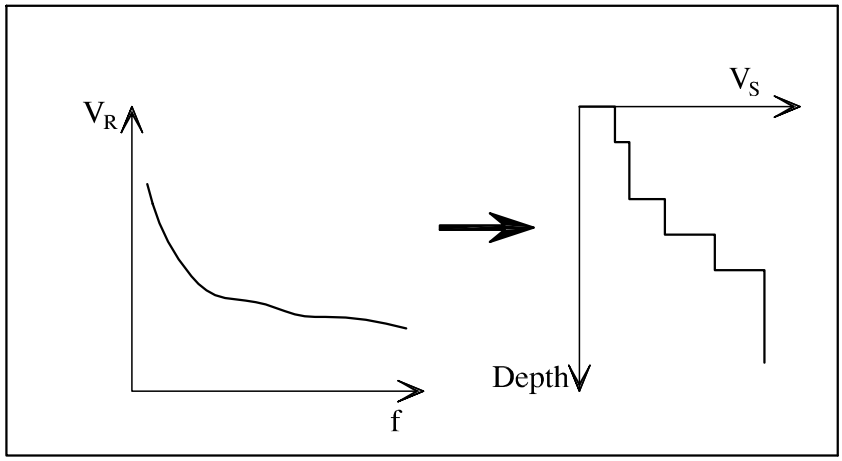

Figure 4.12 Inversion process

Many different techniques of inversion have been proposed to obtain the soil stiffness profile starting from the dispersion curve. Recent improvements in

computational capabilities have made it possible to use more accurate solutions of the forward problem of Rayleigh Wave propagation, which is clearly the basis of the inversion process (see Par. 3.3.1.1). Nevertheless it must be recalled that, in general, inversion is a not trivial task since it's not a mathematically well posed problem and the solution is not unique (i.e. more than one stiffness profile can correspond to nearly the same dispersion curve).

A first procedure to invert the dispersion curve is based on a simple trial-error procedure. An initial first tentative profile of the site is set, if it is the case by using a priori information from previous geotechnical tests. The forward problem of wave propagation is then resolved and the computed dispersion curve is compared to the experimental one. In the successive step some parameters of the initial model are changed in the view of improving the fitting between numerical and experimental data. The judgement about the effectiveness of the fitting is usually done by a least-square criterion and by visual inspection. The process follows an iterative scheme and eventually it converges to an acceptable solution. Such a method has been used since the first applications of the SASW method. Clearly it is a tedious time consuming job and moreover the convergence requires the expertise of the operator in adjusting the trial parameters.

To overcome such difficulties several automated inversion processes have been successively proposed (Yuan and Nazarian 1993, Lai 1998, Ganji et al. 1998). A crucial step in this regard is the computation of the Rayleigh phase velocity derivatives with respect to layers thickness or to layers stiffness that are needed for the (weighted) least-square procedure. Their numerical evaluation can be inaccurate and very time consuming. The convergence of the procedure is strongly dependent on the initial guess, not only in terms of convergence velocity but also regarding the effective convergence of the process to the right solution (local minima problem).

A very appealing possibility can be given by the use of neural networks trained with results of many numerical solutions of the forward problem regarding different soil layer configurations (Meier and Rix 1993, Williams and Gukunski 1995). This "black box" approach has given many interesting results in other fields, but the problem is the computational effort required to train the network and the risk of overspecialisation that can be caused by the use of too much training cases.

Apart from the inversion algorithm, a big deal in inversion processes is the choice of the wave propagation simulation procedure (i.e. the forward problem), which can be considered its engine. A short review of the most common methods used to build the governing equations has been reported in Chapter 3.3.1.1. A great difference between inversion codes is the possibility of accounting for mode superposition. In a fundamental mode analysis, only the first of the free vibration modes is considered. This can be an acceptable solution if effectively the

fundamental mode is predominant (see Par. 3.3.1.2), but in general it can be very misleading. Many problems can arise from the presence of softer layers between stiffer ones or of a stiff top layer. In such situations the influence of higher modes is very strong and hence it is essential that their contribution be considered in the interpretation of the experimental dispersion curve (Gukunski and Woods 1991, 1992).

A more accurate solution can be obtained considering mode superposition in evaluating the effective Rayleigh phase velocity, associated to the case of forced vibration (Roesset et al. 1991, Tokimatsu 1995, Lai 1998). It is important to remark that the effective phase velocity is spatially dependent and hence in the inversion process a choice must be made about the points in which it is evaluated. This problem is not trivial and must be examined carefully, also with respect to the actual receivers position in the testing procedure.

It is noteworthy to mention that to avoid the use of a conventional quantity such as the effective dispersion curve, a very appealing procedure is to invert directly the Fourier frequency spectra of observed ground motion associated to surface wave propagation (Szelwis and Behle 1987). This different perspective, although certainly computationally expensive, is very promising for future applications.

4.3.2.4 Controlled Source SASW and Continuous Surface Wave methods

These are variants of the SASW method, the main difference being the use of a sinusoidal input signal generated by an electromagnetic vertical vibrator, that produces a series of amplitude modulate pulses at various frequencies.

The comparison between the characteristics of signals generated by different kind of sources, such as impact sources, vibrators and random noise sources shows the great advantages that a continuos source can give in terms of higher value of the signal-to-noise ratio (Rix 1988).

Data acquisition at different frequencies can be easily automated connecting source and receivers to an adequate device. One of the main problem is given by the limited mass of the portable shakers that are usually adopted, indeed with these sources it is difficult to perform the test at low frequencies and hence to obtain information about deep layers. One possible solution is given by the use of large truck-mounted seismic vibrators (or vibroseis) (Andrus et al. 1998) often used as sources in large scale geophysical surveys, but the cost of this kind of apparatuses is prohibitive for usual geotechnical testing. Anyway using adequate vibrators, significant depths can be investigated, up to 100 m, whereas using impulsive sources the limitation is stronger due to the greater influence of ambient noise.

Often the continuous source is adopted in the classical framework of SASW

test and the dispersion curve is evaluated using the same signal processing technique, with the difference that in this case the linear spectra of recorded signals are characterised by a predominant frequency. On the other hand, taking advantage of the enhanced signal quality and of the harmonic nature, some other techniques for the derivation of the phase velocity have been developed.

In the CSW (Continuous Surface Wave) method (Matthews et al. 1996, Menzies and Matthews 1996), the dispersion curve is obtained using an array of receivers. It can be shown that for steady state signals the Rayleigh wave wavelength can be computed as the slope of the resulting phase angles plotted against source-to-receiver distance. If the fundamental mode is the predominant one, an advantage of using several geophones is that the best fitting line passing through experimental data minimise the influence of variations in the data caused by internal phase in the instruments and by small local discontinuities. Another advantage can be the possibility of attenuating the possibility of errors in phase unwrapping. Adequate attention must be paid to near field effects.

The CS-SASW (Controlled-Source Spectral Analysis of Surface Waves) technique is a sort of combination of the Steady State Rayleigh method and the SASW method (Satoh et al. 1991). Using a harmonic source and a pair of receivers that are connected to a signal-conditioning unit the travel time of a steady state surface wave along a certain distance is derived and from it the phase velocity. With a sweep in frequency the whole dispersion curve can be obtained. Inversion techniques are similar to those used in the SASW test, also if an approximate solution, based on a modified version of the procedure of Figure 4.3, has been proposed and it seems to work quite well, reducing substantially the computation time.

An interesting solution proposed for the inversion process of data obtained with an electromechanical shaker makes use of vertical and horizontal particle motion to discern between modes of propagation (Tokimatsu 1991). It is based on superposition factors for modes calculated with Haskell-Thomson approach, as found by Harkrider (1964) for a point source. Layering is then estimated using a non-linear least square procedure. The non-uniqueness of the solution can be mitigated using information from horizontal radial displacements: comparing particle orbits from simulation with different solution of layering with the observed ones it’s possible to obtain the most likely solution. In this last case the advantage of using a controlled source is essentially related to the possibility of having better signals than those of impulsive source testing.

4.3.2.5 A time-frequency approach for dispersion curve evaluation

The use of time-frequency distribution techniques is gaining interest in many fields where signals with strong non-stationary components have to be analysed. SASW signals, that are generated by impulsive sources, are inherently non-stationary and often they show low values of signal-to-noise ratio requiring a technique that minimises noise effects.

Recently a time-frequency algorithm for dispersion curve evaluation for SASW test conducted using impulsive sources has been proposed (Audisio et al. 1999). It seem to be very promising for automation of dispersion curve evaluation since no subjective decisions based on coherence or other indicators of data quality are needed and the unwrapping of the CPS phase is avoided.

Using appropriate transforms any signal can be represented by its energy density $C(t, f)$, function of frequency and time. With such procedures a one-dimensional signal is transformed in a two-dimensional spectrum and the momentary signal characteristics can be analysed at different times. The classical example of a time-frequency distribution is the *Short Time Fourier Transform*: the signal is sampled by a moving window in time and each portion is analysed separately with a Fourier Transform. Many other time-frequency distributions have been defined in the past to enhance the potentiality of the analysis for particular fields of application.

For the case of surface waves analysis, a two-station model is considered. In absence of additive noise and neglecting attenuation, the two signals can be represented as $x(t) = s(t)$ and $y(t) = s(t - d)$, where d is the frequency dependent time delay to be estimated. Applying the time-frequency analysis, it is possible to get the relative representations $X(t, f)$ and $Y(t, f)$, equal to each other but with the second delayed of d. Then, using these representations, time delay can be easily computed, for a particular frequency f_0, as the difference of two generic moments when the two functions $X(t, f)\big|_{f=f_0}$ and $Y(t, f)\big|_{f=f_0}$ assume the same value. Repeating this process for the whole band, the time delay as a function of frequency is obtained.

If $x(t)$ and $y(t)$ are corrupted by additive noise, $X(t, f)\big|_{f=f_0}$ and $Y(t, f)\big|_{f=f_0}$ have different shapes, thus it's necessary to define a conventional quantity on which estimating the time delay for $f = f_0$. One possible solution is given by the use of the barycentres of $X(t, f)\big|_{f=f_0}$ and $Y(t, f)\big|_{f=f_0}$ (Figure 4.13), that are defined by the following formulas:

$$B_x = \frac{\int_{-\infty}^{+\infty} t\,X(t,f)\big|_{f=f_0}\,\mathrm{d}t}{\int_{-\infty}^{+\infty} X(t,f)\big|_{f=f_0}\,\mathrm{d}t} \tag{4.16}$$

$$B_y = \frac{\int_{-\infty}^{+\infty} t\,Y(t,f)\big|_{f=f_0}\,\mathrm{d}t}{\int_{-\infty}^{+\infty} Y(t,f)\big|_{f=f_0}\,\mathrm{d}t} \tag{4.17}$$

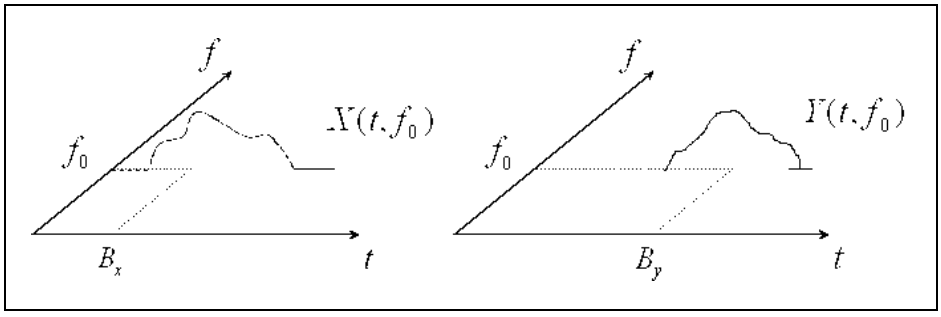

Figure 4.13 Graphical representation of barycentres (from Audisio et al. 1999)

The difference between the two barycentres is the time delay d for that given frequency f_0:

$$d\big|_{f=f_0} = B_y - B_x \tag{4.18}$$

Once the frequency dependent time delay has been obtained repeating the above calculation over the pertinent frequency range, the phase velocity and wavelength of surface waves are found using the same procedure of the standard algorithm.

Time delay estimation using this algorithm is less influenced by signal to noise ratio if compared to the standard procedure for impulsive source SASW test, because noise distribution in both frequency and time domains is considered. The

influence of noise on the barycentres, which are the fundamental quantities of this procedure, is usually of minor importance if compared to the modifications that noise can produce in the cross power spectrum.

4.4 Attenuation and Damping

An open problem in geotechnical testing is the determination of damping ratio for hard-to-sample soils. Indeed quite all the procedures to estimate dissipative properties of geomaterials are laboratory ones and therefore are best suitable for cohesive soils. Nevertheless attenuation properties of soils have a great influence in the determination of the seismic response of a site.

One of the main problems for damping assessment in situ is represented by the difficulty of separating the intrinsic attenuation of the medium from other damping mechanisms such as geometrical attenuation, reflection, scattering and near-field spreading. As a consequence in situ estimates tend to overestimate the damping properties of the medium and as much care as it is possible must be taken to account for the different attenuation mechanisms.

Some applications have been proposed based on the cross-hole method to obtain the damping ratio together with small strain stiffness of soils (Hoar and Stokoe 1984, Mancuso 1992). The damping ratio is computed from particle motion attenuation, evaluated between two detection points, taking into account the geometric attenuation factor. This technique allows the reconstruction of a damping ratio profile with depth, that in conjunction with the stiffness profile represents a good characterization of the site. It must be noted that the procedure requires the adoption of a three boreholes scheme and hence it is quite expansive.

Other geophysical applications have been also developed to estimate the damping properties of soils. Techniques such as the Spectral Ratio Method and the Rise-Time Method have proven to be suitable for the determination of a mean value of the attenuation from seismograms recorded on the surface, without the need for boreholes (Jongmans 1992). The resolution of such methods is very poor, but the rough estimate can be useful for some applications.

Many techniques based on the study of surface waves propagation have been applied in seismology and extended to geophysics to determine respectively the attenuation characteristics of Earth's crust layers (Anderson et al. 1965, Mitchell 1975) and of large basins (Malagnini et al. 1995, Jongmans and Campillo 1993). As for shear wave velocity, also in this case, the big difference in comparison to geotechnics is the scale of application.

The underlying concept of shear damping ratio assessment from surface

waves propagation measurements is analogous to that of shear stiffness determination. Once surface waves attenuation as a function of frequency has been obtained from field measurements, an inversion process is applied to infer the shear damping ratio profile (Figure 4.14).

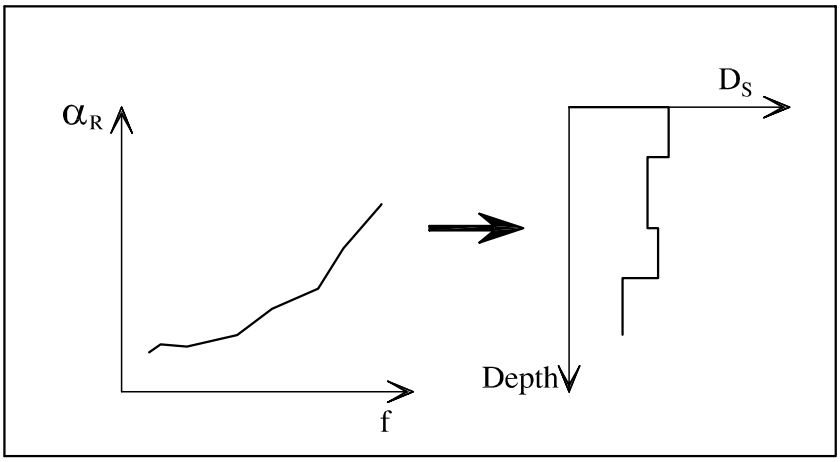

Figure 4.14 Inversion process to get damping ration profile from attenuation curve

Actually there is a strong coupling between Rayleigh wave attenuation and dispersion (Lai 1998, Aki and Richards 1980) so that the inversion process can't be seen as the mere conjunction of two separated steps.

A comprehensive overview of the algorithms that can be used for the inversion process can be found in Lai (1998), where various algorithms are proposed (with different combinations of coupled/uncoupled inversion algorithms with fundamental-mode-only/mode-superposition analysis). The more rigorous solution is given by a coupled algorithm for the simultaneous inversion of dispersion and attenuation curves, accounting for mode superposition in the solution of the forward problem. The complexity of a similar procedure is very high and it requires a robust and coherent determination of the experimental curves.

In the following two experimental procedures for the determination of Rayleigh dispersion and attenuation curves are described.

4.4.1 Uncoupled measurements

In this case, the experimental dispersion and attenuation curves are evaluated separately in two different testing sessions (Rix et al.1999b). Firstly the dispersion curve is obtained, using the classical two-station approach of the SASW method, and the relative inversion process is carried out to get information about the stiffness profile at the site. This preliminary estimate of the stiffness profile is necessary because the geometrical attenuation factor (see Par. 3.3.2) is not known a priori and hence surface wave material attenuation cannot be properly evaluated.

The subsequent measurement of the surface wave attenuation is based on a multi-station scheme (Figure 4.15), in which particle velocity is measured at several locations along a straight line. From these raw data, particle displacements are computed and, with a regression analysis, the surface wave attenuation coefficients are obtained.

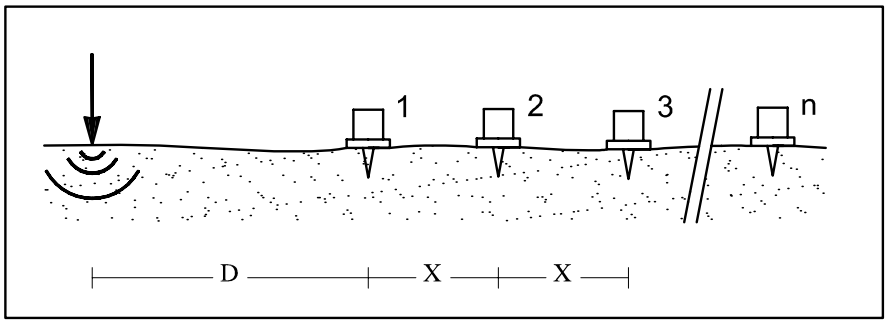

Figure 4.15 Multistation array configuration

For a reliable estimation of the displacement spectra a correction of the particle velocity spectra in frequency domain is necessary to mitigate the effect of uncorrelated noise. In this respect it is necessary to characterise the input of the system (the soil) that produces the given output (the motion at the geophone location). For example if a shaker is used as controlled harmonic source, the acceleration of its frame is measured and it represents a valid estimate of the input.

The correction factor is the coherence function γ_{sr} that can be computed considering the mean input acceleration spectrum, the mean output velocity spectrum G_{rr} and the relative cross power spectrum, obtained averaging several measurements.

The noise corrected velocity spectrum $\overline{G_{rr}}$ is then given by (Bendat and Piersol 1993):

$$\overline{G_{rr}}(\omega) = \gamma_{sr}^2(\omega) G_{rr}(\omega) \tag{4.19}$$

and consequently the experimental particle displacements spectrum $U_z(r,\omega)$ for the receiver position r, can be evaluated as:

$$\left|U_z(r,\omega)\right| = \frac{\left|\dot{U}_z(r,\omega)\right|}{\omega} = \frac{\sqrt{\overline{G_{rr}}(\omega)}}{\omega \cdot C(\omega)} \tag{4.20}$$

where $C(\omega)$ is the frequency dependent calibration factor of the geophone.

After particle displacements spectra have been measured for a number of receiver locations, the attenuation factors α_R are evaluated with a non-linear regression process based on the mathematical formulation for particle displacements spectra in a weakly dissipative medium (Lai 1998):

$$\left|\mathrm{U}_z(r,\omega)\right| = F_z \cdot \mathrm{G}(r,\omega) \cdot e^{-\alpha_R(\omega) r} \tag{4.21}$$

where F_z is the dynamic force transmitted by the vibrator, that can be seen as a second unknown of the regression, and $\mathrm{G}(r,\omega)$ is a function that represents the geometrical attenuation law for Rayleigh waves in a vertically layered system (see Par. 3.3.1.1).

For a homogeneous halfspace this law simply reduces to a constant b divided by the well-known geometric attenuation factor $\sqrt{r}$ (see Equation 3.8):

$$\mathrm{G}(r,\omega) = \frac{b}{\sqrt{r}} \tag{4.22}$$

The general expression for a stratified medium is a complicated function that comes out from mode superposition and it depends on frequency (Lai 1998). The stiffness profile of the site has to be evaluated in advance, since it is a necessary information for computing the function $\mathrm{G}(r,\omega)$.

4.4.2 Coupled measurements using transfer functions

Recently a new method has been proposed to simultaneously measure the dispersion and attenuation curves at a site, using a coupled regression process on a

single set of measurements (Rix et al 1999a). This allows not only a great saving of testing time, but especially the possibility of accounting for the strong coupling between phase velocity and attenuation. As a consequence the subsequent inversion process is globally more stable from a mathematical point of view, because a consistent set of data is used as input. The greater amount of information can be beneficial also if only the stiffness profile is of interest, because the problem is more well-posed in general.

The proposed method is based on the use of the transfer function concept, which is a classical tool for the analysis of linear time invariant dynamic systems (Santamarina and Fratta 1998). Considering a given physical system, the transfer function is defined in the frequency domain as the ratio between the output and the related input (Figure 4.16). Since the input signal is modified by the system, the transfer function carries all the information that is needed to characterize the system. The main problem is to extract such information and for this purpose a model of the system has to be set.

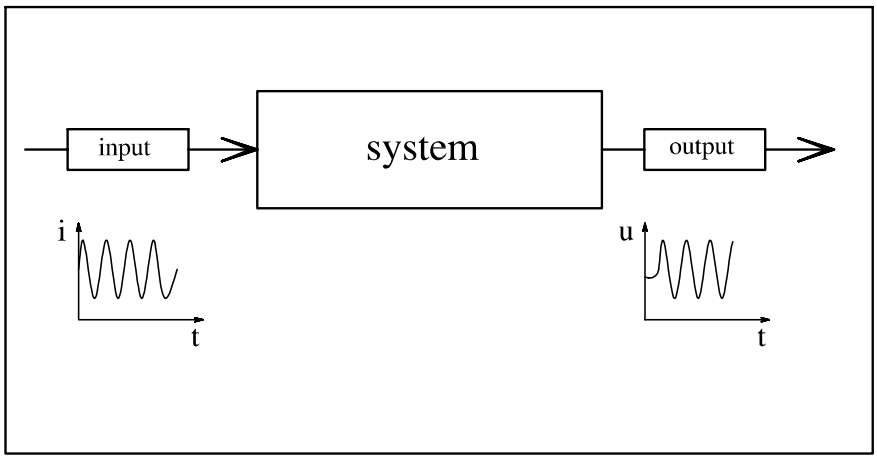

Figure 4.16 Transfer function concept

The test setup is based on the same multistation scheme adopted for the measurement of surface wave attenuation (Figure 4.15). Using an accelerometer mounted on the top of the vibrator to characterise the input and one receiver placed on the ground surface for the output, the transfer function can be measured using the controlled source with a sweep in frequency (Figure 4.17). The process is then repeated for different receiver locations. In case using a multichannel signal

analyser and many receivers data collecting can be done at once.

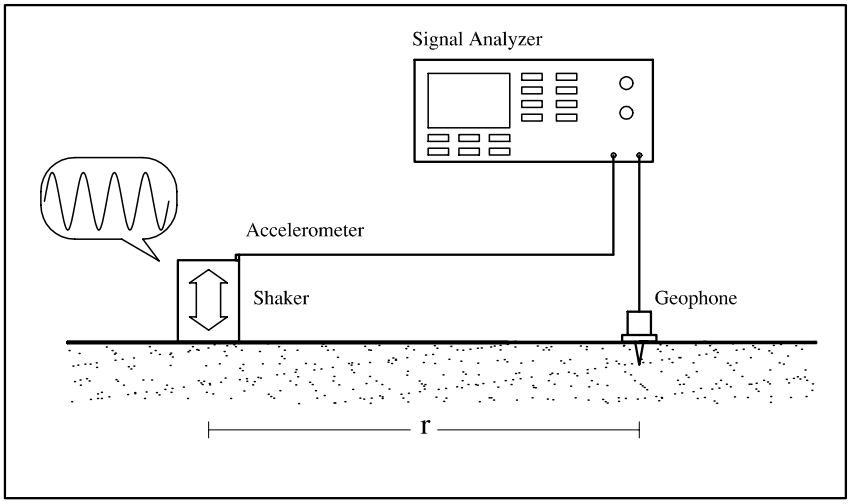

Figure 4.17 Testing configuration for transfer function measurement on the field

Once the experimental transfer function has been obtained with such measurements, a regression analysis is used to estimate Rayleigh phase velocity and attenuation. The basis for such fitting process is the analytical expression of the transfer function, which can be obtained choosing a consistent soil model.

Modelling the soil as a stack of viscoelastic plane and parallel layers and neglecting body waves contributions, the vertical displacements U_z at a certain distance from the source r and at a given frequency ω can be expressed as (Lai 1998):

$$\mathrm{U}_z(r,\omega) = F_z \cdot \mathrm{G}(r,\omega) \cdot e^{i[\omega t - \Psi(r,\omega)]} \tag{4.23}$$

where F_z and $\mathrm{G}(r,\omega)$ are again respectively the dynamic force transmitted by the vibrator and the geometrical attenuation law and $\Psi(r,\omega)$ is a complex-valued phase angle. From Equation (4.23) and considering that the input force is harmonic in time, the *displacement transfer function* $T(r,\omega)$ can be written as:

$$\mathrm{T}(r,\omega) = \frac{U_z(r,\omega)}{F_z \cdot e^{i\omega t}} = \mathrm{G}(r,\omega) \cdot e^{-i \cdot \Psi(r,\omega)} \tag{4.24}$$

This expression can't be used directly for the regression process on experimental data because the complex-valued phase angle is implicitly dependent on the source-receiver distance. Introducing the hypothesis that the phase angle $\Psi(r,\omega)$ corresponds to a single mode of propagation, its dependence on the source to receiver distance becomes linear with a complex coefficient $K(\omega)$ (complex wavenumber), whose expression is:

$$K(\omega)=\left[\frac{\omega}{V_R(\omega)}+i\alpha_R(\omega)\right] \tag{4.25}$$

Accordingly, the analytical expression of the displacement transfer function is now explicit in r :

$$\mathrm{T}(r,\omega)=\frac{U_z(r,\omega)}{F_z\cdot e^{i\omega t}}=\mathrm{G}(r,\omega)\cdot e^{-i\cdot K(\omega)\cdot r} \tag{4.26}$$

There is still a major problem to be solved, indeed the geometric spreading function $\mathrm{G}(r,\omega)$ is not known a priori. As stated above it is a function of the shear stiffness profile of the site, that is one of the final objectives of the testing procedure. This problem could be solved rigorously using an iterative procedure that is likely to converge in a few steps: a first iteration is made considering the classical geometrical spreading law of a homogeneous halfspace (Equation (4.22)). Subsequently using the resulting shear stiffness profile the function $\mathrm{G}(r,\omega)$ is evaluated and the process is repeated.

It is important to note that both the displacements transfer function and the wavenumber $K(\omega)$ are complex valued quantities. The regression process can be conducted using a classical minimisation algorithm, but it needs the definition of a consistent norm, which has to be valid in the complex numbers space.

Once the complex wavenumber has been estimate, it is possible to obtain directly from its real and imaginary parts the average effective Rayleigh phase velocity and attenuation coefficient relative to the zone covered by the receiver array . The dispersion and attenuation curves of the site are obtained repeating the process over the frequencies of interest.

A noteworthy aspect of this testing procedure is that phase velocity and attenuation are obtained from the same set of data and moreover the regression process minimise a combined quantity, so that it is much well conditioned and stable than an uncoupled regression.

4.5 Geophysical Approaches

Very often, in geophysical testing, surface waves are seen as a disturbance. Indeed what is usually named ground roll, i.e. the correlated noise always present in the traces that partially obscures the arrivals of reflected body waves, is essentially given by the surface wave components of the motion. For this reason geophysicists developed many techniques to separate surface waves from the rest of the signal due to body waves. Some of these techniques can be usefully applied to estimate the experimental dispersion curve at a site.

On the other side, seismological techniques have been often used to analyse Earthquakes or microtremors measurements in the view of assessing the macrostructure of Earth on a geologic scale (Dorman and Ewing 1962, Aki and Richards 1980). The distances involved in such phenomena are much bigger than the usual distances in geotechnical testing. This is for sure a great difference because of mode separation, nevertheless these applications paved the way for geotechnical methods based on surface wave propagation and possible applications of the relative analysis techniques can be explored.

4.5.1 Frequency-wavenumber analysis

The most common use of discrete Fourier transform is made to map data from the time domain to the frequency domain and this is undoubtedly the basis of all signal analysis techniques. Nevertheless the same basic concept can be extended to any sequential series other than time. Thus the discrete Fourier transform applied along a straight line in space leads to the wavenumber domain. The application in two independent variables is the essence of the double transform, such that for example a series of time histories recorded along a straight line in space is converted in its frequency-wavenumber spectrum with no loss of information (see Appendix A).

The 2D Fourier transform that has been described above is a standard tool for processing of multichannel data and it is widely used in geophysics because the change of domain gives the possibility of discriminating noise and hence enhancing data quality through a filtering process (see Appendix A).

The implementation of a 2D Fourier transform is straightforward since it comes from two successive applications of the 1D transform: a first application in time takes the raw data from the *tx* domain to the *fx* domain, a second application in the spatial direction leads to the *fk* domain. Obviously the sequence can be reverted.

One main concern about the 2D discrete Fourier transform is related to spatial aliasing. Aliasing in the wavenumber domain is a relatively more serious problem

than in the frequency domain. Indeed for the latter it is possible to implement filtering processes and moreover most of modern instruments have a hardware antialias filter for time domain acquisitions, that is very effective in mitigating the problem. For spatial aliasing neither a hardware filter exist nor a software filter can be implemented, hence it is very important the choice of distance between sampling points (receiver locations). It must be selected as small as required to make the transformed data representative of the phenomenon of interest. A visual inspection of the *fk* spectrum can reveal the presence of spatial aliasing and in case also the frequency range in which spatial aliasing is not a concern can be roughly determined (Yilmaz 1987).

One main application of the 2D DFT in geophysics is the *fk* dip filtering. The representation in the *fk* domain of an event recorded on the ground surface using an active source gives a clear idea of different kind of events that are present in the records. Indeed events having different dips in the (*x*,*t*) plane can be separated in the (*f*,*k*) plane by their dips. A selective filtering process using an appropriate window can eliminate most of the undesired energy related to ground roll (mainly surface waves), guided waves and side-scattered waves. The result is a much clear representation in time and space of arrivals of reflected and refracted waves, on which geophysical seismic methods are based.

The possible application of the *fk* transform to surface waves is suggested by the synthesis method that allows the reconstruction of Rayleigh wave time histories for stratified media.

Moreover Rayleigh waves dominate the signals recorded at a certain distance from the source, because they carry most of the energy and they attenuate less with distance (see Par 3.2.1).

The combination of the above factors relates the energy spectral peaks in the *fk* domain to Rayleigh wave dispersion. As shown below, the local maxima can be associated to modes of propagation and from their location in the (*f*,*k*) plane the surface wave phase velocity as a function of frequency (dispersion curve) can be determined.

Modelling the soil as a vertically heterogeneous medium and neglecting the body waves contributions, the displacements that are caused by an impulsive point source acting on the ground surface can be evaluated by mode superposition as (Aki and Richards 1980):

$$s(x,t) = \frac{1}{2\pi} \int_{-\infty}^{+\infty} \sum_{m} S_m(\omega, x) \cdot e^{i(\omega t - k_m(\omega) x)} d\omega \tag{4.27}$$

where m is the mode number and the factor

$$S_m(\omega, x) = I(\omega) \cdot P_m(\omega) \cdot R_m(\omega) \cdot \frac{e^{-\alpha_m(\omega)x}}{\sqrt{x}} \tag{4.28}$$

is a combination of instrument response $I(\omega)$, source spectrum $P_m(\omega)$ and path response $R_m(\omega)$ with geometric (represented by the factor $\frac{1}{\sqrt{x}}$) and material (coefficient α_m) attenuation.

The modal wavenumber k_m is inversely proportional to phase velocity V_{R_m} or equivalently proportional to its inverse, i.e. the slowness $p_m(\omega)$:

$$k_m(\omega) = \frac{\omega}{V_{Rm}(\omega)} = \omega \cdot p_m(\omega) \tag{4.29}$$

and considering a spacing between geophones equal to Δx, the phase offset between any two geophones can be written as $k_m(\omega) \cdot \Delta x$.

Applying a discrete slant stack transform (see Appendix A) on the displacement field given by Equation 4.28:

$$\begin{aligned} &\sum_{n=1}^{N} s(x_n, \tau + p \cdot x_n) = \\ &= \sum_{n=1}^{N} \frac{1}{2\pi} \int_{-\infty}^{+\infty} \sum_m S_m(\omega, x_n) \cdot e^{i(\omega\tau + \omega p x_n - k_m(\omega) x_n)} d\omega = \\ &= \frac{1}{2\pi} \int_{-\infty}^{+\infty} e^{i\omega\tau} \sum_m \sum_{n=1}^{N} S_m(\omega, x_n) \cdot e^{i(\omega p - k_m(\omega)) \cdot x_n} d\omega \end{aligned} \tag{4.30}$$

The dependence of S_m on distance from the source is only related to the attenuation phenomenon. The influence of the geometric attenuation can be easily removed by multiplying each contribution for the square root of the source-receiver distance and it will be therefore neglected in the following, assuming that such correction is applied on the original data. As the material attenuation is concerned, its contribute can be taken out from the expression of S_m, so that this last quantity becomes a function of frequency only.

Finally applying the Fourier transform over the time τ and recalling the relationship between k and p (Equation 4.29), the *fk* spectrum can be written as (Tselentis and Delis 1998):

$$F(f,k) = \sum_m S_m(f) \cdot \left[\sum_{n=1}^{N} e^{-\alpha_m(f)\cdot x_n} \cdot e^{i(k-k_m(f))\cdot x_n} \right] \tag{4.31}$$

If we neglect the material attenuation contribution, it is evident that differentiating the quantity in the square bracket with respect to k and setting the results equal to zero, the maximum of the energy spectra is obtained for $k = k_m(f)$. Furthermore it can be shown that also if the above differentiation is conducted without neglecting the material attenuation the conclusion is the same, i.e. the accuracy is not conditioned by material attenuation (Tselentis and Delis 1998).

Once the modal wavenumbers have been estimated for each frequency, they can be used to evaluate the dispersion curve from Equation 4.29.

Working in the *fk* domain can be very interesting for two main reasons. Firstly it is possible to get separated dispersion curves for different modes, instead of only one cumulated curve as in SASW test. Moreover the resulting dispersion curves are smoother since they represent the average over a given spatial extent. These factors give the opportunity of applying more stable and robust inversion processes, partially mitigating the non-uniqueness problem.

On another side the *fk* spectrum analysis is less sensitive to near field effects if compared to SASW approach. Indeed using a numerical simulation of a wavefield composed by both Rayleigh and body waves, it has been shown that the undesired distortions produced by body waves on the computed dispersion curve are minimised (Tokimatsu 1995).

An interesting application of this procedure for shallow soil characterization has been reported by Gabriels et al. (1987). They were able to evaluate the dispersion curves of the first six modes of propagation using a FFT algorithm on a 256-trace record. The data were collected with an array of 24 vertical geophones having inter-geophone distance equal to 1 m and moving back the source (a simple weight drop source with a mass of 30kg) by steps of 24 meters. The procedure to individuate the maxima that are related to different mode of propagation was based on a process of successive muting in the *fk* domain. Using such algorithm, after the dispersion curve for a mode is determined, the corresponding zone in the (*x*,*t*) space is muted and data are again reported in the *fk* domain to reveal the maxima that are related to next higher mode. The inversion of the obtained dispersion curve (covering the frequency range 5-30 Hz) led to the reconstruction of the stiffness profile over a depth of about 50m.

The above results are very encouraging in the view of applying a similar procedure for geotechnical site characterization. Still there is the problem of the very large ensemble of traces needed to obtain a good resolution in wavenumber.

Indeed, while the inter-geophone distance controls the highest obtainable wavenumber, the extent in space of the array controls the resolution. The need of a very large number of traces is very restrictive regarding the topographic characteristics of the site, which has to be flat and free from obstacles over a wide extension, that is not always the case. Moreover, considering the usual number of channels of seismic instrumentation, the traces have to be recorded moving the source or the geophone array, that is a main disadvantage both for repetitiveness problems and for required testing time.

To overcome the requirement of a large number of traces, the usual trick of adding a substantial number of zero traces at the end of the field record can be profitably applied. It is the equivalent of zero padding time histories to improve resolution in the frequency domain when a 1D DFT is applied. It is however required that the effective number of measured traces be sufficient to ensure a total spatial aperture at least equal to the maximum wavelength of interest. The undesirable effect, which is connected to the procedure of spatial padding of the measurements, is the possible and in some cases substantial increment of leakage in the power spectrum (Al Hunaidi and Rainer 1995). The leakage phenomenon is essentially constituted by fictitious values in the spectrum associated to frequency and wavenumbers that are not present in the real data, but are introduced by the abrupt change at the edge of the actual data (see Appendix A).

Because of the zero-padding procedure, leakage can eventually make critical the individuation of closely spaced (in the *fk* domain) modes or modes that are characterised by small amplitude maxima. A possible mitigation of leakage effects can be obtained applying a filter in space to the actual data before zero-padding.

Also it is important to consider that the limited extension of the receiver array can also influence the number of modes that it is possible to extract from the field data since some features are anyway lost, depending also on the minimum source-receiver distance.

The effectiveness of the above-described procedure for a pavement site has been tested using synthetic data (Al Hunaidi and Rainer 1995).

An even more appealing possibility is given by the application of spectral estimation techniques based on a limited number of sensors (Tokimatsu 1995). These techniques are essentially the same used for passive measurements (see Par. 4.6) but while in that case a 2D spatial array of receivers is employed, in the active source case, receivers are deployed on a linear array (classical multistation configuration, see Figure 4.15).

The starting point of such techniques is the cross power spectral matrix, which elements G_{ij} are the cross spectra between all the possible receiver couples (*i*-*j*). So if S_i represents the Fourier transform of the signal at the i^{th} receiver, the

average cross power spectral matrix is defined in index notation as:

$$G_{ij}(f) = \frac{1}{M}\sum_{m=1}^{M} S_{im}(f) \cdot \overline{S_{jm}(f)} \tag{4.32}$$

where M is the number of available measurements and the symbol $\bar{}$ denotes the complex conjugate. Obviously the main diagonal ($i = j$) is made of the auto-power spectra of the receivers. The off diagonal terms are the estimated cross power spectra and they contain the phase change between receivers (Zywicki and Rix 1999).

In the conventional Frequency Domain Beam-Former (FDBF) method the spectrum $F(f,k)$ is obtained by steering the array with exponential phase shifts determined using trial wavenumbers k, that must be in the range defined by receivers spacing. For a particular *fk* pair the corresponding energy is estimated by multiplying the measured cross power spectrum by the phase shift and summing over all possible receiver couples (Capon 1969):

$$F(f,k) = \sum_{i=1}^{N}\sum_{j=1}^{N} G_{ij}(f) \cdot e^{ik(x_i - x_j)} \tag{4.33}$$

where N is the number of receivers and x_i is the position of the i^{th} receiver.

The high-resolution method proposed by Capon in 1969 is based on *"a maximum-likelihood filter, whose design is determined by the sensor data and is different for each wavenumber k_0, which passes undistorted any mono-chromatic plane wave travelling at a velocity corresponding to the wavenumber k_0 and suppress in an optimum least-square sense the power of those waves travelling at velocities corresponding to wavenumbers other than k_0"*.

The corresponding mathematical formulation is (Capon 1969):

$$F(f,k) = \left[\sum_{i=1}^{N}\sum_{j=1}^{N} q_{ij}(f) \cdot e^{ik(x_i - x_j)} \right]^{-1} \tag{4.34}$$

where $q_{ij}(f)$ is the inverse of the cross power spectral matrix $G_{ij}(f)$. This inversion is basically the only additional heavy processing step that is required by the high-resolution method, nevertheless the gain in resolution can be really substantial in many cases because of the adaptive nature of the filter (Capon 1969).

4.5.2 Frequency-slowness analysis

As seen above the 2D DFT gives the opportunity of representing the ensemble of traces, which are recorded in a multistation session, in a domain different from the travel time-offset one (*t*,*x*). A similar possibility can be given by the use of other mathematical transforms. The basic concept is essentially the same: to represent an ensemble of data as the superposition of some kind of functions. Thus, as the Fourier transform is based on harmonics, the τp transform or slant stack represents the collected data as the superposition of straight-line events (Telford et al.1990). The τp transform is a particular case of the more general Radon transform, in which the projection is not necessarily along a straight line but along a generalised line. As all the other transforms, an inverse transform can be defined such that in principle it is possible to go back in the initial *tx* domain without any loss of information (but discretization and side effects produce some differences between transformed and original data).

The usefulness of the τp transform for seismic reflection and refraction methods is due to the clear separation in the new domain between different seismic events such as reflections, refractions, diffractions and surface-wave ground roll. In particular the latter maps into a delimited area close to time zero. This separation allows for powerful filtering processing in the τp domain to clear the data from unwanted events (Doyle 1995).

A description of the procedure that is utilised to construct a slant slack gather from a seismic record and the vice versa, together with a comprehensive description of the possible uses of the transform can be found in Yilmaz (1987).

An algorithm for the extraction of the dispersion curve from a common shot wave field using the slant stack transform has been proposed by McMechan and Yedlin (1981). According to their procedure, the successive application of a slant stack and of a 1D discrete Fourier transform take the original data into the frequency-slowness domain, where dispersion curves can be identified.

Indeed, considering the synthesis formula proposed by Chapman (1978), the frequency-wavenumber representation of a general wave field $s(x,t)$ is given by:

$$s(x,t) = \int\int \frac{N(k,\omega)}{D(k,\omega)} e^{i(kx-\omega t)} d\omega \cdot dk \tag{4.35}$$

where $N(k,\omega)$ characterises the source and $D(k,\omega)$ is the dispersion relation for the vertically heterogeneous medium. Applying the slant stack transform to the wavefield described by Equation (4.35), it is possible to obtain:

$$
\begin{aligned}
S(p,\tau) &= \int s(x,\tau + px)\cdot dx = \\
&= \int\int\int \frac{N(k,\omega)}{D(k,\omega)} e^{i[kx-\omega(\tau+px)]} d\omega \cdot dk \cdot dx = \\
&= \int \frac{N(\omega p,\omega)}{D(\omega p,\omega)} e^{-i\omega\tau} d\omega
\end{aligned}
\tag{4.36}
$$

and the successive application of a Fourier transform over τ yields:

$$
S(p,\omega) = \frac{N(\omega p,\omega)}{D(\omega p,\omega)} \tag{4.37}
$$

Analysing this representation of the original wave field (recalling that all information are kept through a transform process) and remembering that for surface waves $D(\omega p,\omega) = 0$, it comes out that $S(p,\omega)$ tends to infinity for this kind of waves. Thus the dispersion curve in terms of slowness can be identified directly as the locus in the plane *p*-ω of the maxima of the transformed data.

This results is not surprising since it can be demonstrated the formal equivalence from a mathematical point of view of the 2D Fourier transform with the successive application of a Radon transform and a 1D Fourier transform on the τ variable (Sherif and Geldart 1995).

In this method the dispersion curve is evaluated from the whole data ensemble without any need for subjective selection of data and hence it can be very interesting for an automation process. Moreover the resolution in the slowness domain can be fixed with no need for particular tricks such as zero-padding for the frequency-wavenumber analysis.

McMechan and Yeldin (1981) tested the method both on synthetic and real marine data. They were able to solve up to the first three modes for the synthetic records, but only the fundamental mode for the real data.

In comparison to the analysis in the frequency-wavenumber domain, the localisation of peaks in the frequency-slowness domain defined by this technique is directly informative about the shape of the dispersion curve. Thus also if the two methods are in principle equivalent the one based on the slant stack transform gives a clearer and faster image of the dispersion property.

4.5.3 Group velocity based methods

As described above the first use of surface waves for characterization purposes was related to Earth's crust properties identification from high period seismic signals.

The great travel distance causes in that case a strong mode separation, because of the existing difference between phase velocity and group velocity of Rayleigh waves. For this reason the tools usually applied in seismological application are capable of tracing not only the dispersion curve that is associated to the fundamental mode but also those relative to the first higher modes.

Applications of such techniques have been also used at a smaller scale for geological basin characterization.

The use of similar methods for geotechnical application is appealing because it could allow for mode separation using only a pair of receivers as in the classical SASW configuration (Lefebre and Karray 1999). As explained above the possibility of having the dispersion curves related to the participating modes is very welcomed because it allows the development of more stable inversion processes, reducing the non-uniqueness in comparison to the inversion processes based on the effective Rayleigh phase velocity.

4.5.3.1 Multiple filter method

The method, that was originally proposed by Dziewonski et al. (1969) to study multi-mode dispersed signals of seismograms, is based on the use of band-pass frequency filters. Every filter can be seen as a system, which is passed through by the signal. Applying narrow band-pass filters with different center frequencies, different wave groups are separated in the signal (Figure 4.18). These different packets of oscillation can be associated to different modes of propagation and the peak of each envelope can be used to evaluate the corresponding wave group time delay and hence its velocity.

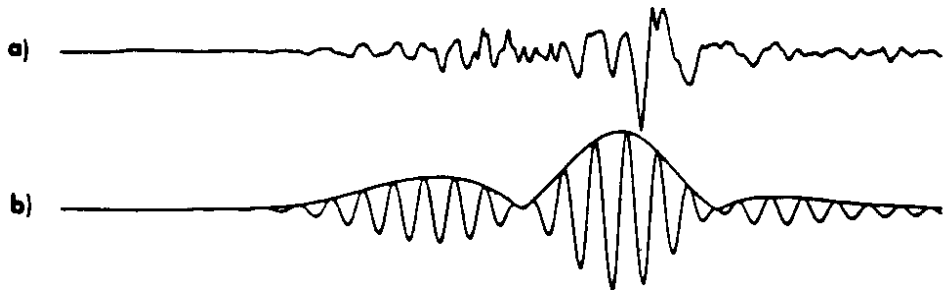

Figure 4.18 Example of narrow bandpass filtering: (a) original earthquake signal; (b) filtered signal (from Dziewonski et Al. 1969)

The main problem concerning the application of this technique to SASW measurements is related to interference between the modes, which is frequent when different modes have similar velocities or the source is too close to the receivers. Such problem can disable the method from being effective in resolving the different dispersion curves. Gabriels et al. (1987) reported such difficulties in their attempt to analyse with the multiple filter technique the data collected in a multistation session.

4.5.3.2 Multiple filter/Time-variable filter

The time-variable filter technique, originally proposed to filter out noise and then applied to the analysis of multi-mode signals for seismological and geophysical applications, attempts to cut off the energy that is not associated to a selected wave group. The combination of multiple filter and time-variable filter techniques can successfully be used for SASW measurements, in the view of obtaining the dispersion curve for the first and higher modes (Lefebre and Karray 1999).

In the MASW (Modal Analysis of Surface Wave) method, the group velocities of the participating modes are firstly individuated using the multiple filter technique. Then for each mode, the original records are passed through a time-variable filter to eliminate the contribution of the other modes and the phase velocity is calculated using techniques similar to the SASW test one. Once the dispersion curves have been reconstructed for all the modes that can be isolated, the inversion process is done using a specific algorithm. The proposed procedure has been successfully applied to real data, showing its ability to resolve the fundamental and the first or the first two higher modes.

4.5.3.3 Cross-correlation method

Once the group velocities have been found using the multiple filter techniques, another procedure to determine phase velocity in SASW measurement can be based on cross-correlation method (Al Hunaidi 1994).

Generally speaking the time delay between two signals y_1 and y_2 can be obtained, under the hypothesis that it is not dependent on frequency, as the time shift that yields the maximum value of the cross-correlation function:

$$R_{12}(\tau) = \int_{-\infty}^{+\infty} y_1(t) \cdot y_2(t+\tau) \cdot dt \tag{4.38}$$

where τ is the time shift.

In the proposed procedure, both signals of a SASW session are processed using the multiple filter technique and from the envelopes the group time delays and hence the group velocities are individuated for the resolved modes. Then, accounting for the relative relations between phase and group velocities (see Equation 3.23), the cross-correlation is applied on segments extracted from the filtered signals to evaluate the phase time delay and hence the phase velocity at each frequency (Bloch and Hales 1968).

Application to synthetic data showed the good performances of the method, except when the receivers are not as far from the source as required for the modes being well separated by the multiple filter technique.

4.6 Passive methods

One of the main difficulties in SASW testing concerns the ability to explore the profile up to a great depth. Indeed the possibility of obtaining the stiffness characteristics of deep strata is directly connected to the lowest testing frequency (highest wavelength) and in turn this is connected with the energy that the source is able to transmit into the soil. To overcome this problem, very massive sources need to be used, but this imply also an increase in the total cost of performing the field data collection, that usually is considered one of the advantage of non-invasive methods such as the SASW. Moreover testing for long wavelength implies the possibility of having a quite long extension of free field to comply with the requirements for the near field effects minimisation (see Par. 4.3.2.2)

One possible alternative can be the use of short-period microtremors (T<1s), due to natural events or human activities in the nearby of the site. Because of the absence of a specific source, such methods are often called passive methods. It is important to remark that in favourable circumstances these methods can be used to characterize up to depth of more than one hundred meters (Horike 1985), going much deeper than any active source method can do. The optimal solution for geotechnical characterization can be obtained with an hybrid method, using short period microtremors, for deeper layer identification, jointly with forced vibration, to cover the need of high frequency waves since in this range microtremors are strongly affected by noise.

The possibility of using records obtained from microtremors is strictly connected to the condition that such signals can be essentially associated to Rayleigh wave. This requirement is usually satisfied if the observation are conducted in favourable weather condition, i.e. in absence of strong winds (Horike

1985).

The basic steps of the procedure for soil characterization using microtremors (Horike 1985, Tokimatsu 1995, Zwycki and Rix 1999) are essentially the same of the SASW test: field measurements, dispersion curve evaluation and inversion. Several sensors are required because there is no restriction to a single mode or a single direction of propagation, because the actual source position is unknown. Usually receivers are deployed in a circular array either with or without a receiver in the center of the array (Figure 4.19). Using three-dimensional receivers it is possible to analyse both vertical and horizontal particle motion related to microtremors.

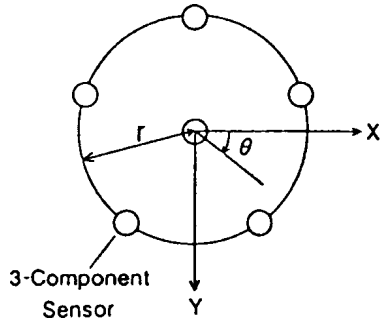

Figure 4.19 Passive noise measurements: example of receivers array configuration (from Tokimatsu 1995)

Ambient noise measurements are conducted for a length of time that must be sufficient to obtain a congruent number of non-overlapping data segments, whose parameter of acquisition have to be fixed as a function of the required resolution in frequency and of the maximum frequency of interest. The test is typically repeated for different receiver distances for the same reasons that have been analysed for SASW test (see Par 4.3.2.2).

Analysis of data is performed using high-resolution frequency-wave number spectral estimation techniques (see Par. 4.5.1), considering the non-overlapping data segments of the record in place of the different repetition of the active source case. Since in this case the receivers are not placed along a straight line the steering of the data array with the trial wavenumber is done in many directions. The resulting spectrum can be represented as a 2D wavenumber (k_x-k_y) contour plot for each analysed frequency (Figure 4.20). The peak of this spatial plot is used to

evaluate the wavenumber that is associated to the dominant surface wave and its direction of propagation. Repeating the process for different frequencies, the dispersion curves is determined.

Inversion procedures are similar to those of the SASW test.

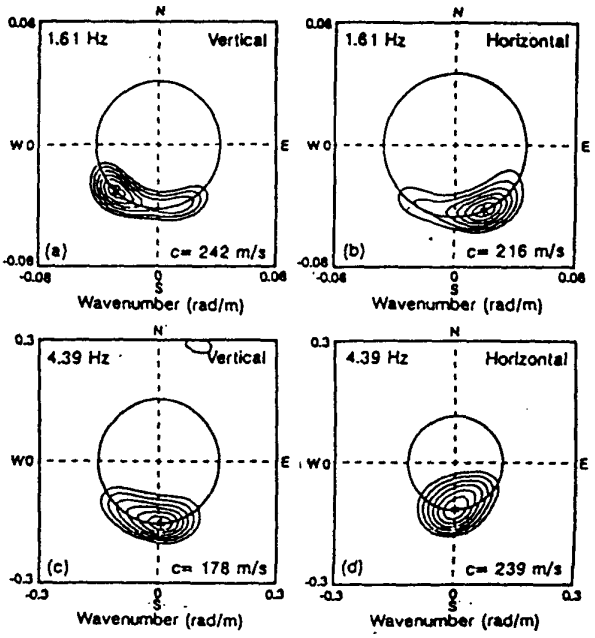

Figure 4.20 Example of fk spectra of noise ambient measurements: both vertical and horizontal components are shown for two different frequencies (from Tokimatsu 1995)

Chapter 5

Dispersion curve evaluation: numerical simulations

To compare different procedures for the dispersion curve evaluation (two-station vs. multistation), a set of numerical simulations has been conducted using synthetic seismograms computed with computer programs written by prof. R.B. Herrmann of Saint Louis University and his co-workers.

Some ideal stiffness profiles were adopted, but their properties has been chosen such that they were representative of various situations. Typical critical profiles for site characterization using surface waves, such as the soft layer trapped between stiffer ones and the stiff top layer over a softer soil, have been considered.

The synthetic data were firstly analysed using the classical approach of the SASW test (Par. 4.3.2), i.e. considering pairs of receivers and extracting the phase velocity from the phase of the cross power spectrum. Thereafter the dispersion curves were computed with the multistation approach based on the 2D Fourier Transform (Par. 4.5.1) considering different options for what concerns the number of receivers used for the analysis.

The dispersion curves computed as described above were then compared between each other and to the ones relative to the different Rayleigh modes. To have a comparison also with the effective phase velocity arising from mode superposition, an estimate of this last quantity has been evaluated for the different profiles.

Finally some notes about the use of the frequency-slowness analysis on multistation data and about effectiveness of the approximate procedure for the estimate of the relation between stiffness and depth are reported.

5.1 Synthetic signals

Initially the synthetic seismograms (that are relative to the vertical motion caused by a vertical point impulse force) were computed considering Rayleigh waves only, with no account for body waves, for 256 receivers placed at intervals of 1m, starting at 1m from the source. Source and receivers are placed on the free surface.

The parameters of the time histories have been chosen in accordance to the acquisition parameters used for field-testing (see Chapter 7). In particular considering the usual range of frequencies of interest in SASW testing, the sample interval in time was taken equal to 0.002 s (it corresponds to a Nyquist frequency of 250 Hz, that is well above the highest frequencies that are needed for soil characterization). To obtain a sufficient resolution in the frequency domain a record length of 2048 samples has been chosen (the total duration of the time histories is consequently 4.096 s, which corresponds to a resolution in frequency equal to 0.244 Hz).

The computer code that has been used for the computation is part of a set of computer programs for seismological purposes, that has been realised by the researchers of Saint Louis University (USA) under the guidance of prof. R.B. Herrmann. The code creates synthetic seismograms using modal superposition of surface waves and hence it doesn't account for body waves contribution.

Firstly the eigenvalue problem that gives the solution for the free Rayleigh modes is set up using the Haskell-Thomson propagator matrix approach (see Paragraph 3.3.1.1). Then the eigenvalues and the corresponding eigenfunctions are used in a mode superposition process to generate the synthetic seismograms with a inverse discrete Fourier transform.

The program allows different kind of sources to be used and arbitrary position of both source and receivers. For the applications presented in the following the impulsive source acting on the ground surface has been considered.

5.2 Dispersion curve evaluation

The synthetic data have been used for testing the different procedure commonly adopted to compute the experimental dispersion curve from field data. Considering the different methods, sets of receiver configurations have been tested on three different profiles, reproducing different possible set-ups of the field-testing.

5.2.1 SASW approach

The procedure usually adopted to compute dispersion curves in SASW test has been described in Paragraphs 4.3.2.1 and 4.3.2.2. Although different combinations of source-first receiver/inter-receivers distances can be used, the choice here has been that of computing the dispersion curve using the most common situation of equal distances.

In the view of reproducing a real test, the first 50 seismograms have been used. With the usual filtering criterion of the SASW test this is a testing configuration that allows the computation of wavelengths as long as 50m, that results in the ability to invert the data up to a depth of roughly 20m.

In the aim of simulating the effective procedure of a real SASW test 7 pairs of signals, corresponding to 7 different test setups, have been considered, choosing the following inter-receiver distances: 1m, 2m, 5m, 10m, 15m, 20m, 25m. The filtering criterion reported in Equation 4.15 has been applied to the data obtained from each source-receivers configuration, also if synthetic data are not affected by near-field side effects, because they have been obtained by modal superposition of surface waves modes only. This procedure reproduce exactly not only the field setup but also the data processing of the common test.

After all points have been evaluated from the different pairs of receivers, the reduced dispersion curve has been evaluated subdividing the frequency range and then assigning the mean values to the central frequencies. This is part of the standard practice of SASW, also in the view of reducing the number of points for the inversion process (Nazarian 1984).

5.2.2 Multichannel fk domain approach

The synthetic data have been successively analysed using the multistation procedure based on the translation of the traces into the fk space, as described in Paragraph 4.5.1. Firstly the fk spectrum has been estimated using the whole ensemble of 256 traces and a FFT algorithm. Resolution in the k domain is an essential feature in the transformed data because it strongly influences the accuracy in the localisation of the spectral peaks for each frequency. This is the reason why a large number of traces is required to obtain good results with this approach. To further improve the resolution also in the case of 256 traces, the ensemble of data has been padded using zero-traces, so that the total number of traces is 2048. In this way the global ensemble was composed of 2048 traces each one of which composed by 2048 points in time.

Clearly a field record of 256 traces is not practical for actual data acquisition,

both because of the limited number of channels of seismic instrumentation and because of the large extension of free from obstacles and plane ground surface that such an approach would require.

For this reason the fk method has been successively applied to a restricted subset of the synthetic data, to test its performance with configurations that can be effectively used in standard practice. Among all the possibilities, the choice has been to use 24 traces, because this is the number of channels available in the seismograph that has been used for the experimental part of the research (see Chapter 6).

Two possibilities have been explored considering in both cases traces spaced 1m. In the first case the array of virtual receivers was placed starting at 1m from the source and in the other starting at 20m.

The second array configuration has been selected considering the actual necessity of reducing near field effects during the experimental tests. In this respect the following remarks must be considered about multistation measurements.

First of all the effects of the near field on the estimate of the dispersion curve should be less important than for the case of classical SASW test. Indeed, while the latter is based on local measurements in only two points, the multistation approach is based on several points and hence the ones closer to source can also be to a certain extent affected by near field effects without strong repercussions on the evaluated dispersion curve. This physical consideration is also supported by the fact that when the traces are translated in the fk domain there is a separation of the different events (Yilmaz 1987), so that the local maxima associated to surface waves should not be much affected by other kind of events.

The above considerations lead to the conclusion that the application of SASW filtering criteria for near field effects to the dispersion curve evaluated from the multistation fk domain approach is not desirable because the only effect would be to discard information that probably are not strongly influenced by body waves.

Another important remark concerning the distance between the receiver array and the source is connected to mode separation due to the dispersion phenomena. As long as the surface wave-packet goes away from the source the separation between different modes increases because of the existing difference between phase and group velocities of Rayleigh waves (see Paragraph 3.3.1.2). Hence if the waves are detected far from the source it is more probably that the different modes are well separated. This could lead to a dispersion curve that is neither the one relative to Rayleigh modes nor the one coming from modal superposition.

In the view of the above remarks the comparison has been made for different source-first receiver distances also to show how this distance affects the evaluated dispersion curve. This analysis is aimed also at assessing which are the

consequences for different types of stiffness profile.

5.2.3 Effective phase velocity

The effect of mode superposition is very important in determining the measured quantity associated to surface wave propagation. To account for it, it is necessary to define an effective phase velocity. Being it a local quantity, a conventional definition has been taken, evaluating it from the response at two receivers located respectively at 2 and 4 wavelengths from the source at each frequency (Figure 5.1). This definition is strongly related to the classical two-station procedure of the SASW test and it is often adopted in inversion programs. It has been chosen as reference because it is widely adopted, also if it is a quantity not directly associated to multistation measurements.

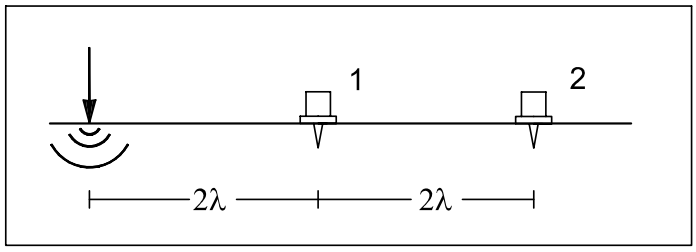

Figure 5.1 Conventional definition of the effective phase velocity

5.3 Results

Three stiffness profiles have been used for the comparative analysis: profile A represents the case of a normally dispersive medium with no big contrasts of mechanical impedance and stiffness always increasing with depth; profile B represents the case of a softer layer between two stiff ones, that can constitute a typical difficulty encountered on the field; profile C represents another complicated case because of the presence of a stiff top layer.

For the sake of generality for each one of the three testing profiles the same procedures of synthetics computation and dispersion curve evaluation have been applied. Actually a distinction should be made about the filtering criteria to be applied to minimise near field effects, since profile B and C are not normally dispersive and for them the near field effect could be sensible up to about 2 wavelengths from the source (see Par. 4.3.2.2). Anyway since synthetic seismograms used for this analysis do not account for body waves effects, the same

filtering criterion has been used.

One observation could be that for strongly inversely dispersive profiles such as profile C, the filtering criterion should be adapted to account for the much more relevant extension of the near field. Actually this is not the case for most of real field testing since a very restrictive filtering criterion would make the test hard to implement.

As seen in Paragraph 4.5.1, one main concern is constituted by the potential effect of spatial aliasing on the data. The Nyquist wavenumber, that represents the maximum wavenumber not affected by spatial aliasing that can be obtained from the 2D Fourier transform, is expressed in relation to the inter-receiver distance:

$$k_{Nyquist} = \frac{2\pi}{2 \cdot \Delta x} = \frac{\pi}{\Delta x} \tag{5.1}$$

A visual inspection of the bidimensional spectrum can give important indications, indeed the presence of spatial aliasing causes the phenomenon of wrap-around in the wavenumber domain. Above a given frequency, part of the energy is concentrated in location above the Nyquist wavenumber, and since conventionally such location are represented as negative wavenumbers, the spectrum 'wraps around' (see Yilmaz 1988 for a detailed description). The frequencies for which no wrap-around is noted should not be affected by spatial aliasing.

Since in this case the starting profile is known a-priori, another important check can be done on the maximum wavenumber of interest that has to be minor than the Nyquist wavenumber for the test configuration. The maximum wavenumber that is expected in the frequency range of interest can be evaluated from the mechanical properties of the top layer.

5.3.1 Case A

To represent the case of a normally dispersive medium, a two-layer over halfspace system has been considered (see Table 5.1 and Figure 5.2).

Table 5.1 Profile A: layers characteristics

Thickness (m)	V_S *(m/s)*	V_P *(m/s)*	*Density* (kg/m^3)
5	350	600	1800
10	400	700	1800
∞	450	800	1800

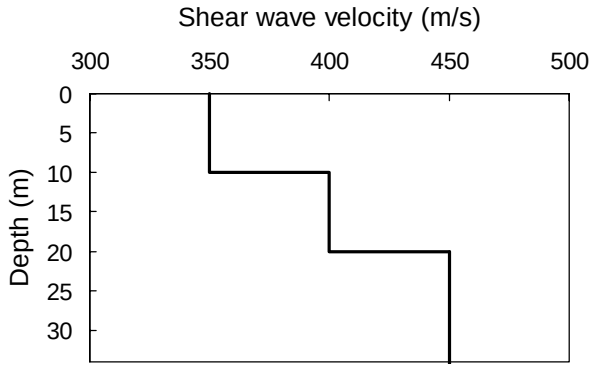

Figure 5.2 Profile A

The dispersion curve for the free Rayleigh modes and the effective phase velocity are reported in Figure 5.3. As expected (see Paragraph 3.4.1) in this normally dispersive case the fundamental Rayleigh mode is dominant over the whole frequency range and its phase velocity practically coincides with the effective one.

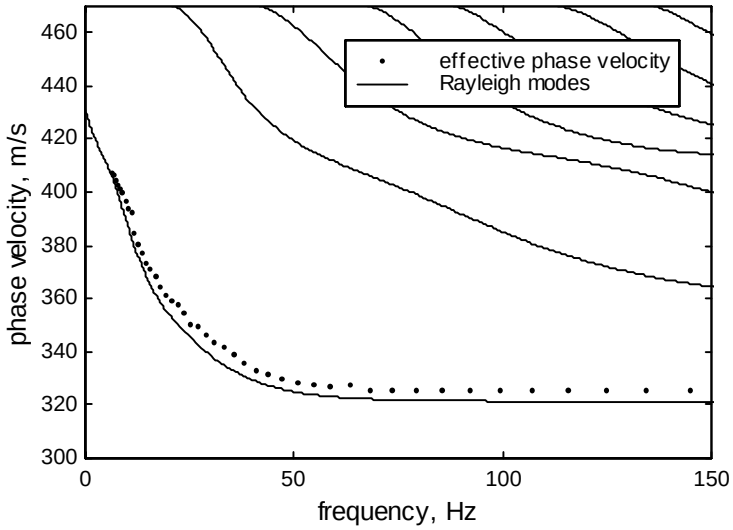

Figure 5.3 Rayleigh modes and effective dispersion curve for profile A

Using the synthetic seismograms, a simulation of the SASW test has been performed, as described in Paragraph 5.2.1. Obviously in the low frequency range, where only one mode of propagation exists, there are no differences between the phase velocity evaluated by different receiver pairs, while when other modes interfere with the fundamental one, the phase velocity has some fluctuations (Figure 5.4). To obtain a consistent mean dispersion curve it is important to have a sufficient number of receivers pairs in the testing configuration. In the analysed cases, this effect is not particularly marked, but it seems that such problem could lead to erroneous evaluations of the dispersion curves.

Figure 5.5 shows a comparison between the fundamental mode dispersion curve, the effective one and the dispersion curve obtained with the classical approach of SASW test. It is important to note that the latter is closer to the fundamental mode one than to the effective one. This can be explained by the fact that the effective phase velocity is here evaluated from the displacement values at two and four wavelength from the source, while minor distances have a strong influence on the SASW dispersion curve. This effect appears to be negligible in this particular case.

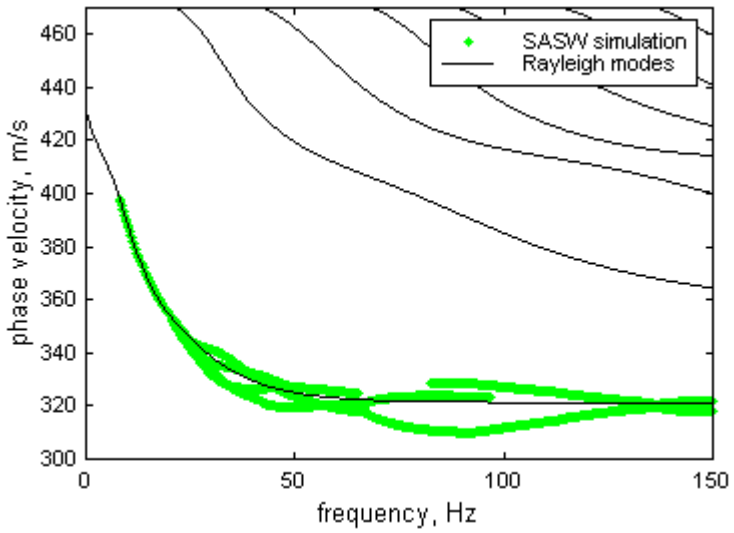

Figure 5.4 Profile A: complete ensemble of data from the SASW simulation

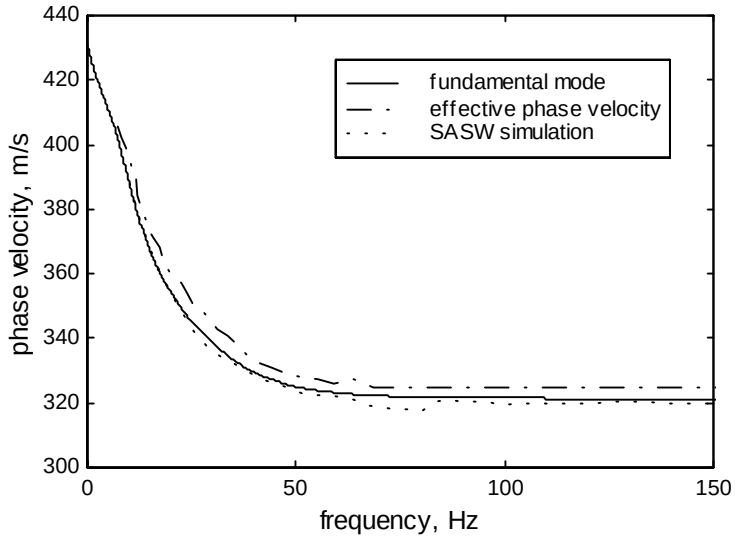

Figure 5.5 Profile A: comparison between dispersion curves

The dispersion curve has been successively estimated using the *fk* domain approach. The estimated spectrum is not affected by spatial aliasing in the frequency range that has been taken in consideration (up to 150 Hz). Indeed for the highest frequency the phase velocity should be equal to its asymptotic values, i.e. to the Rayleigh wave phase velocity of a homogeneous halfspace having the same mechanical characteristics of the top layer ($V_S = 350\,m/s$ *and* $\nu = 0.25$). Hence the corresponding wavenumber can be estimated as:

$$V_R = \frac{0.87 + 1.12\upsilon}{1+\upsilon} \cdot V_S = 0.92 \cdot V_S = 320\ m/s$$

$$k = \frac{2\pi \cdot f}{V_R} = \frac{2\pi \cdot 150}{320} = 2.95\ \ 1/m$$

On the other hand the maximum wavenumber that can be obtained from the 2D Fourier transform is the equivalent of the Nyquist frequency in the wavenumber domain, hence, recalling that the inter-receiver distance is 1m:

$$k_{Nyquist} = \frac{2\pi}{2 \cdot \Delta x} = \frac{2\pi}{1 \cdot 2} = \pi \quad 1/m$$

The conclusion that spatial aliasing doesn't affect the considered traces for the frequency range of interest is confirmed by the visual inspection of the *fk* spectrum (Figure 5.6), for which no wrap-around in wavenumber domain is noted for the frequency range of interest.

The *fk* spectrum (Figure 5.6) clearly shows that in this case only one mode dominates the wavefield, indeed the locus of maxima is continuous while when more modes participate there are some zones of transition along frequency and the maxima are located on different ridges of the spectrum.

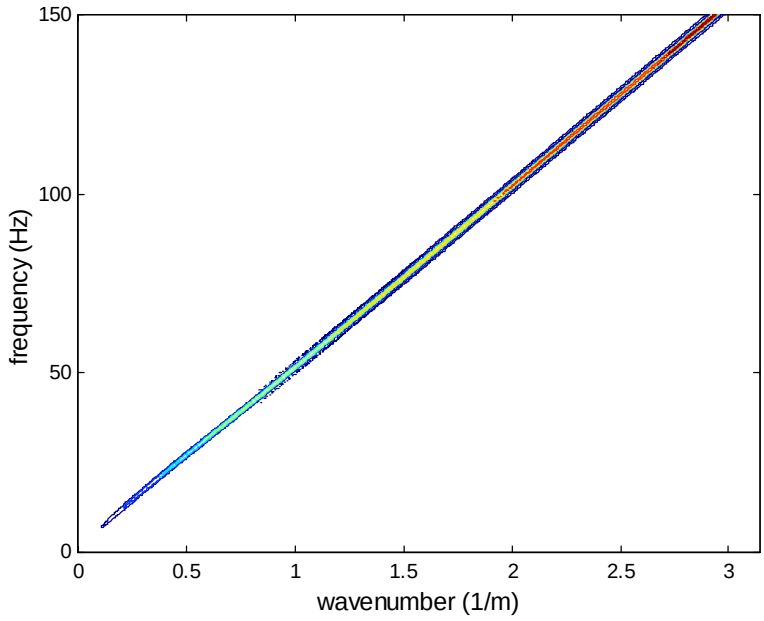

Figure 5.6 Profile A: fk spectrum from 256-receiver array

The dispersion curve obtained considering the maxima in the *fk* spectrum is practically coincident with the fundamental mode one (Figure 5.7). Minor differences can be observed when only 24 traces are used in place of the whole ensemble (256). The conclusion is that in a normally dispersive profile, for which the fundamental mode dominates the response of the soil, the *fk* method can be used with a number of geophones absolutely not prohibitive.

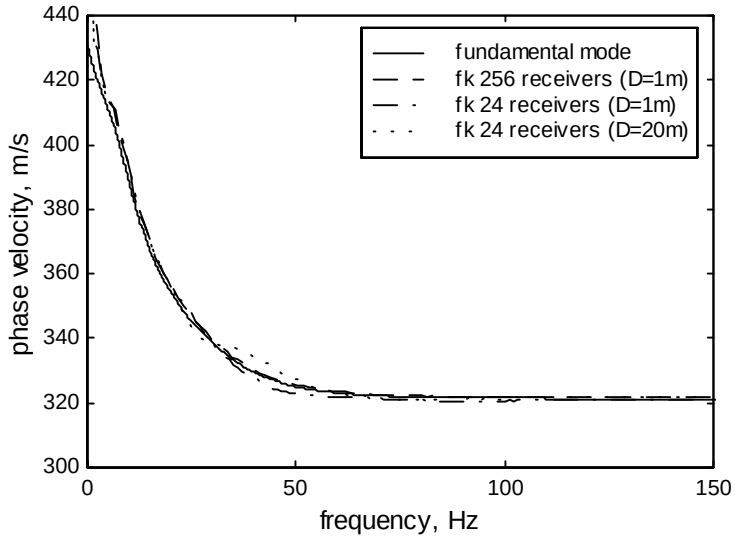

Figure 5.7 Profile A: comparison between the dispersion curves evaluated using the fk approach and the fundamental Rayleigh mode

5.3.2 Case B

To represent the case of a soft layer trapped between two stiffer ones, two layers over halfspace have been considered (see Table 5.2 and Figure 5.8). The choice has been to use a thinner intermediate layer, also to strongly differentiate this case from profile C, in which a stiff top layer is considered.

Table 5.2 Profile B: layers characteristics

Thickness (m)	V_S *(m/s)*	V_P *(m/s)*	*Density* (kg/m^3)
5	400	700	1800
3	300	500	1800
∞	450	800	1800

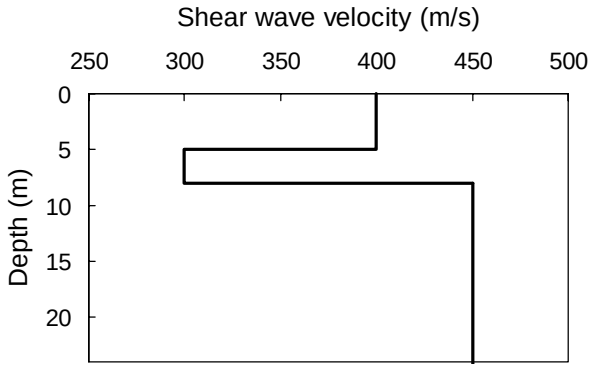

Figure 5.8 Profile B

As expected, in this case the fundamental mode is not predominant over the entire range of frequency, but for higher frequencies there is a transition towards higher modes. In the frequency range of interest the behaviour is dominated by the fundamental and the first higher mode and the transition between one and the other is concentrated in the frequency range between 50 and 80 Hz.

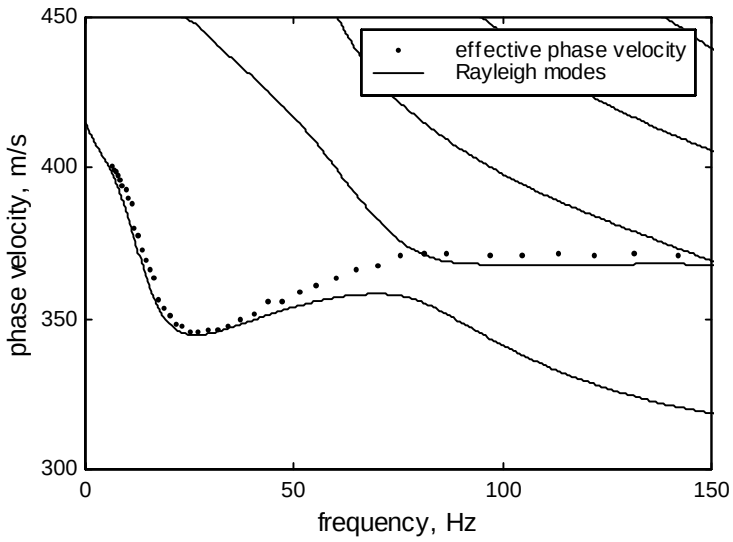

Figure 5.9 Rayleigh modes and effective dispersion curves for profile B

Concerning the results of the SASW simulation, for frequencies up to about 35 Hz, either only the fundamental mode exists or it strongly prevails (see Figure 5.10). The passage from the predominance of the fundamental mode to the prevalence of the first higher mode is characterised by strong fluctuations that are definitely dependent from the position of the two receivers that are used for the spectral estimation of phase velocity. Thus in cases like this one the choice regarding the test setup can be very important. Moreover it is not guaranteed that the subsequent process of averaging of points between different test configuration leads to a stable estimate of the effective phase velocity.

The resulting estimate of the dispersion curve shows a global underestimation of the effective phase velocity, also if quantitatively such differences are not marked (see Figure 5.11).

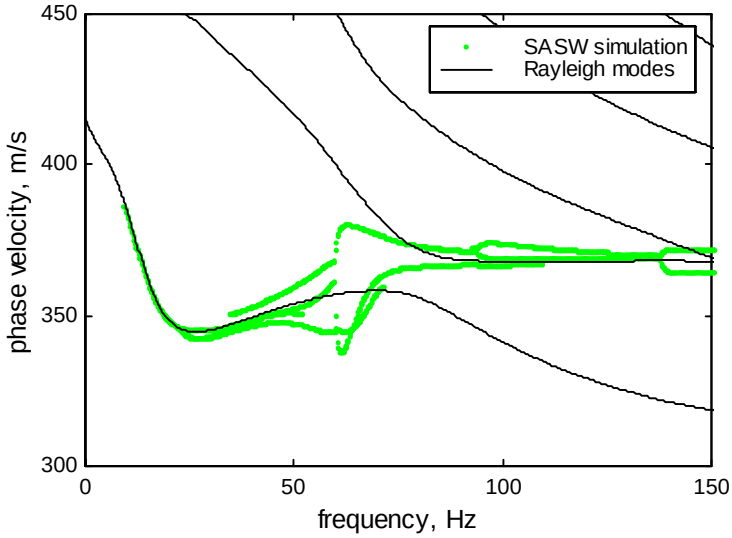

Figure 5.10 Profile B: complete ensemble of data from the SASW simulation

As the construction of the dispersion curve from the maxima of the *fk* spectrum is concerned, things get more complex if compared to the case of normally dispersive soil profile.

No problem of spatial aliasing arise in this case since the inter-receiver distance (and hence the Nyquist wavenumber) is the same of profile A, while the maximum wavenumber in the frequency range of interest is minor, because in this case the top layer is stiffer.

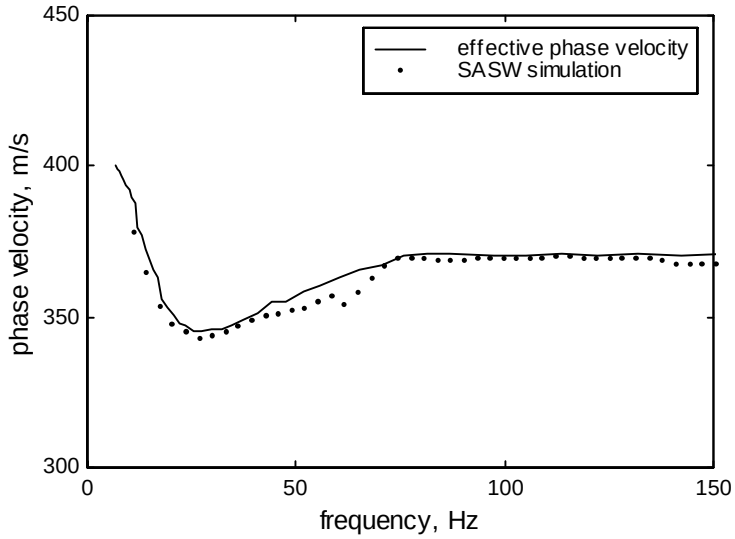

Figure 5.11 Profile B: comparison between dispersion curves

Using all the available traces (256) the resolution of the spectrum (Figure 5.12) is quite good and it is possible to locate the zones where there is the prevalence of the fundamental or of the first higher mode. The main difference with respect to the case of the normally dispersion profile (Figure 5.6) is that in this case two main systems of ridge exist, denoting the fact that there isn't a single dominating mode. Moreover following the respective ridges it is possible to obtain from the spectrum also additional portions of the dispersion curves relative to different modes, which are represented in the spectrum by local maxima (Figure 5.13). Clearly, for a given frequency, the local maximum corresponding to the fundamental mode is the one that is associated to the highest wavenumber, because the fundamental mode has the lowest phase velocity, and so on for the successive higher modes.

The possibility of evaluating the phase velocity associated to different modes would be very interesting in the view of the inversion process, indeed more information than the single effective phase velocity would result in a better posed mathematical problem to be solved.

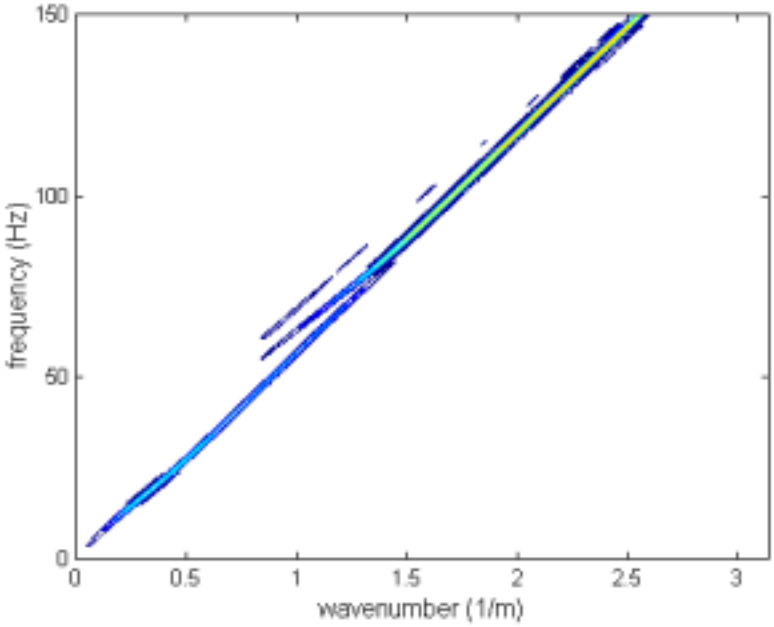

Figure 5.12 Profile B: fk spectrum from 256-receiver array

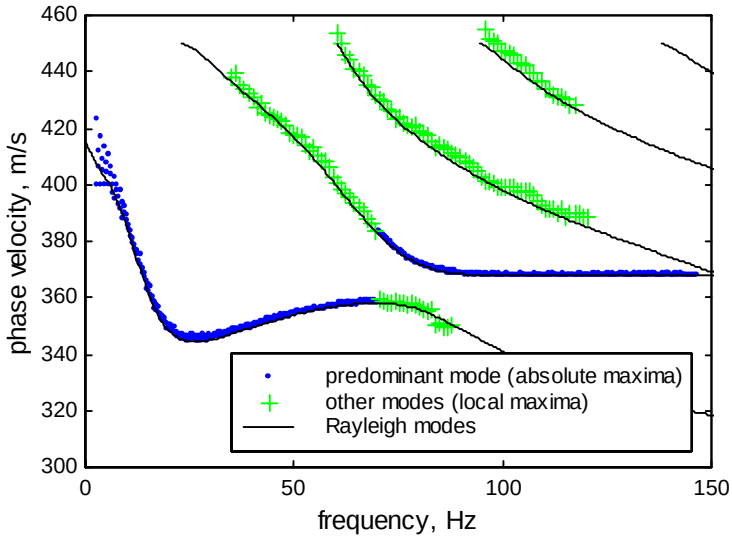

Figure 5.13 Profile B: dispersion curves from fk analysis (256 receivers)

Things change when a minor number of receivers is used. For both cases of the receiver array placed at 1m or at 20m from the source, there are some problems in the definition of the dispersion curve in the transition zone, i.e. where there is the shift from the fundamental mode to the first higher mode. The situation appears quite different for the two cases above.

If the 24-receiver array is deployed starting at a distance of 1m from the source, modes are not well separated (Figure 5.14) and the dispersion curve obtained from the maxima of the *fk* spectrum is very similar to the effective dispersion curve (Figure 5.15).

Instead if the source to first receiver distance is taken equal to 20m, the phenomenon of mode separation is sensible and the fundamental mode velocity is well defined below 50 Hz while the first higher mode velocity is found for frequencies above 75 Hz (Figure 5.17). However the transition zone is not well defined because none of the two modes prevails. This aspect is evident from the dispersion curve obtained from the maxima, moreover a visual inspection of the *fk* spectrum makes it clear the absence of a specified ridge in the frequency range from 50 to 75 Hz (Figure 5.16).

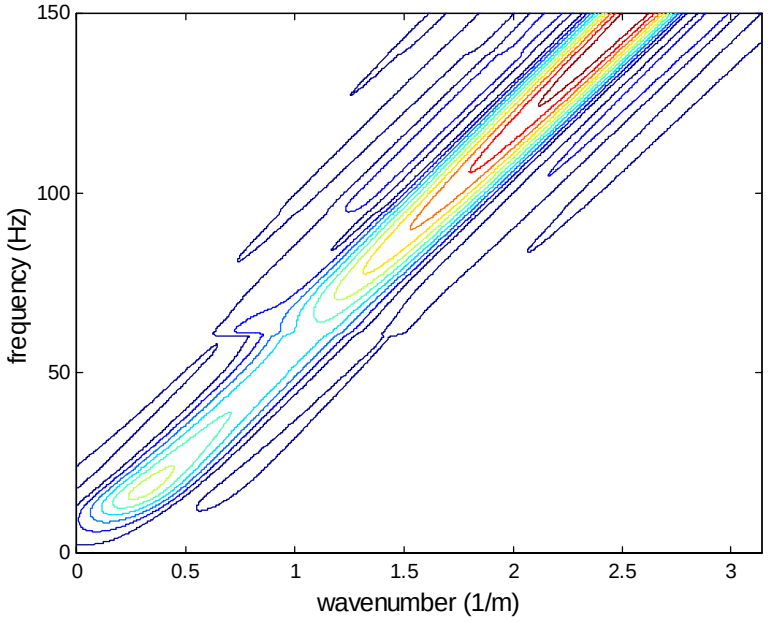

Figure 5.14 Profile B: fk spectrum from 24-receiver array (D=1m)

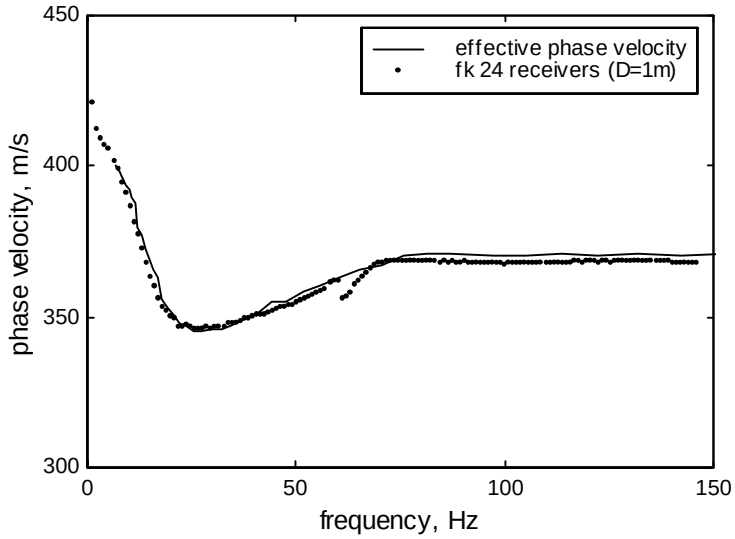

Figure 5.15 Profile B: dispersion curve from 24-receivers array (D=1m)

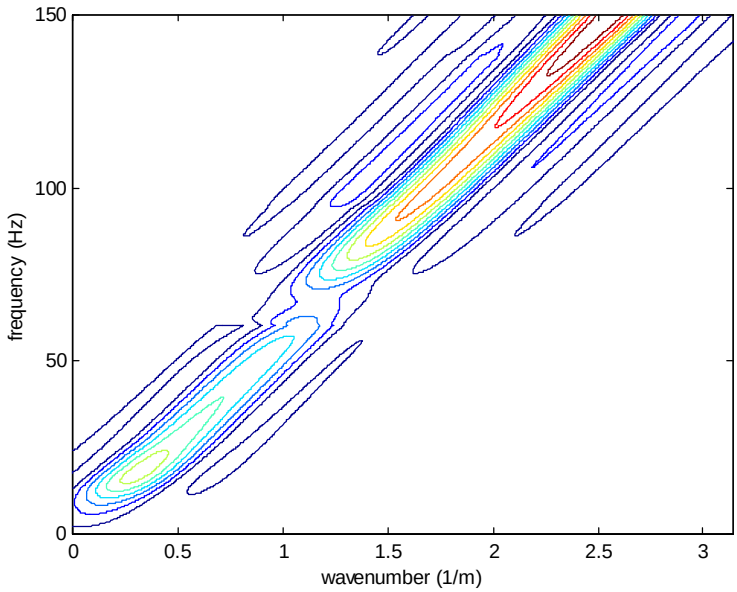

Figure 5.16 Profile B: fk spectrum from 24-receivers array (D=20)

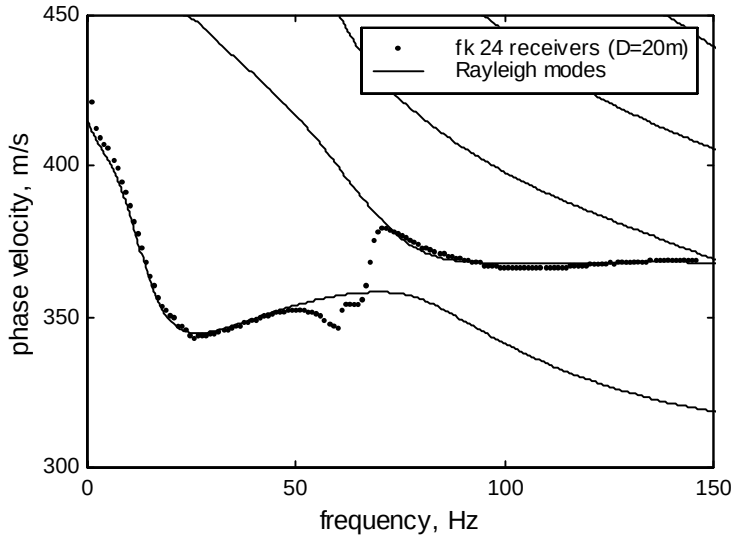

Figure 5.17 Profile B: dispersion curve from 24-receivers array (D=20m)

5.3.3 Case C

Finally to represent the case of a stiff top layer over a softer soil, the profile used for case A has been considered, with the addition of a top layer as stiff as the halfspace (see Table 5.3 and Figure 5.18). The effective dispersion curve reported in Figure 5.19 shows that in this case several modes have a strong influence. In the frequency range of interest (up to 150 Hz) the asymptotic value equal to the Rayleigh wave velocity characteristic of the first layer is not reached, this is due essentially to the fact that in this case the surface layer is quite thin. The fundamental mode prevails only for frequencies smaller than 40 Hz; above this threshold value a continuous transition of dominant mode can be observed.

Table 5.3 Profile C: layers characteristics

Thickness (m)	V_S *(m/s)*	V_P *(m/s)*	*Density* (kg/m^3)
3	450	800	1800
5	350	600	1800
10	400	700	1800
∞	450	800	1800

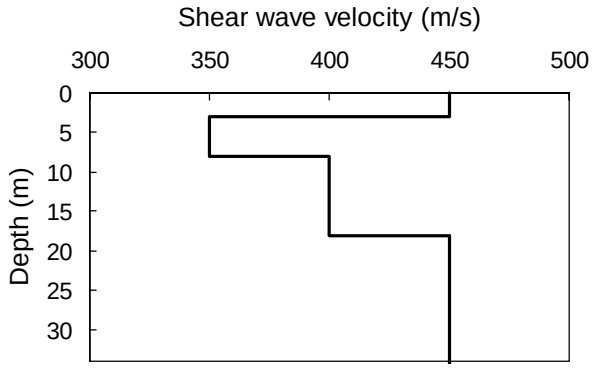

Figure 5.18 Profile C

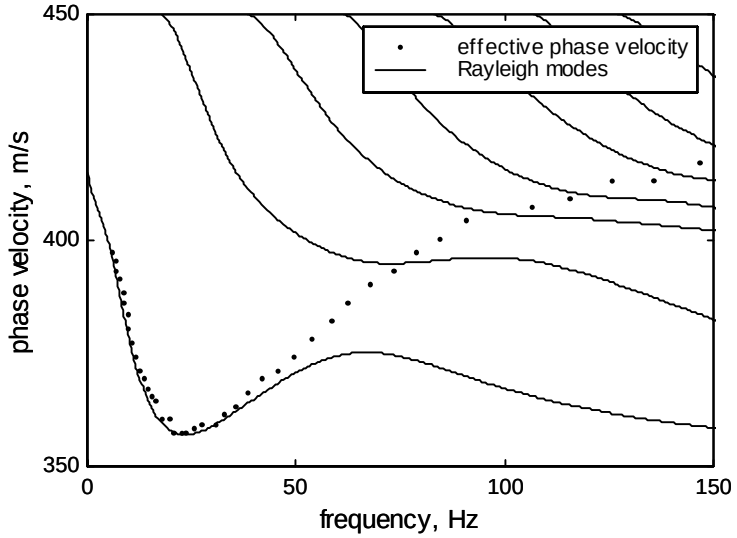

Figure 5.19 Rayleigh modes and effective dispersion curves for profile C

In this case the fluctuation of phase velocity evaluated from different SASW test configurations are not as marked as for profile B (Figure 5.20). This leads to a more stable global estimate from the averaging process and the final result is that the obtained dispersion curve is very close to the effective phase velocity.

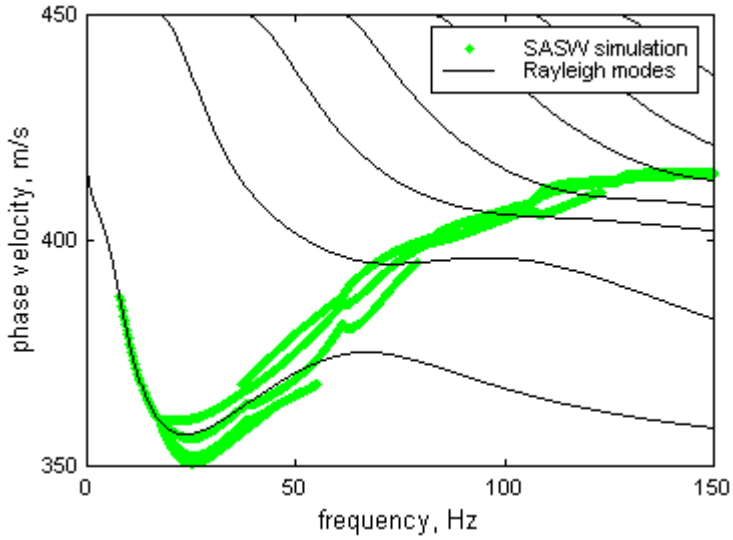

Figure 5.20 profile C: complete ensemble of data from SASW simulation

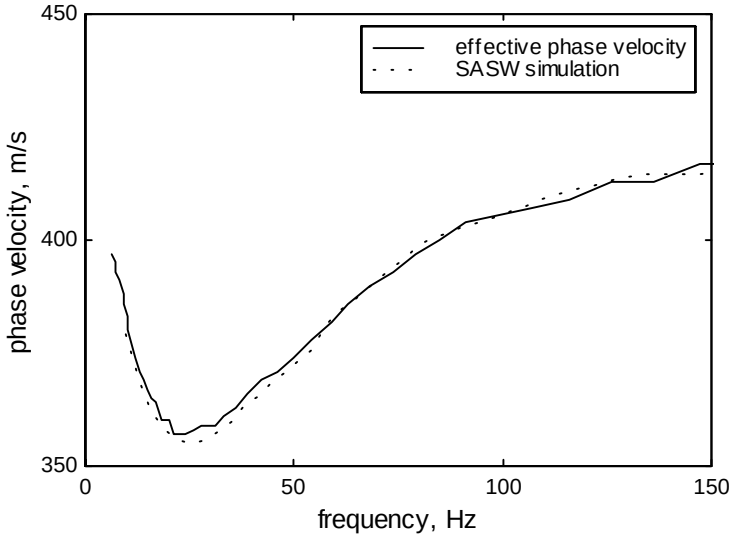

Figure 5.21 Profile C: comparison between dispersion curves

Passing to the multistation *fk* domain analysis, also in this case the trace spacing in time is such that considering the mechanical properties of the system there is no spatial aliasing problem, as it is also confirmed by the visual inspection of the spectrum.

In this case the dominant mode continually shift toward the higher ones as frequency increases, as it is confirmed by the dispersion curve obtained from the absolute maxima of the *fk* spectrum estimated using 256 receivers. Indeed segments relative to different modes constitute this dispersion curve (Figure 5.23). Clearly following the ridges that correspond to these segments in the *fk* spectrum (Figure 5.22) it would be possible to trace a larger segment for each mode from the local maxima, as have been done for Profile B (see Figure 5.13).

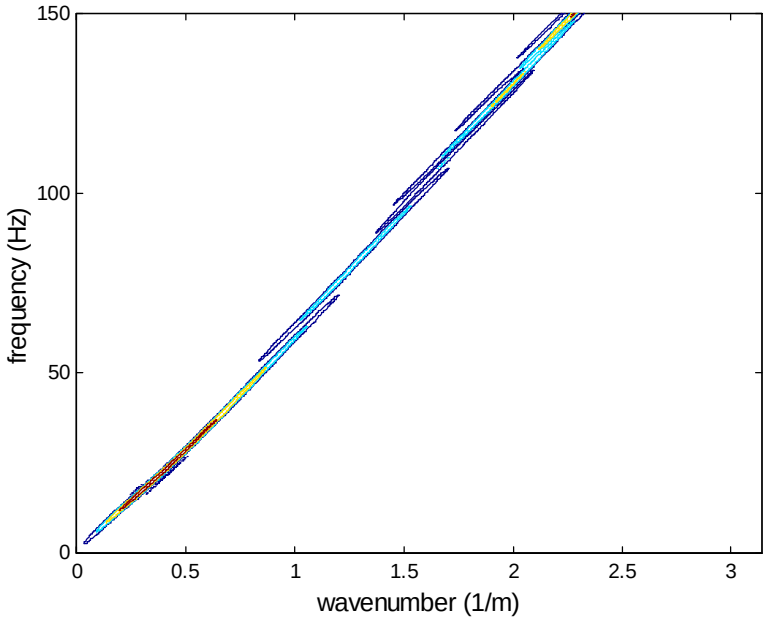

Figure 5.22 Profile C: fk spectrum from 256-receiver array

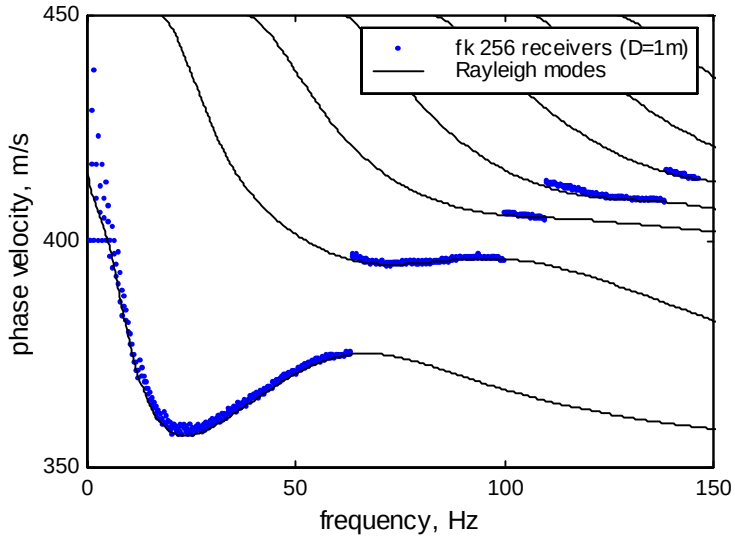

Figure 5.23 Profile C: Rayleigh modes and segments of them that can be found as absolute maxima of the fk spectrum (256 receivers)

Considering the more interesting case in which a reduced number of receivers is employed, the choice of the source to first-receiver distance induces some differences in the results. Indeed, considering 24 receivers, the *fk* spectrum that is obtained with the first receiver at only 1m from the source shows that no mode separation is allowed (Figure 5.24) and hence the dispersion curve obtained is practically identical to the effective phase velocity (Figure 5.25). Only a very slight overestimation of the values of velocity in the range between 25 and 50 Hz can be noted, but this is likely to have not a significant effect on a possible inversion process.

If the distance of the receiver array is augmented to 20m, the result is somewhat worse. Indeed in this case the dispersion curve is identical to the effective one up to about 25 Hz, while for higher frequencies there is a continuous underestimation (Figure 5.25). The distance from the effective curve is greater than the previous case, nevertheless it remains very low, being in the order of the 5% or less.

The conclusion is that substantially the results obtained with 24 receivers can be considered a good approximation of the effective dispersion curve.

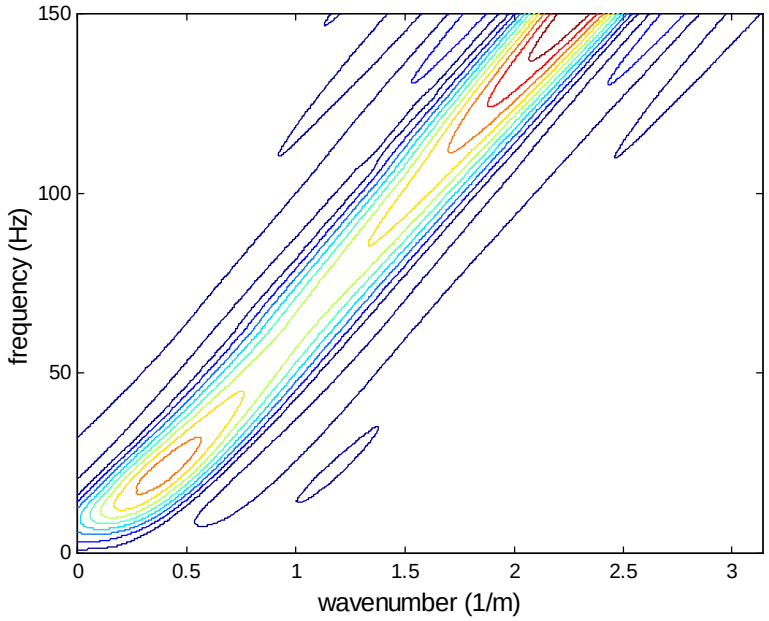

Figure 5.24 Profile C: fk spectrum from 24-receiver array (D=1m)

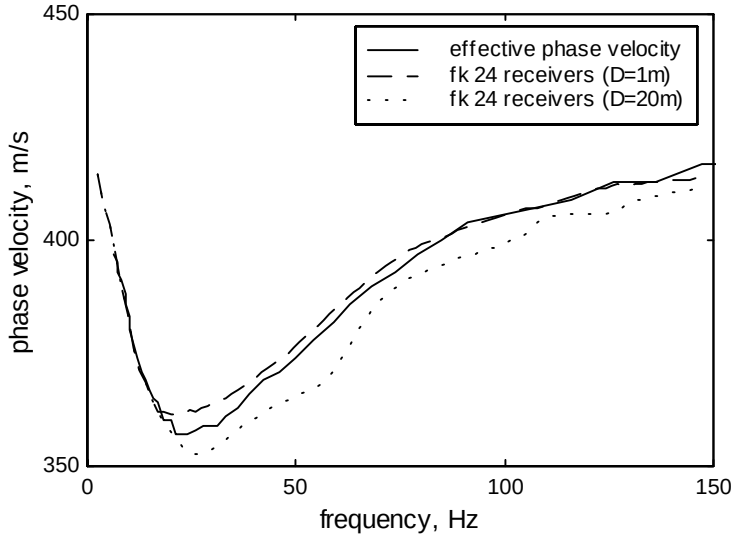

Figure 5.25 Profile C: dispersion curves from fk approach (24-receiver array)

5.4 Near field effects

Up to this point, no near field effect has been considered in the simulation of the wavefield generated by a point source. This choice is justified by the idea of focusing the attention on the effects of mode superposition, to understand which implication it has on the methods used to evaluate the dispersion curve.

Nevertheless it must be considered that in reality the effect of body waves can be substantial, especially in some cases. For this reason some of the above analysis have been repeated to assess the magnitude of the problems that body waves can produce on the dispersion curve evaluation process.

To accomplish this task a new set of synthetic signals has been created using another computer code created by Prof. Herrmann and his co-workers (Herrmann and Wang 1985). This code is based on the wavenumber integration method that consists of evaluating the double integral:

$$g(r,t) = \int_{-\infty}^{\infty} g(r,\omega) \cdot e^{i\omega t} d\omega \tag{5.2}$$

with

$$\overline{g}(r,\omega) = \int_{0}^{\infty} g(k,\omega) \cdot J_n(kr) \cdot k \cdot dk \tag{5.3}$$

where J_n is the Bessel function of the n^{th} order and $g(k,\omega)$ is the motion characteristic in the frequency-wavenumber domain due to a unit surface load (Green's function) that can be obtained for a layered halfspace with the usual techniques (see Paragraph 3.3.1.1) but accounting also for body waves.

The integral in Equation 5.2 represents an inverse Fourier transform and it gives only minor numerical problems for its evaluation. The wavenumber integration of Equation 5.3 is complicated numerically. Main sources of error can be the finite integration limit and the particular rule of integration used.

The code is divided in three sections: the first read the input data, the second solve the layered medium eigenvalue problem and accomplish the task of the wavenumber integration and the third compute the inverse Fourier transform. The second block is by far the most computationally intensive and requires a quite long CPU-time.

The effect of body waves has been considered for the case of profile C, since this is the most complex situation and data from the literature show that the near field constitutes a great problem for inversely dispersive layered media (Sanchez-Salinero 1987, Tokimatsu 1995).

The synthetic seismograms where computed for 43 receiver positions along a straight line starting from the source with a space interval of 1m.

The dispersion curve was evaluated both with the classical two-station approach of SASW test and the multistation fk method.

Figure 5.26 shows the dispersion curve evaluated using the SASW approach and averaged over frequency intervals to reduce the number of points. The inter-receiver distance was assumed equal to the source to first-receiver distance and the following values of such distances were used: 3m, 5m, 7m, 10m, 15m and 20m for a total of 6 test configurations. Since this profile represent one of the cases were near field effects should produce major problems, the curve has been estimated considering three different filtering criteria, corresponding to near field extensions respectively of 1/2, 1 or 2 wavelengths. The problems due to body waves are evident in the whole frequency range of interest and are only attenuated by the more restrictive criterion. Considering a near field extension of about two wavelength the fluctuation of the estimated curve attenuate, but an high price is paid since no information are obtained for frequencies below 40 Hz.

In practice the use of a so restrictive criterion results in a very poor extension to depth of the estimated stiffness profile. E.g. for the test configuration used for this simulation, considering the fact that the two station method works better using the common receiver midpoint geometry (see Paragraph 4.3.2.1), the possibility of testing along a plane and free from obstacles straight line of 60m is required. Using that filtering criterion, wavelength no longer than 10m can be inferred and hence the profile can be inverted only up to about 5m, that is a very poor result.

The fact that body waves have a such adverse effects on the dispersion curve evaluation process could seem in contrast with the observations that were done in Chapter 3, regarding the prevalence of surface waves in the wavefield generated by a point force, also due to their minor geometric attenuation. First of all it must be considered that that discussion was centred on the homogeneous halfspace, while in a layered medium several things can change. Second, and most important, it must be noted that the two-station approach for the evaluation of phase velocity is based only on the phase of the signals at the two receivers and not on their amplitude. For this reason it is strongly affected by perturbations due to any kind of noise and body waves constitute a sort of correlated noise in the signals.

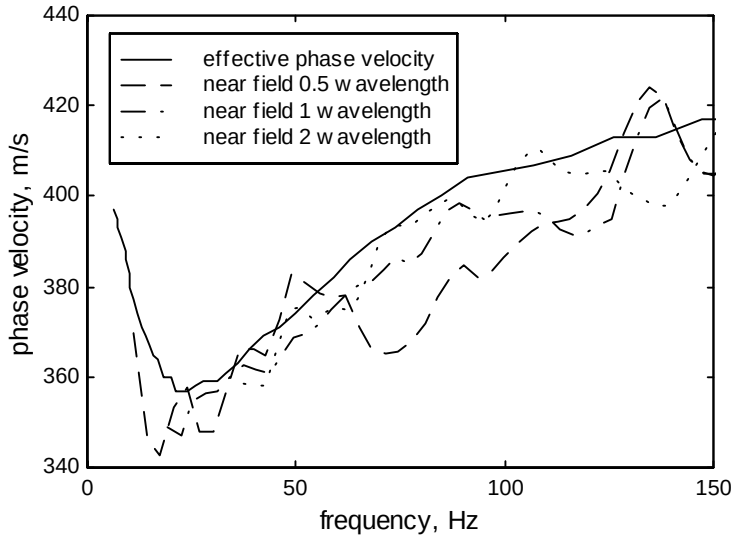

Figure 5.26 Profile C: comparison between the effective phase velocity and the dispersion curve from the SASW approach using different filtering criteria for the estimation of the near field extension

Following the motivation given above about the problems that arise in the evaluation of the dispersion curve from the two-station method, it appears that the *fk* analysis should be more robust in this context. Indeed first of all it is based on the analysis of several signals at once and hence should be less affected by perturbations that interest few receivers (e.g. the closer ones to the source). Moreover the signal amplitudes have a strong influence on the estimated spectrum and hence on the phase velocity evaluation. In particular for this last reason the body waves are expected to have a minor influence since their amplitude is minor and it attenuates more with distance.

These remarks are partially confirmed by the simulations that have been conducted. Indeed Figure 5.27 shows that the fluctuations are much more attenuated with respect to the results from the two-station approach. Nevertheless it must be noted that some local deviations in the values more than in the shape are present with respect to the effective phase velocity evaluated for surface waves only.

The results presented have been both obtained considering an array of 24 receivers with inter-receiver distance of 1m. The difference is the source to first-receiver distance that in one case has been taken equal to 1m and in the other to

20m. In the first case the agreement between effective phase velocity and the estimated value is very good for frequencies above 30 Hz, while below this threshold value the *fk* method underestimates the Rayleigh wave velocity, also if the shape of the curve is quite correct. In the second case there is a general but minor than the previous underestimation of the velocity and moreover there is a lack of information in the range 5 to 10 Hz.

Notwithstanding these lack of precision, the results are globally much better than those obtained using the two-station approach.

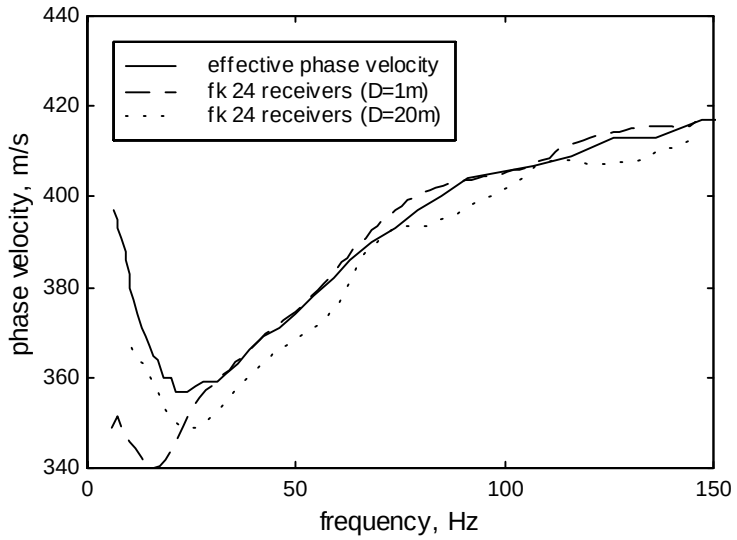

Figure 5.27 Profile C: comparison between the effective phase velocity and the dispersion curve obtained from the fk approach, considering different choices of the source to first-receiver distance (in presence of near field effects)

5.5 The frequency-slowness domain

As discussed in Paragraph 4.5.2, from multistation data the surface wave phase velocity can be extracted also considering the frequency-slowness spectrum, that is obtained applying to the original data a slant stack transform and subsequently a one dimensional Fourier transform.

Although in principle this approach should lead to the same result of the analysis in the frequency-wavenumber domain, because of the equivalence of the

transform processes, some differences could arise in the actual application to real data.

The application of the frequency-slowness algorithm on the simulated data of the present Chapter has led only to minor changes with respect to the frequency-wavenumber analysis. Some discordance are present in the very low frequency range (below 5 Hz), where the frequency-slowness approach fail to individuate the correct dispersion curve (that in that zone is always the one related to the fundamental mode for all the analysed cases).

A distinctive point is related to the visual analysis of the data. Indeed the frequency slowness spectra give a very clear picture of the dispersion curves without the need of extracting the maxima. For example in Figure 5.28 are reported the spectra relative to the three profile considered in the present Chapter when the whole ensemble of 256 traces is considered. Since the slowness is the inverse of the velocity, the spectra clearly show in their maxima the relative dispersion curves (just rotated of 90 degrees counterclockwise with respect to the classical representation phase velocity vs. frequency). Note also that in this case the transition of dominant mode is more evident than in a frequency-wavenumber spectrum.

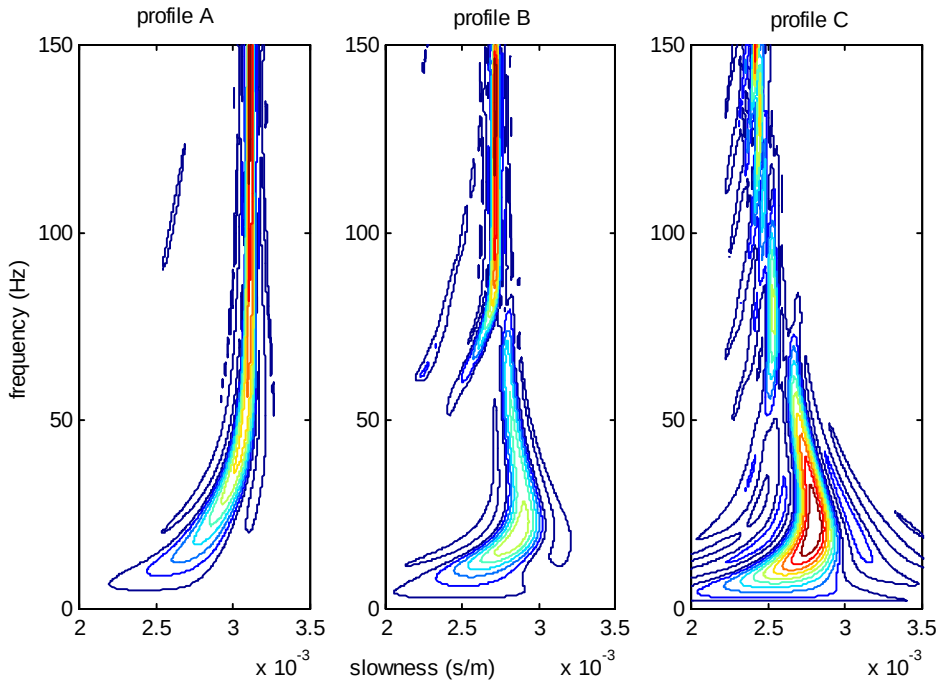

Figure 5.28 Frequency-Slowness spectra (256 receivers)

5.6 Some remarks about approximate inversion

In Paragraph 4.3.1 discussing the Steady State Rayleigh method, an approximate method to estimate the shear wave profile from the experimental dispersion curve was presented (see Figure 4.3). It was emphasised that the method could produce a fast rough estimate for normally dispersive profile, but it fails in the cases where stiffness is not monotonically increasing with depth. To confirm this sentence the method was applied on the effective dispersion curves relative to the three profiles considered in this Chapter.

In such approximate inversion, for each single point of the experimental curve a shear wave velocity slightly higher than the Rayleigh velocity is assigned to a depth equal to a fraction of the correspondent wavelength. Usually on the basis of displacements distribution with depth for a propagating surface wave one half or one third of the wavelength is used for the empirical estimate. To make a comparison, the evaluation has been repeated considering both the above possibilities and an intermediate one.

The results, reported in Figure 5.29, clearly show that effectively the method gives an acceptable estimate only for case A, which represents a normally dispersive profile. The estimate obtained can be considered sufficient for some applications, without the need for an accurate inversion process, but in general it can constitute a good first guess for an iterative inversion algorithm.

The estimate is not acceptable for inversely dispersive profiles, still it is important to remark that the trend related to the presence of softer intermediate layers or stiff top layers is revealed by its shape.

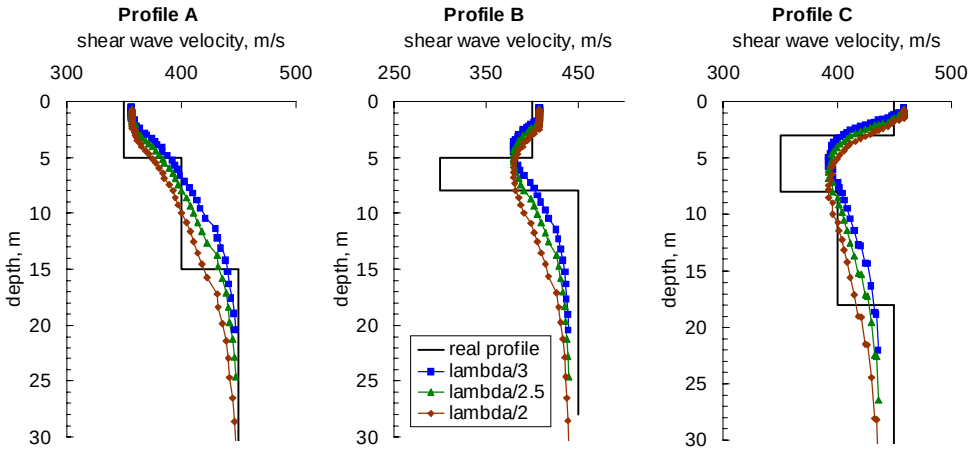

Figure 5.29 Application of the approximate method for estimation of stiffness profile

5.7 Discussion and conclusions

The objective of the numerical simulations that have been reported in this Chapter was essentially to test the effectiveness of different methods that can be used for the evaluation of the dispersion curve of a site from experimental data: one based on a two-station configuration (the traditional case of the SASW test) and the other on multistation measurements. In particular, the flexibility of these methods to different soil stiffness profiles and hence different responses to a dynamic excitation has been assessed.

Two set of simulations have been conducted one considering only surface waves, the other simulating the complete wavefield generated by a point source.

An initial remark must be done about the use of the multistation fk domain approach with a very large number of receivers (256 in the analysed case). As it was expected this configuration leads to a very good reconstruction of the dispersion curves associated to all the participating modes. This would be the ideal case for a stable and efficient inversion process since many information can be used to partially solve the problem of the non-uniqueness of the solution (see Paragraph 4.3.2.3). Nevertheless it must be noted that such a high number of receivers makes unpractical the application of the method to standard problems of geotechnical characterization.

For this reason in the following only the results of the two-station method and of the multistation method with 24 receivers are considered. The first session of simulation of the tests was done considering only surface waves and neglecting the body waves effects.

The profile A was chosen to be representative of a normally dispersive soil. As it was expected, in this case, since the fundamental mode dominates all over the frequencies, both methods performed well. Practically all the tested configurations led to the same dispersion curve, which represents at once the effective and the fundamental mode ones.

In the case of profile B, representing an inversely dispersive medium with a soft layer trapped between stiffer ones, both the SASW approach and the fk method have given some problem. The two station method has shown a frequency range in which strong fluctuation were present, also if this problem was partially attenuated by the averaging over frequencies to reduce the number of point. Globally there was a similarity with the effective dispersion curve.

For what concerns the fk analysis, it performed well when a distance source to first receiver of 1m was considered. In that case the obtained dispersion curve was pretty close to the effective one, with only some points out of trend in the zone of transition from the dominance of the fundamental mode to that of the first higher

mode. More troubles arose when the distance of the array from the source was chosen to be 20m, in that case the external part of the dispersion curve, where one of the two mode was effectively prevailing, was in good accordance to the free Rayleigh modes. But in the middle zone the effective trend was not detected. This can be explained with the effect of mode separation: since the distance from the source is large, the signals do not represent anymore a single wave-packet, nevertheless the number of receivers is not high enough to give a good reconstruction of the two modes.

Profile C was chosen to be representative of the case in which a stiff top layer exists, that must be considered one of the most complex cases, since many modes actively participate in the definition of the soil response. Again as for profile A all the considered configurations and associated methods of estimating the dispersion curve performed well, leading to a good estimate of the effective dispersion curve.

In the case of a strongly inversely dispersive medium, as profile C, the effect of body waves is likely to be more important. For this reason the simulation was repeated constructing a set of complete synthetic seismograms for profile C. In this case the results obtained with the two-station method were not satisfactory, independently from the assumption made about the extension of the near field zone. On the contrary the results from the multistation approach were quite good also if in some ranges of frequency they led to a certain underestimation of the velocity values.

In conclusion both methods showed some troubles, but the multistation method has performed generally as well as the SASW approach or better.

Another important remark must be done about the dispersion curve that is obtained from the fk analysis using a relatively small number of geophones at short distances from the source. In almost all cases the obtained curve was very close to the effective Rayleigh phase velocity. This conclusion is very important in the view of the inversion process, which, for inversely dispersive cases, must be conducted considering modal superposition and not the free Rayleigh modes.

About the generality of the above results, it must be considered that the real signals are also corrupted by external ambient noise. This fact has not been assessed in this work, but it is likely to have major effects at least for some ranges of frequency.

Chapter 6

Testing sites and equipment

One important phase of this research has been field-testing, which was conducted for evaluating the different procedures and develop the associated tools for analysis of surface wave methods.

The above field testing program can be divided in two main sections: a first testing campaign was undertaken in Georgia (USA) using the equipment of Georgia Institute of Technology. It was aimed at developing the transfer function method, which has been described in Paragraph 4.4.2.

A second testing campaign was undertaken in Italy in the Piemonte District and it was essentially directed at assessing the applicability of multistation methods, such as those based on *fk* (Par. 4.5.1) or *fp* (Par. 4.5.2) analysis, for geotechnical characterization.

Because of logistic problem and also because of the difference in the testing procedure the field equipment that has been used for each testing campaign is substantially different.

In both cases it was decided to collect and analyse data also using the classical SASW approach, such that a comparison between the obtained dispersion curve is possible.

In the following the testing sites, with all the available geotechnical information for each of them, and the field equipment are described.

6.1 Testing for stiffness and damping

The possibility of obtaining from surface waves testing not only the stiffness profile, but also the damping ratio profile is very appealing because of the importance that attenuation has in assessing the dynamic response of a site. In this perspective it is important to recall the necessity of working simultaneously on shear wave velocity and attenuation (Lai, 1998). The applicability of the transfer function method for coupled measurements of phase velocity and attenuation (Par. 4.4.2) has been assessed in two testing campaigns. In both cases traditional SASW measurements were conducted for a comparison on the obtained surface waves velocity. For what concerns the possible comparison with the uncoupled method for surface wave attenuation assessment (see Par. 4.4.1), the necessary field data are essentially the same collected for the transfer function method and hence no additional measurements are needed.

6.1.1 Testing sites

6.1.1.1 GTRI Cobb County testing site

The GeorgiaTech Research Institute testing site is located in the nearby of Atlanta, Georgia (USA) in the Cobb County district.

The deposit is essentially constituted of a 7 meters cover of Silt overlying a substratum constituted by Partially Weathered Rock, that is a typical formation of that geographic region, characterised by stiffness values intermediate between those of an altered rock and those of a dense soil. The water table is located below 10m, that is the depth reached during the SPT test, whose results are summarised in Figure 6.1, in conjunction with the log of the borehole. Unfortunately these are the only information available about the site and there are no data about seismic velocities for a direct comparison.

6.1.1.2 ISC 98 GeorgiaTech Campus testing site

This site, located on the Georgia Institute of Technology campus in downtown Atlanta, has been used for field demonstrations during the International Conference on Site Characterization, held in Atlanta on April 1998.

Also for this site the only available information is that of a boring and the correspondent SPT values. The soil is composed in the upper part (3-4m) of

reconstituted fill (mainly silty sands), underlain by a softer layer of residual silt and by a more compact stratum of sand (see Figure 6.2)

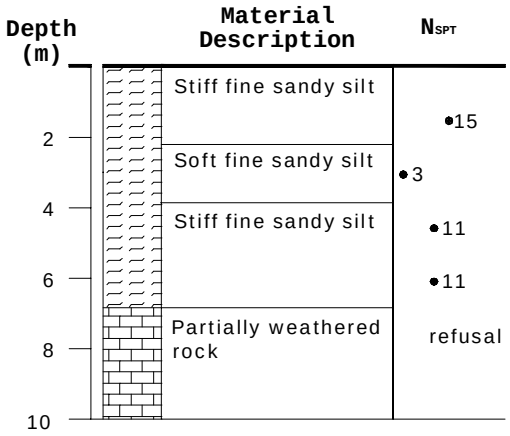

Figure 6.1 GTRI testing site (Cobb County): borehole log and SPT results

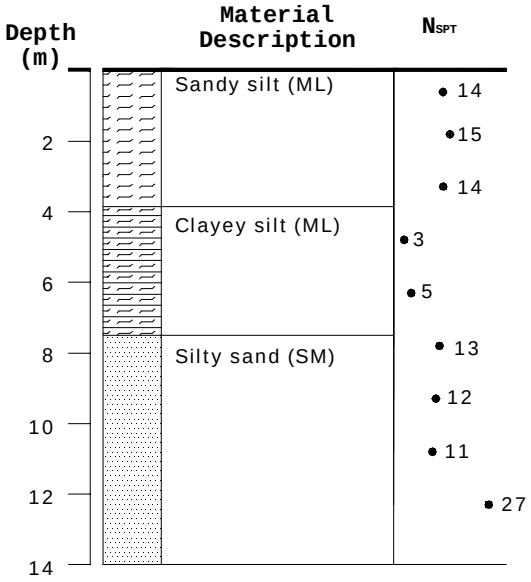

Figure 6.2 ISC 98 testing site (GaTech campus): borehole log and SPT results

6.1.2 Field equipment

The equipment that has been used for this campaign can be considered the classical one for SASW testing. Surface waves were detected using vertical 1Hz geophones and recorded with a digital signal analyser. The use of a controlled source has to be considered mandatory for attenuation measurements, because of the need of characterising the input. The same source has been used also for classical two-station phase velocity measurements. Additionally as required by the testing procedure (described in Par. 4.4.2) an accelerometer has been placed on the frame of the source to measure the input signal, that is required for the computation of the transfer functions.

The continuous source was an electro-mechanical vibratory shaker (Model 400 Electro-Seis® Shaker manufactured by APS Dynamics, Inc.). This shaker, thanks to the long stroke of its armature, is capable of impart its maximum dynamic force at low frequencies. It has a maximum stroke of 6.25 inches (16 cm) and can be operated in the frequency range 1-200 Hz. An input voltage from a function generator is converted by the shaker in a dynamical force that has the same frequency characteristic and magnitude controlled by the magnitude of the input voltage. The shaker mass is 30.6 kg and it gives on the frequency range adopted for the test (5-100 Hz) using the maximum input voltage amplitude (2 V) force amplitudes ranging from 445 N to 60 N. (indeed the acceleration spectrum range from about 1.5g @ 5 Hz to 0.2g @ 100 Hz). The force envelope is depicted in Figure 6.3 (the amplifier that has been used for the test is a model 144).

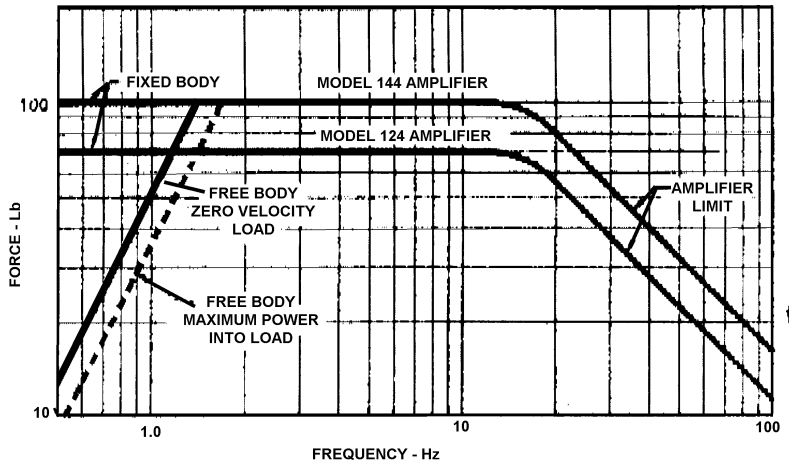

Figure 6.3 Frequency response of the shaker (from APS-Dynamics)

The acquisition device is a Hewlett-Packard Model 3562A, Dual-channel Fast Fourier Transform (FFT) Analyzer, which can be used for measurements with frequencies ranging from 64 μHz to 100 kHz. Its resolution in frequency is given by Span/800 (i.e. 801 calculated frequency points), and the time records have a maximum length of 2048 points (samples). The analyser has a built-in anti-aliasing filter.

An important feature of this analyzer is a built-in function generator that has been employed to furnish the swept sine input to drive the shaker. In the swept sine mode a sinusoidal voltage is created with frequency that varies incrementally (on a linear basis) inside the given range of interest.

The analyzer is able to average a number of measurements ranging from 1 to 32767. During the test an average of 10 measurement at each frequency was used, since further measurements do not improve significantly the results (Spang 1996).

With AC coupling of the input signal, the FFT analyzer inserts a series of capacitor to remove DC components and drifts associated with DC from the geophone input signals (Hewlett-Packard, 1985).

Using a signal analyser it was possible to plot on the graphical display in the field the spectral quantities and hence to assess signal quality by visual inspection. Moreover the signal analyser has an internal algorithm for transfer function evaluation from the receivers signals and hence the required elaboration in the office are reduced.

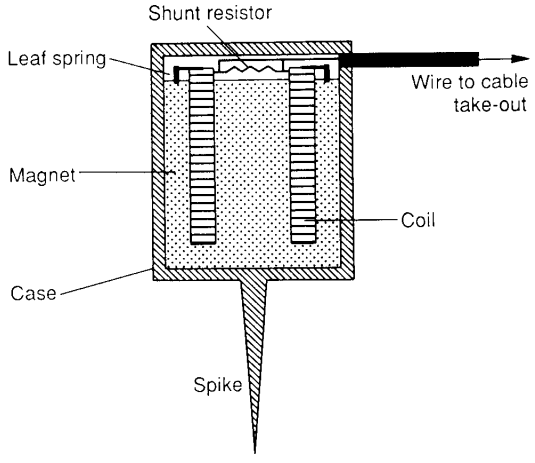

Figure 6.4 Constructive scheme of a moving-coil geophone (from Doyle 1995)

To detect particle motion velocity on the ground surface, the following vertical geophones were used: Mark Products Inc. Model L-4C with a sensitivity of 13.5 Volts/in./s. These geophones, which have a natural frequency of 1 Hz and a mass of 981 grams, measure particle velocities in vertical direction using a magnet, attached to the geophone case and an electric coil system mounted on a suspended mass (Figure 6.4). The relative movement between the two, due to a vertical movement at the base of the geophone and to inertia forces on the mass, produces a voltage in the electric coil proportional to the velocity of motion. The shunt resistor, that is drawn in Figure 6.4, is needed to damp the mass movement and to stop its resonant vibration that would swamp the records, so that the instrument response (Figure 6.5) be flat enough over the frequency range of interest (in our case from 5 to 100 Hz). It is important to note that this is the classical scheme of most geophones. The shunt resistor is an electrical resistance that absorbs the unwanted vibrational energy (Doyle 1995).

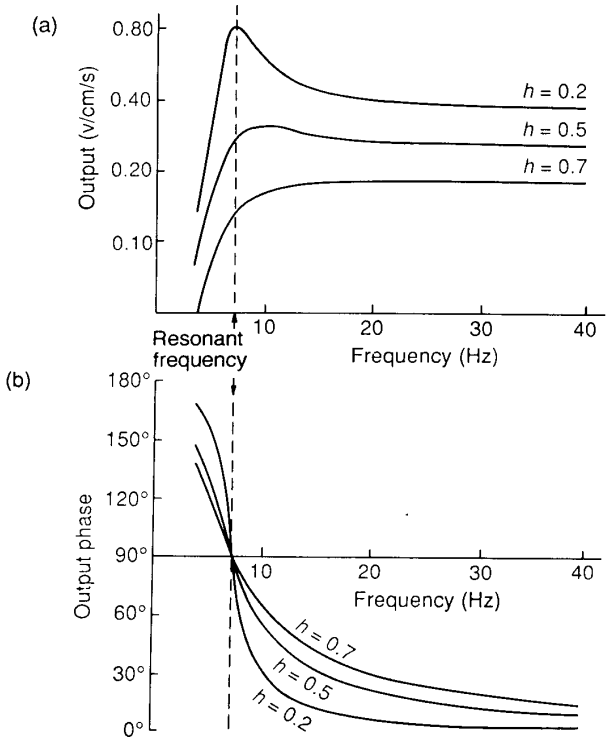

Figure 6.5 Example of geophone response for different damping factors h (7.5 Hz natural frequency) (from Doyle 1995)

The difference between geophones having different natural frequencies is essentially the suspended mass. Indeed the natural period of vibration of the instrument can be evaluated with the classical formula:

$$T_0 = 2\pi\sqrt{\frac{m}{k}} \tag{6.1}$$

where k is the spring constant.

Thus low frequency geophones, as the one used for these experiments, need a quite large mass, so that the sensitivity must be higher and they are largely more expensive than other ones (e.g. 4.5 or 11 Hz geophones). Moreover the high weight of the suspended mass makes this kind of geophones more delicate, because it can damage the spring during the setup operations.

Finally a piezo-electric accelerometer manufactured by Wilcoxon Research (Model 728T), having an acceleration constant of 510 mV per g, was mounted on the top of the shaker armature for the transfer function measurements.

6.2 Multistation impact source tests

During the testing session aimed at assessing the possibility of using *fk* or *fp* approaches, many different source-receivers configurations have been used. In particular the geophones have been usually placed with equal inter-receiver distance and several source-first receiver distances have been used. To evaluate the dispersion curve using the usual two station signal processing of SASW test (see Par. 4.3.2.2), pairs of receivers from the whole array have been considered such that the source-first receiver distance and the inter-receivers distance be equal. In this way a common source array (see Par. 4.3.2.1) field-testing has been obtained. Obviously this doesn't respect the usual practice on inverting the source position adopted for SASW test, but this should be a minor concern since a refraction survey has shown that the inclination of the layers is negligible at the testing site.

6.2.1 Some notes on cross-hole and seismic refraction methods

In view of exposing the available data about the testing site where this testing campaign took place, some notes on two seismic methods are reported in the following: the cross-hole test and the seismic refraction test.

When a detailed profile of stiffness with depth is required, the use of borehole

seismic methods is the standard of practice in geotechnical engineering. The most widely diffused methods of this class are the cross-hole and the down-hole methods (Figure 6.6), while less diffused are the up-hole method and the P-S suspension logging. Undoubtedly the cross-hole method is the most accurate, still it is also the more expensive since while other methods require only one borehole, cross-hole method requires two or, according to the ASTM standard recommendations, three boreholes.

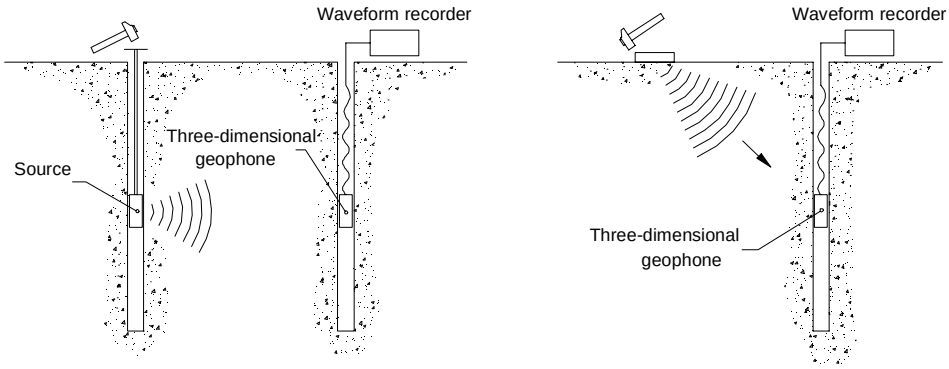

Figure 6.6 Schemes of cross-hole and down-hole tests

In the cross-hole method, the stiffness of the material at a given depth is determined using its relationship with body waves phase velocity. In turn the latter is determined evaluating the travel-time of a wave generated in the first borehole and detected at the other borehole or boreholes by three-dimensional geophones. The execution of the test involves a quite long and costly procedure. Indeed boreholes need to be cased and moreover, since an accurate measure of the effective travel distance is needed, an inclinometer measurement must be used to estimate the deviation from verticality of each borehole. For this reason very often only two boreholes are used, measuring the travel-time from the start of the impulse and the arrival of the wave at a single receiver (see Figure 6.6). The accurateness of this procedure is strictly related to the precision of the triggering mechanism at the source.

Some modified procedures for the analysis of the recorded signals have been implemented to improve the accuracy in the definition of the travel-time, working either in time or in frequency domain (Mancuso 1992).

Usually the distance that the wave covers is assumed to be exactly equal to source-receiver distance, using the assumption of a straight wave-path. This hypothesis can lead to some mistakes because in vertically heterogeneous media the ray-path is in general curvilinear. Moreover for a layered medium a serious problem can be constituted by head waves (Figure 6.7) that, when the cross-over distance is less than the distance from source and receiver, can constitute the first arrivals (see below the description of the refraction method). Such a problem is common when the measurement is made in a soft layer in a point close to the interface with a stiffer layer. The detection of a refracted wave as first arrival can lead to an overestimation of the actual stiffness of a layer.

Different kind of sources can be used to generate either mainly shear waves or longitudinal waves and hence leading to an estimated of the respective velocity. The distinction between different kind of waves can be made in relation to the component of the signal at the three-dimensional receiver. The measurement of the both V_P and V_S can be useful because it gives an estimate of both the shear stiffness modulus and the Poisson Ratio.

The measurements from the cross-holes testing performed using three boreholes can be also successfully used to estimate the local damping from the attenuation of the signal at the two receivers (Hoar 1987, Mancuso 1992).

Non invasive seismic methods are between the most important branches of geophysics. The petroleum industry applications have brought large investments to the developments of accurate signal processing tools for their interpretation (see for example Yilmaz 1987). Their use in civil engineering is generally restricted to the measurement of the depth to the bedrock. Indeed their resolution is usually not so good at the scale that is typical of geotechnical engineering problems. Nevertheless in presence of sensible contrasts of stiffness between layers, high resolution applications of both reflection and refraction methods can work quite well for shallow profile investigations (for some examples see the special section on shallow seismic reflection papers in Geophysics Vol.43, n.4 (1998)).

While the reflection method is based on arrivals of waves reflected by the interface between layers having a contrast in stiffness, refraction method is based on the measurements of the first arrival of the head waves that travel for a given distance along a interface. In general the refraction method has the strong advantage that it is based on first arrivals only, whereas reflected waves are often difficult to distinguish from the direct arrivals. In general both methods can be based on the use of either longitudinal or shear waves, even if usually it is much more simple generating longitudinal waves.

As mentioned above the refraction method is based on the arrival of head waves. Waves coming from the surface and critically refracted at one interface

generate a disturbance that travels along the interface, from which head waves in the upper layer are in turn generated (Figure 6.7). If a perturbation is generated on the ground surface, for given values of layers stiffness and depth, the head wave constitutes the first arrival at a certain distance from the source. The concept is synthesised in Figure 6.8. Going farther from the source, head waves relative to waves that are refracted by deeper and deeper interfaces constitute the first arrival and hence different layers can be characterised.

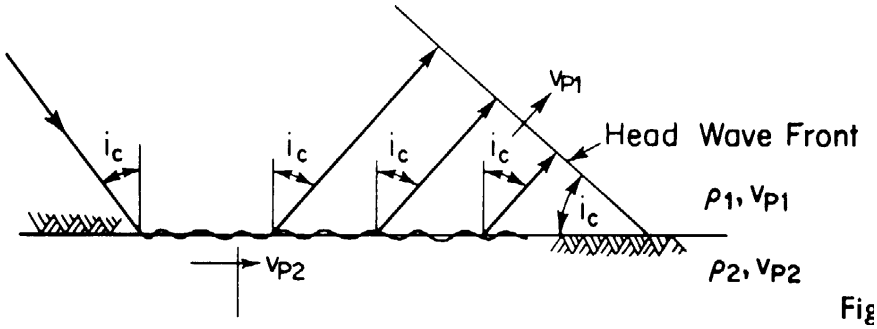

Figure 6.7 Head wave generated by two successive critical refractions (from Richart et al. 1970)

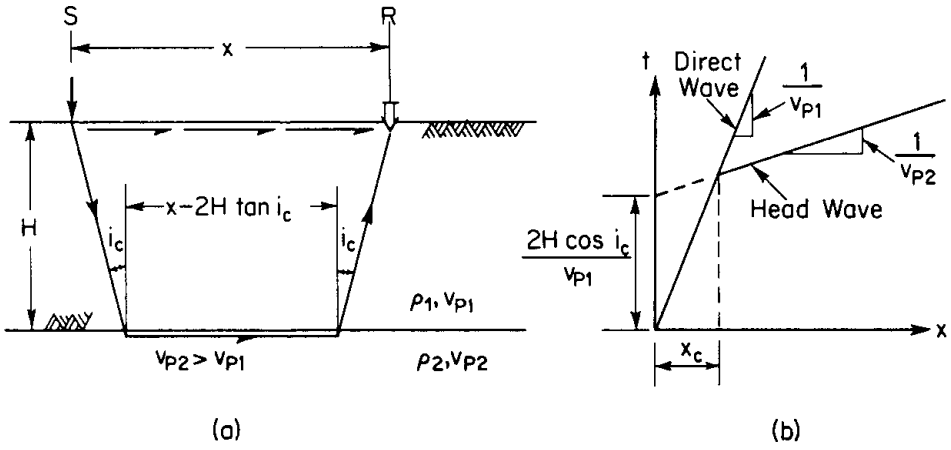

Figure 6.8 Ray paths and travel-time curves for direct and head waves (from Richart et al 1970)

One major problem in refraction surveys is given by the presence of a soft layer between stiffer ones. Indeed the method is not able to detect these layers and their presence can substantially false the final results. Another important problem that is inherent in the method is the so-called *hidden layer* problem. It arises when a thin layer precedes a stiffer layer and the dimension are such that the head wave generated by this second interface arrives on the surface before of the one related to the thin layer.

If the survey is conducted using longitudinal waves the water table can be detected if the layers above are characterised by a longitudinal wave velocity less than that of saturated soils (that can't be less than the velocity of water, i.e. about 1480 m/s). Obviously the presence of water masks all the layers which are under the water table and are characterised by a lower longitudinal wave velocity.

6.2.2 Testing site

The testing site is located in the nearby of a research center of ENEA, the Italian National Agency for Alternative Energy, in Saluggia (VC) in the northern part of Italy. The choice of this site was essentially related to the logistic ease of access and to the relatively large amount of available geotechnical information.

The site is located close to the Dora Baltea River and it is part of a large flat area, that is composed essentially of fluvial sediments. The soil is composed basically of gravels and gravelly sands, with the presence of fine sand and clayey silt, in the form of lenses. The water table can be found at very shallow depth, because of the vicinity of the river, and it can fluctuate seasonally between 2 and 3 meters below the ground surface.

The site has been subjected to a large testing campaign in the past. Several borehole logs are available, together with results from Standard Penetration Tests and a Cross-Hole Test. Figure 6.9 reports a plan view of the testing site with the location of all the boreholes together with the alignment used for surface wave testing and for the refraction survey that will be described in the following.

The above alignment has been chosen considering the following criteria

- Position as close as possible to the profile that was investigated with the Cross-Hole test
- Ground surface as much as possible flat
- Eventually, alignment be place between two of the existing boreholes.

Only the logs of boreholes G and CH are reported (Figure 6.11) because they are those of interest. For boreholes G and CHb also the results of a Standard Penetration Test are reported in Figure 6.10. Parts of these results seem to be controversial, propably because of the gravelly nature of the soil.

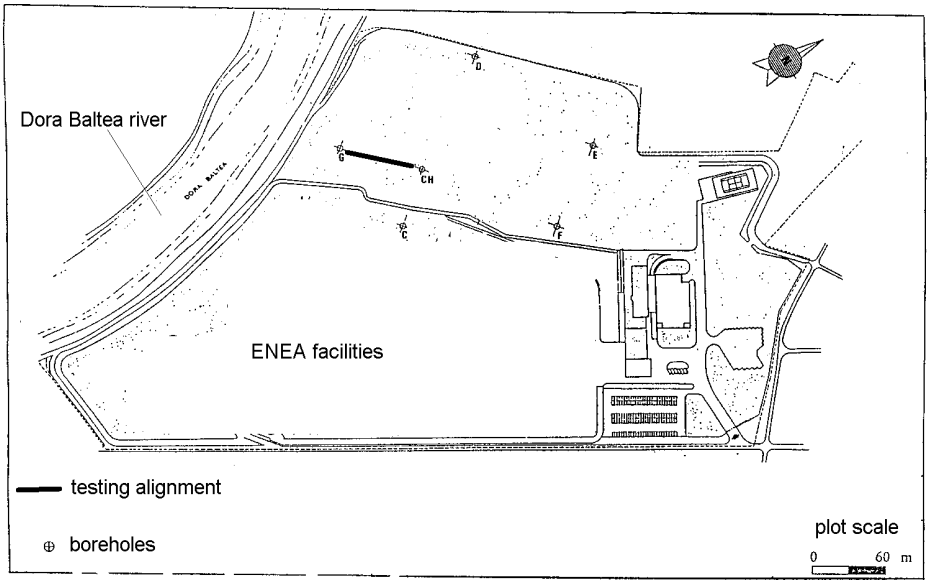

Figure 6.9 Testing site at ENEA facilities (VC, Italy): location of boreholes and testing alignment for SASW and refraction surveys

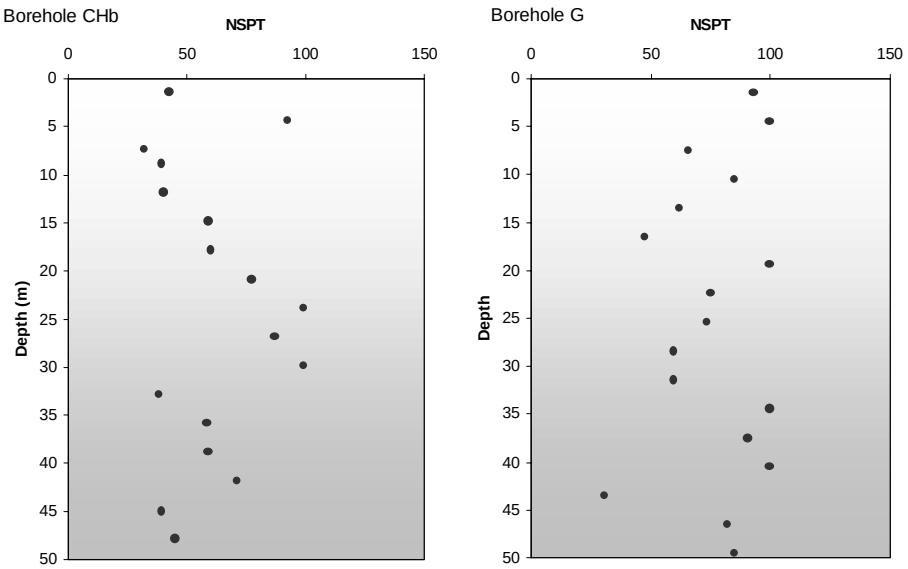

Figure 6.10 Results of Standard Penetration test for borehole CHb (left) and G (right)

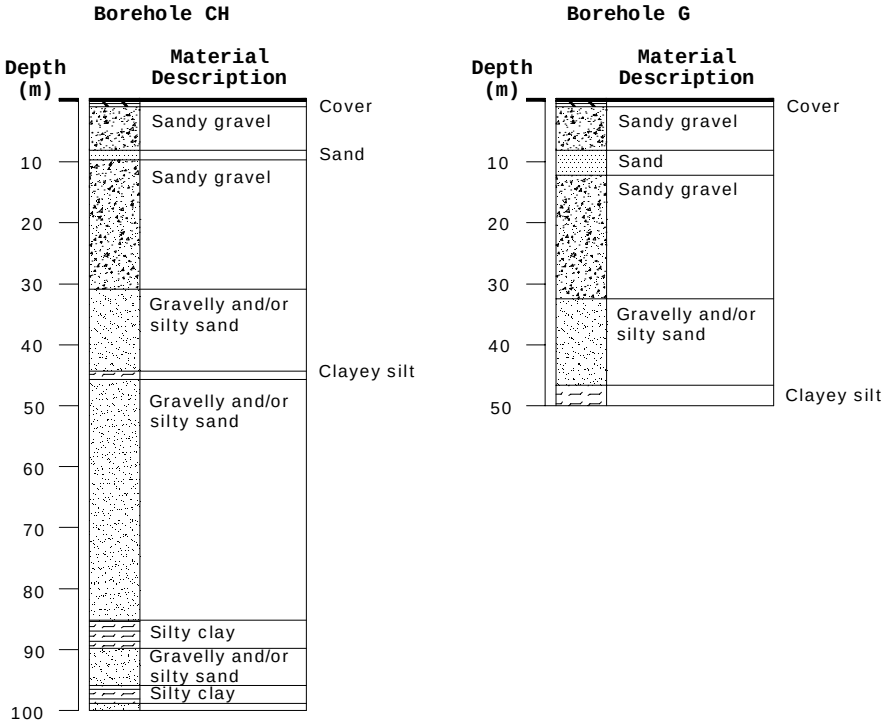

Figure 6.11 ENEA site: borehole logs

A rough description of the global layering of the soil up to a great depth (100m) can be obtained by the borehole CH (Figure 6.11) that has been realised with continuous sampling. Recent alluvial coarse gravels constitute a first layer of about 31m, with the presence of sandy seams; up to 85m there are more or less silty sands with thin gravelly or silty layers; at greater depth there is an alternation of thin layers of different materials. The comparison of the log of borehole G with that of borehole CH leads to the conclusion that the hypothesis of plane and parallel layers should be acceptable for this site, indeed the succession of the interfaces between different materials is at about the same depth. Apparently it seems also that lateral inhomogeneities are negligible for the site, also considering that the shallow soils are essentially alluvial deposits.

At the ENEA site, the Cross-Hole measurements have been conducted using

the borehole CH and another borehole (CHb, that is not reported in Figure 6.9), with an axial distance between the two of about 5 meters. The exact values of the distance have been estimated after the inclination measurements and range from 4.94m at the ground surface to 3.79m at the boreholes bottom (100m). Measurements for both longitudinal and shear wave velocities were conducted starting at 3m below the surface and ending at depth of 100 m, with step 1m. The results in terms of V_P and V_S are reported in Figure 6.12.

Using the above results it is also possible to evaluate the dynamic Poisson ratio that has, for the whole depth investigated by the cross-hole, a quite constant value, with a mean value of 0.47.

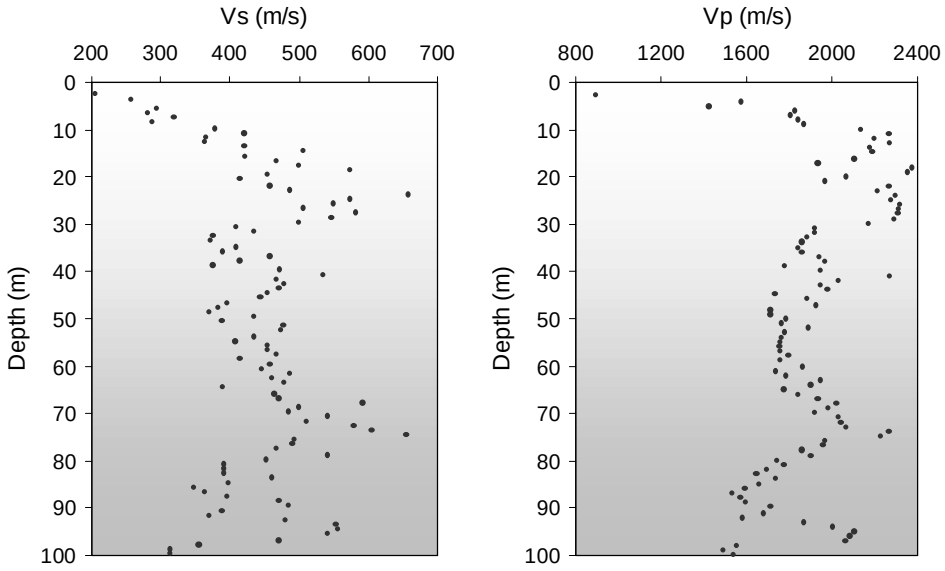

Figure 6.12 ENEA site: results from the cross-hole test

Together with surface waves measurements, which are the objects of this dissertation, also seismic refraction measurements were conducted at the same site, in the view of exploring possible synergies between the two methods.

The refraction survey that has been conducted at the ENEA site, used the same sources and about the same receiver configurations of the multichannel measurements conducted for soil characterization using surface waves. The main

difference was essentially in the acquisition parameters. Indeed the refraction method requires a good resolution in time and it is interested only in the first arrival of the wave but not in the whole waveform. On the contrary the SASW method and the multistation method for characterization through surface wave propagation require a good resolution in the low frequencies (<150 Hz) and hence a long record regardless of resolution in time domain.

The topographical level of the ground surface was preliminary checked. Based on that results the ground surface has been considered horizontal and no correction have been applied to the results from the refraction test. Moreover in the perspective of the SASW testing campaign, the fact that the free surface is practically horizontal, in addition to the information from boreholes CH and G reported above, assures that the usual condition of plane layering system that is fundamental for SASW test is practically satisfied at the site.

The profile for V_P waves obtained from the refraction survey at the ENEA site (Rafanelli 1999) is reported in Figure 6.13, The comparison with the results from the cross-hole test shows a good agreement of the longitudinal wave velocity estimated using the two methods.

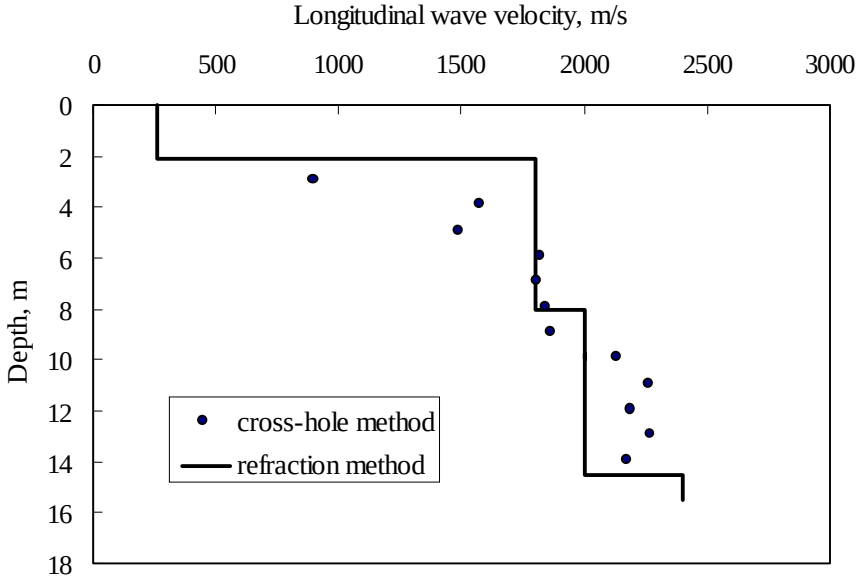

Figure 6.13 ENEA site: profile for longitudinal waves velocity

6.2.3 Field equipment

In view of having a large enough number of receivers a 24 channels seismograph was used for this testing session. The geophones were 4.5 Hz natural frequency velocity transducers, although other geophones were used for special purposes as described below. Many different impact sources were used in the aim of covering as much as possible the frequencies of interest for a deep enough characterization process.

The seismograph is a 24 channels ABEM model TERRALOC MK6. The sampling interval in time can be set between 25 μs and 2 ms and the acquisition window can be as long as 16384 sample/trace. The resolution of the a/d converter is of 18 bits + 3 bit IFP, for a total of 21 bits. The frequency range that can be covered by the instrument is comprised between 2 and 4000 Hz, widely covering the range that is required for SASW test. The seismograph has a built-in analog anti-aliasing filter, that is set automatically according to the selected acquisition parameters. Unfortunately this instrument has no real time capabilities for frequency domain processing and hence all elaboration of the recorded signals had to be done in the office, loosing part of the flexibility that field processing can give in terms of signal quality assessment.

The geophones, which have been used for this testing session, are SENSOR model SM-6/U-B vertical transducers, having a natural resonant frequency of 4.5 Hz. It is important to note that while in the common two-station SASW test only the information about the phases is used, in the multichannel approach the amplitude of the geophone response is very important. For this reason it is important to set the internal damping of the geophones such that their response is as much as possible flat in the frequency range of interest. Hence the shunt resistor (Figure 6.4) was set such that the damping factor is about equal to 0.6, so that the instruments response is more or less equal for all frequencies above the natural one (Figure 6.5). Anyway it must be considered that geophones work also below their natural frequency, even though in this case their response is not uniform.

On this testing site also some coupled vertical and horizontal geophones have been used to detect the elliptical partical motion associated to Rayleigh waves (see Par. 3.5). In that case vertical velocity transducers of frequency 11 Hz and horizontal velocity transducers of natural frequency 14 Hz were used. The two geophones were mounted on a small and rigid steel support, in the view of coupling their movements.

Several sources were used at this site: sledge hammers, a weight drop seismic source and a minibang.

Two sledgehammers (2 and 6 kg mass respectively) were used to energise at high frequencies. The trigger was a small piezo-electric switch that has been

mounted on the backside of the hammer. The switch detects the vibrations that are induced by the impact of the hammer on the ground and closes the electrical circuit.

The weight drop seismic source is mounted on a car trolley. The mass can be either 80 or 130 kg and is lifted up to 3 m in height using an electrical engine. The source has been used in two different configurations with or without a blow plate placed on the ground. When the plate was used the triggering was obtained by the closing of an electrical circuit, that was connected for one side to the plate and for the other to the falling mass. When the mass was falling directly on the ground surface a geophone placed very close to the blow point was used as trigger.

The minibang is a classical seismic source, often used for refraction and reflection surveys. It is a gun that is placed perpendicularly to the ground surface, using a plate that is hold down by the weight of the operators. The energy generated by the shot goes mostly in longitudinal and surface waves. Triggering is realised also in this case through a piezo-electric switch.

Chapter 7

Experimental results

The experimental results obtained during the different testing sessions have been divided as outlined in Chapter 6, in two main classes: the first one is composed by impact source multichannel records aimed at assessing the real capabilities of *fk* and *fp* domain approaches for geotechnical characterization purposes. The second class is that of the measurements based on the transfer function approach, which is proposed for the simultaneous estimate of stiffness and damping.

7.1 Impact Source Tests

7.1.1 Dispersion curve evaluation

In tests conducted with impact sources at the ENEA-Saluggia site, the experimental measurements were made considering a testing configuration designed for multistation methods. Nevertheless it must be considered that signals from a multistation session can be analysed with the classical SASW two-station procedure, just taking pairs of geophone responses.

In this regard, it must be noted that since the acquisitions have been made with a seismograph, all the spectral quantities had to be evaluated once back in the office.

7.1.1.1 SASW measurements

In analysing the traces with the two-station method, only those configurations having the source to first-receiver distance equal to the inter-receivers distance have been considered.

Some typical problems of Discrete Fourier Transform must be taken into account during the elaboration of the traces.

Concerning aliasing, as seen in Paragraph 6.2.2, the seismograph has a built-in internal anti-aliasing filter that is automatically set once the sample interval in time is fixed. Moreover it must be noted that since the highest sample interval is equal to 0.002s, the Nyquist frequency is well above the range of interest for soil characterization using surface waves properties.

Discrete Fourier Transform presumes the periodicity of signals. When a signal is digitised and transformed, the sharp brakes that can arise in the point of contact between the end and the beginning of the signal can cause the presence in the spectrum of some high frequency spurious components. This phenomenon is known with the name of leakage because part of the energy that should be associated to the effective predominant frequencies is leaked into other frequencies.

The phenomenon of leakage is partially attenuated choosing a lengthy window of acquisition in time such that the impulsive signal is concentrated in the central zone of it. Nevertheless it must be noted that because of the presence of ambient noise in the zone supposed to have zero amplitude, the phenomenon of leakage is only partially removed. Leakage can be reduced applying a windowing process with a smooth gradual function (Santamarina and Fratta 1998). The windowing process has been applied considering a Hanning window (Figure 7.1). Note that such a window keep unchanged the amplitude in the central zone of the signal and gradually weighs the outer zone, up to totally lower to zero the boundary points.

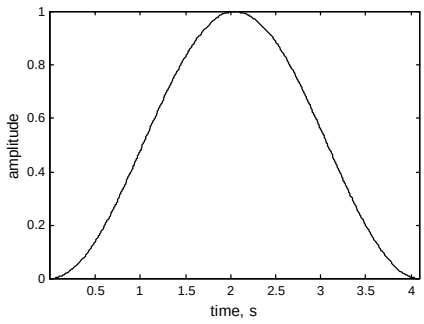

Figure 7.1 Hanning Window

From the whole ensemble of multistation data, some representative pairs of records have been chosen to be analysed with the classical two-station procedure for dispersion curve evaluation of the SASW test. To reproduce a classical acquisition, 6 different pairs have been selected spanning a range of inter-receiver distances between 3 and 30 meters.

Figure 7.2 show an example of the spectral quantities needed for the phase velocity evaluation (see Paragraph 4.3.2.2). A set of traces from 7 repetitions of the impact has been used to calculate all the average quantities. The cross-power spectrum phase is used to estimate the frequency dependent time delay between the receivers and hence, since the inter-receiver distance is known, the phase velocity. The other quantities are used to locate the distribution of energy (through the auto-power spectrum at the two receivers) and the frequency ranges with a high signal-to-noise ratio (corresponding to coherence function close to 1). This information is used to recognise the frequency range over which the information from the cross power spectrum is reliable.

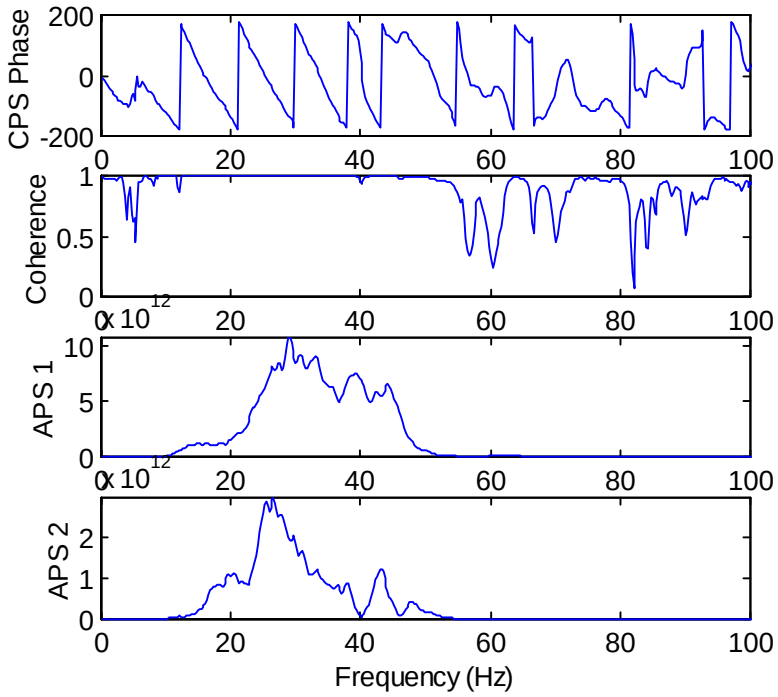

Figure 7.2 Example of SASW data (source: weight drop; inter-receiver distance 18m)

Considering each pair of signals, an estimate of the dispersion curve over a certain frequency range is obtained. Note that at this step the filtering criterion is applied (see Paragraph 4.3.2.2) to restrict the possible influence of body waves and of signal degradation. Hence only frequency corresponding to wavelength not less than one third and not more than twice of the source-to-receiver distance are effectively considered.

Assembling the information from the different pairs of receivers the composite dispersion curve is obtained (Figure 7.3). Note that over certain frequency ranges there is a wide overlap of data, while over other ones only information from one pair of receivers is available. This effect is produced by the combination of filtering criterion for near field effects and actual quality of the data. In particular while the central range of frequency is filled with a great quantity of data, for high and low frequency ranges only information from a single test configuration are present. This inequality can cause unwanted effects.

It is important to remark that since the traces have been collected for multichannel analysis, the common source array geometry has been used in place of the more usual common receiver midpoint one.

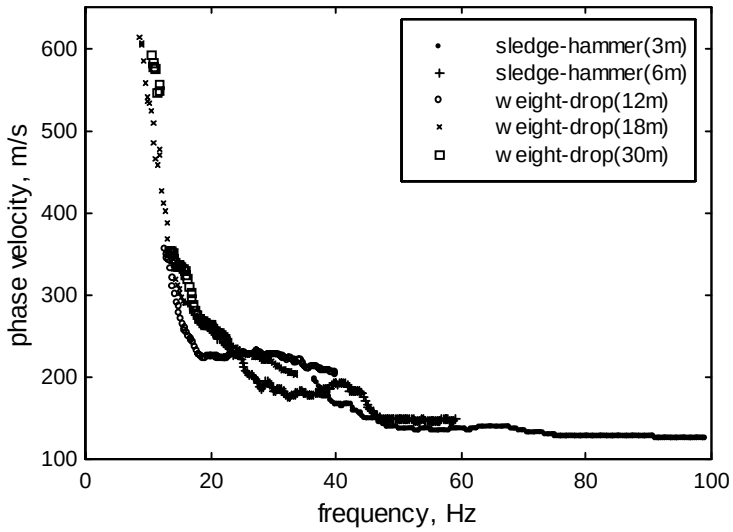

Figure 7.3 Experimental raw dispersion curve from SASW test

Since the number of points in the composite dispersion curve is not manageable for the successive inversion process, it is necessary to reduce it by an

averaging operation. In this regard the choice has been to divide the frequency range over which information are available in a given number of equal segments and for each of it to evaluate the mean value, assigning it to the central frequency of the interval. Using this criterion a 50-point dispersion curve has been built. Figure 7.4 shows the final experimental dispersion curve, where the average values are reported jointly with the relative standard deviations.

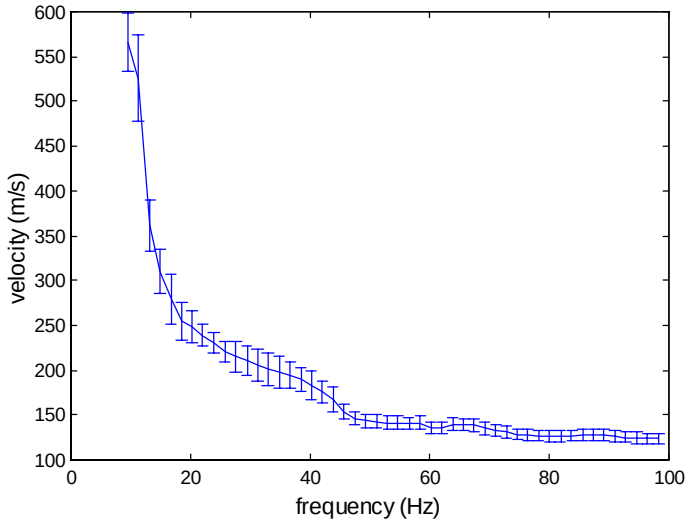

Figure 7.4 Dispersion curve from SASW test: reduced number of point with standard deviation representation

Some peculiarities of the final dispersion curve need to be remarked. First note that the standard deviation varies quite a lot with frequencies. This is essentially due to the presence of information coming from different receiver configurations, indeed has shown in Chapter 3, the phase velocity is a function not only of frequency, but also of space.

Moreover the absence of continuity in the information from a give source-receivers configuration, due to poor quality of data can cause the presence of gaps in some zones and hence small fictitious changes of slope of the dispersion curve. In the present case this effect is not very marked.

7.1.1.2 Multistation approach: *fk* domain

For the application of the multistation approach based on *fk* domain analysis of data, the common shot gather has been translated from the time-space domain to the frequency-wavenumber domain by two successive application of a FFT algorithm. To increase the resolution in the wavenumber domain, that is required for the accurate determination of spectral peaks, the ensemble of trace has been zero padded in space (i.e. a series of null valued traces has been added at the end of the shot gather).

As shown in Chapter 5 using numerical simulations, this algorithm provides a fast and fully automated estimate of the effective dispersion curve, provided that a sufficient number of receivers is used.

The results reported in the following are relative to two different testing configurations, both with an array of 24 receivers deployed at close distance from the source.

To explore the low frequency range the weight drop impact source and an inter-receiver distance equal to 3m have been used. The corresponding Nyquist wavenumber, that is the analogous of Nyquist frequency, is 1.047 1/m. This value limits the zone over which the *fk* spectrum is not affected by spatial aliasing. Figure 7.5 reports the main portion of the traces and the corresponding *fk* spectrum. The maxima associated to surface waves propagation are quite clear and from their location in the spectrum it is possible to evaluate the dispersion curve over a wide range of frequency (8 to 35 Hz) using the relation:

$$V = \frac{2\pi \cdot f}{k} \tag{7.1}$$

Analogously in Figure 7.6 the data relative to the second testing configuration are shown. In this case the sledgehammer having a mass of 6kg has been used and the receivers have been deployed with interval 1m starting at 1m from the source location. In this case information regarding a frequency range spanning from 15 to 68 Hz can be obtained.

It is important to remark that both data reported in Figure 7.5 and Figure 7.6 are relative to only one energising of the source. It has been established that a stacking process do not change significantly the results obtained in terms of dispersion curve.

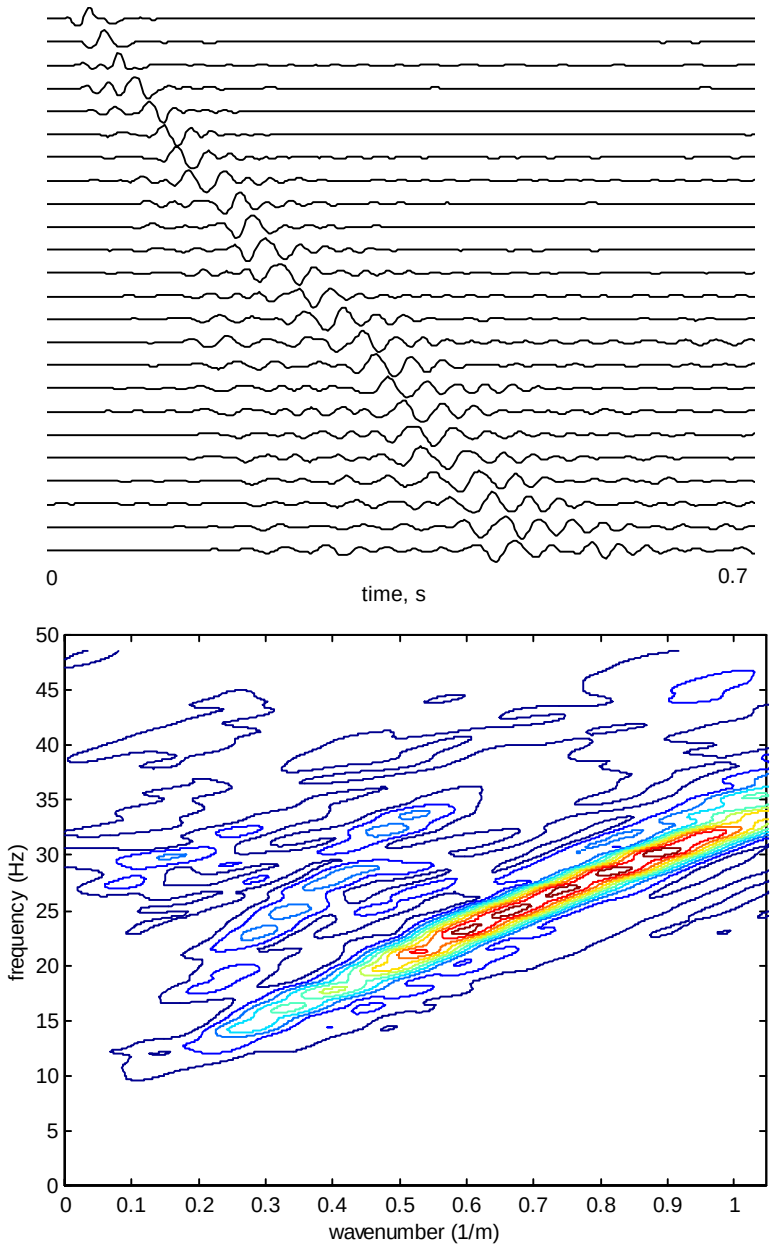

Figure 7.5 Traces and fk spectrum (source: weight drop; inter-receiver distance: 3m)

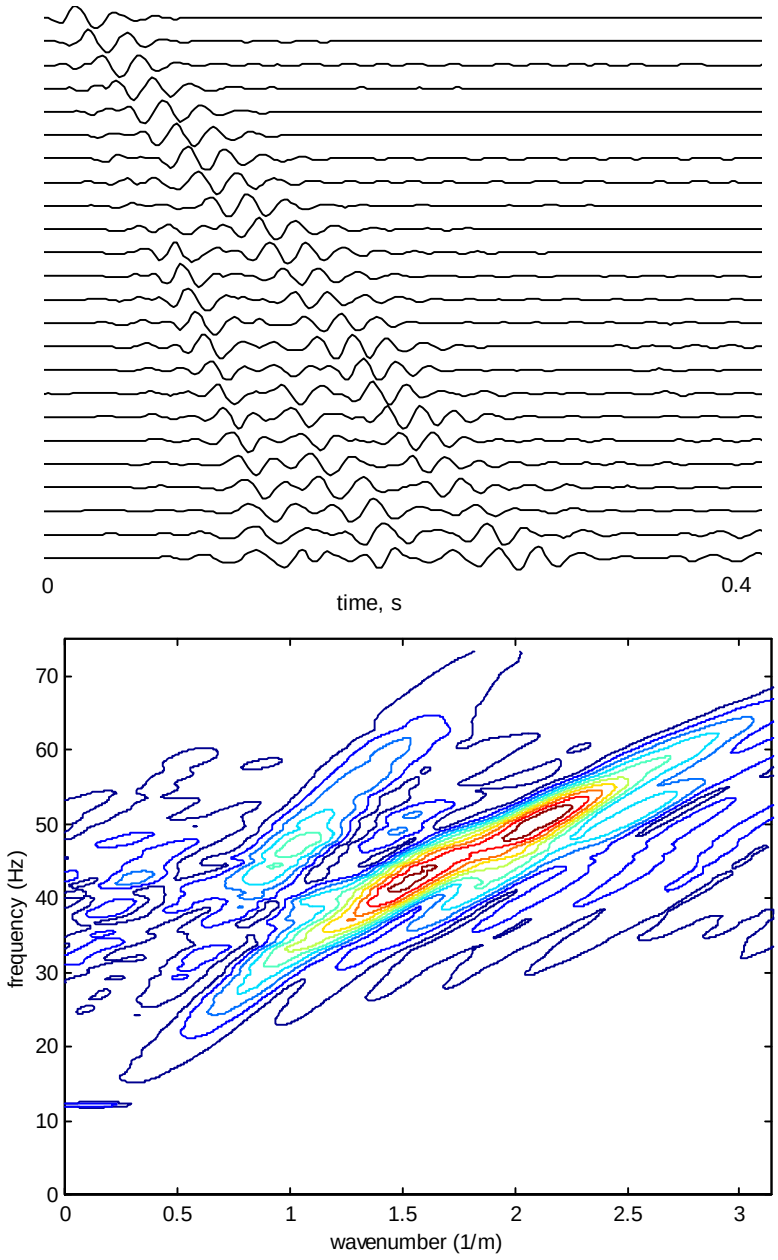

Figure 7.6 Traces and fk spectrum(source: sledgehammer; inter-receiver distance 1m)

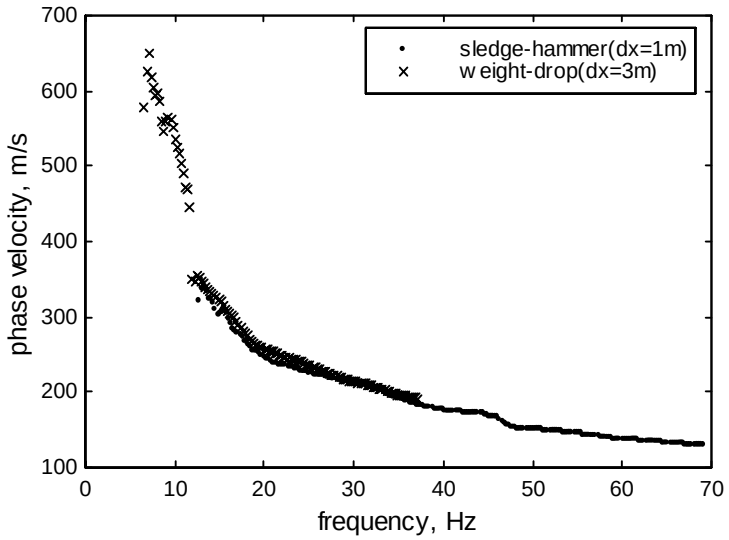

Figure 7.7 Experimental raw dispersion curve from fk analysis

Figure 7.7 reports the composite dispersion curve obtained by the *fk* analysis of the two shot gathers that are considered. Globally the frequency range between 8 and 68 Hz is covered. For low frequencies (below 15Hz) only information from the 3m gather are available, while for high frequencies (above 35Hz) the other gather supplies the information. In the central zone there is an overlap of information. It is remarkably that the values obtained by the two test configurations practically coincide, as it is confirmed also by Figure 7.8, showing the final dispersion curve with 50 representative points and the relative standard deviation, that is quite small in the overlapping zone.

An explanation of the good accordance of the results from the two test configurations is that since the values coming from the *fk* analysis are relative to a wide range of receiver position they are less influenced by the oscillation of phase velocity at a single position. The obtained dispersion curve is a sort of effective mean value corresponding to the whole space covered by the array of geophones.

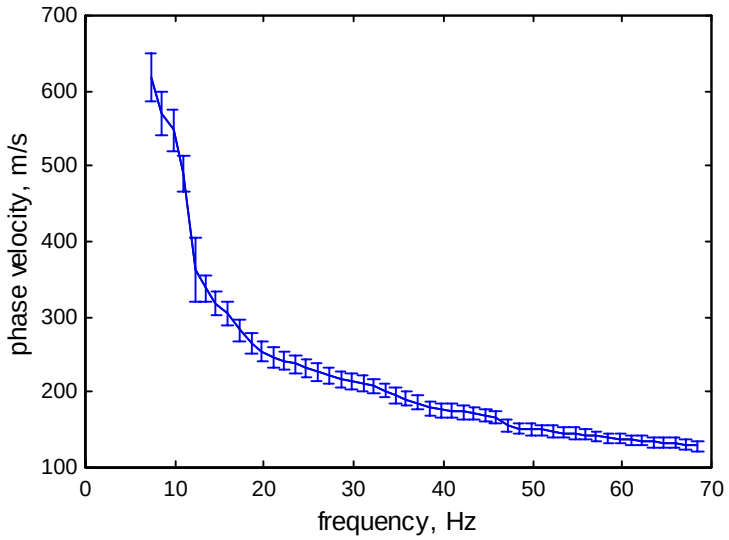

Figure 7.8 Dispersion curve from fk analysis, reduced number of point with standard deviation representation

7.1.1.3 Multistation approach: *fp* domain

Another promising multistation approach that can be used for geotechnical applications is based on the τp transform (see Paragraph 4.5.2). If a seismic shot gather undergoes a cascade of two transformations: first a τp (slant stack) and subsequently a 1D FFT over the τ domain, the dispersion curve can be evaluated from the maxima of the obtained fp spectrum. As shown in appendix A, this double transform is strictly related from a mathematical point of view to a 2D Fourier transform.

Since this process is based on a projection technique over an assigned velocity array (more precisely a slowness array), the resolution can be accurate without the necessity of particular artifices (such as the zero-padding used for 2D FFT) that could eventually introduce disturbances. Moreover since the operator chooses the slowness array over which the traces are steered to obtain the transformed field, it can be adjusted as a function of the expected soil properties, by then improving the resolution.

Another advantage is that a clear qualitative representation of the dispersion

curve is given directly by the spectrum, indeed recalling that velocity is the inverse of slowness the location of spectral maxima is analogous to the usual representation of the dispersion curve, just rotated of 90 degrees counterclockwise.

This kind of approach has been applied to the same data sets used for *fk* analysis. The relative spectra are reported in Figure 7.9 and Figure 7.10.

The dispersion curve evaluated considering the maxima of both spectra shows good accordance of data over the frequency range for which there is an overlap of information (Figure 7.11).

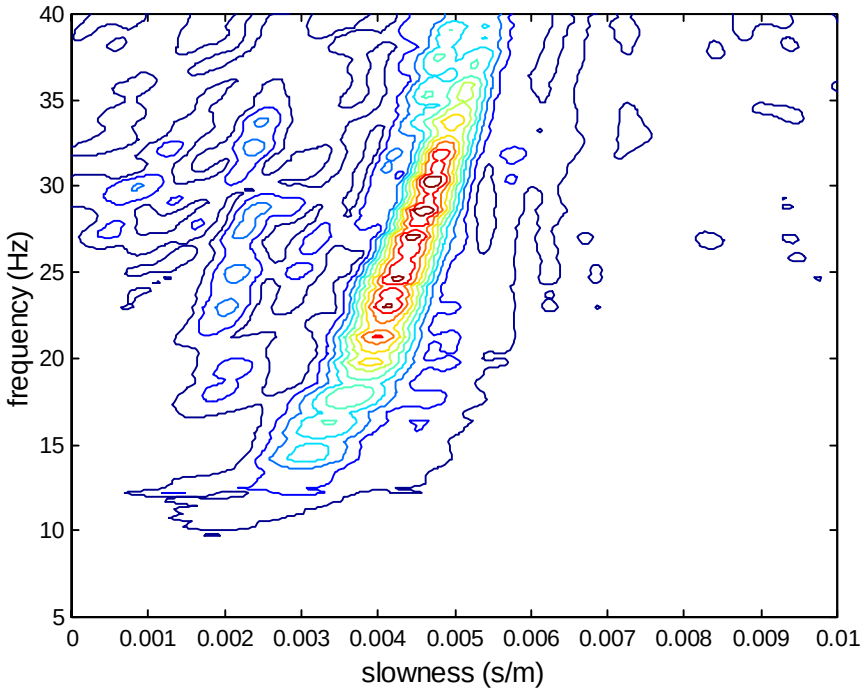

Figure 7.9 fp spectrum (source: weight drop; inter-receiver distance: 3m)

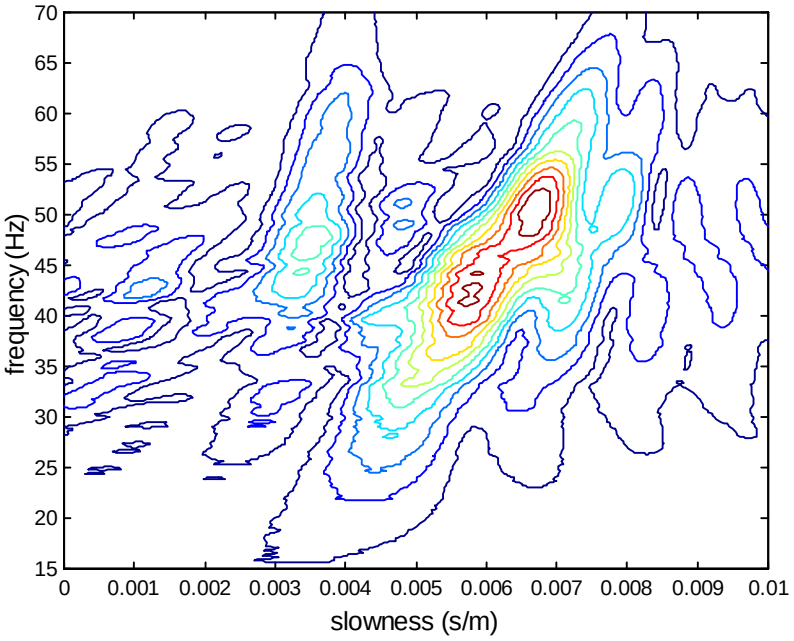

Figure 7.10 fp spectrum (source: weight drop; inter-receiver distance: 1m)

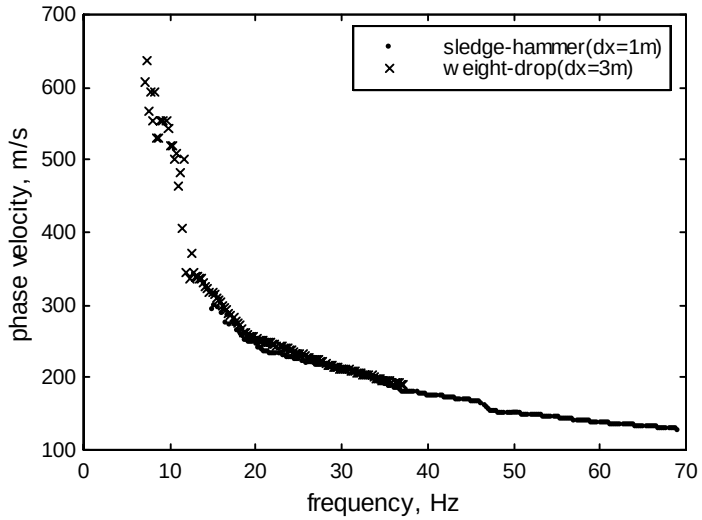

Figure 7.11 Experimental raw dispersion curve from fp analysis

7.1.1.4 Dispersion curves comparison

The experimental dispersion curves obtained using SASW and multistation *fk* methods are compared in Figure 7.12. The accordance between the two is very good all over the frequency range. It is important to recall that the averaging process has a great influence on the data from the SASW test, while it has only a minor effect on those relative to the *fk* analysis. This sentence is clarified by a look at the raw dispersion curves relative to the two cases (Figure 7.3 and Figure 7.7).

It is important to note that, with about the same global span of testing space the multistation *fk* methods is able to give information at lower frequencies. This is due essentially to the minor influence that noise and body waves effects have on multistation methods. On the other side during this testing session the information regarding the high frequencies range are restricted to about 68Hz. This is due to spatial aliasing: if higher frequencies would have been necessary a third receiver configuration with smaller inter-receiver spacing should have been used. In this case it hasn't been considered influent for the purposes of soil characterization.

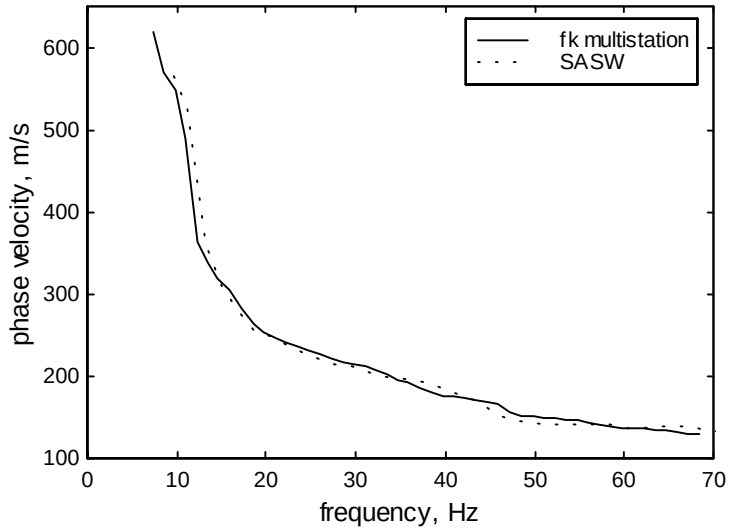

Figure 7.12 Comparison between SASW method and fk multistation method

Figure 7.13 represents the comparison between the dispersion curves obtained using the two different multistation approaches the one based on the 2D Fourier

transform and the other on the slant-stack (τp transform). The coincidence of the two curves is not surprising because of the very strict link between the two procedures. Nevertheless it is important to emphasise that according to this result the use of one or the other procedure makes no difference and can be left to the analyst.

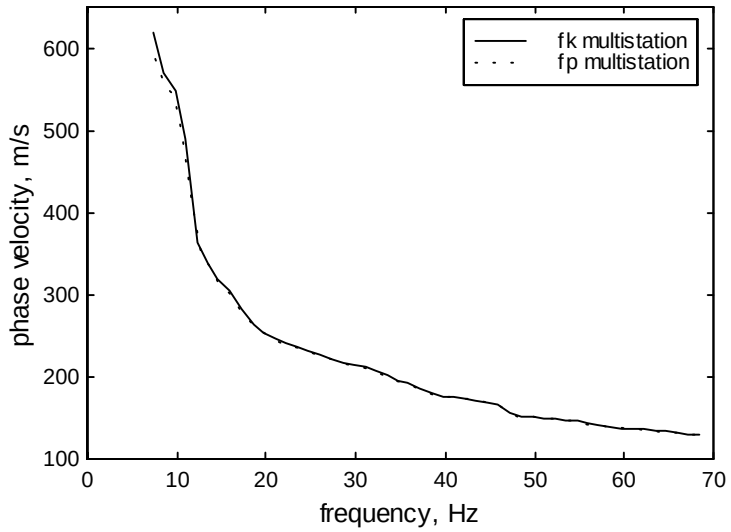

Figure 7.13 Comparison between *fk* and *fp* multistation methods

7.1.2 Inversion process

For the inversion process the dispersion curve obtained from the *fk* analysis has been used. In the present dissertation, the representation of the dispersion curve in the frequency vs. phase velocity plane has been widely adopted, nevertheless the same information plotted as phase velocity vs. wavelength give a clear picture of the general trend of stiffness with depth. Figure 7.14 shows that the general trend at the ENEA-Saluggia testing site is the one of a normally dispersive profile, i.e. a site having increasing stiffness with depth. Note also that the information regarding the highest wavelengths is given by a limited number of points. This is a very important aspect since such information strongly affects the resolution at great depth of the inversion process.

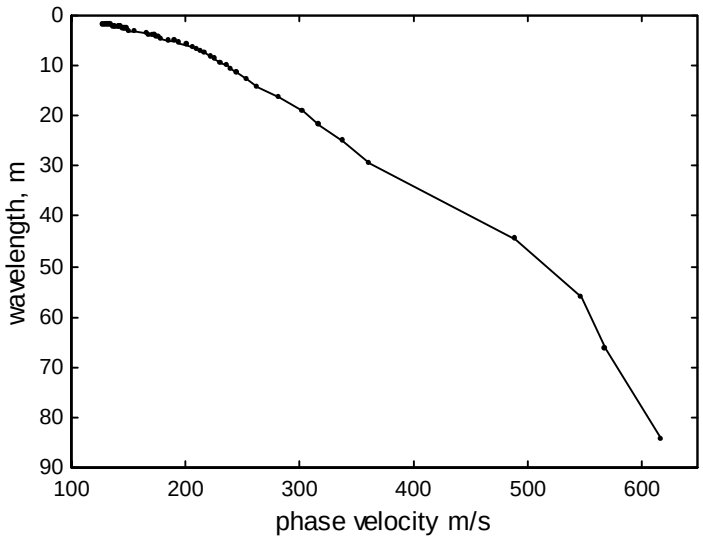

Figure 7.14 Dispersion curve from the fk analysis used for the inversion process

A preliminary shear wave velocity profile can be obtained using the rule adopted for the Steady State Rayleigh Method, i.e. assigning to a depth of $1/3 \cdot \lambda_R$ a shear velocity equal to $1.1 \cdot V_R$ (see Paragraph 4.3.1). This rule gives good results for normally dispersive profiles and it can be adopted to obtain a profile to be used as starting profile in a more rigorous iterative inversion process, based on the forward simulation of wave propagation in layered media.

The practise of assigning that stiffness to a certain depth is related to the shape of the eigenfunction of the Rayleigh fundamental mode (see Chapter 3). The factor three is chosen only considering a rough estimate of the concentration of the propagation energy with depth. Considering the importance that the initial profile has regarding the convergence of the inversion process, three different possibilities ($1/2 \cdot \lambda_R$, $1/2.5 \cdot \lambda_R$ and $1/3 \cdot \lambda_R$) for estimating the starting profile have been considered. The one that gives the minimum root square mean of the distance between the experimental and computed dispersion curves has been adopted. In this case it turns out that a good starting profile can be obtained using the above rule with a factor of reduction of wavelength equal to 1/2.5.

Starting from this preliminary estimate, the thickness and the shear velocity of an idealised layered medium have been fixed as shown in Figure 7.15. As it has been mentioned in Paragraph 4.3.2.3, usually the influence of soil density and

Poisson Ratio on the dispersion curve is negligible and hence they are assumed a-priori. In the present case the choice has been to have a constant density equal to 1900 kg/m^3 and a constant Poisson Ratio equal to 0.45 for all the layers.

The initial model used for the inversion process is a 8 layers over halfspace model, which properties are summarised in Table 7.1.

Table 7.1 Starting profile

Layer	Thickness (m)	V_s (m/s)	ν	Density (kg/m^3)
1	1	155	0.45	1900
2	1.5	190	0.45	1900
3	2	250	0.45	1900
4	2	290	0.45	1900
5	3.5	340	0.45	1900
6	6	400	0.45	1900
7	6	540	0.45	1900
8	5	600	0.45	1900
Halfspace	∞	650	0.45	1900

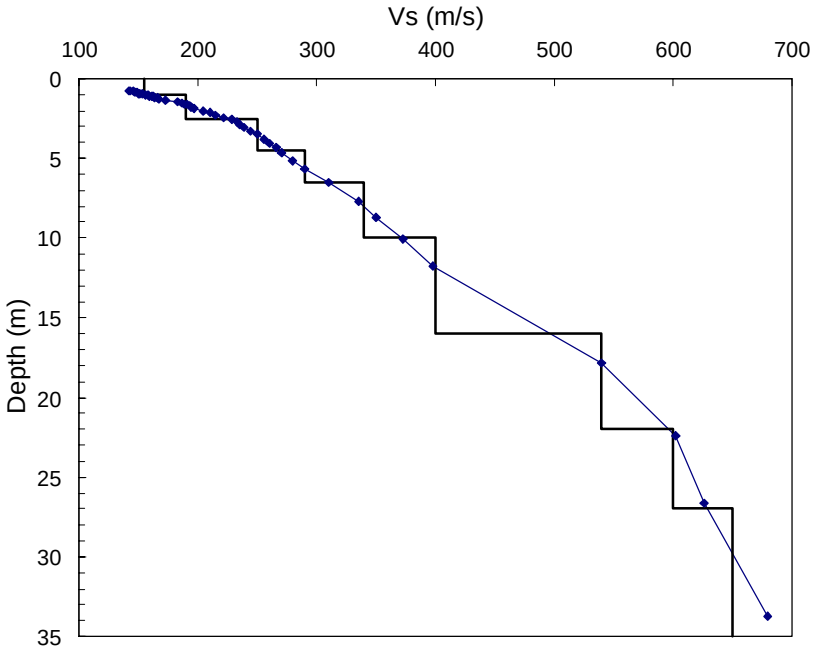

Figure 7.15 Starting profile for the inversion process

The inversion process has been conducted using the code SURF developed at S.Louis University by Prof. Herrmann and his co-workers (Herrmann 1994). The forward simulation of the Rayleigh wave propagation in a layered medium is obtained by a modified version of the Haskell-Thomson algorithm (see Chapter 3). The program does not account for mode superposition and hence it is not suitable for application on inversely dispersive profiles.

The inversion algorithm is based on a damped least square procedure with singular value decomposition of the resulting matrix. It is also possible to use a weighted inversion, so that known or unstable layers can be prevented from great changes during the process. This option has not been used in the present case since no information about specific interfaces was known.

Starting from the initial profile the solution is step by step achieved minimising the error between measured data and values derived from the solution of the forward problem. The program allows the inversion for layer thickness or shear velocity, through the numerical evaluation of the correspondent partial derivatives.

As shown in Figure 7.16 the dispersion curve corresponding to the initial profile (Table 7.1) is quite in good accordance with experimental data. This is a proof of the effectiveness of the approximate rule in the case of normally dispersive media. The fitting corresponding to the last iteration is excellent.

The final result in terms of shear wave velocity profile is reported in Table 7.2. The comparison of the final profile with the cross-hole test results that are available at the site (Figure 7.17) shows globally a good agreement especially for shallow depth. Going deeper the surface wave method is able to catch the general trend of stiffness, but the resolution of soft thin layers is not good. This problem can be easily explained considering the very limited information that is available at low frequencies (long wavelength).

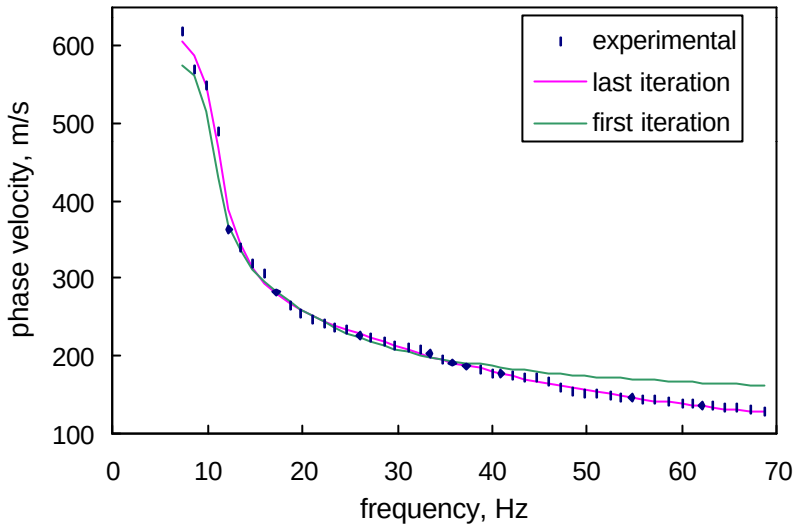

Figure 7.16 Inversion process: fitting between experimental and simulated dispersion curves

Table 7.2 Shear wave velocity profile at ENEA testing site

Layer	Thickness (m)	V_s (m/s)
1	0.9	120
2	1.5	190
3	2.1	265
4	2	275
5	3.4	335
6	5.9	430
7	6	560
8	5	610
Halfspace	∞	685

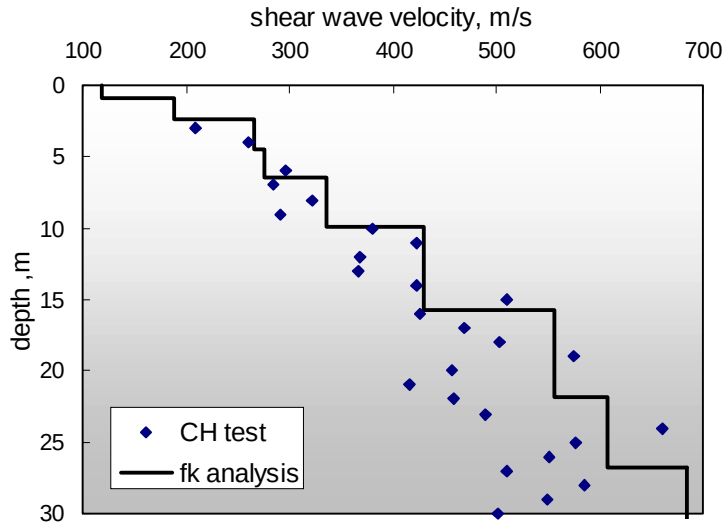

Figure 7.17 Comparison between shear waves velocity profiles from fk multistation analysis of surface waves and cross-hole method

7.1.3 A back-analysis of the *fk* data

The results from the multistation fk surface wave test reported in the previous Paragraph showed that the resolution at relatively large depth is certainly not excellent. Moreover it must be noted that below the depth of 30m that is the maximum depth tested with the surface wave method, there is a thick softer zone with an average shear wave velocity around 400 m/s (see complete results from the CH test in Chapter 6).

Hence starting from the results that are known from the cross-hole test is possible to make some observation about the dispersion curve evaluated from the *fk* method. In Figure 7.18 the raw results corresponding to the absolute maxima of the *fk* spectrum for frequencies less than 12 Hz are reported. Note that the first datum is at a frequency less than 6 Hz and show a phase velocity value of less that 400 m/s. At first sight this value was discarded together with values at 6 and 6.5 Hz that are meaningless, because it seemed to be an isolated outlier. However this datum can be linked to the inversion of stiffness at depth greater than 30m that is shown by the cross-hole results.

The other important features of the data in the range 6.5 to 12 Hz is given by the alternation of higher and lower values. These small perturbations can be considered indicative of the presence of small softer layers at great depth, as shown by the cross-hole test. Unfortunately these features are missed during the inversion process.

In this respect one problem is constituted by the necessity of averaging to reduce the number of points for the inversion. Indeed the first 4 points of the dispersion curve that has been effectively used for the inversion do not show any perturbation that can be linked to soft strata (see Figure 7.4). On the other hand a really detailed inversion, which would be able to follow these perturbation, can hardly be implemented because of the necessity for a very large number of strata in the model, that would result in a very high number of parameter to optimise (this would be a big concern regarding the non-uniqueness issue).

It is very important to emphasise that the above remarks apply only to the dispersion curve obtained from the multistation analysis and they do not apply at all to data from the SASW approach. Indeed looking at raw dispersion curve from the two-station method (Figure 7.3) it is clear that data at low frequency are very poor and moreover they do not show any trend that can be linked to the inversion of stiffness with depth.

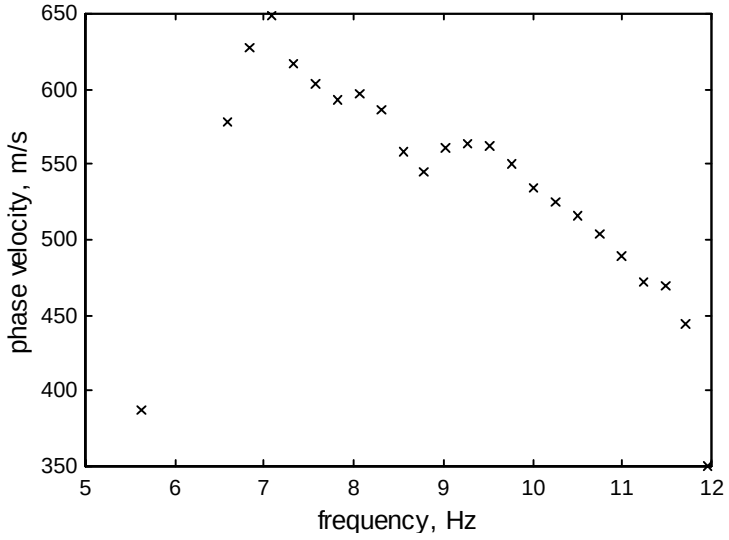

Figure 7.18 Raw results from fk multistation at low frequency (source: weight drop; inter-receiver distance: 3m)

7.2 Testing for Stiffness and Damping

The test session for stiffness and damping has been used to compare the results from the new transfer function method (Paragraph 4.4.2) with those from classical separate determination of stiffness and damping (Paragraph 4.4.1).

The ideal testing equipment for transfer function measurements would be a multichannel signal analyser, indeed it would allow for simultaneous measurements of the transfer function at many receiver locations. Unfortunately this was not the case for the testing session since only a two-channel signal analyser was available. Hence the test was repeated changing the position of the geophone on the ground surface and running again the sweep in frequency of the source maintained in the same position. Obviously even if the excitation could be considered very repeatable, this procedure introduces some differences for each test repetition and the results are not as good as they could be from a single multistation session.

Considering that the input is measured in terms of acceleration of the source mass (i.e. the input force divided by the constant mass) and the output in terms of velocity, the quantity that is obtained as the ratio of the two is what is commonly named *Mobility*. From the mobility $M(r,\omega)$, the experimental displacement transfer function can be readily computed by:

$$T(r,\omega)=\frac{M(r,\omega)\cdot C_2(\omega)}{i\cdot\omega\cdot C_1(\omega)} \tag{7.2}$$

where $C_1(\omega)$ and $C_2(\omega)$ are the frequency dependent *calibration factors* of the velocity transducer and of the accelerometer, respectively. The mass of the shaker armature is included in $C_2(\omega)$. The dynamic signal analyzer calculates the transfer function in such a way that uncorrelated output noise is eliminated (Bendat and Piersol, 1993).

Stored data for each receiver offset consists of the following 5 quantities, directly evaluated by the internal processor of the signal analyzer: 1) frequency response function between the accelerometer mounted on the electromagnetic shaker armature (i.e., the source) and the vertical 1-Hz natural frequency velocity transducer (i.e., the receiver) placed at a particular offset from the source; 2) ordinary coherence measurement between the source and the receiver; 3) auto power spectrum of the source accelerometer; 4) auto power spectrum of the receiver; 5) cross power spectrum between the source and the receiver.

The signal from the receiver is differentially amplified. It is important to account for the gain applied at every source-receiver configuration before any

interpretation based on the amplitude is done.

The frequency range of acquisition was comprised between 5 and 100 Hz. The total number of sample in time is equal to 2048, that means that since the signal analyser used for the test adopts a antialias factor of 2.56 a total of 800 samples in frequency are taken. Considering the frequency range to be covered this means a resolution in frequency of 0.125 Hz. To improve signal quality averaging has been made considering 10 successive acquisitions for each testing frequency.

The global ensemble of the obtained raw data constitutes a complex-valued matrix, containing the transfer function for different source-receiver distances and different frequencies.

A visual inspection of the available data has been conducted, plotting both amplitude and phase of the transfer function against distance for different frequencies. As a consequence raw data relative to some receiver positions were discarded. This can be ascribed to near field effects, poor signal to noise ratio or simply problems due to the repeatability of the test.

On the other side the frequency range for which a poor signal to noise ratio was detected on the basis of the inspection of the coherence function were also discarded.

This process led to a smaller ensemble of clear data through the elimination of rows and columns of the raw transfer function matrix.

Because of the peculiarity of the continuous source that is quite heavy to move and makes unpractical the use of the common receiver midpoint array, the classical two-station measurements of SASW have been conducted using the common source array geometry (Figure 4.6). Moreover this seems to be more consistent with the attenuation measurements that must necessarily be conducted using this geometry.

It must be noted that for the uncoupled estimate of the attenuation the necessary information is obtained during the transfer function testing session. Indeed both the geophone response amplitude spectra and the coherence function relating input and output signals, that is needed to correct the raw amplitude, have been recorded during the testing session.

The inversion process for stiffness and damping has been conducted using the code SURF written by Prof. Hermann of S. Louis University and his co-workers, described in Paragraph 7.1.2. This program allows both coupled and uncoupled inversion processes for stiffness and damping.

Unfortunately this program do not allow for the use of effective quantities since only modal phase velocity, group velocity and surface attenuation can be inserted as data to be inverted. This can constitute a strong limitation in presence of inversely dispersive soils.

7.2.1 ISC 98 site

7.2.1.1 Transfer function measurements

Transfer function measurements have been conducted at this site considering the following positions of the receiver (in terms of distance from the source):

- receiver positions: 1, 2, 3, 4, 5, 6, 8, 10, 15, 20, 25, 30, 40, 50, 60 m

It is noteworthy to recall that the quantity measured on site is directly related to the mobility, i.e. the ratio between output particle velocity and input force. The estimate of the displacement transfer function can be obtained from Equation 7.2.

Unfortunately due to the limited mass of the shaker the low frequency range showed a very low signal to noise ratio. Thus the frequency range considered in the regression process was restricted taking only frequencies above 9.98 Hz.

Some examples of the estimate complex displacements transfer functions are plotted in Figure 7.19 (in terms of phase and amplitude).

Moreover the visual inspection of transfer function amplitude and phase plotted against distance for different frequencies suggested to discard the information related to the closest receiver distance (1m) and to the farthest ones (40, 50, 60 m). While the elimination of the first one can be explained by near field effects, the impossibility of obtaining good results for far receivers is essentially due to the small mass of the source. This effect is quite limiting in view of going deeper with the inversion process, but can be bypassed using more massive harmonic sources.

The regression process on the experimental results has been performed for each testing frequency through a modified least square procedure in the complex number domain. To account for near field effects only receivers placed at minimum half a wavelength from the source have been considered in the regression. Obviously this require an iterative procedure because for a given frequency the wavelength is not known a priori. The choice of considering a near field of about half a wavelength has been done in consideration of the common requirements for the two-station SASW test. Since in this multistation approach the influence on the final results of the closer receiver is less marked than in the two-station approach, the consequences of body waves effects should be less important. Thus the criterion is likely to be acceptable also for inversely dispersive media, whereas for normally dispersive media it can be perhaps over-conservative. This aspect need to be further investigated using some numerical simulations.

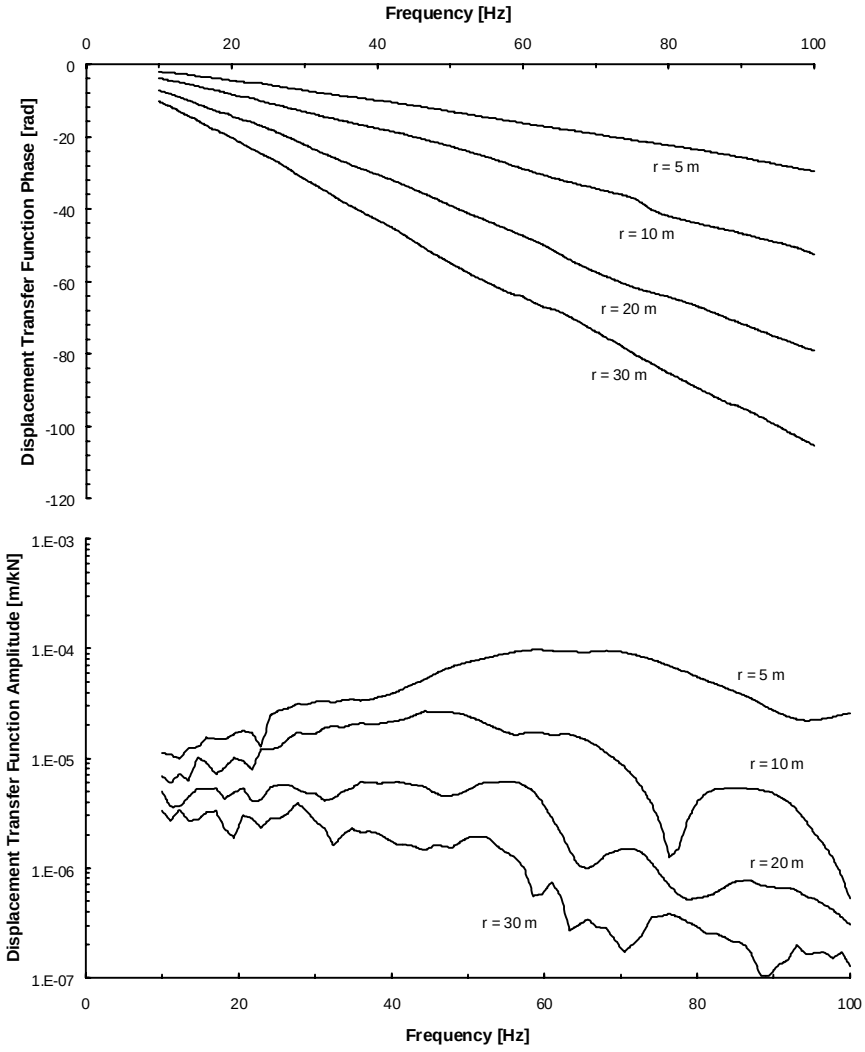

Figure 7.19 Displacement transfer function amplitude measured at the ISC'98 site

Some examples for two different frequencies are reported in Figure 7.20 and Figure 7.21. The regression is conducted in the complex plane, also if the representation is obviously made in terms of phase and amplitude of the transfer function. Considering that Equation 4.25, that is the base of the regression process, can be rewritten (accordingly to the introduced simplifications) as:

$$T(r,\omega) = \frac{b(\omega)}{\sqrt{r}} e^{-\alpha_R(\omega)\cdot r} e^{-i\cdot k_R(\omega)\cdot r} \tag{7.3}$$

it is clear that the phase of the transfer function is directly linked to the Rayleigh wavenumber (and hence to phase velocity) while the amplitude, after the correction for geometrical attenuation, is directly linked to the attenuation. This remark could lead to the idea of two different regression processes in real number domain. Nevertheless it must be remarked that in the view of the coupling of measurements it is undoubtedly more correct to perform a single regression process to obtain simultaneously the two quantities. Moreover, performing the regression directly in the complex number domain, the necessity of phase unwrapping is avoided and, since this is a very ticklish task, a great source of error is skipped.

Obviously, when the quantities are plotted in terms of amplitude and phase angle for necessity of representation the fitting of the experimental data apparently is not the best one, but it is globally the best fit of the complex quantity.

It is noteworthy to mention that during the regression process also the complex constant $b(\omega)$ is determined. This quantity incorporate the effects of the coupling between the source and the soil both in terms of magnitude of transmitted energy and in terms of actual difference in phase between the movement of the shaker and the input effectively transmitted.

The comparison between Figure 7.20 and Figure 7.21 shows that for increasing frequencies a greater number of receivers is considered in the regression process, because the near field extension is linked to the wavelength. Only frequencies for which at least 5 measurements were available in the far field zone have been considered in view of having a sufficient data set for the regression process. This choice, together with some problems of convergence, has restrained the range of frequency for which the dispersion and attenuation curves have been effectively obtained.

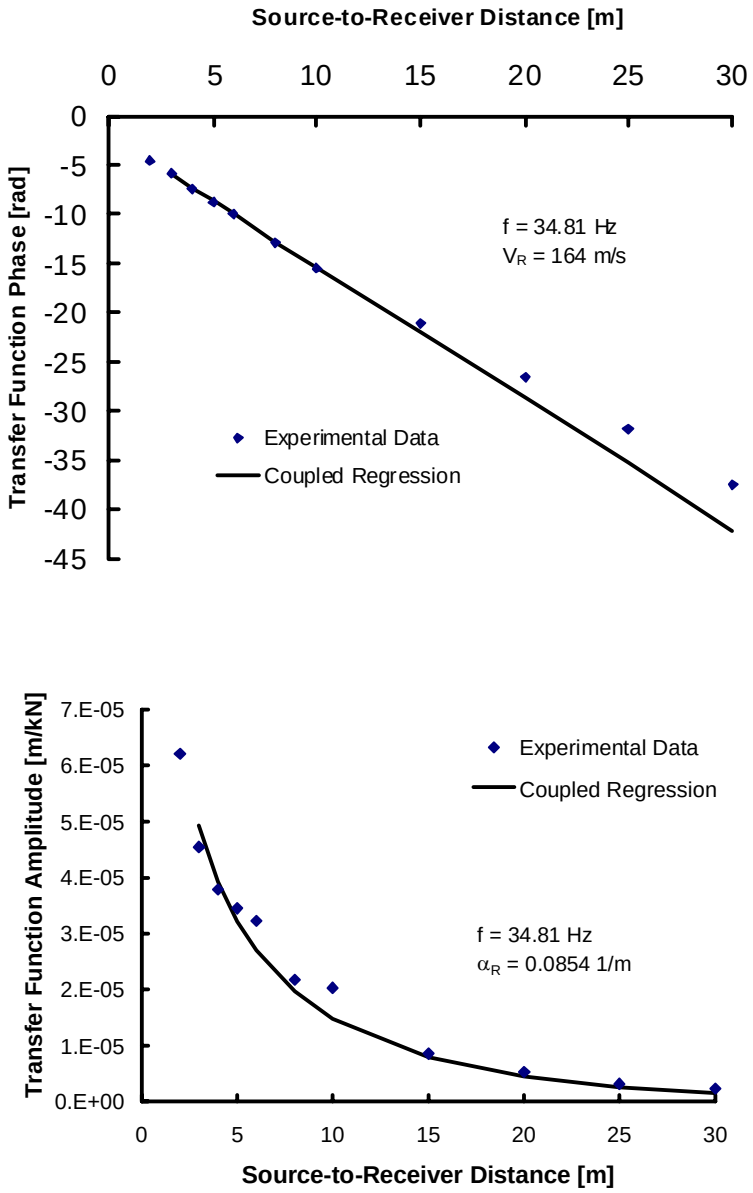

Figure 7.20 Coupled transfer function inversion at the ISC'98 site (34.81 Hz)

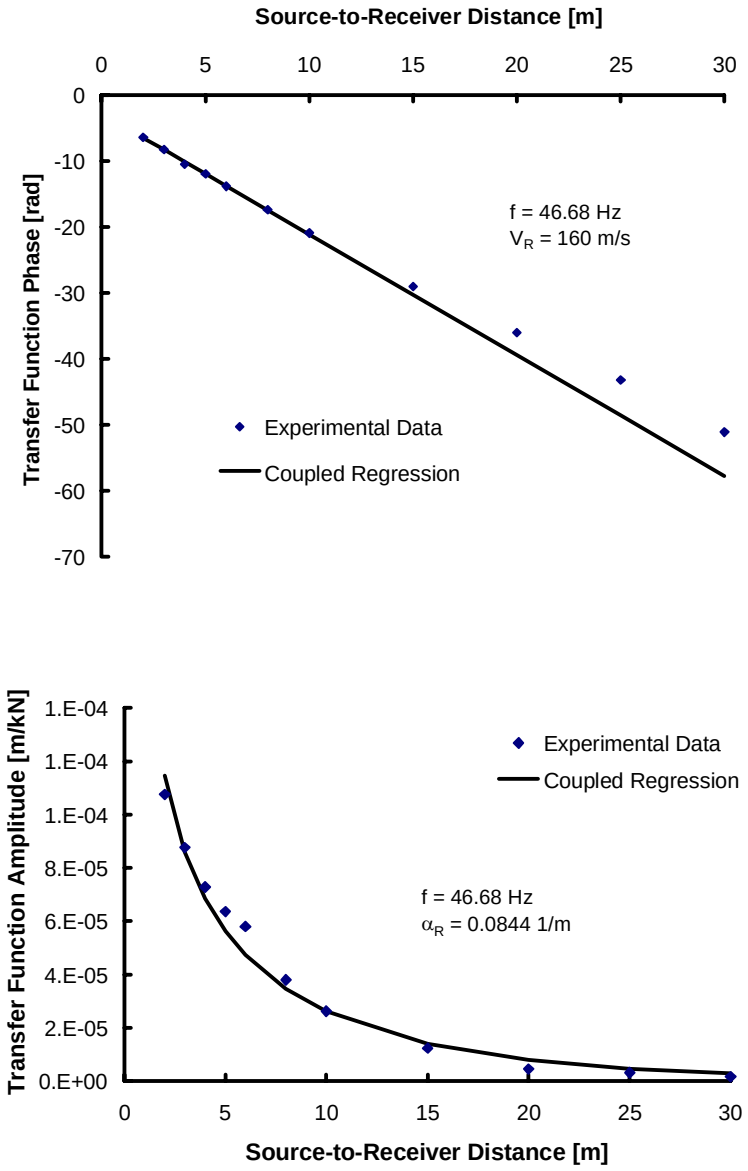

Figure 7.21 Coupled transfer function inversion at the ISC'98 site (46.68 Hz)

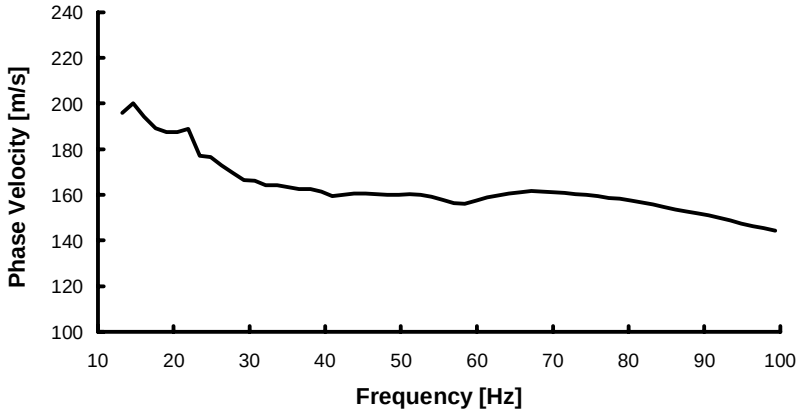

Figure 7.22 Experimental dispersion curve from transfer function at ISC'98 site

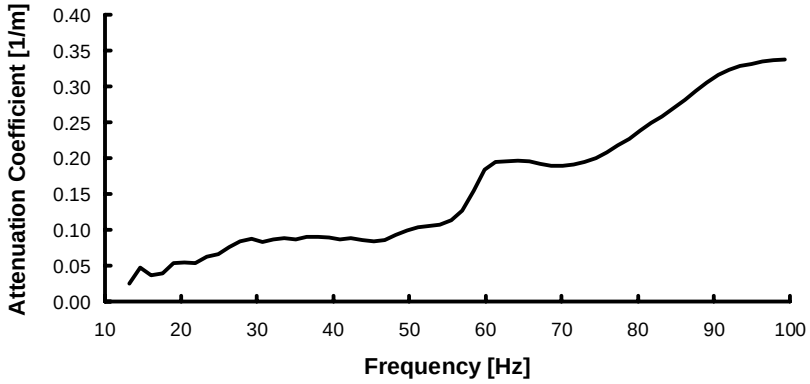

Figure 7.23 Experimental attenuation curve from transfer function at ISC'98 site

7.2.1.2 Uncoupled measurements of dispersion and attenuation

The classical two-station measurements for time delay estimation using the cross-power spectrum approach have been conducted considering the following inter-receiver distances: 5m, 10m and 20m. It has been considered useless to extend the measurements to greater inter-receiver distances because of the modest mass of the shaker. As an examples the data obtained for the testing configuration with inter-receiver distance equal to 5m are reported in Figure 7.24. Note that for such distances the shaker performs very well and the signal to noise ratio is very high all

over the entire frequency range that has been tested, as it is shown by the coherence function that is equal to 1 for all the frequencies above 20Hz. It is also noteworthy to observe the comparison between the auto-power spectra at the two receivers that clearly shows the effect of the soil as a band pass filter.

Figure 7.25 shows instead the experimental data obtained for the highest inter-receiver distance that has been taken in consideration. First of all note that in this case the sweep in frequency of the source has been limited to 50 Hz because short wavelength waves are not of interest in this case. The data are clearly much more degraded since the low mass of the shaker do not allow for a good signal to noise ratio at a great distance from the source.

In such cases many problems could arise during the unwrapping of the phase of the cross-power spectrum, a process that is necessary for the estimation of the time delay. Indeed the very low signal to noise ratio at low frequencies, confirmed by the low values of the coherence function, can lead to erroneous interpretation of the jumps of the phase spectrum. It is noteworthy that this task is usually accomplished directly by the operator on the basis of critical judgement: considering the frequency range of interest, the number of jumps in the cross power spectrum preceding this range must be estimated. The underlined task can be time consuming and it prevents for the application of automated procedures. Finally note that the autopower spectrum at the farthest location clearly shows the insufficiency of energy and the filtering effect of the soil if compared to the other spectrum.

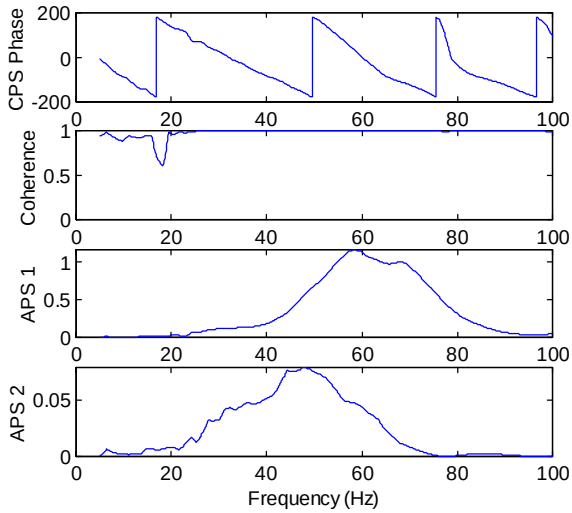

Figure 7.24 Example of SASW data obtained at the ISC'98 site (distance: 5m)

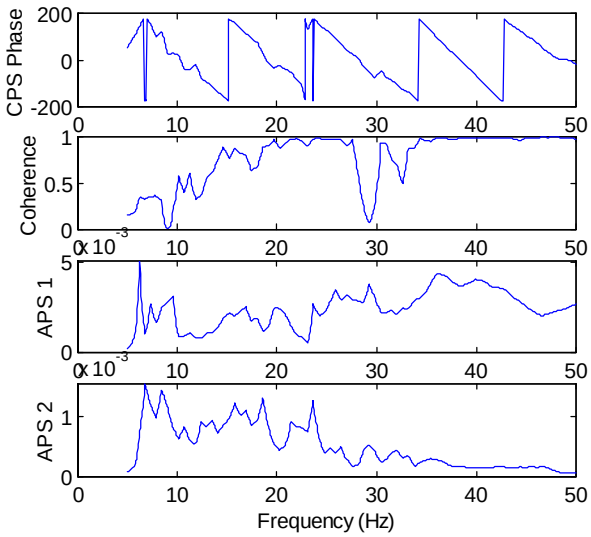

Figure 7.25 Example of SASW data obtained at the ISC'98 site (inter-receiver distance: 20m)

The dispersion curve obtained combining the results of the three different testing configuration considered are shown in Figure 7.26. Note that an averaging process have been applied to the data considering equal intervals in frequency to reduce the number of point to a manageable quantity in the view of the successive inversion process.

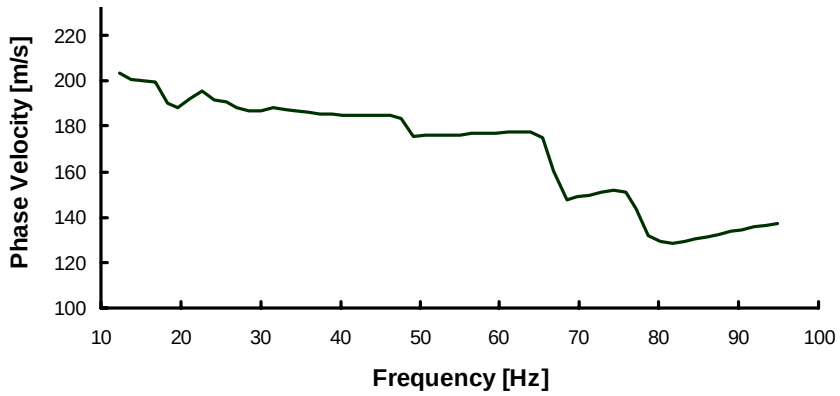

Figure 7.26 Experimental dispersion curve from classical SASW two station technique at the ISC'98 site

Concerning the estimate of the attenuation curve, the preliminary step for the uncoupled process is constituted by the correction of the autopower spectra obtained for different positions of the receiver to get the estimate of the particle displacements (see Par. 4.4.1). The latter ones are successively used for the regression process to get the attenuation coefficients.

Figure 7.27 shows some particle displacements spectra at different positions. Once they have been evaluated for various receiver position, they can be assembled and the regression process can be done for a given frequency, by considering all the data obtained along the spatial dimension given by the receiver positions with respect to the source.

As seen in Paragraph 4.4.1, the regression process should be performed after the inversion for stiffness has been conducted because the estimate of the geometrical spreading function is needed for the non-linear optimisation. Nevertheless considering that in this case the main purpose is to compare the estimate of the attenuation curve with the one obtained using the coupled transfer function method, the geometric attenuation has been taken proportional to the inverse of the square root of the source to receiver distance. In summary the regression process has been conducted considering the simplified expression of particle displacements amplitudes $\mathrm{U}_z(r,\omega)$:

$$\left|\mathrm{U}_z(r,\omega)\right| = \frac{F_z}{\sqrt{r}} \cdot e^{-\alpha_R(\omega)r} \tag{7.4}$$

The results of the non-linear optimisation process is constituted at each frequency by an estimate of the magnitude of the harmonic force applied at the free surface F_z, that is related to the amplitude of the effective acceleration of the shaker mass, and an estimate of the attenuation coefficient. The regression process has been conducted using a classical least square algorithm.

An example for a given frequency is presented in Figure 7.28, while Figure 7.29 represents the global estimate of the attenuation curve. It is important to note that the regression led to quite poor results in terms of fitting and that for a wide frequency range there was no convergence to a positive value of the attenuation, as it is required by conservation of energy. The cause of this problem could be the lack of robustness of the process and it led globally to an unsatisfying result.

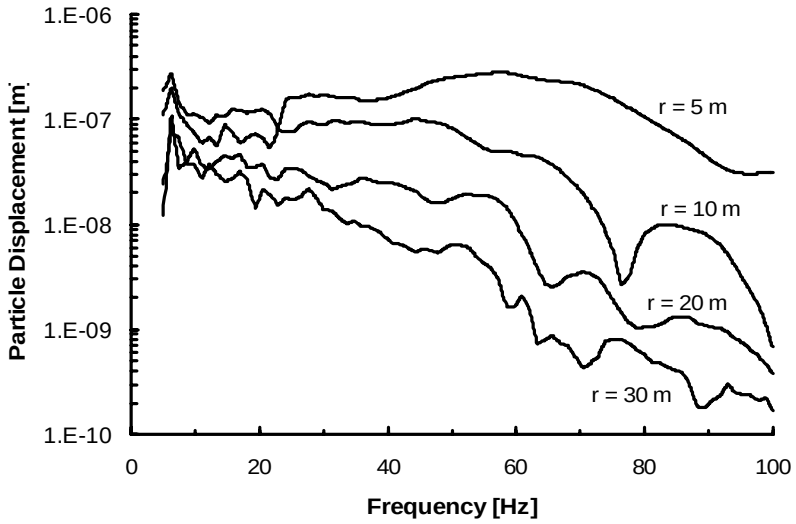

Figure 7.27 Experimental particle displacement spectra at the ISC'98 site

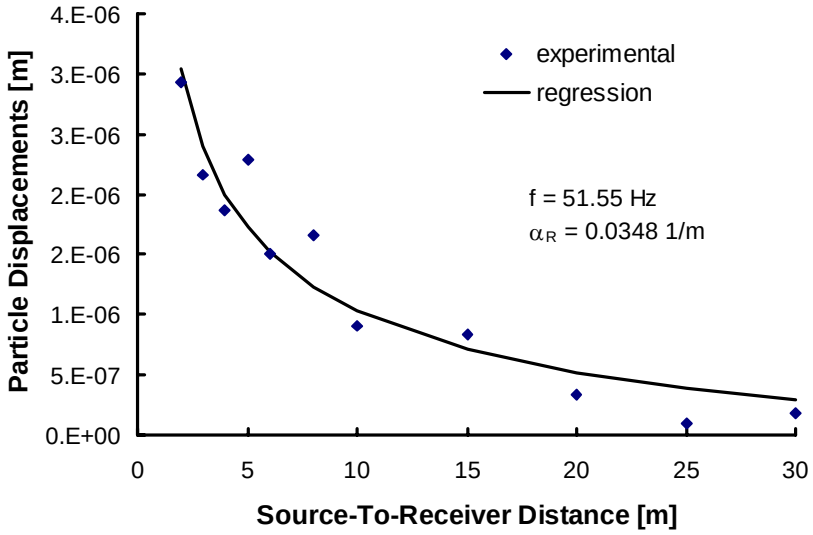

Figure 7.28 Uncoupled particle displacement inversion at the ISC'98 site (51.55 Hz)

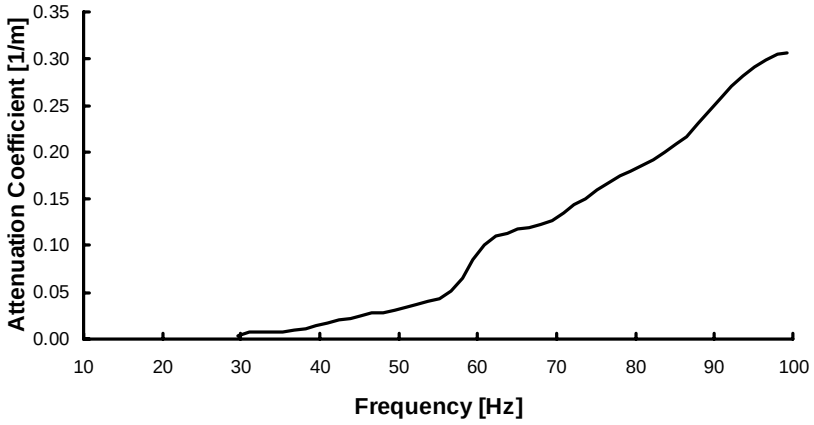

Figure 7.29 Experimental attenuation curve from uncoupled multistation method at the ISC'98 site

7.2.1.3 Dispersion and Attenuation curves comparison

Figure 7.30 and Figure 7.31 report the comparison of results from coupled and uncoupled measurements of dispersion and attenuation curves at the ISC'98 testing site.

As it concerns the dispersion curve, the coupled multistation method based on experimental transfer functions leads to a smoother curve, but the magnitude and the general trend of the data is about the same. This is not an unexpected result since as seen in Chapter 3 the effective phase velocity is a function not only of frequency but also of space. Hence the estimate obtained from a multistation method is an average over the tested zone, while the two-station case the estimate for different testing frequency is more conditioned by some receiver configurations.

As seen above the uncoupled method for the estimation of attenuation, based on particle displacements, gave some problems especially at low frequencies, because the regression didn't converge to a positive value of the attenuation coefficient. Globally it seem that the uncoupled method underestimate the attenuation if compared to the coupled method, also if the trend is quite similar. Moreover the latter appear to be more stable also at low frequencies, probably because of the control that is exerted on the source output.

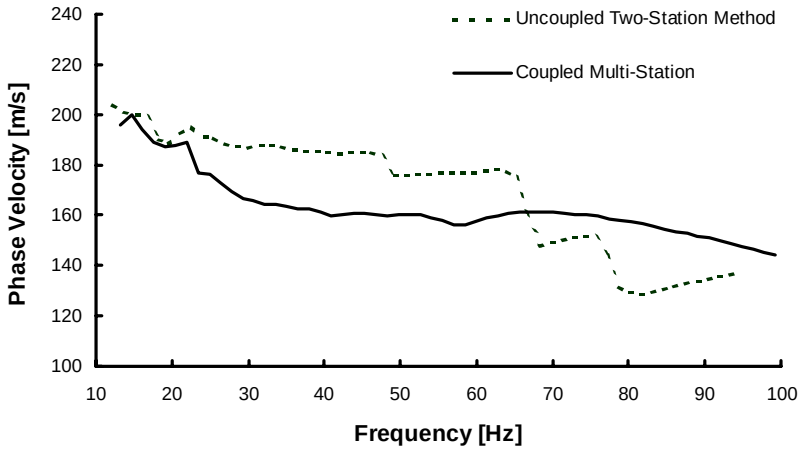

Figure 7.30 Experimental dispersion curves obtained with conventional and new measurement techniques at the ISC'98 site

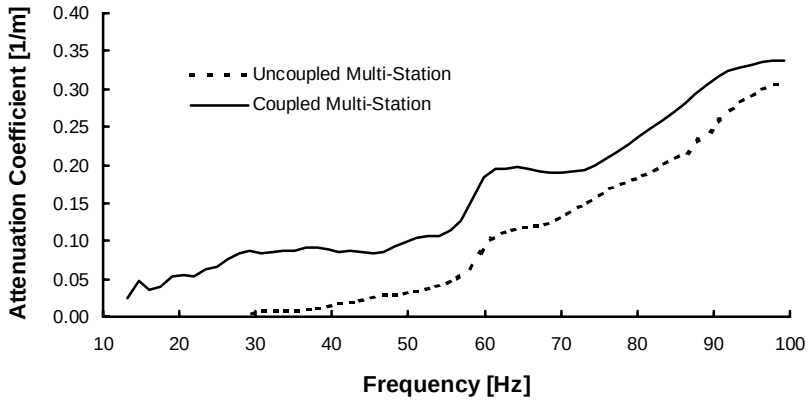

Figure 7.31 Experimental attenuation curves obtained with conventional and new measurement techniques at the ISC'98 site

7.2.1.4 Inversion and final results

The inversion process has been conducted using the data obtained from the transfer function approach and inverting simultaneously surface wave dispersion and attenuation to obtain the soil profile in terms of shear wave velocity and shear damping ratio.

Also in this case some parameters of the layers are assumed a priori since their value has a minor influence on the dispersion and attenuation curve at the site. In particular a fixed value of the following quantities has been taken constant for all the layers:

- Poisson ratio: 0.3
- Density: 1800 kg/m^3
- Ratio Q_P/Q_S: 2.25

The last quantity represents the relationship between shear and constrained damping ratio. Indeed the program uses the seismological convention with the expression of material attenuation through the quality factor Q that is linked to the damping ratio D through the following expression (see Paragraph 2.3.3):

$$D = \frac{1}{2 \cdot Q} \tag{7.5}$$

The choice of having a constant ratio Q_P/Q_S is mainly related to the observation that Q_P has a minor influence on Rayleigh wave attenuation (see Figure 3.6).

In the present case no preliminary estimation of the shear wave velocity and damping profiles has been used. Hence the first iteration was conducted using a stack of uniform layers.

Figure 7.32 reports the final fitting between the experimental data and the solution of the forward problem corresponding to the final profiles obtained through the inversion process that are reported in Figure 7.33.

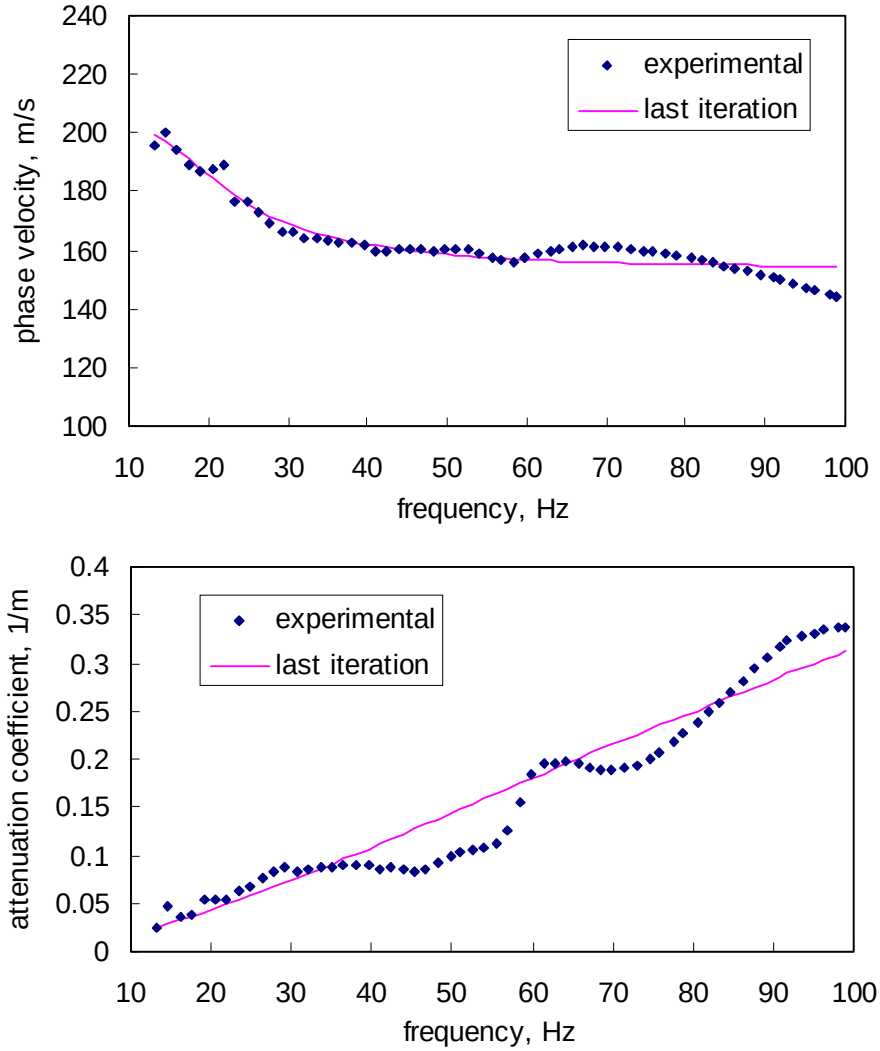

Figure 7.32 Inversion process: fitting between the experimental dispersion and attenuation curves and the simulations corresponding to the final profiles

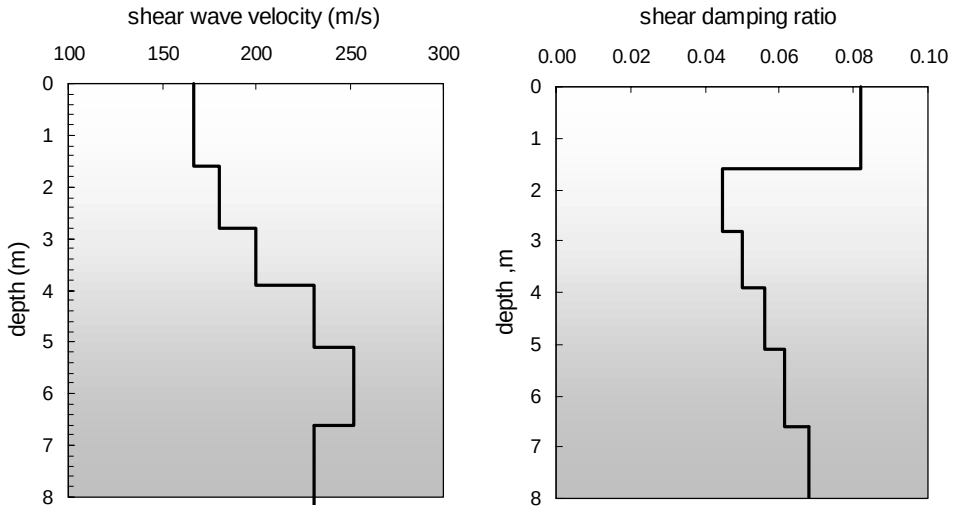

Figure 7.33 Shear wave velocity and damping ratio profiles at ISC'98 testing site

7.2.2 GTRI site

Transfer function measurements have been conducted at this site considering the following positions of the receiver (in terms of distance from the source):

- receiver positions: 1, 2, 3, 4, 5, 6, 8, 10, 15, 20, 25, 30, 40, 50, 60 m

Unfortunately due to the limited mass of the shaker the low frequency range showed a very low signal to noise ratio. Thus the frequency range considered in the regression process was restricted taking only frequencies above 10.22 Hz.

Moreover the visual inspection of transfer function amplitude and phase plotted against distance for different frequencies suggested to discard the information related to the closest receiver distances (1 and 2 m), the farthest ones (30, 40, 50 m) and also one intermediate measurement (15 m). While the elimination of the first two can be attributed to near field effects, the impossibility of obtaining good results for far receivers is essentially due to the small mass of the source. The problems with the measurements with the receiver placed at 15m from the source are not related to any particular factor and can be attributed to some unexpected experimental trouble.

Figure 7.34 and Figure 7.35 represent two example of fitting at high frequencies were the accordance with the experimental data is clearly quite good.

On the contrary some trouble have been encountered on this site for lower frequencies as will be remarked later on.

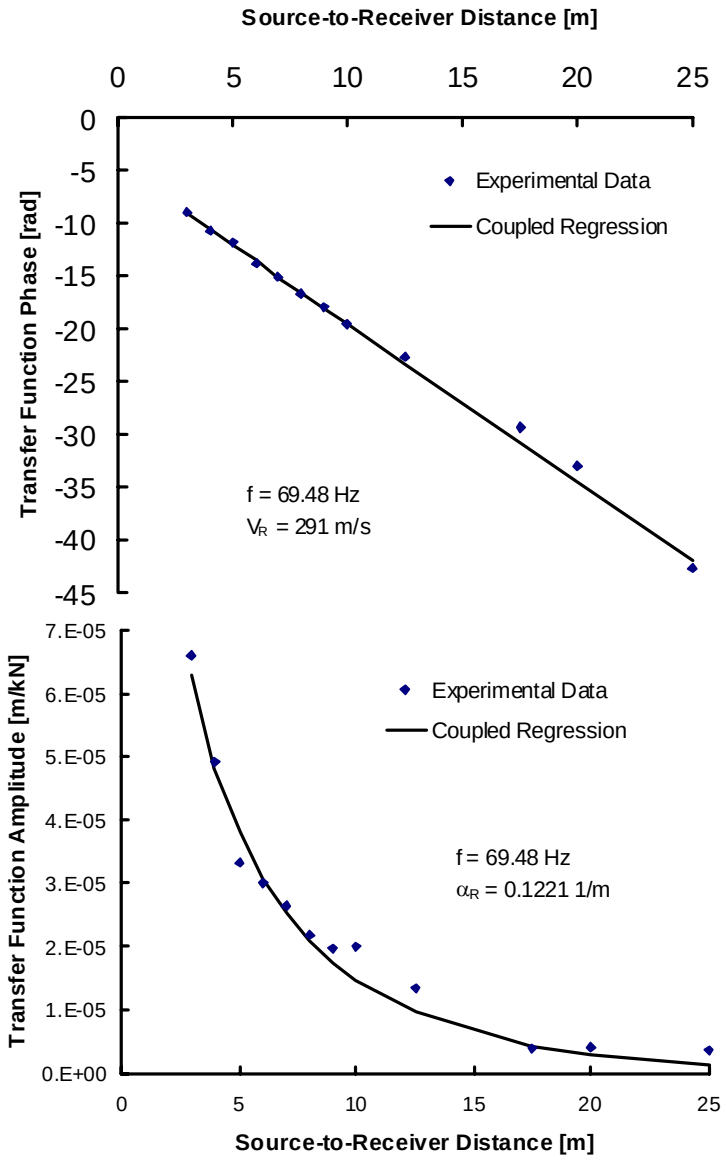

Figure 7.34 Coupled transfer function inversion at the GTRI site (69.48 Hz)

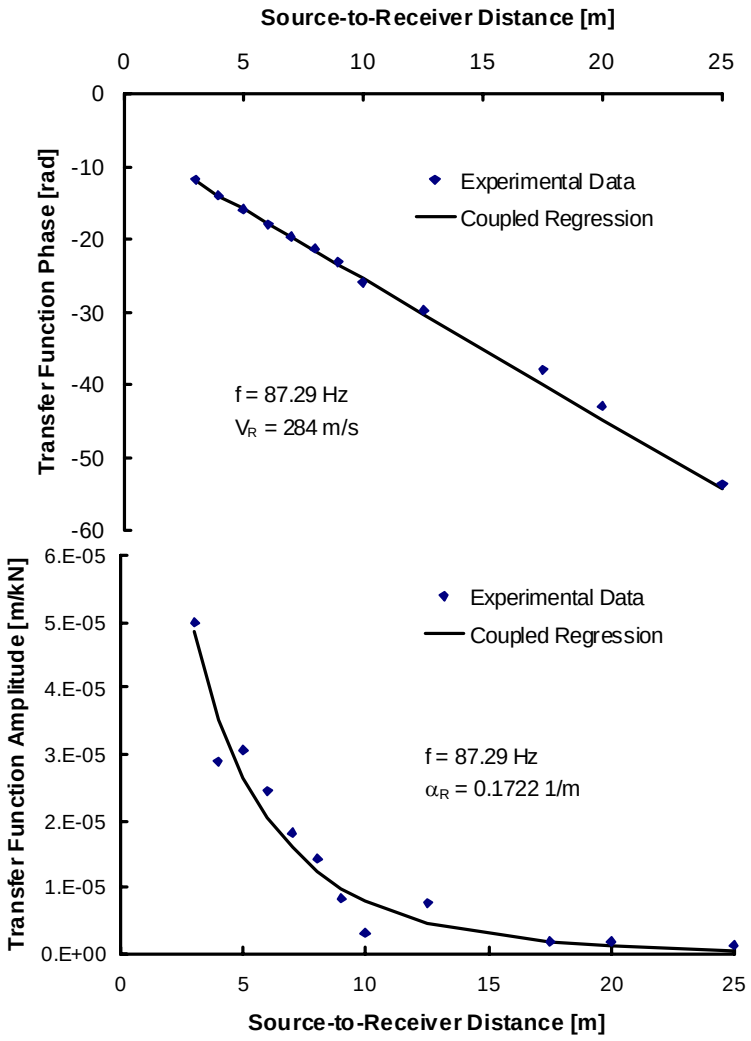

Figure 7.35 Coupled transfer function inversion at the GTRI site (87.29 Hz)

The classical two station measurements for time delay estimation using the cross-power spectrum approach have been conducted considering the following inter-receiver distances: 5m, 10m and 20m. It has been considered useless to extend the measurements to greater inter-receiver distances because of the modest mass of the shaker.

Finally the uncoupled estimate of the attenuation curve from the particle

displacements regression has been conducted as for the ISC'98 testing site using data collected during the testing session for the transfer function method.

The dispersion and attenuation curves obtained using both coupled and uncoupled methods are reported in Figure 7.36 and Figure 7.37.

Compared to the previous case, the results obtained at GTRI site are less satisfactory. First of all the lack of convergence for the low frequencies is now much more evident and it is not possible to obtain results below a frequency of 30Hz. This can be essentially attributed to the limited mass of the shaker used for the test.

As it concerns the comparison between uncoupled and coupled measurements, the same remarks that have been done for ISC'98 testing site apply also for the GTRI testing site. In particular in this case the underestimation of the attenuation coefficient and the instability at low frequency of the uncoupled multistation method is even more evident.

Because of the strong restrain in the frequency range of the obtained data at this site their inversion would be meaningless since it would give only information related to a very shallow depth.

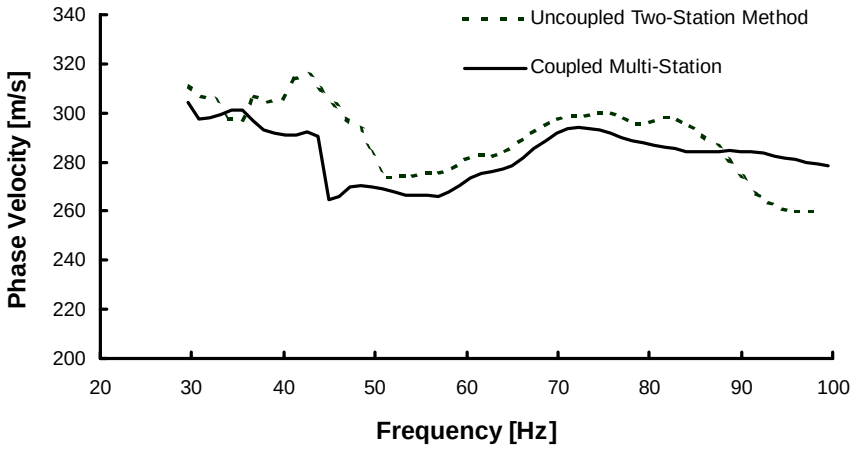

Figure 7.36 Experimental dispersion curves at the GTRI site

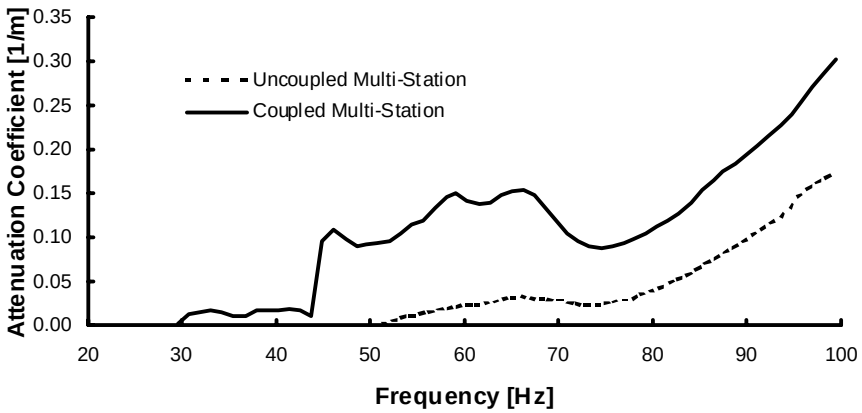

Figure 7.37 Experimental attenuation curves at the GTRI site

7.3 Some issues about sources

Some typical features of different sources can be observed comparing the spectral quantities relative to the same test configuration. The choice has been to compare the autopower spectrum at a certain source-to-receiver distance and the coherence function that can be obtained using two receivers.

The first quantity gives a clear picture not only of the energy associated to each source, but also to energy location in frequency domain, that is very important in the view of using the source for characterization purposes.

The coherence function is a clear indicator of the signal-to-noise ratio and thus it can be used to assess the effectiveness of the different sources, adding information regarding the range of frequencies for which every source works better.

Firstly it is important to observe the differences between harmonic and impulsive sources, for this purpose some relevant features from testing at the GTRI test site are compared. Figure 7.38 and Figure 7.39 represent respectively autopower spectra and coherence function obtained using the electromechanical shaker and a 6 Kg sledge hammer. The difference in the autopower spectra is justified by the different input and also by the different coupling with the tested medium. It is important to point out that the shaker is able to give an output with a high signal to noise ratio over a very wide spectrum of frequencies as confirmed by

the coherence function. Instead the hammer gives acceptable values of the coherence only for limited intervals of high frequencies, where the energy of the signal is higher as confirmed by the autopower spectrum.

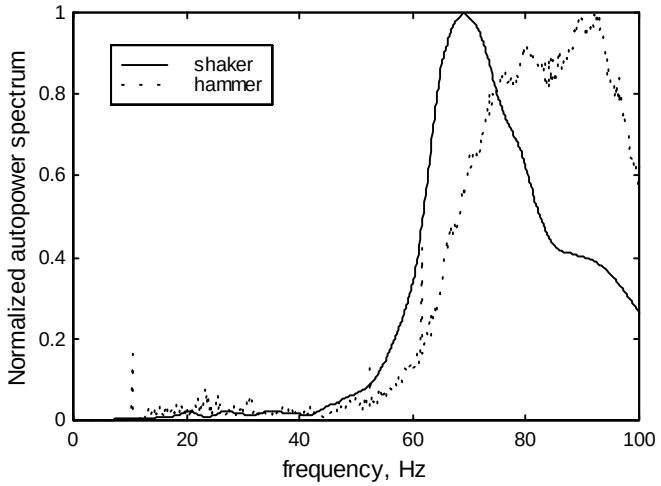

Figure 7.38 Comparison between autopower spectra at 5m from the source

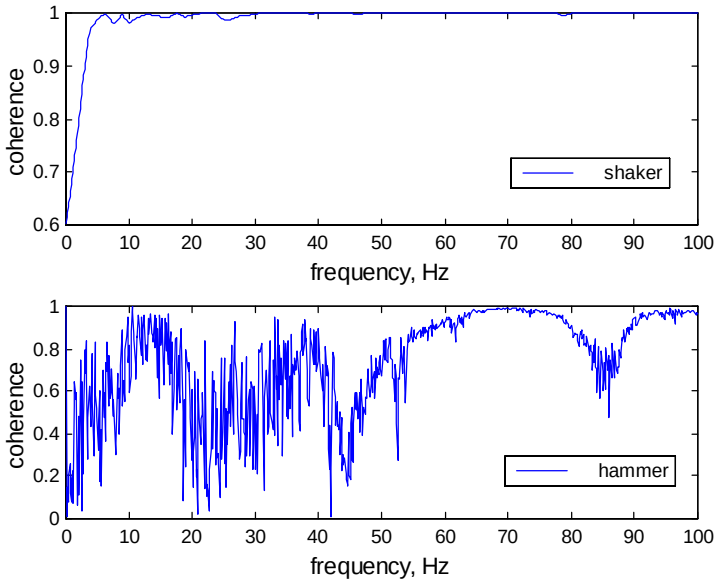

Figure 7.39 Coherence function with receivers at 5 and 10m from the source

On the other hand it can be interesting to compare different impulsive sources. In this case the comparison can be done on the data obtained at ENEA testing site where some different impulsive sources have been used.

Figure 7.40 and Figure 7.41 report the comparison between the impact weight drop source and the two different hammers (to distinguish between the two the 1kg hammer has been indicated as hammer and the 6kg one as sledge-hammer) for receiver locations quite close to the source. The comparison of the autopower spectrum at a distance of 3m clearly shows that the energy of the weight drop source is by far higher of that of the two hammers. Nevertheless the comparison of the coherence functions clearly shows that the energy distribution plays a very important role in determining the frequency range with best signal quality.

Similar conclusions can be drawn from Figure 7.42 and Figure 7.43 that report the comparison at greater distance between the sledgehammer, the weight drop impact source and the minibang.

The comparison is in this case made only for frequencies up to 80 Hz because at such distances the higher components of the signal are strongly attenuated and hence the signals are degraded.

It is important to remark the performances of the minibang source that is rarely used for geotechnical soil characterization. Because of the explosive nature of this source it was expected to give better performance over the high frequency range. Instead the associated cross power spectrum and coherence function show that it stands in between the massive weight drop source and the sledge hammer, qualifying for being a good source for intermediate frequencies.

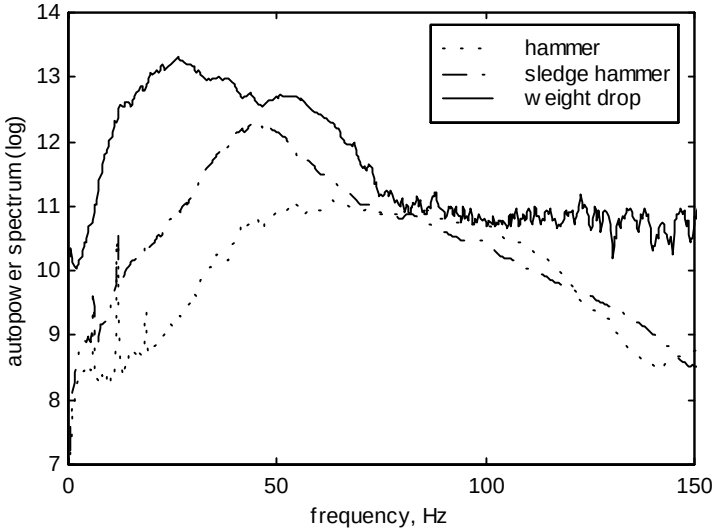

Figure 7.40 Autopower spectra at 3m from the source, number of stack: 7

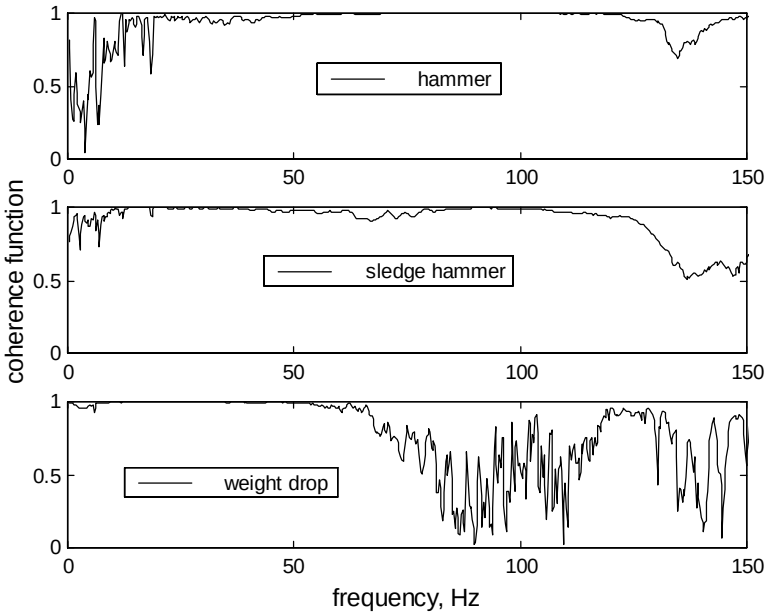

Figure 7.41 Coherence functions with receivers at 3 and 6m from the source

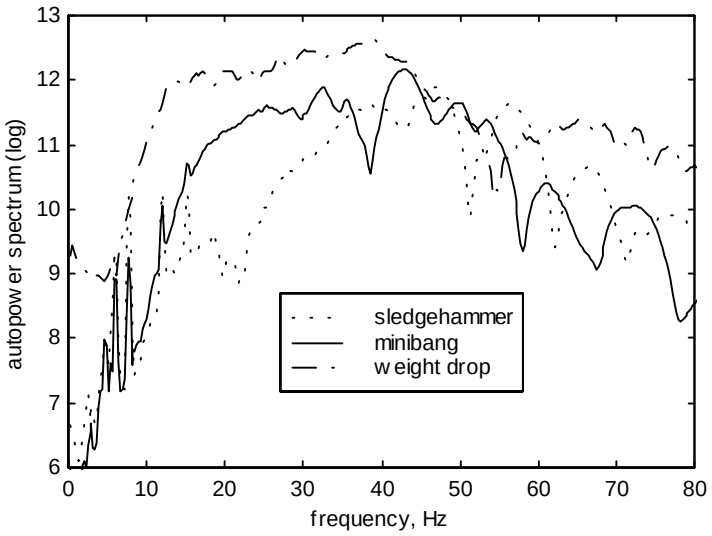

Figure 7.42 Autopower spectra at 12m from the source, number of stack: 5

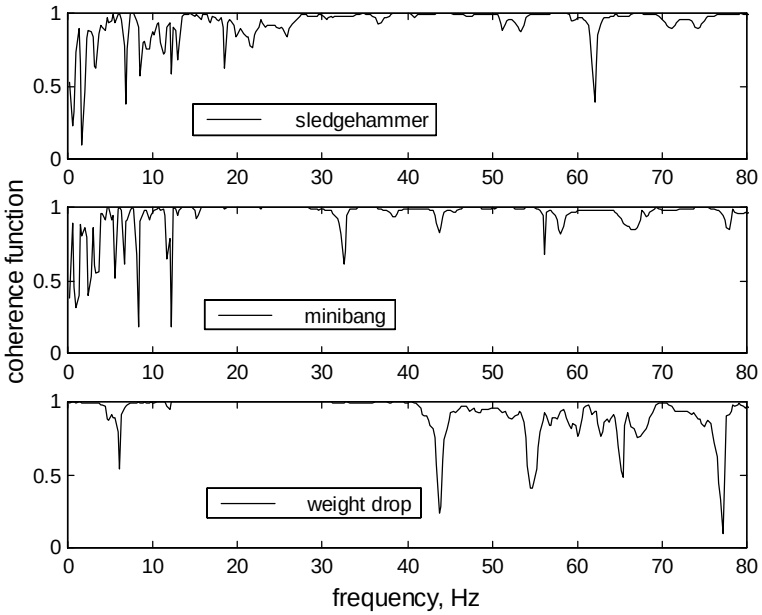

Figure 7.43 Coherence functions with receivers at 12 and 24m from the source

7.4 Comments

The test performed have shown on one hand the advantages associated to multistation methods for soil characterization using impulsive sources and on the other hand the feasibility of the new transfer function method, which has been proposed for the simultaneous determination of stiffness and damping profiles at a site.

The multistation *fk* analysis method for the determination of the dispersion curve has proven to be faster and more robust than the classical two-station method of the SASW test. The following main advantages can be emphasised:

- The procedure can be easily automated while in the classical two-station method the engineering judgement of the operator is continuously needed to assess the portion of the cross-power spectrum phase to be used, with a long and time consuming process to be conducted back in the office. The fast estimate that is assured by the *fk* method can be very useful for preliminary assessment of stiffness profile directly on site.
- There is no need for phase unwrapping that is one of the most controversial aspect and, especially when the signal to noise ratio is low, can cause large mistakes and/or loss of information.
- The method gives directly an estimate of the average phase velocity over the testing space, with reduced need for averaging process of many repetitions with different test configuration that could lead to improper results.
- The testing time on field is drastically reduced. This is the consequence of several factors: first of all since the determination of the dispersion curve comes from many receivers there is no need to adopt the common receiver midpoint geometry with the reversing of the source. Indeed such necessity arises in the SASW test to mitigate the possible error due to internal phases of the instrumentation, which is more likely to occur when only two receivers are used. The second important factor is that with the *fk* method the estimate of the dispersion curve can be successfully made with a single shot gather, with no necessity for several repetition of the test as required by the SASW procedure.
- Last but not least the multistation procedure gives the possibility of obtaining more information on the low frequency range, that often is a weak point for the SASW test. This aspect can be ascribed essentially to the minor influence of ambient noise and near field effects on the multiple receiver measurements.

Chapter 8

Conclusions and Recommendations

This research was essentially focused on surface wave methods for site characterization and in particular on the implementation of multistation procedures, in the view of overcoming the drawbacks associated to the two-station procedure, which is the standard of practice for geotechnical applications.

In this respect the interest was twofold: from one side the necessity of improving the interpretation of impulsive signals, related to the use of impact sources. Indeed such sources, although less efficient than controlled ones, present undoubtedly great benefices concerning costs and save of testing time.

On the other side, when a controlled source is available, it can be possible to extract from the high quality signals more information about the mechanical properties of the medium. In particular it can be interesting to evaluate the dissipative characteristics in terms of damping ratio as a function of depth.

A series of numerical simulations and experimental tests has been conducted, which results are summarised in the following.

Globally multistation methods appear to be very promising for both of the above applications and the advantages, that they showed with respect to the traditional two-station approach of the SASW test, let to think that there is room for these methods in the standard of practice.

Still many aspects related in general to geotechnical site characterization using surface waves and to the application of multistation methods need further studies. In this respect some suggestions will be given in the recommendations.

The following sections are organised maintaining the basic distinction between impact source tests and controlled sources tests, reporting before the general comments, which hold for both.

8.1 Conclusions

In general multistation procedures lead to an estimate of an average dispersion curve over the testing space. This aspect is very important considering the spatial dependence of the phase velocity, due to mode superposition. In the traditional two-station SASW test, sets of data are obtained from different testing configuration and such procedure doesn't seem sufficiently consistent. On the contrary, in multistation methods the phase velocity is estimated with a simultaneous elaboration of the signals detected at different distances from the source. As a consequence the dispersion curve obtained from multistation tests is generally smoother and this can be a great advantage in the view of the inversion process.

One weak aspect of the spectral analysis typically adopted in the SASW test is the unwrapping of the cross power spectrum phase, a necessary step for the estimation of phase velocity. Usually the presence of near field effects and ambient noise strongly deteriorates the cross power spectrum estimate at low frequencies and hence the unwrapping becomes a very ticklish matter. Phase unwrapping is the problem that essentially inhibits the automation of dispersion curve estimation. With the adoption of a multistation procedure, phase unwrapping is avoided and the dispersion curve estimation is easily automated.

Another important advantage of multistation procedures is related to the testing geometry. While the classical SASW test requires the adoption of the common-receiver-midpoint array geometry with source reversing, for multistation tests the much simpler common-source array geometry can be profitably used. This is a great advantage, especially for massive sources, and the testing time is strongly reduced.

8.1.1 Multichannel impulsive source methods

The multichannel procedures adopted in this research for the analysis of seismic traces related to impulsive sources have some inherent advantages with respect to the two-station method. The whole ensemble of data contributes to the final image in the transformed domain that is thereafter used to get the dispersion curve, i.e. there is no subjective selection. This aspect is very important in the perspective of automating the dispersion curve evaluation. Indeed the process of picking the maxima from the transformed image of the data can be easily implemented on a portable computer to get directly on site the estimate of the dispersion curve. This aspect has a twofold advantage reducing the time for interpretation in the office and producing an important feedback during the in situ

testing.

The numerical simulations, which are reported in Chapter 5, give an important insight regarding the application of the multistation methods in geotechnics. As seen in Chapter 4, Rayleigh waves are often analysed on a seismological scale to get an estimate of the Earth's structure. In that case the travel distance is large enough, so that the experimental modal dispersion curves can be obtained and used for the inversion process. The applications of *fk* and *fp* transforms based methods, which can be found in the literature, regard great distances on which the hypothesis of mode separation is applicable. In such cases the dispersion curves for separated Rayleigh modes is obtained and consequently, if more than one mode is available, the inversion process results to be very stable and the non-uniqueness problem is mitigated (Gabriels at al. 1987).

One important conclusion of the simulation reported in Chapter 5 is that, using a relatively small number of receivers close to the source, the quantity that is obtained from multistation methods is an estimate of the average effective phase velocity, i.e. it is strongly affected by mode superposition. This aspect has a great relevance in the view of the subsequent inversion process. Indeed the inversion algorithm has to be based on a consistent definition of the effective velocity in the spatial range tested. Such a conclusion is extremely important for the application of multistation methods for characterization at a geotechnical scale.

Another open question regards the influence of near field effects. Since in multistation methods the evaluation of the dispersion curve is based on many receivers, some closer and some more distant from the source, it would be expected that body waves should have a minor influence. Moreover if the traces are translated in the *fk* domain, the energy carried by different kinds of wave partially separates. The simulation in presence of body waves effects, partially confirmed the above idea: effectively there is a mitigation of near field effects on the dispersion curve estimation, but at very close positions from the source the near field effects are still sensible.

Finally the experimental part of this research associated to impulsive sources gave really appreciable results. In particular it has been possible to show the successful application of both *fk* and *fp* methods.

The comparison with results obtained from the classical SASW test showed some distinctive experimental advantages, which join the advantages exposed above about multistation methods in general.

First of all the estimate of the dispersion curve is with no doubt more stable in the case of multistation methods. This is true over the whole range of frequency of interest, but it is particularly interesting at low frequency. Indeed the possibility of obtaining a good estimate of the dispersion curve at low frequency is a critical

point for the resolution at depth. The application of the *fk* method allowed not only the reconstruction of the dispersion curve down to lower frequencies if compared to SASW, but also a by far more accurate estimate.

Finally concerning the influence of ambient noise, the SASW approach requires a high signal-to-noise ratio and hence the stacking in frequency of several repetitions of the energising, this is mainly due to problems arising from the unwrapping of the cross-power spectrum phase. With the multistation methods it has been shown that a single shot produces a good estimate of the dispersion curve and the need for stacking is quite totally avoided. Consequently a certain amount of experimental time can be saved.

8.1.2 Transfer function method

The transfer function method has been proposed to enhance the capabilities of surface wave tests when both stiffness and damping profiles have to be determined.

The need for a coupled attenuation and dispersion estimate was stressed by previous works about this subject. Rix et al. (1999b) proposed a method for the uncoupled measurement and inversion of attenuation curves to get the damping profile. Lai (1998) working in the global framework of linear visco-elasticity showed the necessity of a coupled inversion process. Hence for the sake of consistency a new method for the coupled measurements of dispersion and attenuation curves of Rayleigh waves was required.

A method based on the measurement of the experimental transfer function and on simultaneous determination of dispersion and attenuation curves is proposed (see also Rix et al. 1999a). The basis of the regression algorithm is the theoretical expression of the transfer function for a layered linear viscoelastic medium. Using this method, experimental attenuation and dispersion curves can be obtained simultaneously with a coupled inversion of field data.

The use of a controlled harmonic source is compulsory for the application of this method, indeed the input characterization is required for the transfer function evaluation.

Some preliminary results are reported from two different testing sessions. The results are very encouraging, also if it has been possible to collect data only over a narrow frequency range, because of the modest mass of the electromechanical shaker. The loss of information in the low frequency range strongly influence the resolution at depth of stiffness and damping profiles, still the results show a good fitting of the experimental transfer function with the analytical expression.

8.2 Recommendation for Future Research

The use of Rayleigh waves for characterization purposes in geotechnical engineering had a strong impulse with the introduction of the SASW (Spectral Analysis of Surface Waves) method. In the last decade its diffusion rapidly spread over and now it is widely adopted for its versatility and convenience.

Still there is not a standard of practice in this field and many different methods can be adopted to get the experimental dispersion curve from field data (see Chapter 4 for a brief overview). The SASW method gave a great contribute for the spreading of surface wave tests, but it should not be considered the best choice, both because it shows many drawbacks and because it doesn't use all the information carried by the signals.

Still a great effort in research is required to clarify some basic points in this contest, in the view of exploring the possibilities and the limitations of testing using surface waves.

A still open question about the use of surface waves is the bedding inclination. For the analysis of the experimental data a model of the soil has to be selected and all the results are strongly influenced by this choice. Usually a stack of homogeneous and isotropic layers with constant thickness is considered. In case the inclination of the layers strongly violates this basic assumption and consequently it can invalidate the results.

In general it can be stated that soil characterization with surface wave based methods should be used only when horizontal layering is expected at a site.

The usual practice to account for bedding inclination in the SASW test is to average between dispersion measurements with the source placed on one and the other side in a common-receiver-midpoint testing geometry (see Figure 4.5). In the writer's opinion this remedy is not satisfactory, indeed the violation of a basic assumption should be addressed with much caution.

If a common-source array geometry (see Figure 4.6), which is the scheme for multistation testing, is adopted, bedding inclination is totally neglected.

An extensive study of the effects of bedding inclination on the dispersion curve evaluated from surface measurements is then required to clarify if and up to which extent they can be tolerated. Such results could eventually be used in conjunction with an on site estimation of bedding inclination, that can be obtained using other non invasive methods such as the seismic refraction method, to assess the applicability of surface waves based method in controversial situations.

The big issue about soil testing using surface wave methods is the inversion process. The problem of non-uniqueness makes this aspect a very tricky matter from a mathematical point of view. Consequently the inversion is in itself ill posed

and adequate constraints for the solution are needed. Some automated procedures have been proposed, still there is much room for further improvements.

In this dissertation some applications of multistation methods have been presented showing the advantages and the drawbacks that they can have when applied to geotechnical characterization. With respect to each one of them some starting points for further researches are reported in the following.

8.2.1 Multichannel impulsive source methods

The fk domain analysis has been profitably used on a testing site, showing several advantages with respect to the common two-station procedure of the SASW test. Nevertheless the profile of the testing field was essentially normally dispersive, at least for the depth that the usual practice of inversion allows to investigate accurately. A more extensive testing campaign is required to assess the extendibility of such results to inversely dispersive profiles, with reversals of stiffness in layers at shallow depth.

For what it concerns the inversion process, a new, and more consistent with the testing procedure, definition of the effective phase velocity is needed. Indeed in Chapter 5 the phase velocity obtained from the simulation of the multistation test has been compared with the effective phase velocity evaluated in a two-station fashion. The conclusion that what we get from fk analysis is not a modal phase velocity but an effective one is very important. In the view of the inversion process the phase velocity obtained from a multistation approach is a sort of average effective velocity over the extent of space covered by the receiver array (recalling from Chapter 3 that the phase velocity is a function of both frequency and space).

8.2.2 Transfer function method

The transfer function method, which has been suggested for the coupled measurements of Rayleigh dispersion and attenuation curves, appears to be a formally elegant and appealing possibility to enlarge the perspective of surface wave testing.

The experimental transfer function is compared with an analytical expression obtained in the framework of linear viscoelasticity using some hypotheses. Some proofs about such assumptions are required. In particular an extensive study is needed to check the consequence of two basic simplifying assumptions (see Paragraph 4.4.2). The first is related to the transformation of the complex wavenumber $\psi(\omega, r)$, which is required to make explicit its dependence on

distance from the source. The second one is relative to the geometric spreading function $G(\omega, r)$, which in this work has been assumed proportional to the usual attenuation factor for homogeneous media ($1/\sqrt{r}$).

Both assumptions are strictly related to the influence of higher modes in determining the global response of the site to a harmonic excitation. The second assumption could be removed with an iterative procedure in which a starting stiffness and damping profile is obtained and then refined by removing the assumption itself. The consequence of the first assumption should be in general that an effective value of phase velocity and attenuation coefficient is found.

As for the multistation impulsive source tests, also in this case a further effort is required for the development of a robust inversion process in which the quantities to be inverted (phase velocity and attenuation factor) should be defined in a consistent manner with respect to the experimental measurements.

Finally the necessity of a larger testing campaign has to be emphasised. Indeed the results cannot be validated without a comparison with an independent estimation of shear wave velocity and damping ratio, obtained using other seismic methods (e.g. the cross-hole test).

Appendix A

Signal Processing Tools

The possibilities given by the application of signal processing have greatly influenced the approaches in many different branches of engineering especially those related to dynamic problems.

As wave propagation is concerned the interpretation of the relative signals is strongly enhanced by the application of transforms. Using such mathematical tools it is possible to change the domain in which experimental data are represented, choosing appropriate and convenient new domains.

The same data are translated from a domain to another without any loss of information, at least in principle. The convenience is constituted by some peculiar properties that each domain shows, making it convenient to work on it in function of the final scope of the analysis. It is important to remark that, since no loss of information is implied, it is always possible to come back to the original domain using the relative inverse transforms. This possibility of switching from one domain to another and back to the initial one is the basis of many data processing techniques.

An intensive use of wave field transforms is made in geophysics, where many application have been developed to enhance the performances of methods such as seismic reflection and seismic refraction. An intensive use of transforms is also made for seismic tomography, a technique that is founded directly on the application of transforms (Sheriff and Geldart 1995).

An overview of the transforms used in the present dissertation and of the relation between them is useful to clarify some important points. Many of this aspect have been explicitly or implicitly recalled in the dissertation, but they will be here included to get a consistent summary. The intention is not to focus on the

mathematical aspects that can be found in many reference textbooks (Bracewell 1986, Johnson and Dudgeon 1993, Helgason 1980) but on some important properties, that are closely linked to the use that is done of these transforms in general in geophysics and more closely in this dissertation.

A.1 Discrete Fourier Transform

The Fourier transform is undoubtedly the most well known and widely applied signal-processing tool. It is based on the Fourier Series, according to which a given time series can be expressed as the sum of infinite sinusoids having different frequency. Considering that each sinusoid is characterised by its amplitude and phase-lag (relative alignment), these values constitute the frequency-domain representation of the series (Figure A.1).

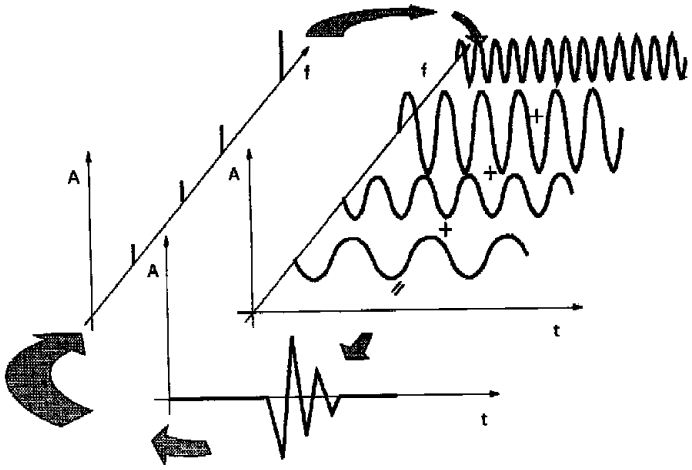

Figure A.1 Exemplification of the Fourier Transform concept

The above concept is totally general meaning that the series can be defined in whatever domain. The most common case is that of a signal in the time domain that is translated in its complex representation in the frequency domain. Another pertinent case is that of a series of values in space that is analogously transformed in a series of sinusoids in space, each one characterised by its wavelength or more commonly by its wavenumber (note that wavelength and wavenumber are related by the same relationship that links period and circular frequency for a sinusoid in time).

Considering a given continuous function $x(t)$ of a single variable t, the mathematical definition of its Fourier transform $X(\omega)$ is:

$$X(\omega) = \int_{-\infty}^{+\infty} x(t) \cdot e^{-i\omega t} dt \tag{A.1}$$

where ω is the transform variable. Since there is no loss of information, the Fourier Transform is reversible and the Inverse Fourier Transform is given by:

$$x(t) = \frac{1}{2\pi} \int_{-\infty}^{+\infty} X(\omega) \cdot e^{i\omega t} d\omega \tag{A.2}$$

Equations A.1 and A.2 are often denoted respectively as Fourier Analysis and Fourier Synthesis equations to indicate their application for signal analysis and construction (or reconstruction).

In general $X(\omega)$ is a complex valued function, hence it can be represented either in terms of its real and imaginary components or more meaningfully of its amplitude and phase:

$$X(\omega) = \mathrm{Re}(X(\omega)) + i \cdot \mathrm{Im}(X(\omega)) = A(\omega) \cdot e^{i\phi(\omega)} \tag{A.3}$$

where $A(\omega)$ and $\phi(\omega)$ are respectively the amplitude and phase spectra.

In reality a signal can't be sampled in a continuous way and hence it is necessary to introduce the concept of series, that can be seen as a discrete function. The digitised form of the continuous function $x(t)$ is a finite array of values taken at constant intervals of the variable t. This is the way in which signals are captured from the real world and used for successive processing and hence this is the form to which engineering is concerned about. Consequently the Discrete Fourier Transform has to be introduced.

Assuming that N samples are taken at interval Δt, the Discrete Fourier Transform pair (i.e. analysis and synthesis equations) can be written as (Santamarina and Fratta 1998):

$$\begin{aligned} X_m &= \sum_{l=0}^{N-1} x_l \cdot e^{-i\left(m\frac{2\pi}{N}l\right)} && m = 0...N-1 \\ x_l &= \frac{1}{N} \sum_{m=0}^{N-1} X_m \cdot e^{i\left(m\frac{2\pi}{N}l\right)} && l = 0...N-1 \end{aligned} \tag{A.4}$$

Because of periodicity of harmonic functions, the DFT presumes periodicity of the signals. This implies that aperiodic signals are analysed as periodic signals with period $N \cdot \Delta t$.

The Discrete Fourier Transform enjoys many important properties, which make of it a distinctive tool (Bracewell 1986).

Some important aspects are related to the discrete formulation and will be shortly discussed in the following.

A.1.1 Aliasing

It is an undesired effect of sampling at discrete time intervals, a procedure that is inevitably linked to the digitisation necessary for storage and subsequent analysis of time histories. A thorough analytical treatment can be found in Oppenhein et al. (1983), while Santamarina and Fratta (1998) report a clear exemplification of the problem.

The highest frequency component that can be extracted by a discrete signal is inversely proportional to the sampling interval and it is commonly called the Nyquist frequency:

$$f_{Nyquist} = \frac{1}{2\Delta t} \tag{A.5}$$

All the frequency components above this value are lost. Aliasing can be summarised as the presence of fictitious low frequency components that are created to compensate the energy of lost high frequency components.

Two main problems are associated to the aliasing phenomenon. First the sampling interval has to be carefully chosen in accordance to the frequencies involved by the phenomenon under study or at least to the frequency range of interest. Under-sampling can induce the loss of important information in the frequency range above the Nyquist value.

The second important problem is that aliasing causes the alteration of the Fourier spectrum if frequency components above the Nyquist threshold are present in the real signal. Indeed the energy associated to those lost components is erroneously related to other frequencies below the Nyquist value (i.e. the energy is aliased in the low frequency range). Alias frequencies can seriously damage the analysis. For this reason an anti-alias filter is required to cut off all the energy effectively associated to high frequency components. In this way a correct evaluation of the frequency spectrum for the frequency range below the Nyquist value can be obtained.

Many recording device (either seismograph or signal analysers) have a built in

analog anti-alias filter placed in series before the digitisation unit. In this way the high frequency components (above $1/2\Delta t$) are removed from the original analog signal arriving from the receiver. Such a process is quite reliable and certainly superior to the implementation of digital filters.

A.1.2 Leakage

Inevitably the application of the DFT introduces some spurious components because of the presumed periodicity and of signal truncation, caused by the finite length of the records. Indeed sharp brakes caused by the forced periodicity that links the end with the start of the signal must be simulated by the DFT, introducing some erroneous high frequency components.

Moreover it must be considered also that the transform is discrete in frequency, thus the frequencies of the original signal not present in the discrete array must be represented by the closest discrete values, either the higher or the lower one.

Both this aspects causes the translation of part the energy from the actual frequencies to close frequencies, in other word energy leaks into other frequencies. For this reason this problem is known as *leakage*.

As the second aspect is concerned, leakage can be reduced increasing the frequency resolution. On the other hand if a wide observation window of the signal is chosen and a pre-trig is applied to the signal, it is possible to obtain a record starting and ending with zero values, eliminating, at least in principles, the effect of forced periodicity.

Nevertheless it must be noted that not always memory storage capability allows the application of this trick. Moreover also when it is used, the presence of noise can introduce truncation errors.

A good strategy to reduce leakage in such cases is the application of a windowing process, using an appropriate gradual windowing function (see Paragraph 7.1.1.1). It must be considered that the global energy of the signal is reduced by the application of windowing and hence, if it is of interest, a correction is required.

A.1.3 Resolution

The sampling interval, i.e. the interval between two consecutive discrete times, fixes the resolution in time. The resolution in frequency is instead determined by the total duration of the record, which, because of the presumed periodicity in DFT, represents the longest resolvable period.

The two resolutions are closely linked each other; indeed the duration of the record is given by the product of the sampling interval per the number of samples. In summary the interval between two consecutive discrete frequencies Δf (resolution in frequency) is related to the sampling interval Δt (resolution in time) by the following relationship:

$$\Delta f = \frac{1}{N \cdot \Delta t} \tag{A.6}$$

As a consequence it is clear that given the number of samples (that is usually dictated by the instrument or by manageability of the digitised signal) there is a trade-off between the two resolution. This is also known as uncertainty principle: the more the signal is defined in time the less it is in frequency. The choice of an acceptable compromise between the two is related to the field of application.

Once a signal has been captured with a given sample interval and number of points, a possible strategy to improve the frequency definition is given by zero-padding that consists in tailing the signal with a series of zero value samples. Care must be taken because zero padding can introduce discontinuity and hence produce leakage in the DFT. For this reason it is desirable to apply zero-padding after a windowing process.

A.2 2D Discrete Fourier Transform

The concept of the one-dimensional Fourier Transform can be extended to more than one dimension. In geophysics the 2D Fourier Transform is interesting for two different classes of applications.

In multichannel processing, several traces collected simultaneously at different locations along a straight line are analysed at once as an ensemble. In this case the 2D DFT allows the conversion from the space-time domain in which traces are collected to the frequency-wavenumber domain in which appropriate elaborations can be performed.

When two different direction in space are involved the 2D DFT allows the translation to a 2D-wavenumber domain. This process is commonly used for image processing and it is the base of tomography.

In the following we will refer to a wavefield, defined in time and space domain ([t, x]), but the formulas are in general valid for any 2D domain.

The bidimensional Fourier Transform (analysis equation) is defined by:

$$P(k,\omega) = \int_{-\infty}^{+\infty}\int_{-\infty}^{+\infty} p(x,t)\cdot e^{i(kx-\omega t)}dxdt \tag{A.7}$$

and its inverse (synthesis equation) by:

$$p(x,t) = \frac{1}{4\pi^2}\int_{-\infty}^{+\infty}\int_{-\infty}^{+\infty} P(k,\omega)\cdot e^{-i(kx-\omega t)}dkd\omega \tag{A.8}$$

For implementation convenience and for a clearer view of the transform, the 2D Fourier Transform can be seen as two successive application of the 1D transform. A first transform over t leads to the frequency-space domain:

$$P(x,\omega) = \int_{-\infty}^{+\infty} p(x,t)\cdot e^{-i\omega t}dt \tag{A.9}$$

while a second application over x gives the 2D FT:

$$P(k,\omega) = \int_{-\infty}^{+\infty} P(x,\omega)\cdot e^{ikx}dx \tag{A.10}$$

Clearly, also in this case the actual use of the transform is made in its discrete formulation, since the acquisition of signals is discrete both in time and in space. In analogy to the one-dimensional case, the 2D DFT and its inverse can be written as (Santamarina and Fratta 1998):

$$\begin{aligned} P_{u,v} &= \sum_{l=0}^{M-1}\left[\sum_{m=0}^{N-1} p_{l,m}\cdot e^{-i\left(v\frac{2\pi}{N}m\right)}\right]\cdot e^{-i\left(u\frac{2\pi}{N}l\right)} \\ p_{l,m} &= \frac{1}{M\cdot N}\sum_{u=0}^{M-1}\left[\sum_{v=0}^{N-1} P_{u,v}\cdot e^{-i\left(v\frac{2\pi}{N}m\right)}\right]\cdot e^{-i\left(u\frac{2\pi}{N}l\right)} \end{aligned} \tag{A.11}$$

assuming that N samples are taken at interval Δt at M receiver positions spaced Δx along a straight line. It is important to note that in this case the original data are given by a matrix, in which each entry is the signal at a given position in space in a given time instant. The 2D DFT can hence be seen as two successive applications of the 1D DFT: before over the rows of the matrix and subsequently over its columns.

The problems of aliasing, leakage and resolution now interest both the

dimension and must be carefully accounted for when choosing the sampling parameters in time and the receiver locations in space.

In particular it is important to remark that:

- ✓ No antialias filter can be built for the space domain (see Yilmaz 1987 for a discussion of aliasing effects on *fk* spectra);
- ✓ The number of detecting points in space is often much more small than the number of samples in time, hence the uncertainty problem is much more stressed;
- ✓ The enhancement of definition in space is obtained adding zero-valued traces at the end of the ensemble of data.

A.2.1 Properties and applications

The advantage of working in the transformed domain when analysing seismic traces is essentially related to the separation of events that are obscurely overlapped in the original time-space domain.

Apparent velocity on the ground surface linked to the different inclination of the wave fronts plays a major role in the separation of energy in the *fk* domain (Doyle 1995). In particular while reflections tend to map close to the frequency axis, surface wave tend to map close to the wavenumber axis (Figure A.2).

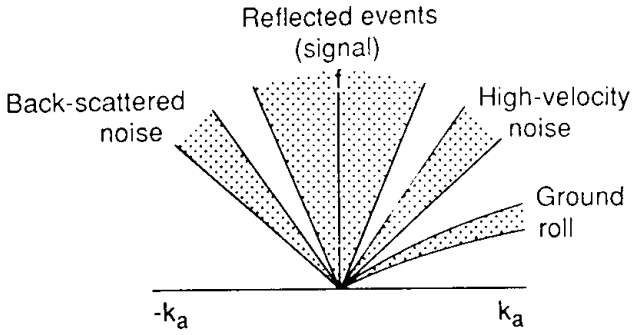

Figure A.2 Idealised frequency-wavenumber spectrum of a seismic gather with reflection and noise localisation (from Doyle 1995)

One application linked to this property is the *fk* filtering that is commonly used for the seismic reflection method. Coherent linear noise (ground roll mainly

due to Rayleigh waves), guided waves and side-scattered energy are a major problem in analysing shot gathers because they can significantly obscure the reflections. Filtering out the energy associated to ground roll in the fk domain and going back to the tx domain, the arrivals of reflected waves can be more easily located. Care must be taken in the filtering process because it can cause signal distortion and smoothing.

Another significant application of the 2D DFT in geophysics is migration, that will not be treated because it has less implication of the objective of the present dissertation.

A.3 Radon Transform

The Radon transform is an integral operator that acts on a given function of a bi-dimensional domain mapping it into a new domain defined by the parameters that specify the line along which integration is performed. Considering for example an arbitrary property defined in a bi-dimensional space $p(x, y)$ and expressing it for convenience in polar coordinates $p(r,\phi)$, its Radon Transform along the line RS (see Figure A.3) univocally defined by the angle ϑ and a radial coordinate l, is given by the integral (Sheriff and Geldart 1995):

$$P(l,\vartheta) = \int_{RS} p(r,\phi)ds \tag{A.12}$$

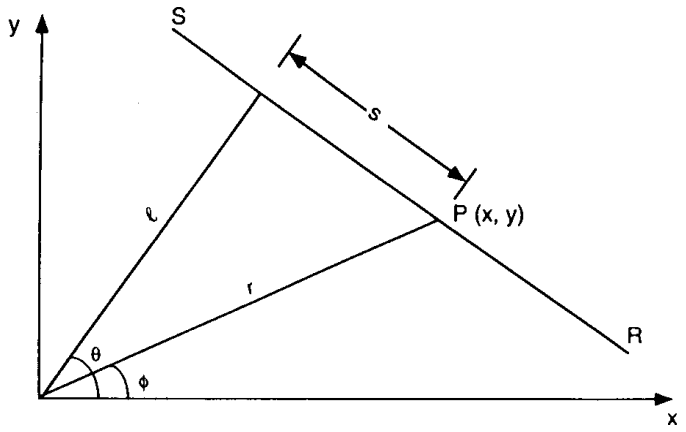

Figure A.3 Definition of the integration line for the Radon transform (from Sheriff and Geldart 1995)

It must be noted that a straight line has been used in this definition, nevertheless considering an arbitrary line the Generalised Radon Transform can be defined.

Considering the equation of the line RS in cartesian coordinates:

$$x\cos\vartheta + y\sin\vartheta = l \tag{A.13}$$

it is possible to reformulate the Radon transform as the integral sum of the values along the straight line in cartesian coordinates using the delta function ($\delta(q)=1 \;\; if \;\; q=0; \;\; \delta(q)=0 \;\; if \;\; q\neq 0$):

$$P(l,\vartheta) = \int_{-\infty}^{+\infty}\int_{-\infty}^{\infty} p(x,y)\delta(x\cos\vartheta + y\sin\vartheta - l)dxdy \tag{A.14}$$

As for the case of Fourier Transform also in this case, since there is no loss of information during the transformation process, an inverse transform can be defined. An important difference is given by the fact that a nontrivial one-dimensional analog of the Radon Transform doesn't exist.

A discrete formulation of the Radon Transform is required for application in engineering problems. Care must be taken because the inverse Discrete Radon Transform can't be derived directly by the definition of the inverse Radon Transform (Beylkin 1987).

A.3.1 Slant Stack or τp Transform

A slightly different form of the Radon Transform is commonly used in geophysical application. It is usually indicated as the τp Transform, because in this case the straight line, along which the integral operation is performed, is defined as:

$$y = \tau - px \tag{A.15}$$

(clearly $\tau = l/\sin\vartheta$ and $p = \cot\vartheta$). Hence the definition of the τp Transform will be (Sheriff and Geldart 1995):

$$P(\tau, p) = \int_{-\infty}^{+\infty}\int_{-\infty}^{\infty} p(x,y)\delta(y + px - \tau)dxdy \tag{A.16}$$

Although mathematically the difference is apparently negligible the τp Transform assumes physically more significance for the analysis of seismic shot gathers, collections of signals related to the same shot but detected by different receivers aligned with constant spacing (note that in this case the original domain is $[tx]$). Indeed in this case such transform is equivalent to a plane-wave decomposition of the wave field, where the slope p is the horizontal slowness (i.e. the inverse of velocity) and the intercept τ is a transformed (linearly moved out) time. Considering that the apparent velocity of body waves on surface in a homogeneous medium is associated only to the inclination of the wavefront, in the new domain each trace represents a wave that propagates at a certain angle from the vertical (Yeldin 1987).

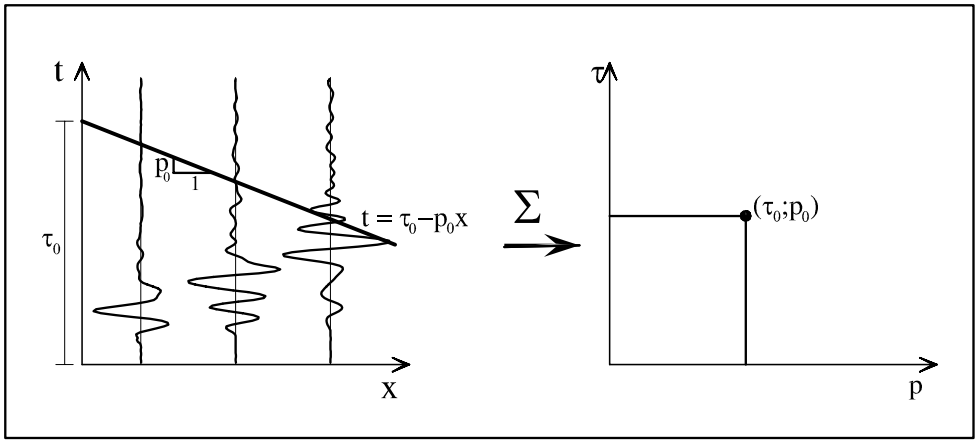

Figure A.4 Exemplification of the Slant Stack transform concept

The transform is often called *Slant-Stack* because considering a wavefield the basic operation is that of stacking all the values along each inclined (slant) line (Robinson 1982). The sum of all the values along the line is then associated to a point in the new domain having as coordinates the slope and the intercept of the line (Figure A.4).

A.3.2 Properties and applications

The Slant Stack transform can be a very useful tool for implementation of filtering techniques for seismic methods. Indeed compared to the 2D Fourier Transform, it

gives a clearer separation between reflections, refractions, diffractions and surface-waves noise (Doyle 1995). Note in particular that both reflection and refraction methods can take advantage in this case.

With the application of a Slant Stack transform to a seismic gather, ground roll (surface waves noise) maps into a small area close to time zero and refractions to points, because they are ideally characterised by a constant slope. Reflections and diffraction hyperbolae transform to ellipses in the new domain, and it is important to remark that also if hyperbolae cross each other the corresponding ellipses do not cross (Figure A.5).

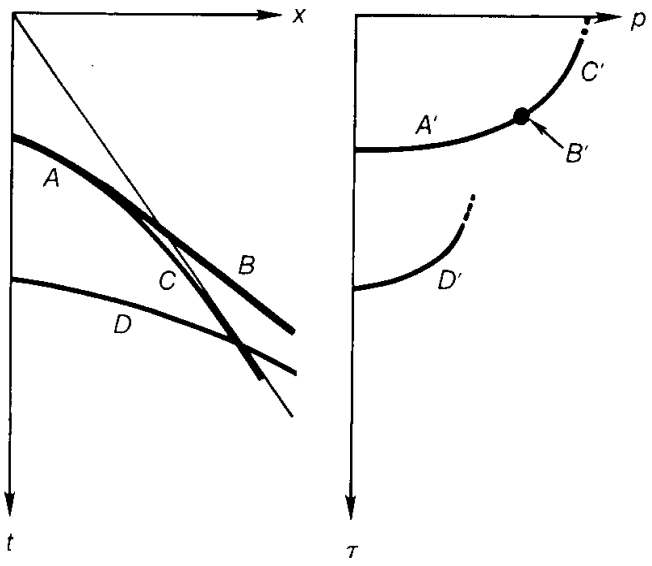

Figure A.5 Various arrivals on a seismic *tx* gather mapped onto the corresponding *τp* gather (from Yilmaz 1987)

Such a clear separation allows for powerful filtering, but the inverse Slant Stack transform, required to switch back to the original *tx* domain for arrival times evaluation, is a very ticklish operation.

A review of the many applications of *τp* Transform in geophysics can be found in Yilmaz (1987).

A.4 The Fourier Slice Theorem

This theorem constitutes an important link between the 2D Fourier Transform and the Radon Transform and it is the base of tomographic imaging (Sheriff and Geldart 1995, Santamarina and Fratta 1998).

Considering an arbitrary property defined in a bi-dimensional space $p(x, y)$, the Fourier Slice Theorem states that its 2D Fourier Transform is equal to the 1D Fourier Transform of its Radon Transform.

This equivalence constitutes the link between the multistation methods applied in this research for the determination of the dispersion curve associated to a wavefield.

References

Achenbach J.D. (1984) “Wave propagation in elastic solids”, North-Holland, Amsterdam, Netherlands

Aki K., Richards P.G. (1980) “Quantitative seismology: theory and methods - 2 vol.”, Freeman, S. Francisco

Al-Hunaidi M.O. (1992) “Difficulties with phase spectrum unwrapping in spectral analysis of surface waves nondestructive testing of pavements”, Can. Geotech. J., vol. 29, pp. 506-511

Al-Hunaidi M.O. (1994) “Analysis of dispersed multi-mode signals of the SASW method using the multiple filter/crosscorrelation technique”, Soil Dynamics and Earthquake Eng., vol. 13, Elsevier, pp. 13-24

Al-Hunaidi M.O., Rainer J.H. (1995) “Analysis of multi-mode signals of the SASW method”, Proc. 7th Int. Conf. Soil Dynamics and Earthquake Eng., pp. 259-266

Alkire B.D. (1992) “Seasonal soil strength by spectral analysis of surface waves”, J. of Cold Regions Eng., vol. 6 (1), ASCE, pp. 22-38

Anderson D.L., Ben-Menahem A., Archambeau C.B. (1965) “Attenuation of Seismic Energy in the Upper Mantle”, J. Geophysical Research, vol. 70, pp. 1441-1448

Andrus R.D., Chung R.M., Stokoe K.H., Bay J.A. (1998) “Delination of densified sand at Treasure Island by SASW testing”, Geotechnical Site Characterization, Robertson & Mayne eds, vol. 1, Balkema, pp. 459-464

Apsel R.J., Luco J.E. (1983) “On the green functions for a layered half-space. Part II”, Bullettin of the Seismological Society of America, vol. 73 (4), pp. 934-951

Audisio A., Bonani S., Foti S. (1999) “Advances in spectral analysis for SASW test”, Pre-Failure Deformation Characteristics of Geomaterials, Jamiolkowski M., Lancellotta R. and Lo Presti D. eds, Balkema, Rotterdam, pp. 395-402

Ballard R.F. (1964) “Determination of soil shear moduli at depth by in situ vibratory techniques”, Waterways Experiment Station, Miscellaneous paper No. 4-691, December

Bendat J.S., Piersol A.G. (1993) "Engineering applications of correlation and spectral analysis", J. Wiley & sons, New York

Beylkin G. (1987) "Discrete Radon Transform", IEEE Transactions on ASSP, vol. 35, pp. 162-172

Bloch S., Hales A.L. (1968) "New techniques for the determination of surface wave phase velocity", Bullettin of the Seismological Society of America, vol. 58, , pp. 1021-1034

Bracewell R.N. (1986) "The Fourier transform and its applications", McGraw-Hill, New York

Buchwald V.T. (1961) "Rayleigh waves in transversely isotropic media", Quart. Journ. Mech. and Appl. Math, vol. 14, , pp. 293-317

Capon J. (1969) "High-Resolution Frequency-Wavenumber Spectrum Analysis", Proceedings of the IEEE, vol. 57, pp. 1408-1418

Chen X. (1993) "A systematic and efficient method of computing normal modes for multilayered half-space", Geophys. J. Int., vol. 115, pp. 391-409

Christensen R.M. (1971) "Theory of viscoelasticity - an introduction", Ed. Academic Press

Dorman J., Ewing M. (1962) "Numerical inversion of seismic surface wave dispersion data and crust-mantle structure in the New York-Pennsylvania Area", J. Geophysical Research, vol. 67 (13), pp. 5227-5241

Doyle H. (1995) "Seismology", J. Wiley & sons, Chichester

Dziewonski A., Bloch S., Landisman M. (1969) "A technique for the analysis of transient seismic signals", Bullettin of the Seismological Society of America, vol. 59, pp. 427-444

Ewing W.M., Jardetzky W.S., Press F. (1957) "Elastic waves in layered media", McGraw-Hill, New York

Gabriels P., Snieder R., Nolet G. (1987) "In situ measurements of shear-wave velocity in sediments with higher-mode Rayleigh waves", Geophys. Prospect., vol. 35, pp. 187-196

Ganji V., Gukunski N., Maher A. (1997) "Detection of underground obstacles by SASW method - Numerical aspects", J. Geotech. and geoenvir. Eng., vol. 123 (3), ASCE, pp. 212-219

Ganji V., Gukunski N., Nazarian S. (1998) "Automated inversion procedure for spectral analysis of surface waves", J. Geotech. and Geoenv. Eng., vol. 124, ASCE, pp. 757-770

Gazetas G. (1982) "Vibration characteristics of soil deposits with variable wave velocity", Int. J. Num. and Anal. Meth. in Geomechanics, vol. 6, J. Wiley & Sons, pp. 1-20

Graff K.F. (1975) "Wave motion in elastic solids", Dover, New York

Gucunski N., Ganji V., Maher M.H. (1996) "Effects of ostacles on Rayleigh wave dispersion obtained from the SASW test", Soil Dynamics and Earthquake eng., vol. 15, Elsevier, pp. 223-231

Gucunski N., Woods R.D. (1991) “Inversion of Rayleigh wave dispersion curve for SASW test”, Prooc. 5th Int. Conf. on Soil Dyn. and Earthq. Eng., Kalsruhe, pp. 127-138

Gucunski N., Woods R.D. (1991) “Use of Rayleigh modes in interpretation of SASW test”, Proc. 2th int. Conf. Recent Advances in Geot. Earthq. Eng. and Soil Dyn.-S.Louis, pp. 1399-1408

Gucunski N., Woods R.D. (1992) “Numerical simulation of SASW test”, Soil Dyn. and Earthq. Eng., vol. 11 (4), Elsevier, pp. 213-227

Gucunski N., Krstic V., Maher M.H. (1998) “Experimental procedures for detection of underground objects”, Geotechnical Site Characterization, Robertson & Mayne eds, vol. 1, Balkema, pp. 469-472

Haegeman W., Van Impe W.F. (1997) “Stiffness parameters for soils - SASW experiences”, Third Geotech. Eng. Conf. - Cairo

Haegeman W., Van Impe W.F. (1998) “SASW control of a vacuum consolidation on a sludge disposal”, Geotechnical Site Characterization, Robertson & Mayne eds, vol. 1, Balkema, pp. 473-477

Harkrider (1964) “Surface waves in multilayered elastic media I. Rayleigh and Love waves from buried sources in multilayered elastic halfspace”, Bulletin of the Seism. Soc. of Am., vol. 54 (2), pp. 627-679

Haskell N.A. (1953) “The dispersion of surface waves on multilayered media”, Bullettin of the Seismological Society of America, vol. 43 (1), pp. 17-34

Heisey J.S., Stokoe K.H. II, Meyer A.H. (1982) “Moduli of pavement systems from spectral analysis of surface waves”, Transp.Res. Rec., vol. 852, pp. 22-31

Helgason S. (1980) “The Radon Transform”, Birkhauser, Boston

Herrmann R.B. (1994) “Computer programs in seismology”, User’s Manual, S.Louis University, Missouri (USA)

Herrmann R.B., Wang C.Y. (1985) “A comparison of synthetic seismograms”, Bullettin of the Seismological Society of America, vol. 75 (1), pp. 41-56

Hisada Y. (1994) “An efficient method for compunting Green's functions for a layered half-space with sources and receivers at close depths”, Bullettin of the Seismological Society of America, vol. 84 (5), pp. 1456-1472

Hisada Y. (1995) “An efficient method for compunting Green's functions for a layered half-space with sources and receivers at close depths (part 2)”, Bullettin of the Seismological Society of America, vol. 85 (4), pp. 1080-1093

Hoar R.J., Stokoe K.H. (1984) “field and laboratory measurements of material damping of soil in shear”, Proc. 8th World Conf. On Earthq. Eng., vol. 3, pp. 47-54

Horike M. (1985) “Inversion of phase velocity of long-period microtremors to the S-wave-velocity structure down to the basement in urbanized areas”, J. Phys. Earth, vol. 33, pp. 59-96

Johnson D.H., Dudgeon D.E. (1993) "Array signal processing", Prentice-Hall, Upple Saddle River (N.J.)

Jones R.B. (1958) "In-situ measurement of the dynamic properties of soil by vibration methods", Geotechnique, vol. 8 (1), pp. 1-21

Jones R.B. (1962) "Surface wave technique for measuring the elastic properties and thickness of roads: theoretical development", British J. of Applied Physics, vol. 13, pp. 21-29

Jongmans D. (1991) "Near-source pulse propagation: application to Q-determination", Geophys. Prospect., vol. 39, pp. 943-952

Jongmans D., Campillo M. (1993) "The determination of soil attenuation by geophysical prospecting and the validity of measured Q values for numerical simulations", Soil Dynamics and Earthquake eng., vol. 12, Elsevier, pp. 149-157

Kalinski M.E., Stokoe K.H. II, Roesset J.M., Cheng D.S. (1998) "Measurements and modeling of surface waves in drilled shaft in rock", Nondestructive and Automated Testing for Soil and Rock Properties, Marr W.A.and Faihurst C.E., ASCE

Kalinski M.E., Stokoe K.H. II, Young Y.L., Roesset J.M. (1999) "In situ log (Gmax) - log (σ') relationships using a Borehole SASW tool", Pre-Failure Deformation Characteristics of Geomaterials, Jamiolkowski M., Lancellotta R. and Lo Presti D. eds, Balkema, Rotterdam, pp. 371-378

Kausel E., Roesset J.M. (1981) "Stiffness matrices for layered soils", Bullettin of the Seismological Society of America, vol. 71 (6), pp. 1743-1761

Kennett B.L.N. (1974) "Reflections, rays and reverberations", Bullettin of the Seismological Society of America, vol. 64 (6), pp. 1685-1696

Kennett B.L.N. (1979) "Seismic waves in stratified half space", Geophysical J. Royal Astron. Soc., vol. 57, pp. 557-583

Kerry N.J. (1981) "Synthesis of seismic surface waves", Geophysical J. Royal Astron. Soc., vol. 64, pp. 425-446

Kramer S.L. (1996) "Geotechnical Earthquake Engineering", Prentice Hall, New York

Lai C.G. (1998) "Simultaneous inversion of Rayleigh phase velocity and attenuation for near-surface site characterization", PhD Diss., Georgia Inst. of Techn., Atlanta (Georgia, USA)

Lai C.G., Lo Presti D.C.F., Pallara O., Rix G.J. (1999) "Misura simultanea del modulo di taglio e dello smorzamento intrinseco dei terreni a piccole deformazioni", Atti convegno ANIDIS (in Italian)

Lai C.G., Rix G.J. (1999) "Inversion of multi-mode effective dispersion curves", Pre-Failure Deformation Characteristics of Geomaterials, Jamiolkowski M., Lancellotta R. and Lo Presti D. eds, Balkema, Rotterdam, pp. 411-418

Lamb H. (1904) "On the propagation of tremors over the surface of an elastic solid", Philos. Trans., vol. CCIII, pp. 1-42

Lefebvre G., Karray M. (1999) "New developments in in-situ characterization using Rayleigh waves", Proc. 51st Canadian Geotechnical Conf.

Love A.E.H. (1911) "Some problems of geodynamics", Cambridge Un. Press

Luco J.E., Apsel R.J. (1983) "On the green functions for a layered half-space. Part I", Bullettin of the Seismological Society of America, vol. 73 (4), pp. 909-929

Luke B.A. (1994) "In situ measurements of stiffness profiles in the seafloor using the Spectral-Analysis-of-Surface-Waves (SASW) method", PhD Diss., Un. of Texas at Austin

Malagnini L., Herrmann R.B., Biella G., de Frando R. (1995) "Rayleigh waves in quaternary alluvium from explosive sources: determination of shear-wave velocity and Q structure", Bull. of Seism. Soc. of A., vol. 85, pp. 900-922

Mancuso C. (1992) "Misura in sito delle proprietà dei terreni mediante prove dinamiche", Tesi di Dottorato (PhD Diss.), Un. Federico II, Napoli (in Italian)

Mancuso C. (1995) "Aspetti metodologici ed applicazione della tecnica sperimentale SASW", Rivista Italiana di Geotecnica, vol. 24, AGI, pp. 271-287 (in Italian)

Manesh S.M. (1991) "Theoretical investigation of the Spectral-Analysis-of-Surface-Waves (SASW) technique for application offshore", PhD Diss., Un. of Texas at Austin

Matthews M.C., Hope V.S., Clayton C.R.I. (1996) "The use of surface waves in the determination of ground stiffness profiles", Geotechnical Eng., vol. 119, Proc. Inst. Civ. Eng, pp. 84-95

McMechan G.A., Yedlin M.J. (1981) "Analysis of dispersive waves by wave field transformation", Geophysics, vol. 46, pp. 869-874

Meier R.W., Rix, G.J. (1993) "An initial study of surface wave inversion using artificial neural networks", Geotech. Testing J., ASTM, pp. 425-431

Menzies B., Matthews M. (1996) "The continuous surface-wave system: a modern technique for site investigation", Special Lecture: Indian Geot. Conf., Madras

Mitchell B.J. (1975) "Regional Rayleigh Wave Attenuation in North America", J. Geophysical Research, vol. 80, pp. 4904-4916

Nazarian S. (1984) "In situ determination of elastic moduli of soil deposits and pavement systems by Spectral-Analysis-of-Surface waves method", PhD Diss., Un. of Texas at Austin

Nazarian S., Desai M.R. (1993) "Automated surface wave method: field testing", J. Geotechnical Eng., vol. 119 (7), ASCE, pp. 1094-1111

Nazarian S., Stokoe II K.H. (1984) "In situ shear wave velocities from spectral analysis of surface waves", Proc. 8th Conf. on Earthquake Eng. - S.Francisco, vol. 3, Prentice-Hall, pp. 31-38

Oppenheim A.V., Willsky (1997) "Signal and systems", Prentice-Hall, New Jersey

Poggiagliolmi E., Berkhout A.J., Boone M.M. (1982) "Phase unwrapping, possibilities and limitations", Geophysical Prospecting, vol. 30, pp. 281-291

Rafanelli A. (1999) “Sperimentazione e comparazione di tecniche sismiche diverse per la determinazione del modulo elastico dinamico dei terreni”, Tesi di Laurea (Master Thesis), Politecnico di Torino, Italy (in Italian)

Rayleigh J.W.S. (1885) “On waves propagated along the plane surface of an elastic solid”, Proc. London Math. Soc., vol. 17, pp. 4-11

Richart F.E. Jr, Wood R.D., Hall J.R. Jr (1970) “Vibration of soils and foundations”, Prentice-Hall, New Jersey

Rix G.J. (1988) “Experimental study of factors affetting the Spectral-Analysis-of-Surface-Waves method”, PhD Diss., Un. of Texas at Austin

Rix G.J., Lai C.G. (1998) “Simultaneous inversion of surface wave velocity and attenuation”, Geotechnical Site Characterization, Robertson & Mayne eds, vol. 1, Balkema, pp. 503-508

Rix G.J., Lai C.G., Foti S. (1999a) “Simultaneous measurement of surface wave dispersion and attenuation curves”, submitted to the ASTM Geotec. Testing J.

Rix G.J., Lai C.G., Foti S., Zywicki D. (1998) “Surface wave tests in landfills and embankments” Geotechnical Earthquake Engineering and Soil Dynamics III, ASCE Geotechnical Special Publication No. 75, Dakoulas, P., Yegian, M., and Holtz, R.D., Eds., pp. 1008-1019

Rix G.J., Lai C.G., Wesley Spang A.W. Jr (1999b) “In situ measurement of damping ratio using surface waves”, accepted for pubblication on J. Geotech. and geoenvir. Eng., ASCE

Robinson E.A. (1982) “Spectral approach to geophysical inversion by Lorentz, Fourier, and Radon transforms”, Proceedings IEEE, vol. 70, pp. 1039-1054

Roesset J.M., Chang D.W., Stokoe K.H. (1991) “Comparison of 2-D and 3-D models for analysis of surface wave tests”, Prooc. 5th Int. Conf. on Soil Dyn. and Earthq. Eng., Kalsruhe, vol. 1, pp. 111-126

Sànchez-Salinero I. (1987) “Analytical investigation of seismic methods used for engineering applications”, PhD Diss., Un. of Texas at Austin

Santamarina J.C., Fratta D. (1998) “Discrete signals and and inverse problems in civil engineering”, ASCE Press, New York

Satoh T., Poran C.J., Yamagata K., Rodriguez J.A. (1991) “Soil profiling by Spectral Analysis of Surface Waves”, Proc. 2th int. Conf. Recent Advances in Geot. Earthq. Eng. and Soil Dyn.-S.Louis, pp. 1429-1434

Sheriff R.E., Geldart L.P. (1990) “Applied geophysics”, University Press, Cambridge

Sheriff R.E., Geldart L.P. (1995) “Exploration seismology”, University Press, Cambridge

Spang A.W. (1995) “In situ measurements of damping ratio using surface waves”, PhD Diss., Georgia Inst. of Techn., Atlanta (Georgia, USA)

Stokoe K.H. II, Nazarian S., Rix G.J., Sanchez-Salinero I., Sheu J., Mok Y. (1988) "In situ seismic testing of hard-to-sample soils by surface wave method", Earthq. Eng. and Soil dyn. II - Recent adv. in ground-motion eval. - Park City, ASCE, pp. 264-277

Stokoe K.H. II, Wright S.G., J.A. Bay, J.M. Roesset (1994) "Characterization of geotechnical sites by SASW method", Geophysical Characterization of Sites (ISSMFE TC#10) by R.D. Woods, Oxford & IBH Publ., pp. 15-25

Szelwis R., Behle A. (1987) "Shallow shear-wave velocity estimation from multimodal Rayleigh waves", in Danbom, S. and Domenico, S. N., Ed., Shear-wave exploration: Soc. Expl. Geophys., pp.214-226

Thomson W.T. (1950) "Transmission of elastic waves through a stratified solid medium", J. Applied Physics, vol. 21 (1), pp. 89-93

Tokimatsu K. (1995) "Geotechnical site characterisation using surface waves", Prooc. 1st Int. Conf. on Earth. Geotechn. Eng., IS-Tokio, pp. 36

Tokimatsu K., Kuwayama S., Tamura S., Miyadera Y. (1991) "Vs determination from steady state Rayleigh Wave mwthod", Soils and Foundations, vol. 31 (2), Jap. Soc. Soil Mech., pp. 153-163

Tokimatsu K., Shinzawa K., Kuwayama S. (1992a) "Use of short-period microtremors for Vs profiling", J. Geotechnical Eng., vol. 118 (10), ASCE, pp. 1544-1558

Tokimatsu K., Tamura S., Kojima H. (1992b) "Effects of multiple modes on Rayleigh wave dispersion characteristics", J. Geotechnical Eng., vol. 118 (10), ASCE, pp. 1529-1543

Tselentis G-A., Delis G. (1998) "Rapid assessment of S-wave profiles from the inversion of multichannel surface wave dispersion data", Annali di Geofisica, vol. 41, pp. 1-15

Viktorov I.A. (1967) "Rayleigh and Lamb Waves: physical theory and applications", Plenum Press, New York

Vucetic M. (1994) "Cyclic threshold shear strains in soils", J. Geotechnical Eng., vol. 120 (12), ASCE, pp. 2208-2228

Williams T.P., Gucunski N. (1995) "Neural networks for backcalculation of moduli from SASW test", J. of Computing in Civil Eng., vol. 9 (1), ASCE, pp. 1-8

Yilmaz O. (1987) "Seismic data processing", Soc. of Expl. Geoph., Tulsa

Yuan D., Nazarian S. (1993) "Automated surface wave method: inversion technique", J. Geotechnical Eng., vol. 119 (7), ASCE, pp. 1112-1126

Zywicki D., Rix G.J. (1999) "Frequency-wavenumber analysis of passive surface waves", Proc. Symp. on the Appl. of Geophysics to Environm. and Eng. Problems, Oakland, pp. 75-84

VITA

Sebastiano Foti was born in Catania (Sicily, Italy) on August the 2nd, 1971. After receiving his high school diploma from the Liceo Scientico "Ettore Mayorana" of Caltagirone, he moved to Torino to attend university.
On May the 14th 1996 he achieved a first class degree in Civil Engineering from Politecnico di Torino. His final thesis on seismic isolation and pile foundation received the award as best thesis of the year on structures from the local Alumni Association and qualified in the Philips Morris Prize for Scientific and Technological Research in Italy. He has also been included in the distinguished graduate list of the Torino Industrial Association.
During the university time, he took apprenticeships at ENEL, the Italian Agency for Electrical Energy; Carl Bro Group, Civil and Transportation division in Edinburgh (UK); MAV Bridge Construction in Budapest (Hungary).
After the university he worked for a short period at SINTECNA Consulting in Torino on bridge design projects. At the end of 1996 he applied for a PhD programme in Geotechnical Engineering at Politecnico di Torino under the guidance of Prof. Renato Lancellotta. His main research theme has been on surface wave propagation and soil characterization. He has been also involved on foundation engineering researches and on a seismic analysis project. He has been a Teaching Assistant for Statics and Construction Theory courses.
He spent seven months at Georgia Institute of Technology, Atlanta (USA), working as Research Scholar with Prof. Glenn Rix and attending courses of the local PhD programme.